

Environmental Sciences Division

**Adapting to Sea-Level Rise in the U.S. Southeast:  
The Influence of Built Infrastructure and Biophysical  
Factors on the Inundation of Coastal Areas**

Richard C. Daniels<sup>1,2</sup>, Vivien M. Gornitz<sup>3</sup>,  
Ashish J. Mehta<sup>4</sup>, Say-Chong Lee<sup>4</sup>,  
and Robert M. Cushman<sup>2</sup>

<sup>1</sup>Energy, Environment and Resources Center  
The University of Tennessee-Knoxville  
Knoxville, TN 37932

<sup>2</sup>Environmental Sciences Division  
Oak Ridge National Laboratory  
Oak Ridge, TN 37831-6335

<sup>3</sup>Goddard Institute for Space Studies  
National Aeronautics and Space Administration  
New York, NY 10025

<sup>4</sup>Coastal and Oceanographic Engineering Department  
University of Florida  
Gainesville, FL 32611

Environmental Sciences Division  
Publication No. 3915

November 1992

Prepared for the  
Office of Environmental Analysis  
U.S. Department of Energy  
Budget Activity Number PE 04 01 00 0

Prepared at  
OAK RIDGE NATIONAL LABORATORY  
Oak Ridge, Tennessee 37831-6335  
managed by  
MARTIN MARIETTA ENERGY SYSTEMS, INC.  
for the  
U.S. DEPARTMENT OF ENERGY  
under contract DE-AC05-84OR21400

**MASTER**

## **DISCLAIMER**

The findings and conclusions in this report do not necessarily reflect the official position of the U.S. Department of Energy, Oak Ridge National Laboratory, or any of its subcontractors. Mention of trade names or products does not constitute an endorsement.

## TABLE OF CONTENTS

ACKNOWLEDGMENTS . . . . .	vii
LIST OF FIGURES . . . . .	ix
LIST OF TABLES . . . . .	xvii
ABSTRACT . . . . .	xxiii
1. IMPACTS OF SEA-LEVEL RISE . . . . .	1-1
1.1 INTRODUCTION . . . . .	1-1
1.2 GOALS OF THIS STUDY . . . . .	1-2
1.3 STRUCTURE OF THE ANALYSIS . . . . .	1-2
1.4 FIGURES . . . . .	1-5
2. GLOBAL CLIMATE CHANGE . . . . .	2-1
2.1 GREENHOUSE EFFECT . . . . .	2-1
2.2 PAST EVIDENCE OF CLIMATE CHANGE . . . . .	2-2
2.3 SEA-LEVEL TRENDS . . . . .	2-3
2.4 SEA-LEVEL-RISE SCENARIOS . . . . .	2-5
2.5 FIGURES . . . . .	2-11
3. VULNERABILITY OF THE U.S. SOUTHEAST TO SEA-LEVEL RISE . . . . .	3-1
3.1 THE COASTAL HAZARDS DATA BASE . . . . .	3-1
3.2 DATA BASE COMPONENTS AND RISK CLASSES . . . . .	3-2
3.3 DEVELOPMENT OF THE COASTAL VULNERABILITY INDEX . . . . .	3-7
3.4 STUDY AREA SELECTION . . . . .	3-14
3.5 FIGURES . . . . .	3-17

<b>4. APPLICATION OF THE SEA-LEVEL SCENARIOS ON THE U.S. SOUTHEAST</b>	<b>4-1</b>
<b>4.1 METHODS AND DATA SOURCES</b>	<b>4-1</b>
4.1.1 Land Use Data	4-1
4.1.2 Digital Elevation Models	4-3
4.1.3 Subsidence Rates	4-3
<b>4.2 THE GULF COAST</b>	<b>4-7</b>
4.2.1 Galveston, Texas	4-8
4.2.2 Caminada Pass, Louisiana	4-12
4.2.3 Bradenton Beach, Florida	4-16
<b>4.3 THE EAST COAST (SOUTHERN HALF)</b>	<b>4-20</b>
4.3.1 Daytona Beach, Florida	4-21
4.3.2 McClellanville, South Carolina	4-25
4.3.3 Nags Head, North Carolina	4-29
<b>4.4 CONCLUSIONS</b>	<b>4-33</b>
<b>4.5 FIGURES</b>	<b>4-35</b>
<b>5. ANALYSIS OF THE EFFECTS OF BIOPHYSICAL FACTORS ON THE EXTENT OF COASTAL INUNDATION</b>	<b>5-1</b>
<b>5.1 INTRODUCTION</b>	<b>5-1</b>
<b>5.2 METHODOLOGY</b>	<b>5-1</b>
5.2.1 Generic Methods in Use for Sandy Coasts	5-1
5.2.2 Wetlands	5-8
5.2.3 Previous Applications	5-13
5.2.4 Adopted Approaches for Sandy Coasts	5-13
5.2.5 Sea-Level-Rise Scenarios	5-14
<b>5.3 GALVESTON, TEXAS</b>	<b>5-14</b>
5.3.1 Site Description	5-14
5.3.2 Sea-Level-Rise Scenarios	5-15
5.3.3 Previous Studies	5-15
5.3.4 Results and Discussion	5-16
5.3.5 Conclusions	5-21

5. (Continued)

5.4	CAMINADA PASS, LOUISIANA . . . . .	5-23
	5.4.1 Site Description . . . . .	5-23
	5.4.2 Sea-Level-Rise Scenarios . . . . .	5-24
	5.4.3 Previous Studies . . . . .	5-24
	5.4.4 Results and Discussion . . . . .	5-28
	5.4.5 Conclusions . . . . .	5-33
5.5	BRADENTON BEACH, FLORIDA . . . . .	5-34
	5.5.1 Site Description . . . . .	5-34
	5.5.2 Sea-Level-Rise Scenarios . . . . .	5-35
	5.5.3 Previous Studies . . . . .	5-35
	5.5.4 Results and Discussion . . . . .	5-38
	5.5.5 Conclusions . . . . .	5-44
5.6	DAYTONA BEACH, FLORIDA . . . . .	5-44
	5.6.1 Site Description . . . . .	5-44
	5.6.2 Sea-Level-Rise Scenarios . . . . .	5-45
	5.6.3 Previous Studies . . . . .	5-45
	5.6.4 Results and Discussion . . . . .	5-47
	5.6.5 Conclusions . . . . .	5-51
5.7	McCLELLANVILLE, SOUTH CAROLINA . . . . .	5-51
	5.7.1 Site Description . . . . .	5-51
	5.7.2 Sea-Level-Rise Scenarios . . . . .	5-53
	5.7.3 Previous Studies . . . . .	5-53
	5.7.4 Results and Discussion . . . . .	5-55
	5.7.5 Conclusions . . . . .	5-60
5.8	NAGS HEAD, NORTH CAROLINA . . . . .	5-61
	5.8.1 Site Description . . . . .	5-61
	5.8.2 Sea-Level-Rise Scenarios . . . . .	5-63
	5.8.3 Previous Studies . . . . .	5-63
	5.8.4 Results and Discussion . . . . .	5-66
	5.8.5 Conclusions . . . . .	5-71
5.9	CONCLUDING COMMENTS . . . . .	5-72
5.10	FIGURES . . . . .	5-77

6. SUMMARY AND FINDINGS . . . . . 6-1

    6.1 SUMMARY . . . . . 6-1

    6.2 FINDINGS . . . . . 6-1

    6.3 IMPLICATIONS FOR FUTURE STUDIES . . . . . 6-3

LITERATURE CITED . . . . . 7-1

MAPS CITED . . . . . 7-14

## ACKNOWLEDGMENTS

We thank the following individuals for their time and efforts: Tammy W. White (Oak Ridge National Laboratory), for her willingness to share her comprehensive knowledge of the Coastal Hazards Data Base and for her "voluntary" review of this document; Thomas A. Chatfield (Miami University, Ohio), whose critical review of this document identified several problems and prompted numerous changes; and Kimberly K. Chapman (East Tennessee State University), who collected and assisted in analyzing the population and income data, used in Sect. 4, from U.S. Census records.

This research was sponsored by the Office of Environmental Analysis, U.S. Department of Energy. Oak Ridge National Laboratory is managed by Martin Marietta Energy Systems, Inc., for the U.S. Department of Energy under Contract DE-AC05-84OR21400. Environmental Sciences Division, publication number 3915.

## LIST OF FIGURES

<b>Figure</b>		<b>Page</b>
1.1	The U.S. Southeast Coastal Zone . . . . .	1-6
1.2	Location of the six case study areas in the U.S. Southeast . . . . .	1-7
2.1	Basic interactions between incoming solar energy and the earth . . . . .	2-12
2.2	Mean annual atmospheric concentration of carbon dioxide at the Mauna Loa Observatory, Hawaii, 1958-1990 . . . . .	2-13
2.3	Global mean temperature change: combined land, air, and sea surface temperatures, 1861-1988 relative to 1950-1979 . . . . .	2-14
2.4	Projected sea-level rise (low) . . . . .	2-15
2.5	Projected sea-level rise (intermediate) . . . . .	2-16
2.6	Projected sea-level rise (high) . . . . .	2-17
2.7	Scenarios of sea-level rise used in this study . . . . .	2-18
3.1	Histogram of the stretched CVI used in this study (values weighted by shore length in meters) . . . . .	3-18
3.2a	Map showing the distribution of low, moderate, high, and very high risk shorelines (Texas) . . . . .	3-19
3.2b	Map showing the distribution of low, moderate, high, and very high risk shorelines (Texas and Louisiana) . . . . .	3-20
3.2c	Map showing the distribution of low, moderate, high, and very high risk shorelines (Louisiana, Mississippi, Alabama, and Florida) . . . . .	3-21



<b>Figure</b>	<b>Page</b>
3.2d Map showing the distribution of low, moderate, high, and very high risk shorelines (Gulf coast of Florida) . . . . .	3-22
3.2e Map showing the distribution of low, moderate, high, and very high risk shorelines (Atlantic coast of Florida) . . . . .	3-23
3.2f Map showing the distribution of low, moderate, high, and very high risk shorelines (Florida, Georgia, and South Carolina) . . . . .	3-24
3.2g Map showing the distribution of low, moderate, high, and very high risk shorelines (South Carolina and North Carolina) . . . . .	3-25
4.1 Location of geologic basins and arches within the U.S. Southeast . . . . .	4-36
4.2 Population per square kilometer in the coastal counties of Texas, Louisiana, Mississippi, Alabama, and the Gulf coast of Florida (values after 1990 were estimated using linear regression) . . . . .	4-37
4.3 Galveston County, Texas: population and per capita income (values after 1990 were estimated using linear regression) . . . . .	4-38
4.4 Galveston study area land use map . . . . .	4-39
4.5 Application of the low sea-level-rise scenario on the Galveston study area. Coastlines shown are for the year 2050 and 2100 . . . . .	4-40
4.6 Application of the medium sea-level-rise scenario on the Galveston study area. Coastlines shown are for the year 2050 and 2100 . . . . .	4-41
4.7 Application of the high sea-level-rise scenario on the Galveston study area. Coastlines shown are for the year 2050 and 2100 . . . . .	4-42

<b>Figure</b>	<b>Page</b>
4.8 Jefferson Parish, Louisiana: population and per capita income (values after 1990 were estimated using linear regression) . . . . .	4-43
4.9 Caminada Pass study area land use map . . . . .	4-44
4.10 Application of the low sea-level-rise scenario on the Caminada Pass study area. Coastlines shown are for the year 2050 and 2100 . . . . .	4-45
4.11 Application of the medium sea-level-rise scenario on the Caminada Pass study area. Coastlines shown are for the year 2050 and 2100 . . . . .	4-46
4.12 Application of the high sea-level-rise scenario on the Caminada Pass study area. Coastlines shown are for the year 2050 and 2100 . . . . .	4-47
4.13 Manatee County, Florida: population and per capita income (values after 1990 were estimated using linear regression) . . . . .	4-48
4.14 Bradenton Beach study area land use map . . . . .	4-49
4.15 Application of the low sea-level-rise scenario on the Bradenton Beach study area. Coastlines shown are for the year 2050 and 2100 . . . . .	4-50
4.16 Application of the medium sea-level-rise scenario on the Bradenton Beach study area. Coastlines shown are for the year 2050 and 2100 . . . . .	4-51
4.17 Application of the high sea-level-rise scenario on the Bradenton Beach study area. Coastlines shown are for the year 2050 and 2100 . . . . .	4-52
4.18 Population per square kilometer in the coastal counties of North Carolina, South Carolina, Georgia, and the Atlantic coast of Florida (values after 1990 were estimated using linear regression) . . . . .	4-53

<b>Figure</b>	<b>Page</b>
4.19 Volusia County, Florida: population and per capita income (values after 1990 were estimated using linear regression) . . . . .	4-54
4.20 Daytona Beach study area land use map . . . . .	4-55
4.21 Application of the low sea-level-rise scenario on the Daytona Beach study area. Coastlines shown are for the year 2050 and 2100 . . . . .	4-56
4.22 Application of the medium sea-level-rise scenario on the Daytona Beach study area. Coastlines shown are for the year 2050 and 2100 . . . . .	4-57
4.23 Application of the high sea-level-rise scenario on the Daytona Beach study area. Coastlines shown are for the year 2050 and 2100 . . . . .	4-58
4.24 Charleston County, South Carolina: population and per capita income (values after 1990 were estimated using linear regression) . . . . .	4-59
4.25 McClellanville study area land use map . . . . .	4-60
4.26 Application of the low sea-level-rise scenario on the McClellanville study area. Coastlines shown are for the year 2050 and 2100 . . . . .	4-61
4.27 Application of the medium sea-level-rise scenario on the McClellanville study area. Coastlines shown are for the year 2050 and 2100 . . . . .	4-62
4.28 Application of the high sea-level-rise scenario on the McClellanville study area. Coastlines shown are for the year 2050 and 2100 . . . . .	4-63
4.29 Dare County, North Carolina: population and per capita income (values after 1990 were estimated using linear regression) . . . . .	4-64
4.30 Nags Head study area land use map . . . . .	4-65

<b>Figure</b>	<b>Page</b>
4.31 Application of the low sea-level-rise scenario on the Nags Head study area. Coastlines shown are for the year 2050 and 2100 . . . . .	4-66
4.32 Application of the medium sea-level-rise scenario on the Nags Head study area. Coastlines shown are for the year 2050 and 2100 . . . . .	4-67
4.33 Application of the high sea-level-rise scenario on the Nags Head study area. Coastlines shown are for the year 2050 and 2100 . . . . .	4-68
5.1 Schematic representation of the Bruun Rule (National Research Council 1987) . . . . .	5-78
5.2 Barrier island equilibrium response (Dean and Margavever 1983) . . . . .	5-79
5.3 Comparison of projected shoreline retreat, Ocean City, Maryland . . . . .	5-80
5.4 Study area, Galveston, Texas . . . . .	5-81
5.5 Offshore profiles, Galveston, Texas (based on U.S. Nautical Charts) . . . . .	5-82
5.6 Location of cross-shore transects, Galveston, Texas. . . . .	5-83
5.7 Sea-level-rise scenarios for Galveston, Texas . . . . .	5-84
5.8 Projected locations of waterline for the year 2100 at transect 1, Galveston, Texas . . . . .	5-85
5.9 Projected locations of waterline for the year 2100 at transect 2, Galveston, Texas . . . . .	5-86
5.10 Projected locations of waterline for the year 2100 at transect 3, Galveston, Texas . . . . .	5-87
5.11 Study area, Caminada Pass, Louisiana . . . . .	5-88

<b>Figure</b>	<b>Page</b>
5.12 Offshore profiles, Caminada Pass, Louisiana (based on U.S. Nautical Charts) . . . . .	5-89
5.13 Location of cross-shore transects, Caminada Pass, Louisiana . . . . .	5-90
5.14 Study area, Bradenton Beach, Florida . . . . .	5-91
5.15 Offshore profiles, Bradenton Beach, Florida . . . . .	5-92
5.16 Location of cross-shore transects, Bradenton Beach, Florida . . . . .	5-93
5.17 Beach segments referenced in Table 5.12 . . . . .	5-94
5.18 Historical shoreline positions, Bradenton Beach, Florida . . . . .	5-95
5.19 Longboat Pass bathymetry, Bradenton Beach, Florida (adapted from Harvey 1982) . . . . .	5-96
5.20 Study area, Daytona Beach, Florida . . . . .	5-97
5.21 Offshore profiles, Daytona Beach, Florida . . . . .	5-98
5.22 Location of cross-shore transects, Daytona Beach, Florida . . . . .	5-99
5.23 Regional histogram of long-term shoreline change rates, Florida (Grant 1992) . . . . .	5-100
5.24 Historical shoreline positions, Daytona Beach, Florida . . . . .	5-101
5.25 Study area, McClellanville, South Carolina . . . . .	5-102
5.26 Offshore profiles, McClellanville, South Carolina (based on U.S. Nautical Charts) . . . . .	5-103

<b>Figure</b>	<b>Page</b>
5.27 Locations of cross-shore transects, McClellanville, South Carolina . . . . .	5-104
5.28 Study area, Nags Head, North Carolina . . . . .	5-105
5.29 Offshore profiles, Nags Head, North Carolina (based on U.S. Nautical Charts) . . . . .	5-106
5.30 Locations of cross-shore transects, Nags Head, North Carolina . . . . .	5-107
5.31 Study area and plot of shoreline rate-of- change values, Cape Hatteras to Oregon Inlet, North Carolina (Dolan et al. 1991) . . . . .	5-108
5.32 Historical inlet locations from the Virginia/ North Carolina state line to Cape Hatteras (Mehta and Montague 1991) . . . . .	5-109

## LIST OF TABLES

<b>Tables</b>	<b>Page</b>
2.1 Estimates of recent rates of global sea-level rise . . . . .	2-3
2.2 Predicted contributions to future sea-level rise (cm) . . . . .	2-6
2.3 Estimates of future sea-level rise (cm) . . . . .	2-8
2.4 Sea-level-rise scenarios used in this study (cm). . . . .	2-9
3.1 Coastal risk classification scheme used in this study . . . . .	3-5
3.2 Percent of shoreline within each coastal hazard class . . . . .	3-6
3.3 Coastal Vulnerability Indices considered for use in previous coastal hazard studies (e.g., Gornitz et al. 1991) . . . . .	3-7
3.4a Sensitivity of CVI <sub>i</sub> to changes in the classification methods used for the risk variables, changing values from 5 to 1 . . . . .	3-9
3.4b Sensitivity of CVI <sub>i</sub> to missing variables . . . . .	3-9
3.5 Revised Coastal Vulnerability Indices considered for use in this study . . . . .	3-10
3.6a Sensitivity of CVI <sub>i</sub> to changes in the classification methods used for the risk variables, changing values from 5 to 1 . . . . .	3-11
3.6b Sensitivity of CVI <sub>i</sub> to missing variables . . . . .	3-12
3.7 Statistics of the CVI used in this study (values weighted by shore length) . . . . .	3-13

<b>Tables</b>	<b>Page</b>
3.8 Case study sites used for this project. Site names are equivalent to the name of the USGS 7.5-min topographic map of each area . . . . .	3-14
4.1 Raw sea-level trend and regional-weighted trend for each long-term tide-gauge station, and the number of stations within the 350-km circles contributing to the average (including center station) . . . . .	4-5
4.2 Data used to interpolate the subsidence trend for Bradenton Beach, Florida; McClellanville, South Carolina; and Nags Head, North Carolina . . . . .	4-6
4.3 Calculated subsidence rates for the six study areas. . . . .	4-6
4.4 Number of hectares within each land use category for Galveston, Texas, in 1990 . . . . .	4-9
4.5 Sea-level-rise scenarios used for Galveston, Texas. Present subsidence rate for Galveston is 4.89 mm/year . . . . .	4-10
4.6 Land above mean sea level at Galveston, Texas, based on sea-level-rise scenarios A, B, and C and current conditions (values in hectares) . . . . .	4-10
4.7 Total land in 1990 (ha) and the percentage of land still above mean sea level for each sea-level-rise scenario for the Galveston study area. . . . .	4-11
4.8 Number of hectares within each land use category for Caminada Pass, Louisiana, in 1990 . . . . .	4-13
4.9 Sea-level-rise scenarios used for Caminada Pass, Louisiana. Present subsidence rate for Caminada Pass is 7.9 mm/year . . . . .	4-14



<b>Tables</b>	<b>Page</b>
4.10 Land above mean sea level at Caminada Pass, Louisiana, based on sea-level-rise scenarios A, B, and C and current conditions (values in hectares) . . . . .	4-14
4.11 Total land in 1990 (ha) and the percentage of land still above mean sea level for each sea-level-rise scenario for the Caminada Pass study area . . . . .	4-15
4.12 Number of hectares within each land use category for Bradenton Beach, Florida, in 1987 . . . . .	4-17
4.13 Sea-level-rise scenarios used for Bradenton Beach, Florida. Present subsidence rate for Bradenton Beach is 0.23 mm/year . . . . .	4-18
4.14 Land above mean sea level at Bradenton Beach, Florida, based on sea-level-rise scenarios A, B, and C and current conditions (values in hectares) . . . . .	4-18
4.15 Total land in 1987 (ha) and the percentage of land still above mean sea level for each sea-level-rise scenario for the Bradenton Beach study area . . . . .	4-19
4.16 Number of hectares within each land use category for Daytona Beach, Florida, in 1988 . . . . .	4-22
4.17 Sea-level-rise scenarios used for Daytona Beach, Florida. Present subsidence rate for Daytona Beach is 0.513 mm/year . . . . .	4-23
4.18 Land above mean sea level at Daytona Beach, Florida, based on sea-level-rise scenarios A, B, and C and current conditions (values in hectares) . . . . .	4-23

<b>Tables</b>	<b>Page</b>
4.19 Total land in 1988 (ha) and the percentage of land still above mean sea level for each sea-level-rise scenario for the Daytona Beach study area . . . . .	4-24
4.20 Number of hectares within each land use category for McClellanville, South Carolina, in 1989 . . . . .	4-26
4.21 Sea-level-rise scenarios used for McClellanville, South Carolina. Present subsidence rate for McClellanville is 1.40 mm/year . . . . .	4-27
4.22 Land above mean sea level at McClellanville, South Carolina, based on sea-level-rise scenarios A, B, and C and current conditions (values in hectares) . . . . .	4-27
4.23 Total land in 1989 (ha) and the percentage of land still above mean sea level for each sea-level-rise scenario for the McClellanville study area . . . . .	4-28
4.24 Number of hectares within each land use category for Nags Head, North Carolina, in 1983 . . . . .	4-30
4.25 Sea-level-rise scenarios used for Nags Head, North Carolina. Present subsidence rate for Nags Head is 1.87 mm/year . . . . .	4-31
4.26 Land above mean sea level at Nags Head, North Carolina, based on sea-level-rise scenarios A, B, and C and current conditions (values in hectares) . . . . .	4-31
4.27 Total land in 1983 (ha) and the percentage of land still above mean sea level for each sea-level-rise scenario for the Nags Head study area . . . . .	4-32

<b>Tables</b>	<b>Page</b>
5.1 Rates of marsh accretion and relative sea-level rise . . . . .	5-10
5.2 Relative sea-level-rise scenarios for Ocean City, Maryland . . . . .	5-13
5.3 Predicted shoreline recession for the year 2050, Galveston, Texas . . . . .	5-19
5.4 Predicted shoreline recession for the year 2100, Galveston, Texas . . . . .	5-20
5.5 Predicted changes in shoreline position, Galveston, Texas. Reference point locations are shown in Figs. 5.8, 5.9, and 5.10 . . . . .	5-22
5.6 Revised estimates of land area lost (ha) for Galveston, Texas . . . . .	5-22
5.7 Barrier shoreline change statistics, Caminada Pass, Louisiana . . . . .	5-26
5.8 Input values used in the various approaches, Caminada Pass, Louisiana . . . . .	5-30
5.9 Comparison of projected shoreline retreat for the year 2050, Caminada Pass, Louisiana . . . . .	5-30
5.10 Comparison of projected shoreline retreat for the year 2100, Caminada Pass, Louisiana . . . . .	5-31
5.11 Projected shoreline retreat based on the Modified Brunn Rule, Caminada Pass, Louisiana . . . . .	5-32
5.12 Trends in shoreline change, North Longboat Key, Florida. Beach segment numbers refer to Fig. 5.17 . . . . .	5-37
5.13 Comparison of projected shoreline retreat for the year 2050, Bradenton Beach, Florida . . . . .	5-41

<b>Tables</b>	<b>Page</b>
5.14 Comparison of projected shoreline retreat for the year 2100, Bradenton Beach, Florida . . . . .	5-42
5.15 Comparison of projected shoreline retreat for the year 2050, Daytona Beach, Florida . . . . .	5-49
5.16 Comparison of projected shoreline retreat for the year 2100, Daytona Beach, Florida . . . . .	5-50
5.17 Comparison of projected shoreline retreats for McClellanville, South Carolina . . . . .	5-56
5.18 Annual net accretion deficits of wetlands, McClellanville, South Carolina . . . . .	5-58
5.19 Revised estimates of land area lost (ha), McClellanville, South Carolina . . . . .	5-60
5.20 Projected ratios of R/S based on the Double Bruun Rule, Nags Head, North Carolina . . . . .	5-67
5.21 Projected shoreline retreat along the seaward margin for the year 2050, Nags Head, North Carolina . . . . .	5-68
5.22 Projected shoreline retreat along the seaward margin for the year 2100, Nags Head, North Carolina . . . . .	5-69
5.23 Predicted changes in shoreline position, Nags Head, North Carolina. Reference point locations are shown in Fig. 5.30 . . . . .	5-70
5.24 Revised estimates of land area lost (ha), Nags Head, North Carolina . . . . .	5-71
5.25 Physical characterization of the study areas . . . . .	5-73
5.26 Predicted land loss, in percent, and the relative influences of biophysical factors and built infrastructure on inundation . . . . .	5-74

## ABSTRACT

DANIELS, R.C., GORNITZ, V.M., MEHTA, A.J., LEE, S.-C., and R.M. CUSHMAN. 1992. Adapting to Sea-Level Rise in the U.S. Southeast: The Influence of Built Infrastructure and Biophysical Factors on the Inundation of Coastal Areas. ORNL/CDIAC-54. Oak Ridge National Laboratory, Oak Ridge, Tennessee. 274 pp.

The earth's global mean surface air temperature has increased by 0.5°C over the past 100 years. This warming trend has occurred concurrently with increases in the concentration and number of greenhouse gases in the atmosphere (e.g., CO<sub>2</sub>, N<sub>2</sub>O, H<sub>2</sub>O, CH<sub>4</sub>, and CFCs). These gases may be partially responsible for this temperature increase and may cause this trend to accelerate in the future due to the increased amount of thermal radiation that will be trapped in the troposphere by these gases. This trapping effect may result in a net increase in the earth's global mean surface air temperature of 1.5 to 4.5°C by the year 2100. An increase in the mean surface air temperature of this magnitude could cause significant changes in the intensity and frequency of storms, and will cause sea surface temperatures to increase. This increase in sea surface temperature will cause sea levels to rise—from thermal expansion of the sea, and the addition of melt waters from alpine glaciers and continental ice sheets.

To allow for the cost-effective analysis of the impacts that sea-level rise may have on the U.S. Southeast, a method is needed that will allow sites that are potentially at risk to be identified for study. Previously, no objective method was available to identify such sites. This project addresses this problem by using a geographic data base with information on both physical and climatological factors to identify coastal areas of the U.S. Southeast that are at risk to inundation or accelerated erosion due to sea-level rise. The following six areas were selected for further study from the many identified as being at high risk: Galveston, Texas; Caminada Pass, Louisiana; Bradenton Beach, Florida; Daytona Beach, Florida; McClellanville, South Carolina; and Nags Head, North Carolina. These six areas are representative of three of the major stages of economic development on the East and Gulf coasts (i.e., urban/residential, undeveloped/rural, resort/recreational), and as such, any conclusions drawn from these case studies may be generalized to other high risk regions with similar geologic and economic histories.

For each study area the amount of land, by land use type, in danger from inundation from three sea-level-rise scenarios was calculated. The calculated values were based on elevation alone. These studies were then extended by considering the effects that built infrastructure (e.g., seawalls) and biophysical factors (e.g., erosion/accretion rates) would have on the actual amount of land that would be inundated if the sea was allowed to advance unchecked. By considering these factors, a best-guess estimation of the amount of land that may be lost to the sea was derived for each study area and each scenario. These estimated values consider both natural (e.g., elevation and erosion/accretion) and anthropogenic (e.g., built infrastructure) effects when predicting the future location of the coastline in the years 2050 and 2100 for each study area, for each scenario.

# IMPACTS OF SEA-LEVEL RISE

## 1.1 INTRODUCTION

Rising sea levels from global warming and coastal storms threaten areas in many parts of the world with erosion, inundation, and temporary flooding. The southeastern United States, however, appears to be one of our nation's most vulnerable regions. The southeast United States, as defined in this report, comprises the coastal counties or parishes of North Carolina, South Carolina, Georgia, Florida, Alabama, Mississippi, Louisiana, and Texas (Fig. 1.1). This region contains more than 50% of the nation's barrier islands and 85% of the nation's coastal wetlands. The area is subject to 84% of the tropical cyclone direct hits and 83% of the major hurricane hits that affect the United States [i.e., major hurricanes have sustained winds of 178 km (111 miles) per hour or greater] (Smith and Titus 1990; Neumann et al. 1987).

The vulnerability of the U.S. Southeast to sea-level rise (SLR) has been demonstrated by a number of case studies, papers, and reports (e.g., Titus 1991; Smith and Tirpak 1989). These studies demonstrated the extent to which the barrier islands and wetlands within this region may be at risk to climate change. For example, if a relative SLR of 1 m occurs by the year 2100, 30 to 90% of the coastal wetlands within the region and an additional 6,700 to 11,800 km<sup>2</sup> of dry land, depending on the extent to which coastal protection structures are erected in response to SLR, would be inundated (Smith and Tirpak 1989).

A common shortcoming of many of the regional and site-specific studies that have examined the potential impacts of SLR is that the loss of land (and the associated economic costs) have been estimated on the basis of elevation alone. Few site-specific case studies have examined the potential effects that long-term erosion/accretion trends, offshore sediment sources, and site geology may have on the amount of land that will be lost to a given rise in sea level. Furthermore, in most of these studies the regions examined were subjectively selected and no rigorous method was used to identify the areas at greatest risk. Other limitations of these early studies are that the role of society as a limiting factor to SLR induced erosion was not considered, and infrastructure (e.g., roads) and land uses (e.g., residential), have not been analyzed in regard to the role they could play in interfering with the inland advance of the sea.

Various options have been proposed as possible responses to the threat that rising sea levels pose (Titus 1990). Chief among these are (1) hardening and protecting the current shoreline (i.e., with seawalls, dikes, beach nourishment) for the entire coast, (2) protecting heavily populated areas only, and (3) abandoning the current coastline and retreating inland. The third option has been suggested as being especially appropriate when the level of investment in built infrastructure does not warrant massive expenditures for more active measures, such as the construction of erosion-control structures or the design and erection of water-exclusion devices (e.g., dikes and seawalls).

## **1.2 GOALS OF THIS STUDY**

A need exists for an evaluation to be made of the impacts that rising sea levels may have on the U.S. Southeast. To fulfill this need in the U.S. Southeast this project undertook the following tasks: (1) the objective identification of high risk coastal areas based on land characteristics (geology, geomorphology, elevation) and marine and climate characteristics (waves, tides, storm frequencies, and storm intensities); (2) the analysis of SLR in terms of its effects on coastal land uses; and (3) the identification of built infrastructure (e.g., seawalls) and biophysical factors (e.g., sediment transport and vertical accretion rates of wetlands) that could interfere with, or mitigate the effects of SLR.

This project identified the coastal areas of the U.S. Southeast that are at high risk to inundation or accelerated erosion due to SLR. From the areas identified as high risk, three areas were selected from each coast for further study. Each of the selected study areas, on the East and Gulf coast, is representative of one of the following stages of economic development: undeveloped/rural, resort/recreational, or urban/residential. Thus, each coast has one study area at each stage of economic development (Fig. 1.2).

## **1.3 STRUCTURE OF THE ANALYSIS**

To determine the differential vulnerability of the U.S. Southeast to future SLR from global climate change, detailed SLR scenarios were needed. These scenarios were based on assumptions of how climate will change in response to increases in the concentration of greenhouse gases within the troposphere. The background assumptions related to the greenhouse effect, used in this report, along with a detailed discussion of the SLR scenarios used in this study are described in Sect. 2.

Before the SLR scenarios could be applied to the study areas, the study areas had to be selected. To do this, a geographic/climatologic data base was used in conjunction with a geographic information system (GIS) to estimate the relative vulnerability of the U.S. Southeast to erosion and inundation from SLR. The data base integrated climatological data from Birdwell and Daniels (1991) with portions of the Global Coastal Hazards Data Base (Gornitz et al. 1991). The composite data base was then used to identify and map the coastal areas of the U.S. Southeast that are at risk to erosion or inundation from increases in the world's mean sea level (Sect. 3).

The six study areas were selected from the high-risk coastal areas identified in Sect. 3. The study areas are distributed more or less equally along each coast, and each area is representative of an undeveloped/rural, resort/recreational, or urban/residential area. These case studies consider the amount of land, by land use type, that will be lost as a result of a gradual rise in sea level to the year 2100. The individual case studies for the East and Gulf coasts are in Sect. 4.

After projecting the amount of land that may be lost to the sea, on the basis of elevation alone, the projections obtained in Sect. 4 were compared to those obtained from transects that were constructed in each study area. These transects were used to compare the predicted amount of coastline inundation (based on elevation) with that predicted when

biophysical factors (e.g., erosion/accretion rates) and the presence of built infrastructure (e.g., seawalls) are considered. These transects consider the effects that offshore and nearshore sediment transport mechanisms will have on each study area, and allow a clearer picture to be obtained as to how a given coastline will respond to SLR (Sect. 5).

The six study areas examined within this report were identified using the risk maps constructed in Sect. 3. Each study area was selected to insure it contained land uses that were representative of those found throughout the U.S. Southeast. Thus, results obtained for each study area may be generalized and applied to similar areas within the region. The findings, generalizations, and suggestions for further research derived from these case studies are contained in Sect. 6.



## **1.4 FIGURES**

Fig. 1.1 The U.S. Southeast Coastal Zone.

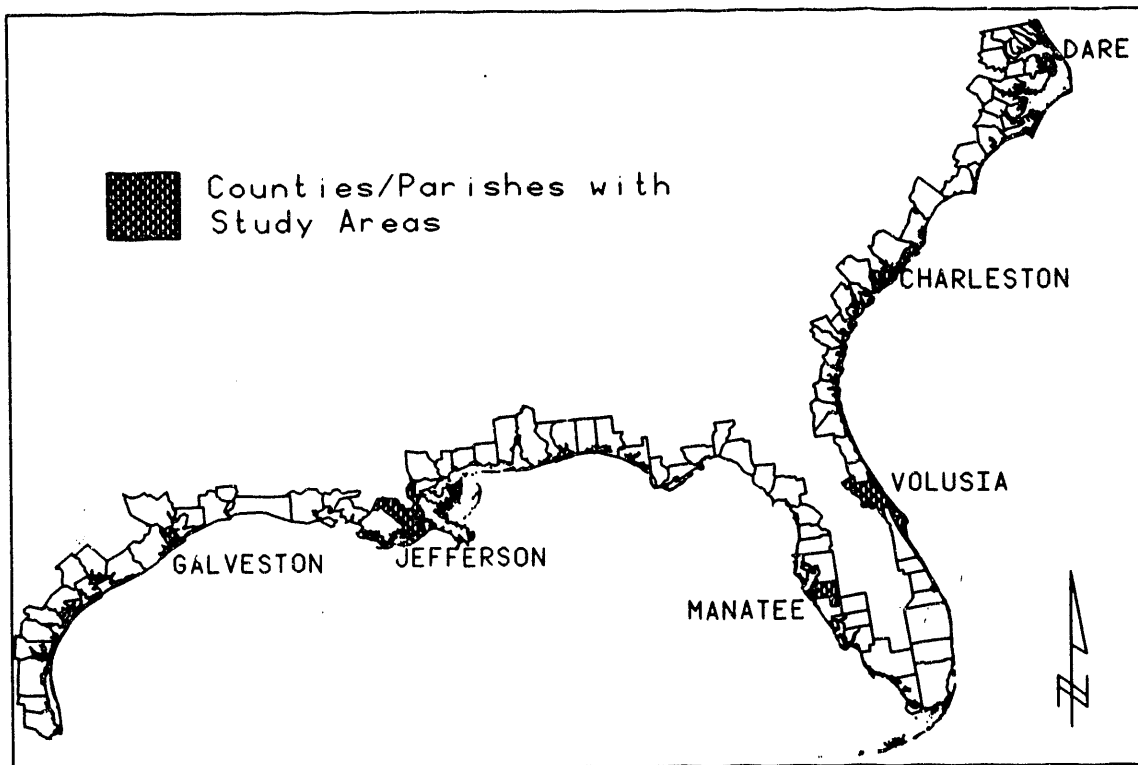
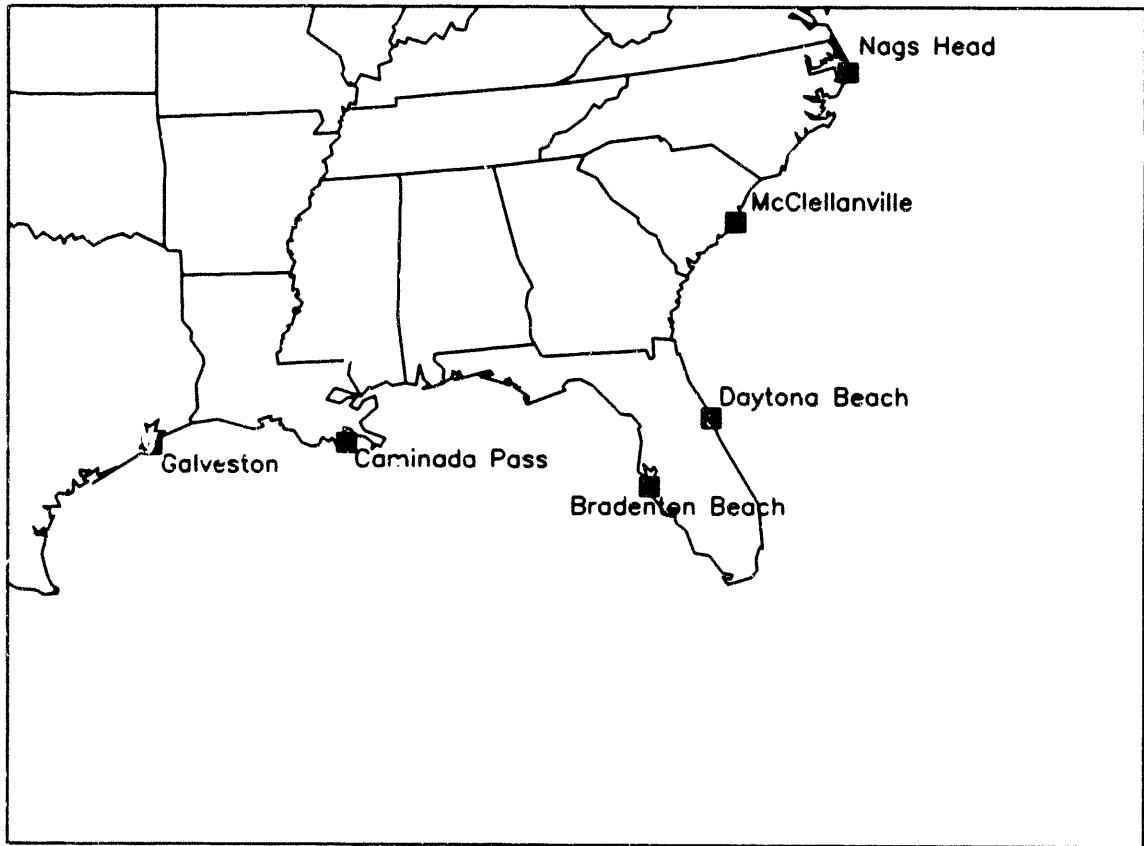


**Fig. 1.2**      **Location of the six case study areas in the U.S. Southeast.**



# GLOBAL CLIMATE CHANGE

## 2.1 GREENHOUSE EFFECT

The earth's surface temperature depends on the amount of incoming shortwave radiation from the sun, the earth's albedo (i.e., ratio of reflected to incident radiant energy), the amount of incident radiation absorbed at the surface, and the amount of energy radiated from the earth. Because the earth's surface temperature has achieved a state of equilibrium, we may assume that the energy gained at the earth's surface must equal the energy lost. The earth has accomplished this state of dynamic equilibrium by radiating the energy absorbed from the sun back into space as long-wave radiation (i.e., heat) as shown in Fig. 2.1 (Blatt 1983). The global mean surface air temperature of the earth, 15°C, is greater than expected, if these are the only factors at work, however (Ramanathan 1987).

The variation between predicted and measured global surface air temperatures is related to the presence of gases such as carbon dioxide (CO<sub>2</sub>), methane (CH<sub>4</sub>), nitrous oxide (N<sub>2</sub>O), and water vapor (H<sub>2</sub>O) within the atmosphere. These "greenhouse gases" are transparent to shortwave radiation, but absorb long-wave radiation radiating back from the earth's surface. This absorption reduces the amount of energy that is lost to space and results in a net warming of the earth's troposphere. To maintain the earth's energy equilibrium a corresponding cooling of the stratosphere also occurs.

The concentration of these "greenhouse gases" within the atmosphere affects the amount of outgoing radiation that will be absorbed. Thus, assuming that the amount of incoming radiation to the earth is constant, as the number and concentration of the greenhouse gases present in the atmosphere increase, the global mean surface air temperature should also increase. In 1938 G.S. Callendar modeled this process and determined that humans have added more than 150 billion tons of CO<sub>2</sub> into the atmosphere and that this increase in CO<sub>2</sub> had the potential to alter climate.

Callendar's study (along with others) sparked interest in the possible effects of CO<sub>2</sub> on the world's global mean surface air temperature. Efforts began after World War II to obtain long-term measurements of atmospheric CO<sub>2</sub> concentrations. The best known of these records is the Mauna Loa Observatory monitoring program in Hawaii. This program was initiated by Dr. David Keeling, Scripps Institute of Oceanography, in 1958. Since measurements began, the concentration of CO<sub>2</sub> has increased by 10%, at a rate >0.4%/year. A graph of this data is shown in Fig. 2.2 (Keeling and Whorf 1991).

The rapid increase in the concentration and number of greenhouse gases in the atmosphere that has occurred since the 1800s may have committed the earth to a long-term warming trend (Houghton and Woodwell 1989). This increase in the concentration of CO<sub>2</sub>, CH<sub>4</sub>, N<sub>2</sub>O, and H<sub>2</sub>O [along with the addition of anthropogenic gases such as chlorofluorocarbons and volatile organic compounds] into the atmosphere has increased the percentage of outgoing long-wave radiation (heat) that is being trapped in the troposphere. To study the long-term effects of this buildup of CO<sub>2</sub> (and other gases) in the atmosphere, modelers have developed several comprehensive general circulation models. These models simulate the complex relationships among the ocean, land, and atmosphere in order to

analyze global climate. The consequences of varying the concentration of greenhouse gases in the atmosphere may be determined using these models. Such models have predicted a global warming trend on the order of 1.5 to 4.5°C when the CO<sub>2</sub> within the models "atmosphere" is doubled (it has been predicted that this will occur on our "real" Earth before the year 2100) (Schneider 1989). An increase in the global mean surface air temperature of this magnitude will have severe repercussions, such as initiating rapid increases in sea surface temperatures, possibly causing variations in tropical storm intensities and precipitation patterns, and causing a rise in the world's sea level (Emanuel 1987; Houghton and Woodwell 1989).

## 2.2 PAST EVIDENCE OF CLIMATE CHANGE

The climate record since the late 19th century provides persuasive indications of a long-term global warming; these indications have been derived from instrumental measurements, historic retreats of alpine glaciers, and other high-latitude temperature proxies. On the other hand, globally coherent precipitation trends over this period are more difficult to discern. Current records of sea ice and snow cover are too short and variable to detect long-term trends with any certainty. Therefore, the following brief summary will focus mainly on the evidence for temperature change.

The increase in global mean temperature over the period 1861 to 1989 for combined data sets of land surface and sea surface temperatures is shown in Fig. 2.3 (Jones et al. 1990). Global temperature has risen by 0.5°C, on average, between 1881 and 1988. Temperatures worldwide have increased more rapidly during the 1920s and 1930s, and also in the 1980s, whereas the period between 1940 and 1970 remained relatively stable (the northern hemisphere, and especially the high-latitude North Atlantic, experienced a sharp temperature drop during these decades; this drop is absent from the southern hemisphere data). Trends of temperature increases have been more pronounced in the nighttime records, even after urban heat-island biases have been accounted for.

There are, however, a number of limitations in the quantity and quality of the available historical temperature data. The extent of global coverage has also increased systematically over time (Jones et al. 1990). Nevertheless, long-term trends calculated from data grids using the areal coverage present in 1861 to 1870, 1901 to 1910, and 1921 to 1930 all show similar values. Potential problems with the data sets commonly used in these temperature analyses include changes in instrumentation and data collection techniques over time, and the effects of urban heating, which have been estimated at 0.1°C/100 years (Hansen and Lebedeff 1987; Jones et al. 1989).

Other evidence suggesting that a recent global warming trend has occurred comes from the worldwide recession of alpine glaciers, boreal forest tree-ring analysis, documented vegetation changes, and near-surface warming of permafrost within the Arctic Circle—detected in bore holes dug by research drilling platforms. However, evidence for changes in the polar ice sheet mass balance budget is more uncertain, and no consistent trend can be inferred at this time.

Alpine glaciers, because of their limited spatial extent, are more sensitive to minor

climate fluctuations. Glacier retreat since the late 19th century has been recorded from widespread mountain localities, such as the Alps, Alaska, the Canadian Rockies, the Andes, and the Himalayas (Grove 1988). Because ice-flow dynamics and local climate affect the behavior of individual glaciers, such a consistent worldwide pattern suggests a common cause, such as a global temperature increase.

According to climate models, the magnitude of greenhouse warming is expected to be amplified at higher latitudes. As a corollary, these warming trends should be detectable earlier at high latitudes. Reconstructed temperatures derived from boreal tree-ring data indicate a prolonged warming since 1840 (Jacoby and D'Arrigo 1989). Historical evidence has also been documented for a significant northward shift in the boreal forest/tundra boundary in Canada (Ball 1986). Finally, analysis of thermal profiles in bore holes drilled in Alaskan permafrost (Lachenbruch and Marshall 1986) and in unfrozen soils in eastern Canada (Beltrami and Mareschal 1991), and elsewhere, suggest that a surface warming of several degrees has occurred within the past 100 years.

### 2.3 SEA-LEVEL TRENDS

Global sea level is sensitive to long-term variations in climate. Global warming contributes to a long-term sea-level rise (SLR) through oceanic thermal expansion (Wigley and Raper 1987; Church et al. 1991), and through the addition of water into the oceans by the melting of mountain glaciers and polar ice sheets (Meier 1984). Sixteen separate studies have examined global mean SLR over the past 100 years using tide-gauge data, largely derived from the Permanent Service for Mean Sea Level, Bidston Observatory, England (Pugh et al. 1987). These studies have found rates of mean SLR ranging between 0.5 and 3 mm/year. The most likely value of the eustatic SLR lies between 1.0 and 2.0 mm/year (Table 2.1).

**Table 2.1** Estimates of recent rates of global sea-level rise

Rate (mm/year)	Comments	References
> 0.50	Cryologic estimate	Thorarinsson (1940)
1.10 ± 0.80	Many stations, 1807-1939	Gutenberg (1941)
1.20 to 1.40	Combined methods	Kuenen (1950)
1.10 ± 0.40	Six stations, 1807-1943	Lisitzin (1958, in Lisitzin 1974)

**Table 2.1 (Continued)**

Rate (mm/year)	Comments	References
1.20	Selected stations, 1900-1950	Fairbridge and Krebs (1962)
3.00	Many stations, 1935-1975	Emery (1980)
$1.20 \pm 0.10^a$	193 stations, 14 regions, 1880-1980	Gornitz et al. (1982)
1.50	Many stations, 1900-1975	Klige (1982)
$1.50 \pm 0.15^a$	Selected stations, 1903-1969	Barnett (1983)
$1.40 \pm 0.14^a$	Many stations, regions, 1881-1980	Barnett (1984)
$1.20 \pm 0.30^a$	130 stations, 1880-1980	Gornitz and Lebedeff (1987) <sup>d</sup>
$1.00 \pm 0.10^a$	130 stations, 11 regions, 1880-1980	Gornitz and Lebedeff (1987) <sup>d</sup>
1.15	155 stations, 1880-1986	Barnett (1988)
$2.40 \pm 0.90^b$	40 stations, 1920-1970	Peltier and Tushingham (1989; 1991) <sup>c</sup>
$1.75 \pm 0.13^b$	84 stations, 1900-1986	Trupin and Wahr (1990) <sup>c</sup>
$1.67 \pm 0.33$	69 stations, 1900-1986	Wahr and Trupin (1990) <sup>c</sup>
$1.80 \pm 0.10^c$	21 stations, 1880-1980	Douglas (1991) <sup>c</sup>

<sup>a</sup> = Values plus 95% confidence interval

<sup>b</sup> = Mean and std. deviation

<sup>c</sup> = Standard error

<sup>d</sup> = Long-term crustal motions removed

<sup>e</sup> = Glacio and hydro-isostatic effects removed

Source: Warrick and Oerlemans 1990.

Numerous factors affect measured sea-level change on local and even global scales. Tide gauges record alterations in sea levels due to variations in atmospheric pressure, wind, ocean currents, long-period tides, river runoff, and vertical land movements (including such effects as glacio-isostasy, neotectonism, and sediment compaction). A major source of error within the tide-gauge records is from the contamination of the data by crustal motions. In the future this inherent ambiguity between land and ocean-level changes, as seen in the tide-gauge record, will probably be resolved through satellite geodesy, but at present the tide gauge data, flawed as they may be, are the only available long-term sea-level record.

Several approaches have been adopted to minimize the effects of crustal motions when calculating eustatic sea levels. One is to select a limited number of stations, with relatively long, complete records, that are assumed to be representative of wider areas, from tectonically stable areas of the world (Fairbridge and Krebs 1962; Barnett 1983; Table 2.1). Another is to average a broader geographic distribution of records, again avoiding areas of known glacial rebound and tectonic activity, so that the net contribution of residual land movements reduces to zero (Barnett 1984; 1988). Long-wavelength crustal motions may also be filtered out by the use of late Holocene paleosealevel indicators (Gornitz et al. 1982; Gornitz and Lebedeff 1987). More recently, elevation changes caused by ice melting and water loading, as determined from glacial rebound models, have been subtracted from tide-gauge data (Peltier and Tushingham 1989; Trupin and Wahr 1990; Douglas 1991; Table 2.1). The glacial rebound models are calibrated by reference to the Holocene sea-level record. Thus the newer studies, shown in Table 2.1, differ in their selection of stations and averaging methods but often use the same basic geophysical model.

The algebraic mean for the sea-level rates shown in Table 2.1 is 1.4 mm/year. The mean was then recalculated excluding Thorarinsson (1940), as his study did not provide a "mostly likely" rate of global SLR. When this was done, a mean sea-level rate of 1.5 mm/year was obtained. This value (i.e., 1.5 mm/year) is in line with the values calculated by recent studies, and will be used throughout this investigation as the base line eustatic trend.

## **2.4 SEA-LEVEL-RISE SCENARIOS**

SLR from global warming will come from the following four major sources:

1. thermal expansion of the oceans;
2. melting of mountain (alpine) glaciers and small ice caps;
3. enhanced melting of the Greenland ice sheet; and
4. enhanced melting of the Antarctic ice sheet, including the potential destruction of the West Antarctic Ice Sheet (WAIS).

The contribution of these four sources to future SLR have been estimated, and are summarized in Table 2.2. The Environmental Protection Agencies (EPA) projections (Hoffman et al. 1983) assumed a global warming of 1.5° to 4.5°C by the year 2100 in a doubled CO<sub>2</sub> world. This warming was predicted on the basis of a world energy model that



projected growth rates of greenhouse gases, and ocean thermal expansion, using a simple box diffusion model (after A. Lacis, Goddard Institute for Space Studies), with thermal diffusion coefficients of 1.18 to 1.9 cm<sup>2</sup>/sec. The future contributions of mountain and polar ice melt were computed, using 1:1 and 2:1 ratios of ice melt to thermal expansion, based on historical rates of SLR (after Gornitz et al. 1982). Subsequently, Hoffman et al. (1986) revised the EPA projections. Nevertheless, their upper limits remained high, mainly because of assumptions of massive increases in iceberg calving in Antarctica, which could cause a SLR of +2 m by the year 2100.

**Table 2.2 Predicted contributions to future sea-level rise (cm)**

Study	Thermal expansion	Alpine glaciers	Greenland	Antarctica	Total	Year
Hoffman et al. (1983)	28-115	-	-	-	56-345 <sup>a</sup>	2100
"most likely"	72.2	-	-	-	144-217 <sup>a</sup>	2100
Hoffman et al. (1986)	28-83	12-37	6-27	12-220	58-367	2100
Thomas (1986)	35-48	12-42	13-34	20-80	80-204	2100
"most likely"	-	20	-	20	110	2100
Oerlemans (1989)	39	26	15	-15	65	2100
Meier (1990)	20 ± 10	16 ± 14	8 ± 12	-30 ± 20	34 ± 42 <sup>b</sup>	2050
IPCC (1990)						
"Business-as-usual"	6.8-14.9	2.3-10.3	0.5-37.0	0-0.8	8.7-28.9	2030
"Best estimate"	10.1	7.0	1.8	-0.6	18.3	2030

<sup>a</sup> = Includes 1 to 2 times contribution from glaciers and ice sheets.

<sup>b</sup> = Includes 20 ± 30 cm from groundwater pumping.

Thomas (1986), however, considered such increased calving rates in Antarctica unlikely in the absence of greater temperature increases than predicted by most climate models. Although Thomas used values of thermal expansion similar to those of Hoffman et al. (1986), he assumed that an increased discharge by ice streams into the ice shelves would replace much of the ice lost by enhanced melting. On the basis of these findings he predicted an Antarctic sea-level contribution between 20 and 80 cm by 2100, with the lower value being considered more probable. He modified the SLR contribution from the melting of mountain glaciers after Meier (1984), but to a different temperature scenario, which

generated an increase in sea level of 12 to 42 cm by 2100. Finally, he modeled the Greenland ice-sheet response to climate warming, yielding an SLR of between 13 and 34 cm (Table 2.2).

Because of the large uncertainties in future SLR, the National Research Council (NRC) (1987) adopted a set of three SLR scenarios, ranging between 0.5 to 1.5 m, for the year 2100, based on the NRC's assessment of the most likely impacts from the continuing increase in greenhouse gas emissions. They provided a simple parabolic-curve-fitting equation, assuming a past eustatic trend of 1.2 mm/year, with adjustments for local subsidence factors.

Oerlemans (1989) simulated the response of alpine glaciers to a temperature increase of +4°C and determined that melting of these glaciers could cause a SLR of +26 cm by 2100 (Table 2.2). This increase in sea level was then added to that expected to occur from the thermal expansion of the world's oceans (i.e., +39 cm), estimated from a simple diffusion model. Predicted increases in snow accumulation in Antarctica nearly compensates for any enhanced ice melting and/or calving that may occur on both the Greenland and Antarctic ice sheets due to global warming. Thus a rapid disintegration of the West Antarctic Ice Sheet is not considered very likely in the near future, given realistic ice-shelf thinning rates. In summary, Oerlemans' results suggest that in the next 110 years the contributions from glaciers and thermal expansion will be roughly comparable, whereas the contributions from Antarctica and Greenland will be negligible, leading to an expected rise in sea level of 65 cm by the year 2100.

The Intergovernmental Panel on Climate Change (IPCC) report (Warrick and Oerlemans 1990) considered three values of climate sensitivity (i.e., 1.5°, 2.5° and 4.5°C) for a doubling of CO<sub>2</sub>, or a radiatively equivalent mix of greenhouse gases, for four energy-growth scenarios: "business-as-usual" (B.A.U.) with no projected curbs on greenhouse gas emissions, except for CFCs, and three others (B through D), with increasing reductions of fossil fuel emissions (Houghton et al. 1990). Thermal expansion was calculated from the upwelling-diffusion model of Wigley and Raper (1987), with a thermal diffusivity of 0.63 cm<sup>2</sup>/sec. The response of mountain glaciers to warming was modeled, using a global glacier melt model with three prescribed parameters, derived from estimated rates of glacier volume loss over the past 100 years. Changes in the Greenland and Antarctic ice sheets were estimated, using sensitivity values (of equivalent SLR per °C warming), on the basis of mass and energy balance studies. In the IPCC study, as in that of Oerlemans (1989), increased snow accumulation on Antarctica outweighs any enhanced ice calving (ablation is negligible), so the net contribution to future SLR is negative. Although the relative proportions of the contributing processes differ somewhat, the total predicted SLR in both the IPCC B.A.U. "best estimate" and Oerlemans (1989) are fairly similar (Table 2.3).

The approach taken for this study is analogous to that of the NRC (1987); namely, a set of three SLR scenarios were developed (low, moderate, and high) based on a review of currently available studies, including the IPCC scenarios.

**Table 2.3 Estimates of future sea-level rise (cm)**

Study	2000	2025	Low					
			2030	2050	2070	2075	2085	2100
Hoffman et al. (1986)	3.5	10.0		20.0		36.0	44.0	57.0
NRC (1987)	2.4	9.3		19.6		33.5		50.8
IPCC (1990) Business-as-usual			8.0		21.0			31.0
Wigley and Raper (1992) IPCC'92 best-guess			4.0		9.5			15.0
Study	2000	2025	Moderate					
			2030	2050	2070	2075	2085	2100
Oerlemans (1989)	6.2	20.5		33.0		50.5		65.6
Meier (1990)				34.0				
Wigley, in Commonwealth Secretariat Report (1989)			17-26		24-38			
IPCC (1990) Business-as-usual			18.0		44.0			66.0
Wigley and Raper (1992) IPCC'92 best-guess			13.0		31.0			48.0
Study	2000	2025	High					
			2030	2050	2070	2075	2085	2100
Thomas (1986)	3.0	20.0		50.0		83.0	95.0	110.0
NRC (1987)	4.2	21.6		52.2		95.9		153.0
IPCC (1990) Business-as-usual			29.0		71.0			110.0
Wigley and Raper (1992) IPCC'92 best-guess			26.0		59.0			90.0

*Note: The IPCC'92 best-guess scenarios were published after the sea-level-rise scenarios used in this report were developed.*

Projections of future SLR have been sorted into low, moderate, and high groups (Table 2.3, Figs. 2.4, 2.5, and 2.6). The IPCC scenarios B, C, and D are not considered further, because at this stage there is no indication that any drastic changes in energy utilization patterns will occur in the near future. Furthermore, the "best estimates" of the B, C, and D scenarios overlap that of the B.A.U. low scenario. The IPCC B.A.U. low estimate is only slightly higher than that derived by linear extrapolation of current trends (Fig. 2.4). The sea-level curves for the Hoffman et al. (1986) low estimate and NRC (1987) low range (0.5 m SLR), while higher than that of the IPCC B.A.U. low, are similar to each other. However, because both of these "low" SLR curves lie fairly close to the intermediate group of curves (Fig. 2.5), the IPCC B.A.U. low curve may be more representative of the lower range of likely SLR.

Sea-level curves in the intermediate range are in close agreement (Fig. 2.5). Thus, either the IPCC (1990) B.A.U. best estimate, or Oerlemans (1989) curves could be used. Therefore, the moderate SLR scenario will use a composite of the two.

As discussed above, the NRC (1987) high scenario of +1.5 m by 2100 is probably too high, although it was based, at the time, on a conservative view of the upper range of SLR. At any rate, all three curves are quite close until 2050. The NRC curve diverges significantly from the IPCC and Thomas (1986) scenarios after that. Both the Thomas (1986) best estimate and IPCC (1990) B.A.U. high curves remain fairly close until 2100 (Fig. 2.5). Therefore, as in the case of the moderate scenario, a composite of these two scenarios will be made. The SLR scenarios use in this study are shown in Table 2.4, and Fig. 2.7.

**Table 2.4 Sea-level-rise scenarios used in this study (cm)**

Scenario	Year				
	2000	2025	2050	2075	2100*
A. Low scenario:	2	6.5	14	22	31
B. Moderate scenario:	5	17	32	48	66
C. High scenario:	8	27	50	78	110

\*Scenario values for 2100 are identical to the IPCC (1990) Business-as-Usual scenarios.

## **2.5 FIGURES**

Fig. 2.1 Basic interactions between incoming solar energy and the earth.

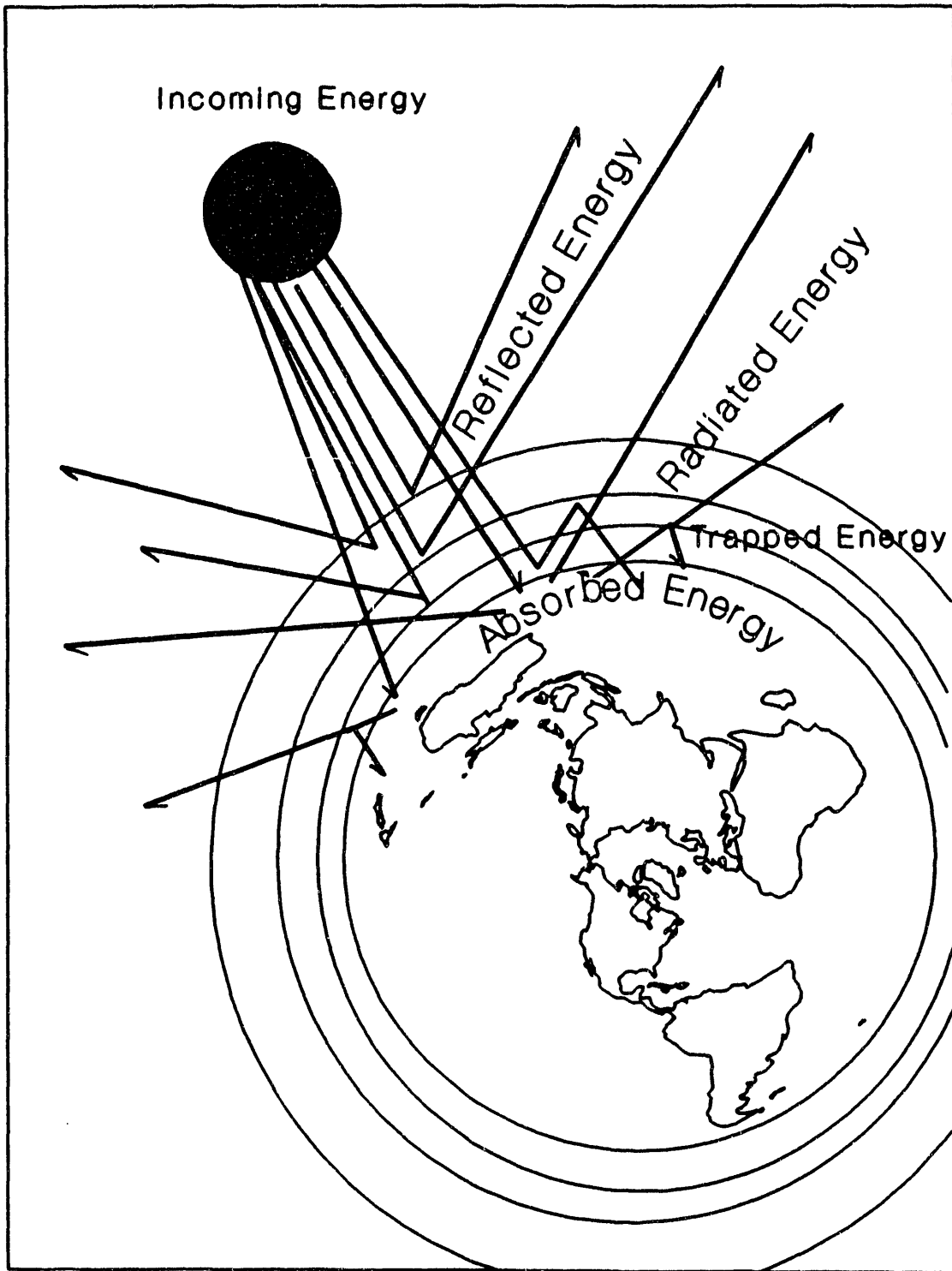


**Fig. 2.2** Mean annual atmospheric concentration of carbon dioxide at the Mauna Loa Observatory, Hawaii, 1958-1990.

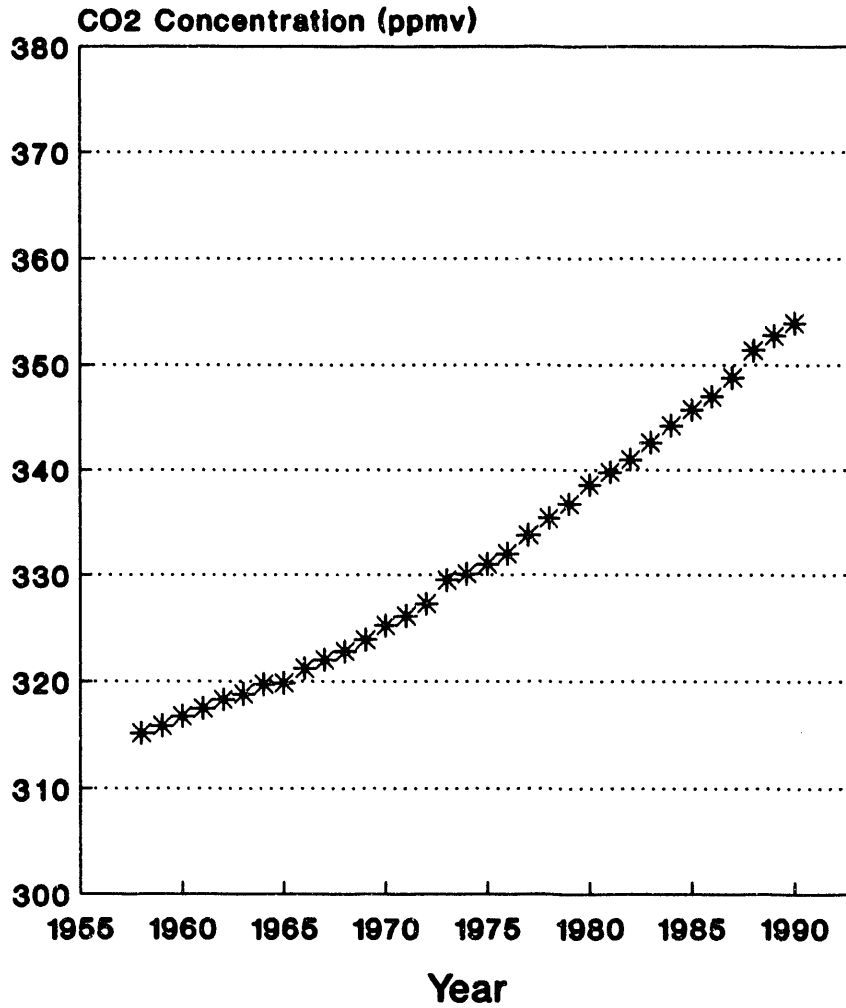


**Fig. 2.3** Global mean temperature change: combined land, air, and sea surface temperatures, 1861-1988 relative to 1950-1979.

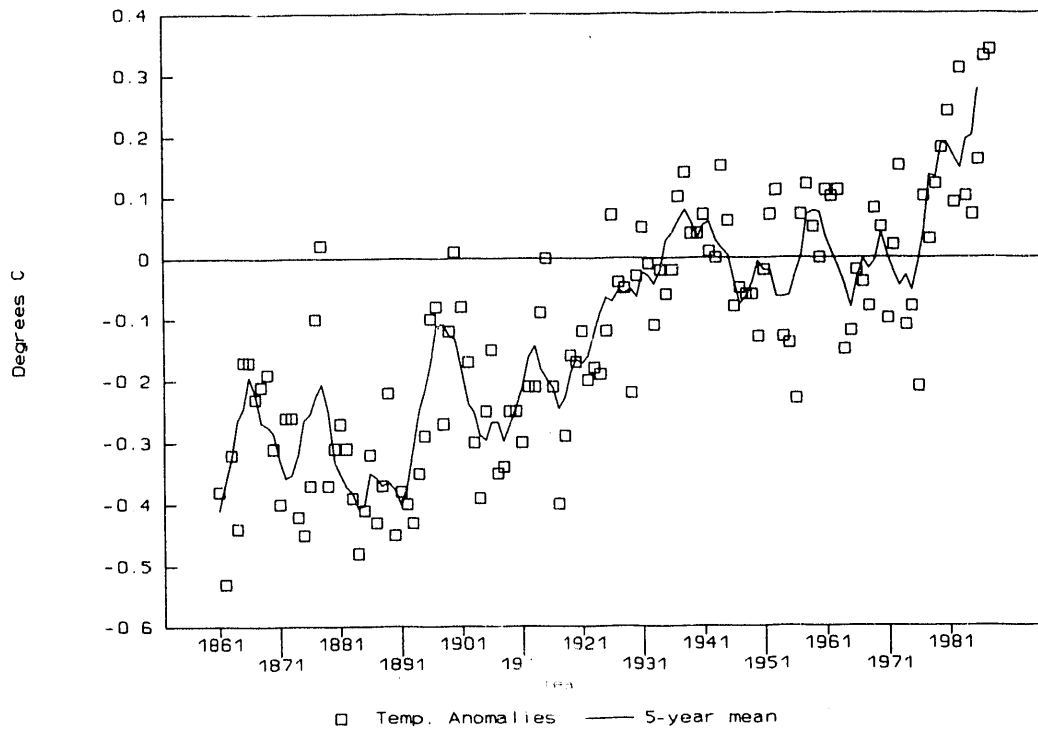




Fig. 2.4 Projected sea-level rise (low).

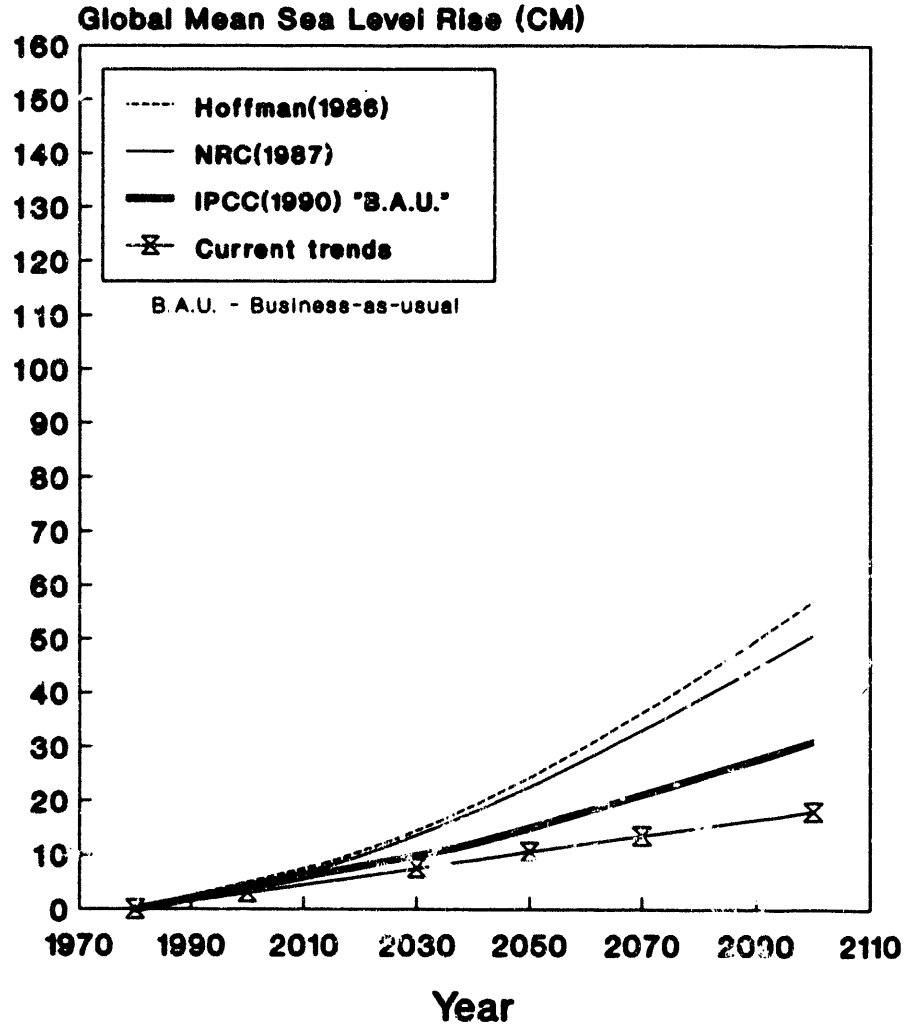
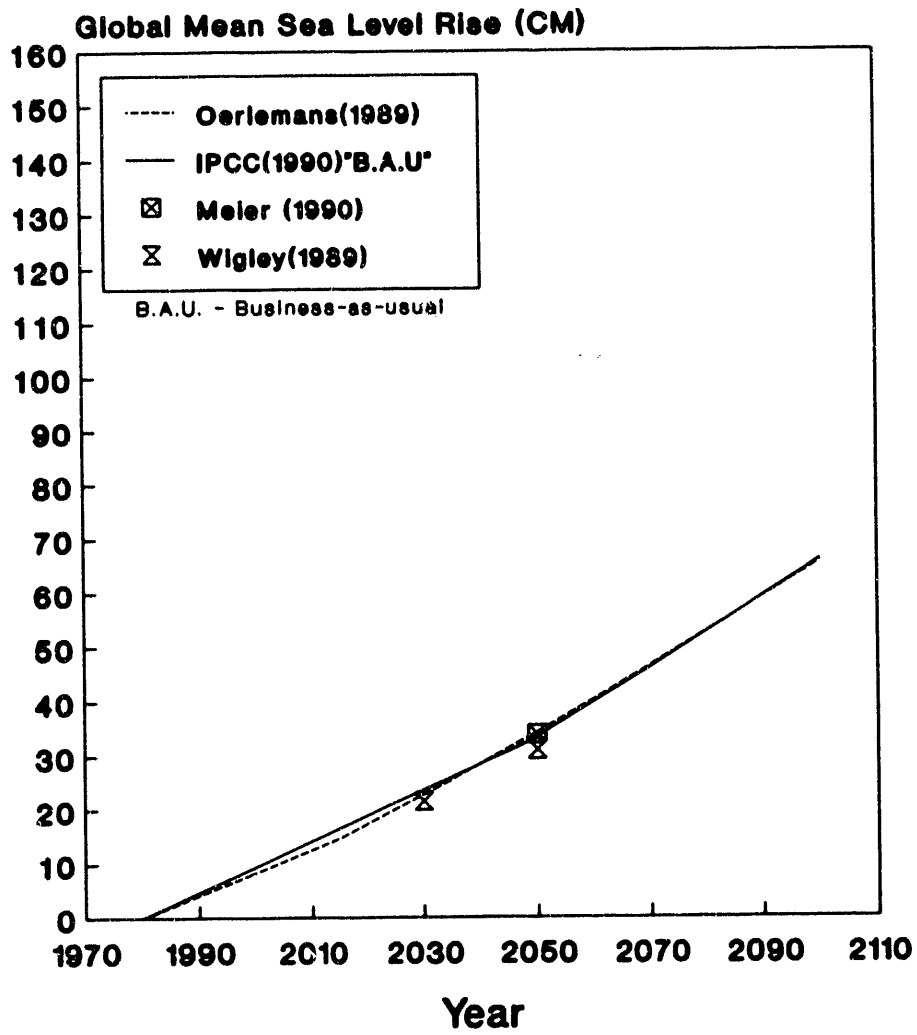


Fig. 2.5 Projected sea-level rise (intermediate).



**Fig. 2.6** Projected sea-level rise (high).

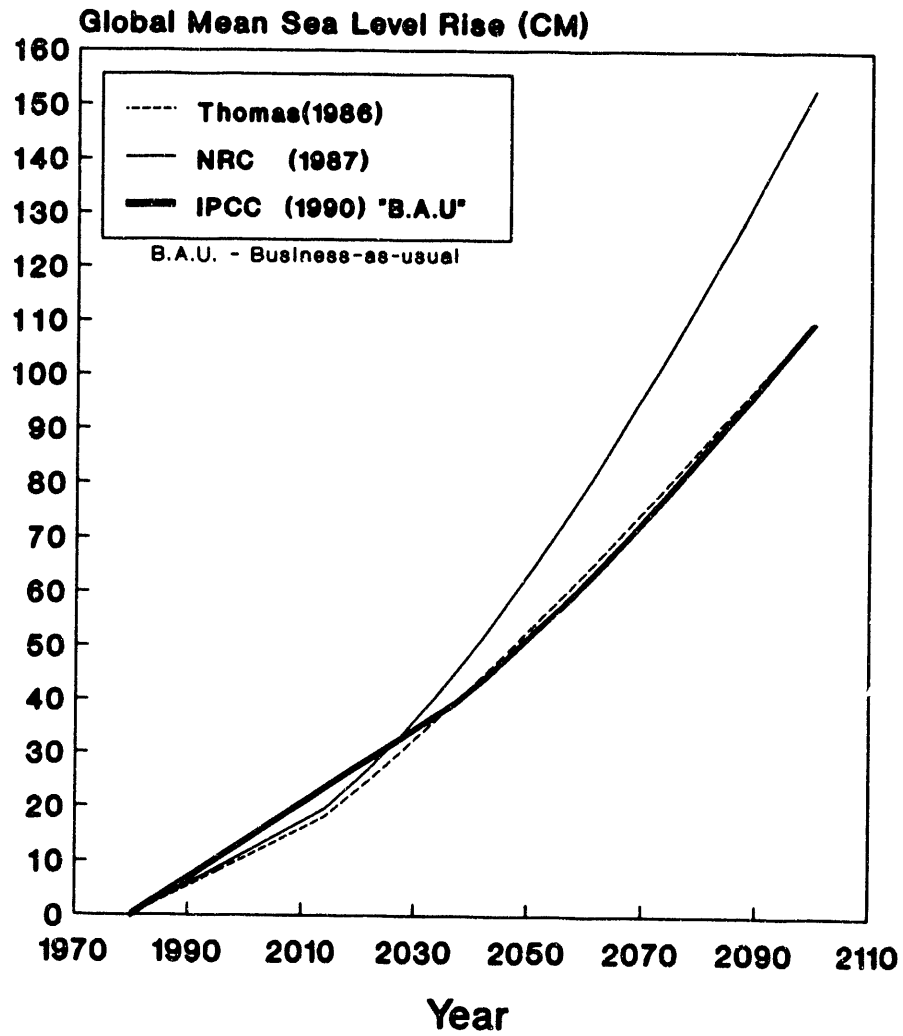
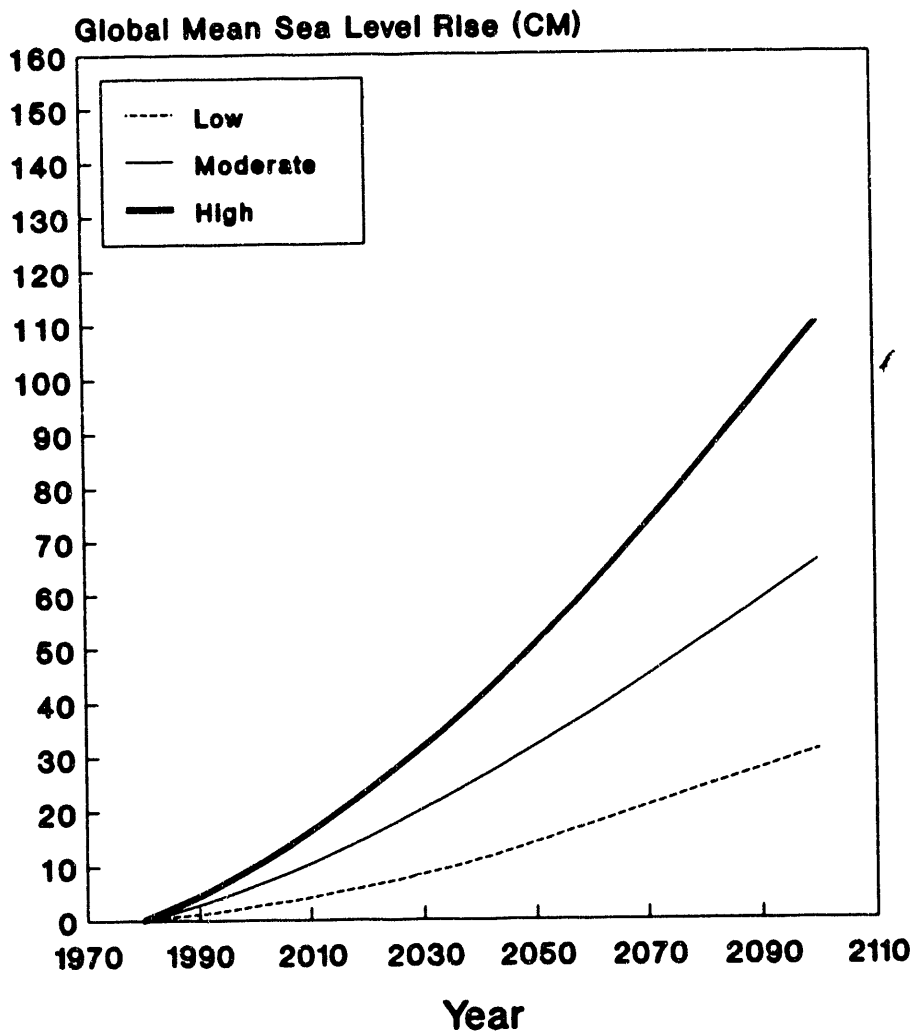


Fig. 2.7 Scenarios of sea-level rise used in this study.



## **VULNERABILITY OF THE U.S. SOUTHEAST TO SEA-LEVEL RISE**

### **3.1 THE COASTAL HAZARDS DATA BASE**

By the year 2100 the rate of global sea-level rise (SLR) may increase to over 10 mm/year (high scenario), which would represent a sevenfold increase over present rates. Local increases could be still greater, depending on local subsidence factors. The potential impacts of accelerated SLR include the permanently inundated of portions of the coastal zone to an elevation equivalent to the vertical rise in sea level. The increase in sea level will also increase the likelihood of episodic flooding events and will cause tidal prisms to be altered (thus changing tidal ranges). Finally, increasing salinization of coastal aquifers and upstream penetration of saltwater resulting from the SLR could contaminate drinking water supplies and adversely affect agriculture. The effects of the global SLR on the shoreline, however, will be spatially nonuniform because of the presence of local vertical crustal movements, differential resistance to erosion, varying wave climates, and variations in longshore currents and sediment supplies.

The ability to identify areas vulnerable to future changes in local sea level as a result of local vertical movements (e.g., subsidence) and SLR is necessary if a timely response is to be made to the rising sea. The original Coastal Hazards Data Base was designed to identify the areas in danger from SLR or erosion on the basis of several physical and marine data variables (Gornitz and Kanciruk 1989). These variables include elevation, geology, geomorphology, mean wave heights, tide ranges, erosion/accretion rates, and local vertical movements. These variables have been obtained for each coastal segment along the U.S. East and Gulf coasts (mean length of a coastal segment is 4.5 km). The physical/marine variables have been evaluated and used in combination with climatological data to determine the differential vulnerability of coastlines to inundation and erosion and to classify and map the spatial distribution of high-risk areas in order to identify targets for future detailed case studies. A vulnerable coastline is characterized by low coastal elevations, an erodible substrate (e.g., sand or other unconsolidated sediments), present and past evidence of subsidence, history of extensive shoreline retreat, high wave/tide energies, and high probabilities of being hit by a extratropical storm, tropical storm, or hurricane.

To map the variations in risk for each coastal segment, an index of vulnerability was developed based on the physical and marine variables in the original Coastal Hazards Data Base and several climatological variables in a data base developed by Birdwell and Daniels (1991). The variables within the expanded Coastal Hazards Data Base, for each coastal segment, were classified into one of five risk/hazard categories and saved in a new "risk" variable. This process was conducted for each data variable in the data base. These risk variables were then used to calculate a Coastal Vulnerability Index for each coastal segment. The index of each coastal segment was then grouped, based on the statistical distribution for all the segments, into a low, moderate, high, or very high risk class.

### 3.2 DATA BASE COMPONENTS AND RISK CLASSES

The original Coastal Hazards Data Base contained information on seven physical and marine variables, relating to permanent and episodic inundation (elevation, vertical land movements, relative sea-level changes) and erosion potential (geology, coastal landforms, erosion/accretion trends, wave heights and tidal ranges) (Gornitz and Kanciruk 1989; Gornitz 1990; Gornitz et al. 1991). Subsequently, six climate variables relating to storm frequency, storm intensity, and surge heights were added.

The 13 risk variables in the expanded Coastal Hazards Data Base were ranked on a scale of 1 to 5, in order of increasing vulnerability (Table 3.1). The rationale for the ranking scheme of the seven physical and marine variables have been described in detail in Gornitz et al. (1991) and will be briefly reviewed here. The methods used to classify the six climatological variables will also be described.

The elevation variable (EL) is a primary indicator of inundation risk. Coastal areas with elevations < 1 m above mean sea level face the highest probability of permanent inundation, while coastal areas with elevations < 5 m above mean sea level are at high risk to above-normal tides or severe storm surges. The hazards for each coastal area decreases progressively for higher average elevations (Table 3.1).

The local vertical movement variable (SL) was deduced from a network of tide-gauge stations (Lyles et al. 1987; Pugh et al. 1987). As discussed in Sect. 2, the relative-sea-level (RSL) change at each locality is a composite of the eustatic component ( $\approx 1.5$  mm/year) and other vertical land motions. Subsiding areas, or those with RSL in excess of the eustatic range ( $> 1.5$  mm/year), regardless of the original cause, face greater inundation hazards and are ranked on the basis of this premise in Table 3.1.

The geology (GL) and the coastal landforms (LF) variables are associated with the erosivity risk of an area. A generalized scale of the resistance of geologic and coastal landforms to erosion was used and is discussed in Gornitz and Kanciruk (1989). Because of the difficulty in quantifying the relative resistance to erosion for each landform, or material type, these two variables were ranked into classes of increasing risk on the basis of the resistance of a given rock type or landform to erosion (Table 3.1).

The historical shoreline displacement (erosion) variable (ER) is a measure of the past tendency of a shoreline to retreat/advance in the face of SLR. In this variable changes of  $\pm 1.0$  m/year lie within the measurement error and are not considered significant. Shores with rates of erosion of -1 m/year or less (more negative) are eroding, and thus are at relatively higher risk. Conversely,

shores with rates  $> 1$  m/year are accreting and are correspondingly at low risk (Table 3.1).

The wave height (WH) variable, and the longshore currents produced by these waves, actively transform the shoreline via sediment transport. Since wave energy is proportional to the square of the wave height, this variable may be used as a measure of a wave's capacity to perform work (i.e., erosion). This variable is an indicator of the amount of beach/coastal materials that may be moved offshore and thus be permanently removed from the coastal sediment system. The risk value assigned in Table 3.1 for WH are based on the maximum significant wave height for each segment.

The tidal range variable (TR) is linked to both permanent and episodic inundation hazards. A large tidal range determines the spatial extent of the coast that is acted upon by waves. The area that is actually experiencing erosion will vary based on the time of day and tidal conditions (e.g., phase of the moon). Areas with large tidal ranges have wide, near-zero relief intertidal zones, susceptible to permanent inundation following SLR. They are also highly susceptible to episodic flooding, associated with storm surges, particularly if these coincide with high tide. Therefore, macrotidal coasts ( $> 4$  m) will be more vulnerable than those with lower tide ranges (Table 3.1).

Climate change will also affect such variables as winds, storm-induced waves, and storm surges. Hurricane intensity, for example, may increase in a doubled  $\text{CO}_2$  world (Emanuel 1987; Daniels 1992). Because of the complexity of modeling the response of these variables to climate warming, changes in the magnitudes of their effects on the relative vulnerability of coastal areas are outside the scope of this study. However, the adverse repercussions of large storms will only be exacerbated by rising sea levels. Ranking schemes for the climatological variables (after Birdwell and Daniels 1991) used in this study are described below.

The tropical storm probability of occurrence (TS) and hurricane/typhoon probability of occurrence (TY) variables define the likelihood, for a  $1^\circ$  by  $1^\circ$  grid cell, that any given year will have at least one tropical storm or hurricane. These variables do not indicate the number of storm (or hurricane) events per year, nor do they provide information on their relative intensities. More precisely, they measure the annual probability of occurrence of a tropical cyclone of at least tropical storm (for TS) or hurricane (for TY) strength in a cell. In the eastern U.S., relatively high TS values are concentrated between Cape Hatteras and northern Florida. TS ranges from a high of 25.3% south of Cape Hatteras to a low of 1.1% in Maine. The

greatest annual likelihood of hurricanes occurs in southern Florida. Annual tropical storm/hurricane probabilities have been sorted into five risk classes based on the range of values shown in Table 3.1.

The hurricane strike frequency/intensity variable (HFI) provides a measure of hurricane frequency and intensity. The total number of hurricane strikes per segment (state or substate) was divided by the record length (91 years) and multiplied by the relative shore length of each segment to obtain a normalized annual average hurricane strike frequency. A weighted-average Saffir-Simpson rating was then derived for each coastal segment by calculating the mean Saffir-Simpson intensity class for all the hurricanes that occurred on each segment on an average year. The maximum sustained wind velocity for the calculated mean intensity class was then obtained by linear interpolation of the lower class boundaries of the Saffir-Simpson classification system. The sustained wind velocities were then scaled to relative energy<sup>1</sup> by squaring to obtain HFI. The "energy" values were then classified based on the risk classes shown in Table 3.1.

The mean forward velocity variable (TC) is the average forward velocity for all tropical cyclones traversing a given 5° by 5° grid cell in the North Atlantic. The data used were originally obtained from the U.S. Department of Commerce (1979). Tropical cyclones moving along the U.S. East Coast accelerate as they head north, while slower moving tropical cyclones, at lower latitudes, have more time in which to inflict greater damage. Therefore, lower mean forward velocities are assigned a greater risk value (Table 3.1).

The annual mean number of extratropical cyclones variable (CN) was obtained from a grid of 5° by 5° cells. The storms measured by CN tend to originate in nontropical areas and, as may be expected, CN decreases southward, ranging from a high of 43.5 per year in Maine to 0.65 in the Florida Keys (Table 3.1). Thus, at least along the U.S. East Coast, CN tends to vary inversely with TS and TY.

Finally, a mean hurricane surge height variable (SS) has been calculated for each of the coastal segments by converting the weighted-average Saffir-Simpson rating to the equivalent sustained wind velocity and deriving the other storm parameters from equations given in Daniels (1992) and the Coastal Engineering Research Center's *Shore Protection Manual* (1984). This calculation neglects geographical variations in the beach slope, which was assumed to be constant at 2%.

---

<sup>1</sup>Energy is proportional to the square of the velocity. The destructive potential of a hurricane is linked to its energy.



**Table 3.1 Coastal risk classification scheme used in this study**

Rank	Very Low	Low	Moderate	High	Very high risk
Variable	1	2	3	4	5
Elevation (m)	≥ 30.0	20.1-30.0	10.1-20.0	5.1-10.0	0-5.0
Geology (relative resistance to erosion)	Plutonic, Volcanic (lava) High-medium grade metamorphics	Low-grade metamor. Sandstone and conglomerate (well-cemented)	Most sedimentary rocks	Coarse and/or poorly sorted unconsolidated sediments	Fine unconsolidated sediment Volcanic ash
Landform	Rocky, cliffed Coasts Fiords Fiards	Medium cliffs Indented coasts	Low cliffs Glacial drift Salt marsh Coral Reefs Mangrove	Beaches (pebbles) Estuary Lagoon Alluvial plains	Barrier beaches Beaches (sand) Mud flats Deltas
Vertical movement (RSL change) (mm/year)	< -1.0 Land rising	-1.0-0.99 <-----	1.0-2.0 within range of eustatic rise	2.1-4.0 Land sinking	> 4.0 ----->
Shoreline displacement (m/yr)	> 2.0 Accretion	1.0-2.0 <-----	-1.0-+1.0 Stable	-1.1-2.0 ----->	< -2.0 Erosion
Mean Tidal Range (m)	< 1.0 Microtidal	1.0-1.9 <-----	2.0-4.0 Mesotidal	4.1-6.0 ----->	> 6.0 Macrotidal
Maximum Wave height (m)	0-2.9	3.0-4.9	5.0-5.9	6.0-6.9	> 6.9
Annual tropical storm prob. (%)	0-8.0	8.1-12.0	12.1-16.0	16.1-20.0	> 20.1
Annual hurricane prob. (%)	0-4.0	4.1-8.0	8.1-12.0	12.1-16.0	16.0-20.0
Hurricane frequency-intensity index	0-20	21-40	41-80	81-120	> 120
Mean forward velocity (m/s)	> 15	15.0-12.0	12.1-9.0	9.1-6.0	< 6.0
Annual mean no. extratropical cyclones	0-10.0	10.1-20.0	20.1-30.0	30.1-40.0	> 40.1
Mean hurricane surge (m)	0-2.0	2.1-4.0	4.1-6.0	6.1-7.0	> 7.0

The percentage of shoreline assigned to each risk class, by variable, in Table 3.1 is shown in Table 3.2. Among the land variables, almost 90% of the segments lie at a mean elevation of 5 m or less and are underlain by unconsolidated sediments. Nearly half of the sampled population consists of erodible beaches, estuary-lagoon complexes, or deltas. Around a quarter is eroding at rates exceeding 2 m/year, 95% of the coast is subsiding, and ≈ 30% is subsiding at rates of 2.5 mm/year or greater, which is faster than the mean global rate of SLR (i.e., 1.5 mm/year). Nearly 18% of the coastal segments have at least a 12% or greater chance of being struck by at least one hurricane per year; 30% have a 16% or

greater chance of experiencing a tropical storm in any given year, and 9% have more than a 20% chance of experiencing a tropical storm annually. These tropical cyclones have the potential to cause massive erosion and to overtop or destroy coastal protection structures. The arrival of a tropical storm or hurricane has the potential to inflict catastrophic losses of land, property, and human life. These losses are caused by the torrential rains, flooding, and storm surges that accompany these storms.

**Table 3.2 Percent of shoreline within each coastal hazard class**

Variable	Risk Class				
	1	2	3	4	5
Elevation (EL)	0.00	0.70	3.40	6.80	89.10
Geology (GL)	0.00	0.00	12.20	58.10	29.70
Landform (LF)	0.00	0.00	53.30	20.80	26.00
Vertical movement (SL)	0.00	0.00	4.70	65.80	29.60
Shoreline displacement (ER)	4.60	3.50	44.70	22.30	24.90
Tidal range (TR)	86.50	8.80	4.70	0.00	0.00
Wave height (WH)	8.70	80.00	11.30	0.00	0.00
Annual Tropical storm prob. (TS)	4.50	29.10	37.00	20.00	9.40
Annual Hurricane Prob. (TY)	6.80	42.10	33.70	16.50	1.00
Hurricane-frequency-intensity index (HFI)	17.90	13.30	26.50	31.20	11.10
Mean forward velocity (TCV)	0.00	0.00	7.00	26.20	66.80
Annual mean number of extratropical cyclones (CN)	66.80	20.20	13.10	0.00	0.00
Mean hurricane surge (SS)	1.20	0.00	35.50	37.50	25.80

Hurricanes can generate storm surges exceeding 7 m along as much as a quarter of the coast and 63% of the coast is potentially subject to surges of 6 m or greater. Clearly, a substantial portion of the coastal segments in the U.S. Southeast are vulnerable to temporary inundation and episodic erosion hazards.

Extratropical storms, although less destructive than hurricanes, can accelerate shoreline erosion. Although the U.S. Southeast has a temperate to subtropical climate regime it can still expect as many as 20 to 30 extratropical cyclones per year over 13% of the coast and 10 to 20 cyclones over 20% of the coast.

After the data were assembled, they were incorporated into a GIS, in which additional variables may be added as new information becomes available. The GIS approach also allows the Coastal Hazards Data Base to be integrated with land use and socioeconomic data sets, for impact assessment.

### 3.3 DEVELOPMENT OF THE COASTAL VULNERABILITY INDEX

The Coastal Vulnerability Index (CVI) originally combined information from the seven physical and marine variables. In these CVI, the value of each variable in each coastal segment was assigned a rank from 1 to 5, with 5 representing the most vulnerable class. The CVI was computed as either the sum or product of the risk classes assigned to the individual variables. The product has the advantage of expanding the range of values, but it is quite sensitive to small changes in individual risk classes. Therefore, a factor was introduced to dampen the extreme range, thus reducing the sensitivity of the calculated CVI. The CVIs originally developed for use with the Coastal Hazards Data Base are shown in Table 3.3.

**Table 3.3 Coastal Vulnerability Indices considered for use in previous coastal hazard studies (e.g., Gornitz et al. 1991)**

---

(1) Product mean

$CVI_1 = 1/n(EL \times SL \times \dots \times TR)$ , where  $n = \#$  of variables present, ( $n = 7$ , max.);  
 EL = elevation, SL = local vertical movement, GL = geology, LF = landform,  
 ER = shoreline displacement (erosion), WH = wave height, TR = tide range.

(2) Modified product mean

$CVI_2 = 1/(n-2)[EL \times SL \times 1/2(GL + LF) \times ER \times 1/2(WH + TR)]$

(3) Average of sum of squares

$CVI_3 = 1/n[EL^2 + SL^2 + \dots + TR^2]$

---

**Table 3.3 (Continued)**

---

(4) Modified product mean

$$CVI_4 = \frac{1}{5^{(n-4)}} (EL \times SL \times \dots TR)$$

(5) Square root of product mean

$$CVI_5 = (CVI_1)^{1/2}$$

(6)  $CVI_6 = 4(EL + SL + ER) + 2(GL + LF + WH + TR) = 100$

---

CVI<sub>1</sub> was the first developed and is the product of the risk classes divided by the number of variables present (i.e., the product mean). The product mean was modified slightly in CVI<sub>2</sub> by averaging the geology and geomorphology risk classes, which are highly correlated in the southeastern United States, and also the tide ranges and wave heights, both of which represent forces that actively shape the coastline. To reduce the possible range of CVI values, a dampening factor was introduced in CVI<sub>4</sub>. The average of the sum of the squares of the risk classes was also computed in CVI<sub>3</sub>. The square root of the product mean was also taken in an attempt to compress the possible range of values for the CVI (i.e., CVI<sub>5</sub>). CVI<sub>5</sub> was used for the East and Gulf coasts in previous studies (Gornitz 1990; Gornitz et al. 1991). Finally, geology/landform ranks (GL and LF) and tide range/wave height ranks (TR and WH) were combined (Table 3.3) in CVI<sub>6</sub> in order to weight lithologic erosion resistance and marine erosion forcing factors equally.

These vulnerability indices were tested on a set of 93 stations (point data), including 59 along the East Coast and 34 along the Gulf Coast. The Pearson correlation coefficient, which compares two sets of ranked CVI<sub>i</sub>, was tested for all combinations of CVI<sub>6</sub> with CVI<sub>1-5</sub>. The correlations obtained ranged from r=0.71 for CVI<sub>4</sub> and CVI<sub>6</sub> to r=0.97 for CVI<sub>2</sub> and CVI<sub>6</sub>. With the exception of CVI<sub>4,6</sub>, all other combinations of CVI yielded an r greater than 0.90, indicating a very high degree of correlation. In particular, the correlation between CVI<sub>5</sub>, previously used on the East Coast, and CVI<sub>6</sub> is 0.92.

To obtain an estimate of the sensitivity of the 6 original CVIs to misclassification in the risk variables, Table 3.4a was constructed. In this table one to three variables were changed from risk class 5 to 1, while holding the remainder constant at 5, for each CVI. This was done to obtain a ratio of the changed from the original CVI (maximum possible score), such that the higher the ratio, the smaller the percentage change. For some CVI, a change in two or more variables results in more than one score; when this occurs only the

minimum possible ratio is shown in Table 3.4a. CVI<sub>3</sub> shows the least sensitivity to change, followed closely by CVI<sub>6</sub>, while CVI<sub>1</sub>, CVI<sub>2</sub>, and CVI<sub>4</sub> are very sensitive. The effect of missing data can be assessed in a similar manner (Table 3.4b). Because of its lower sensitivity to misclassification errors and missing data, and reasonably wide range of possible scores, CVI<sub>6</sub>, based on the sum of variables, may be a better algorithm for coastal vulnerability assessment when only the seven original data variables are used.

**Table 3.4a Sensitivity of CVI<sub>i</sub> to changes in the classification methods used for the risk variables, changing values from 5-1**

No. variables changed	CVI <sub>1</sub>	CVI <sub>2</sub>	CVI <sub>3</sub>	CVI <sub>4</sub>	CVI <sub>5</sub>	CVI <sub>6</sub>
1	0.2	0.2	0.86	0.2	0.44	0.84
2	0.04	0.04	0.73	0.04	0.2	0.68
3	0.008	0.008	0.59	0.008	0.089	0.52

**Table 3.4b Sensitivity of CVI<sub>i</sub> to missing variables**

No. variables missing	CVI <sub>1</sub>	CVI <sub>2</sub>	CVI <sub>3</sub>	CVI <sub>4</sub>	CVI <sub>5</sub>	CVI <sub>6</sub>
1	0.23	0.25	0.047	1.0	0.48	0.80
2	0.056	0.067	0.028	1.0	0.24	0.60
3	0.014	0.020	0.023	1.0	0.12	0.40

Several modified CVI algorithms were derived and tested for use with the expanded version of the Coastal Hazards Data Base used in this study. These new CVIs include both the original 7 physical/marine variables and 6 new climatological variables (listed in Table 3.1), for a total of 13 variables. Because these variables were selected on the basis of their ability to identify coastal areas at risk to both erosion and inundation, these variables were grouped into three factors using principal component analysis. These groups, in order of importance, are permanent inundation, episodic inundation, and erosion potential (see Table 3.5).

The permanent inundation factor is the most important of the three and is used to identify coastal areas at risk to SLR. This factor incorporates the elevation and local vertical movement variables. As both of these variables are of equal importance, they have been weighted equally when used in the modified CVIs.

The second most important factor is the episodic inundation factor. This factor consists primarily of the climatic variables (e.g., tropical storm probabilities, hurricane probabilities, hurricane strike frequency/intensity index, etc.). However, the tidal range

variable also falls within this factor. The tidal range variable was grouped with this factor since it is additive to the storm surge produced by a cyclone (i.e., at astronomical high tide, the peak storm surge produced by a tropical cyclone may be increased by an amount equal to 1/2 the mean tide range). Within the factor, the tropical storm probability and annual hurricane probability variables were averaged with weights of 0.25 and 0.75, respectively. These weights were obtained by taking the wind velocity of the strongest hurricane category (Saffir-Simpson class 5) and converting it into relative energy, taken as the square of the mean sustained wind velocity, and comparing it to the relative energy of a tropical storm (computed in a similar manner). It was found that a tropical storm has 23% of the destructive energy of a hurricane. Based on this relationship, the weighting values of 0.25 and 0.75 were selected.

**Table 3.5 Revised Coastal Vulnerability Indices considered for use in this study**

Coastal hazard variables		
Permanent inundation factor	Episodic inundation factor	Erosion potential factor
1. Elevation (relief) (EL)	3. Annual tropical storm probability(TS)	10. Geology (GL)
2. Vertical movement (SL)	4. Annual hurricane probability (TY)	11. Geomorphology (LF)
	5. Hurricane strike frequency-intensity (HFI)	12. Shoreline displacement (ER) (erosion/accretion)
	6. Mean forward velocity (TC)	13. Wave height (WH)
	7. Annual mean number of extratropical cyclones (CN)	
	8. Hurricane surge height (SS)	
	9. Tidal Range (TR)	

$$CVI_7 = \underbrace{3.5(EL + SL)}_{35\%} + \underbrace{0.6670[(0.25TS + 0.75TY) + HFI + TC + CN + SS + TR]}_{20\%} + \underbrace{3[(GL + LF)/2 + ER + WH]}_{45\%}$$

55%

$$CVI_{8a} = \underbrace{3.5(EL + SL)}_{35\%} + \underbrace{0.8333[(0.25TS + 0.75TY) + HFI + TC + CN + SS + TR]}_{25\%} + \underbrace{2.667[(GL + LF)/2 + ER + WH]}_{40\%}$$

60%

$$CVI_{8b} = \underbrace{3.0(EL + SL)}_{30\%} + \underbrace{1.0000[(0.25TS + 0.75TY) + HFI + TC + CN + SS + TR]}_{30\%} + \underbrace{2.667[(GL + LF)/2 + ER + WH]}_{40\%}$$

60%

$$CVI_9 = 1.818[SL + (0.25TS + 0.75TY) + HFI + TC + CN + SS + TR + (GL + LF)/2 + ER + WH]$$

The last factor is the erosion potential factor. This factor consists of the geology, landform, shoreline displacement (erosion), and wave height variables. Because the geology and landform variables contain similar information they were averaged as in CVI<sub>2</sub> (Table 3.3).

Several weight distributions were examined for use with each factor in the revised CVI algorithms. As inundation is considered a greater hazard than erosion, the combined weight of the two inundation factors has been made greater than that of the erosion factor. Permanent inundation has been treated as a greater hazard than episodic inundation, so the former factor is weighted more heavily than the latter in the revised CVI. In CVI<sub>7</sub>, permanent inundation, episodic inundation, and erosion were weighted 35:20:45%, respectively (as before, each individual variable can receive a maximum rating of 5). To examine the effects of altering the relative weights assigned to each factor, CVI<sub>8a</sub>, using weights of 35:25:40%, and CVI<sub>8b</sub>, using a mix of 30:30:40%, were developed. For comparison with the original algorithms CVI<sub>9</sub> was generated. CVI<sub>9</sub> is not weighted using the factors discussed above; however, the tropical cyclone variables and the geology/geomorphology variables have been averaged, thus reducing the number of variables to eleven (Table 3.5).

Eight representative stations from the U.S. Southeast were selected to test the sensitivity of the new CVIs to misclassification and omission errors. Of the four CVIs tested, CVI<sub>9</sub> (all variables weighted equally) is least sensitive to misclassification errors or missing variables (Table 3.6a). However, differences between CVI<sub>7</sub> and CVI<sub>8</sub> are slight. At any rate, CVI<sub>7,9</sub> are less sensitive, in general, than CVI<sub>1,6</sub> (compare Table 3.4a with Table 3.6a). CVI<sub>8a</sub>, with weighting factors of 35:25:40%, has been adopted as the CVI algorithm to be used in this study for determining the relative vulnerability of the U.S. Southeast coastal zone to SLR. It was adopted because it is highly correlated ( $n=4557$ ,  $r=0.79$ ,  $r^2=0.63$ ) with CVI<sub>5</sub>, used in previous coastal risk studies (Gornitz et al. 1991).

Analysis of the classified risk variables found a high correlation between shoreline erosion and wave heights ( $r=0.66$ ), but little or no correlation among the other land/marine variables. This suggests that, in this region at least, wave energy could be an important cause of coastal erosion.

**Table 3.6a Sensitivity of CVI<sub>i</sub> to changes in the classification methods used for the risk variables, changing values from 5-1**

No. Variables Changed	CVI <sub>7</sub>	CVI <sub>8a</sub>	CVI <sub>8b</sub>	CVI <sub>9</sub>
1	0.86	0.86	0.88	0.93
2	0.72	0.72	0.76	0.85

**Table 3.6b Sensitivity of CVI<sub>i</sub> to missing variables**

No. Variables Missing	CVI <sub>7</sub>	CVI <sub>8a</sub>	CVI <sub>8b</sub>	CVI <sub>9</sub>
1	0.83	0.83	0.85	0.91
2	0.65	0.65	0.70	0.82

Among the climate variables, the mean annual number of extratropical cyclones was found to be inversely correlated ( $r=-0.94$ ) with the mean forward velocity of tropical cyclones (i.e., along the East Coast both tropical and extratropical cyclones show a strong latitudinal dependence). Tropical cyclones, however, tend to accelerate as they track northward. Thus the mean forward velocity of a tropical cyclone tends to increase northward, but its destructive potential decreases. On the other hand, extratropical cyclones become more numerous northward.

The variables most strongly correlated with CVI<sub>8a</sub> include shoreline erosion ( $r=0.73$ ) and wave height ( $r=0.76$ ), a finding also supported by principal components and clustering analysis. A possible reason that CVI<sub>8a</sub> is so heavily weighted toward erosion and wave data is that the other physical variables do not vary significantly in this region because of the relatively low elevations and the uniform geologic and geomorphological characteristics of the Atlantic Coastal Plain.

The impact of a missing variable [in particular, shoreline erosion (ER)] on CVI<sub>8a</sub> has been examined in greater detail for a subset of 1946 coastal segments with the complete set of variables (out of a regional total of 4557). The CVI was calculated using equation CVI<sub>8a</sub> for the 1946 segments with data for all variables, and again for the same set of segments with ER set to 0. When the two runs of CVI<sub>8a</sub> were compared it was found that the range, and general shape of the histogram, were the same for each run, which suggested that the absence of ER did not significantly affect the calculated CVI. However, the absence of the erosion variable did shift the range of CVI<sub>8a</sub> to the left by 2.67 units. To compensate for this reduction in range, CVI<sub>8a</sub> was modified for coastal segments that were missing erosion data by using a higher weight (i.e., 4.000 instead of 2.667) for the erosion-potential factor and by applying a linear stretch to the CVI.

Thus, for the coastal segments with erosion data, CVI<sub>8a</sub> was used to calculate the CVI in this study:

$$CVI_{8a} = \underbrace{3.5(EL + SL)}_{35\%} + \underbrace{0.8333[(0.25TS + 0.75TY) + HFI + TC + CN + SS + TR]}_{25\%} + \underbrace{2.667[(GL + LF)/2 + ER + WH]}_{40\%}$$

60%

The CVI for coastal segments that were missing erosion data, were calculated using the modified CVI equation shown below. The results from CVI<sub>8a mod</sub> were then linearly stretched to minimize variations between the original and modified CVI<sub>8a</sub> (stretch is centered on 71.009).



$$CVI_{8a \text{ mod.}} = 3.5(EL + SL) + 0.8333[(0.25TS + 0.75TY)/2 + HFI + TC + CN + SS + TR] + 4.000[(GL + LP)/2 + WH]$$

If ( $CVI_{8a \text{ mod.}} > 71.009$ .)

then  $CVI_{8a} = CVI_{8a \text{ mod.}} + 0.24290 (CVI_{8a \text{ mod.}} - 71.009)$

else  $CVI_{8a} = CVI_{8a \text{ mod.}} + 0.13317 (71.009 - CVI_{8a \text{ mod.}})$

The above modification may overcompensate the calculated CVI for missing erosion data toward the higher end of the range, because it assumes that the missing erosion data had a distribution similar to that of the data actually present. In reality, the data gaps occur primarily along the inner coast (back barriers, estuaries, etc.), where erosion rates are probably much lower than along the open coast. It is also assumed that the missing wave height data will follow a similar distribution as the erosion data because the two are highly correlated. Thus the correction methods used here would have to be modified if used in different coastal zones, because the correlation of the risk variables will differ, and consequently the correction methods needed for the CVI would also vary.

A histogram and statistical summary for the stretched  $CVI_{8a}$ , weighted by shore length, for the U.S. Southeast are given in Fig. 3.1 and Table 3.7. The CVI scores were divided for mapping into the low, moderate, high, and very high risk categories based on the following quartiles:

1. low CVI 45.1 to 62.4,
2. moderate CVI 62.4 to 66.6,
3. high CVI 66.6 to 72.7, and
4. very high CVI 72.7 to 84.7.

These risk categories are shown for the southeastern United States in Figs. 3.2a through 3.2g.

**Table 3.7 Statistics of the CVI used in this study (values weighted by shore length)**

Percentile	$CVI_{8a}$
100%	84.67
95	79.84
75	72.75
50 (median)	66.59
25	62.44
5	57.02
0	45.18

Range = 45.18 - 84.67	Mode = 74.50	N = 4557 segments
Mean = 67.04		Std. dev. = 7.13

### 3.4 STUDY AREA SELECTION

The CVI described above has been used to identify coastal segments that may be at risk to future changes in sea level (Figs. 3.2a through 3.2g). To select the case study areas to be used in this report, the following criteria were considered: (1) the location of the study areas in high to very high risk coastal zones, (2) the presence of diverse land use and infrastructure types, (3) the equal representation of East and Gulf coasts, and (4) the availability of data.

To determine the mix (in terms of land uses) to be sampled in the case studies, the demographics of the U.S. Southeast were examined. Currently the Southeast has 16 cities with urban populations between 50,000 and 500,000. Two cities (Houston and New Orleans) have populations of 500,000 to 1,000,000, and 1 (Miami) has a population over 1,000,000. Because of these large cities, and the many smaller fishing and resort communities in the region, 66% of the coastline has been modified by man in some way.

On the basis of this ratio, between man-modified shorelines and unmodified shorelines, it was determined that two case studies should be conducted in or near urban areas, two in resort areas, and two in undeveloped/rural areas. The specific location that was chosen for each of the six case study areas was guided by the mapped CVI (Figs. 3.2a through 3.2g), the land use types in each area, and the spatial distribution of the areas.

Another important consideration was the availability and cost of digital elevation data, aerial photos, and land use maps at scales from 1:24,000 to 1:250,000 (Table 3.8). On the basis of the data requirements for this project, the size of each study site was constrained to an 11 by 11 km area (roughly the size of a USGS 7.5-min topographic map). This size is large enough to capture a complete geomorphic landform while small enough for detailed analysis of the effects of coastal inundation from SLR on specific structures to be carried out. The areas selected for study (shown in Fig. 1.2) are identified in Table 3.8.

**Table 3.8 Case study sites used for this project. Site names are equivalent to the name of the USGS 7.5-min topographic map of each area**

Site name	State	County/Parish	Site type
<b>Gulf Coast:</b>			
Galveston	Texas	Galveston	Urban
Caminada Pass	Louisiana	Jefferson	Rural
Bradenton Beach	Florida	Manatee	Resort
<b>East Coast:</b>			
Daytona Beach	Florida	Volusia	Urban
McClellanville	South Carolina	Charleston	Rural
Nags Head	North Carolina	Dare	Resort

The study areas selected reflect the range of land uses and infrastructure types found along the coastal zone of the U.S. Southeast. As such, the conclusions derived for each study area may be generalized and applied to other areas in the Southeast with similar hazard ratings (from the CVI) and stages of economic development. The following Sects. apply the sea-level scenarios developed in Sect. 2 to these study areas. Sect. 4 will determine the amount of land, by land use type, that would be lost to SLR if elevation is considered alone. In Sect. 5 the effects of biophysical factors, land use, and infrastructure, on the ability of the sea to advance inland will be considered.

### **3.5 FIGURES**

**Fig. 3.1** Histogram of the stretched CVI used in this study (values weighted by shore length in meters).

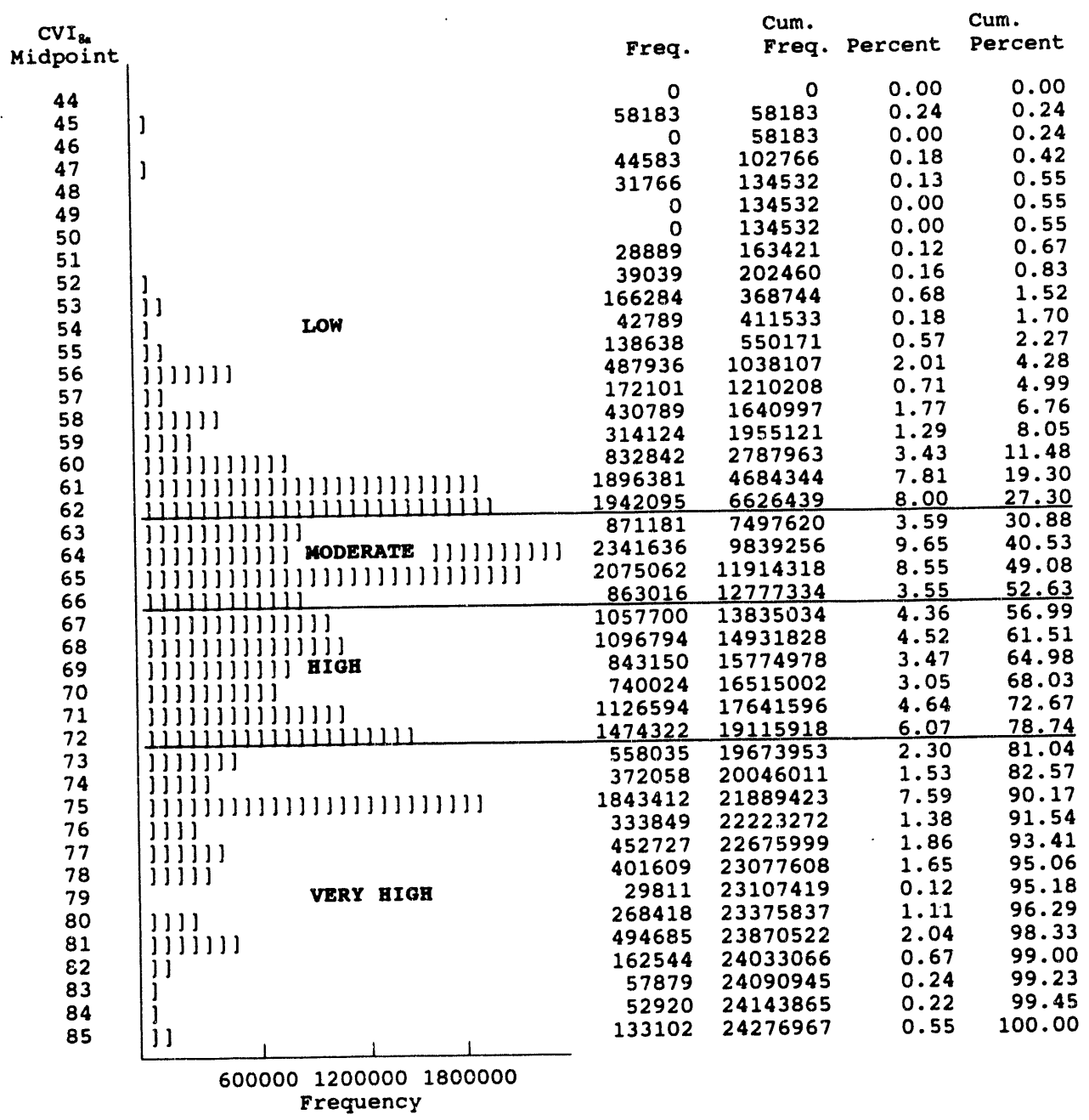


**Fig. 3.2a** Map showing the distribution of low, moderate, high, and very high risk shorelines (Texas).

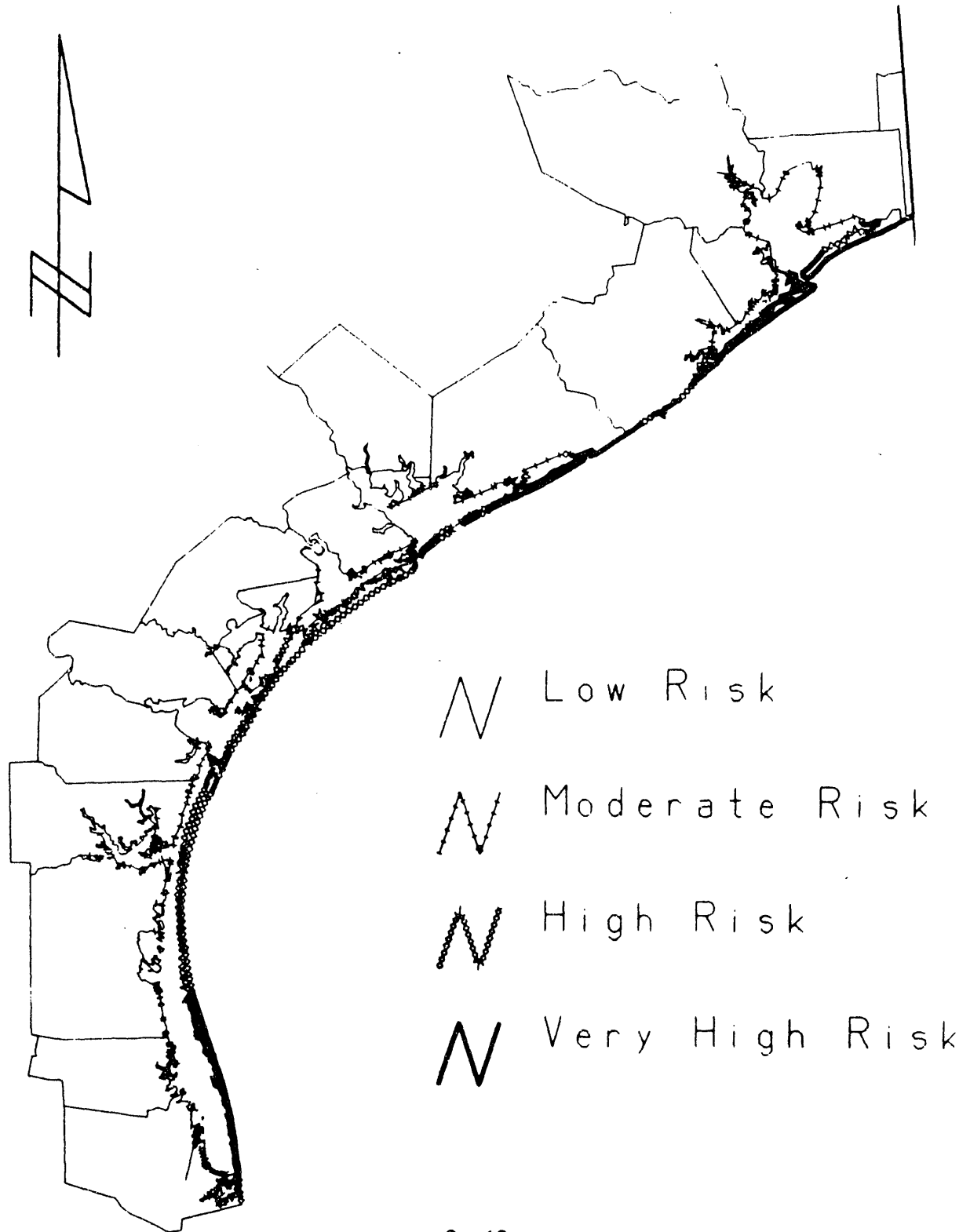
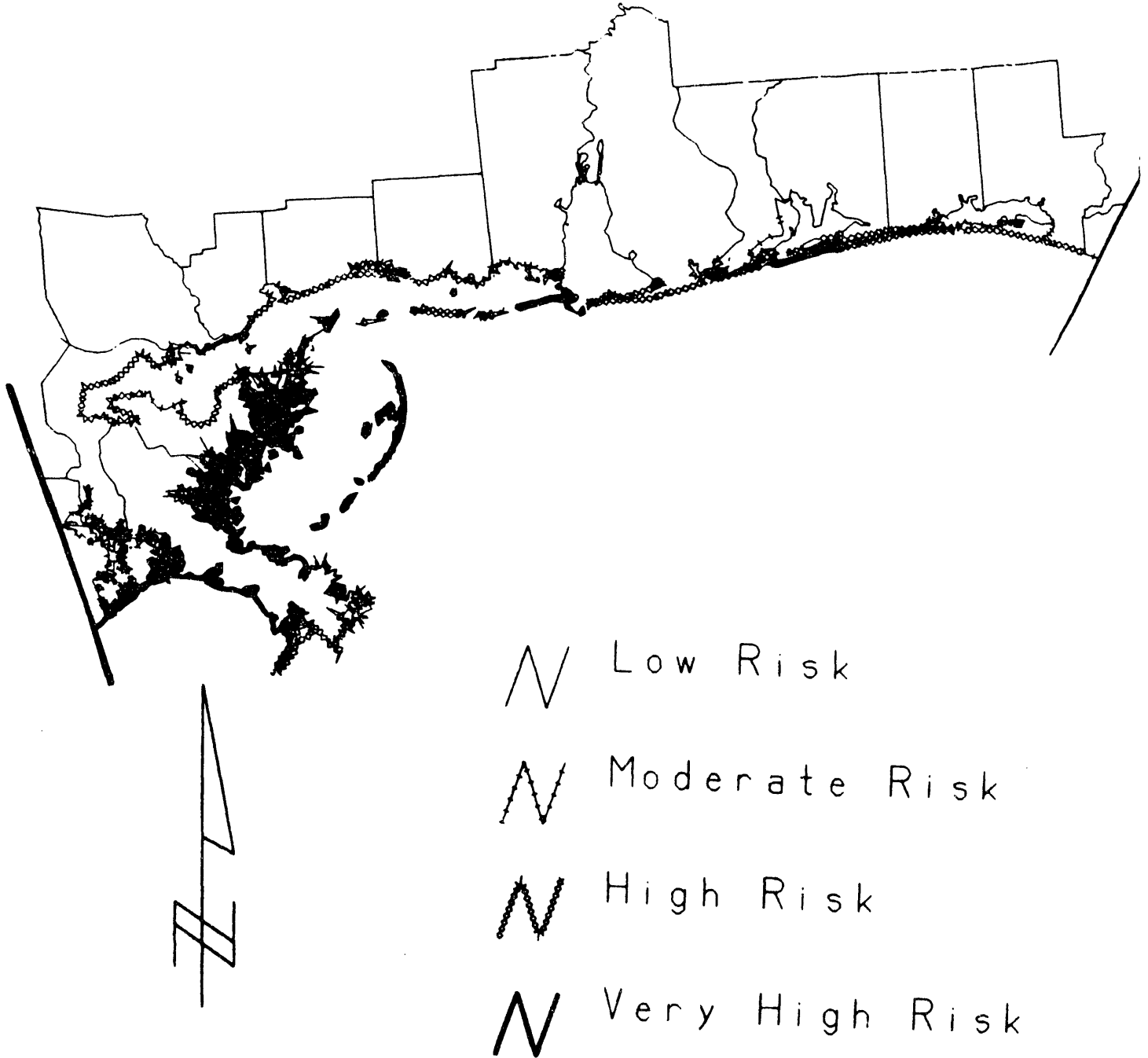


**Fig. 3.2b** Map showing the distribution of low, moderate, high, and very high risk shorelines (Texas and Louisiana).



- N Low Risk
- N Moderate Risk
- N High Risk
- N Very High Risk

**Fig. 3.2c** Map showing the distribution of low, moderate, high, and very high risk shorelines (Louisiana, Mississippi, Alabama, and Florida).







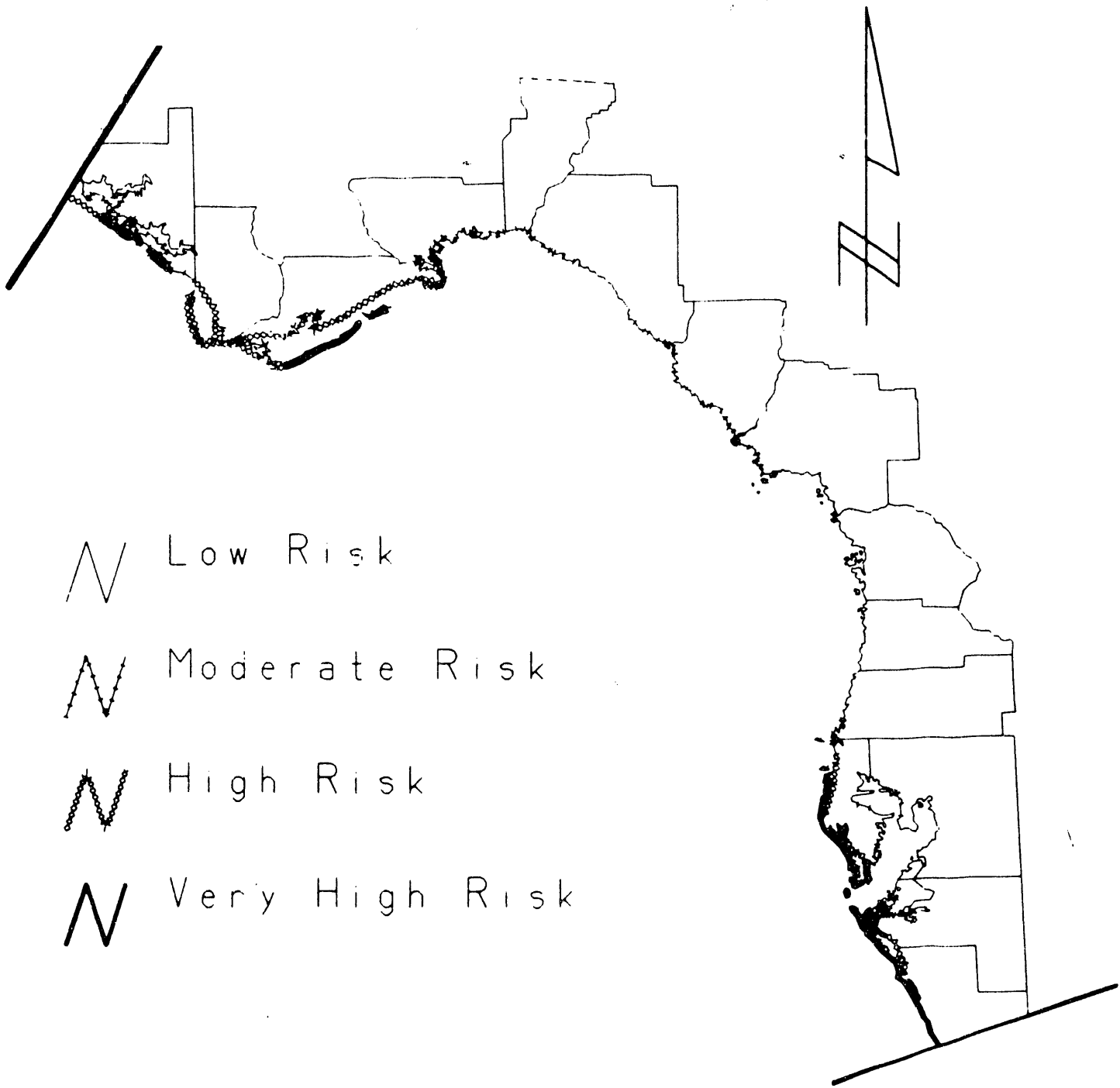


**Fig. 3.2d** Map showing the distribution of low, moderate, high, and very high risk shorelines (Gulf coast of Florida).



**Fig. 3.2e**

**Map showing the distribution of low, moderate, high, and very high risk shorelines (Atlantic coast of Florida).**

-  Low Risk
-  Moderate Risk
-  High Risk
-  Very High Risk

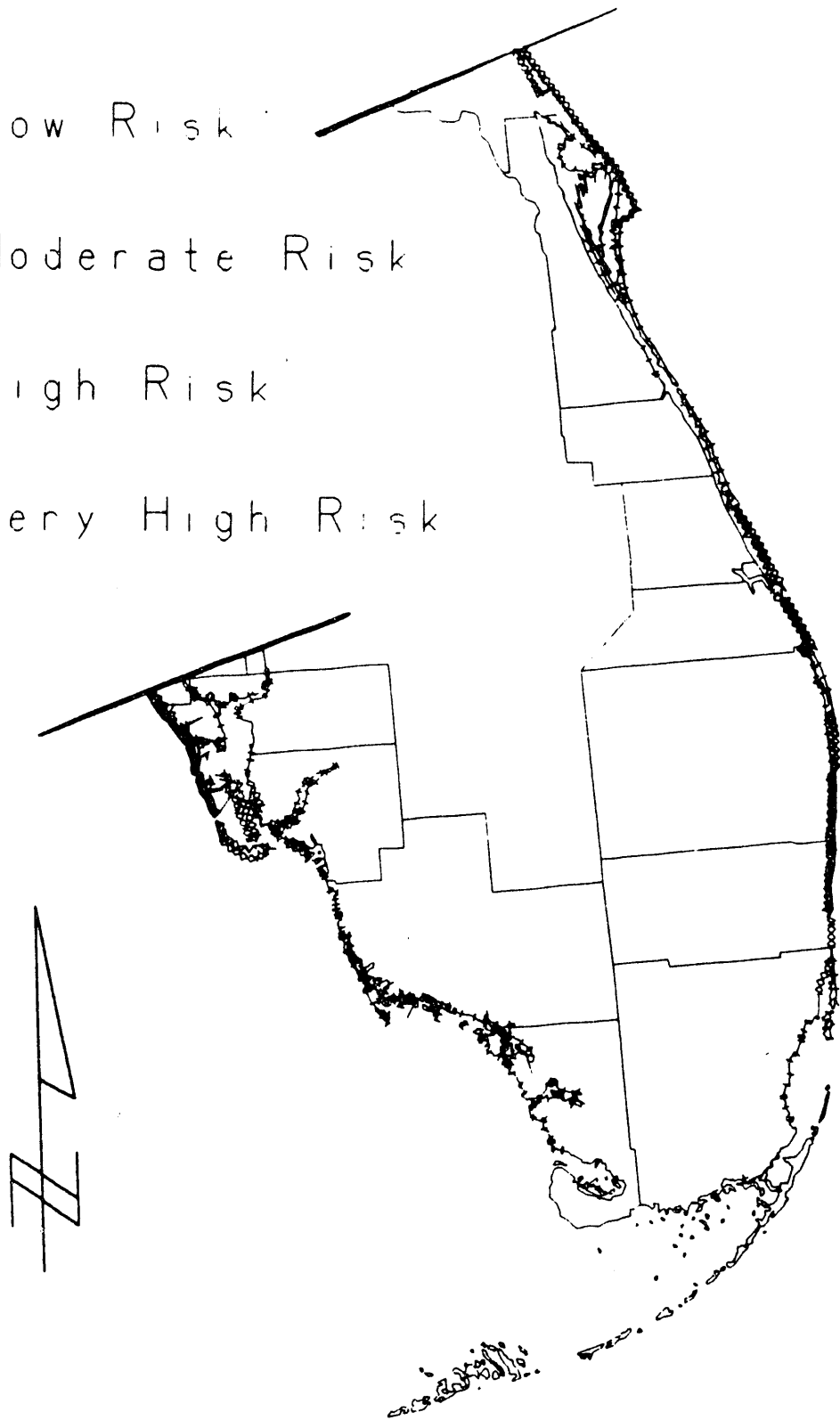


**Fig. 3.2f** Map showing the distribution of low, moderate, high, and very high risk shorelines (Florida, Georgia, and South Carolina).

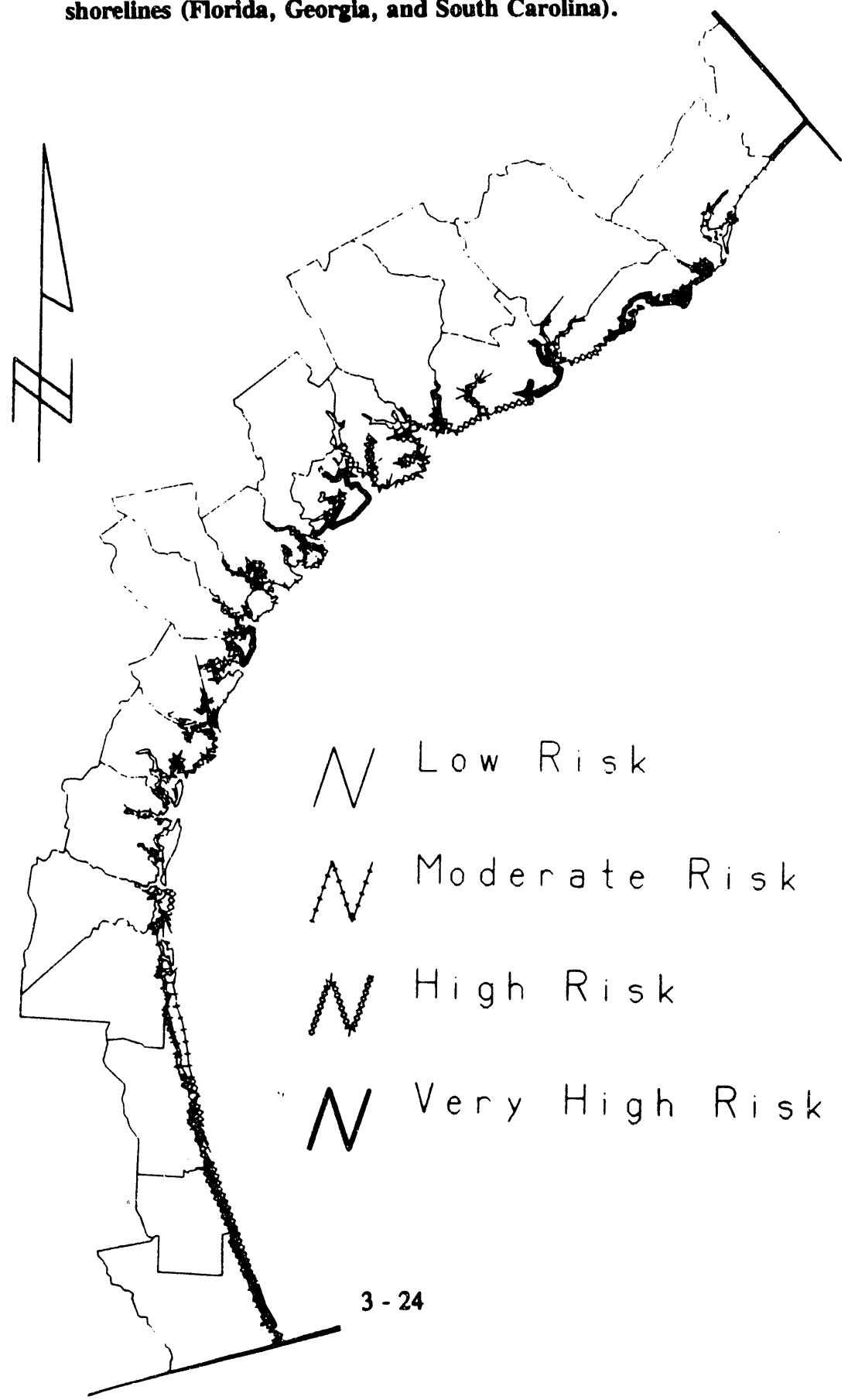
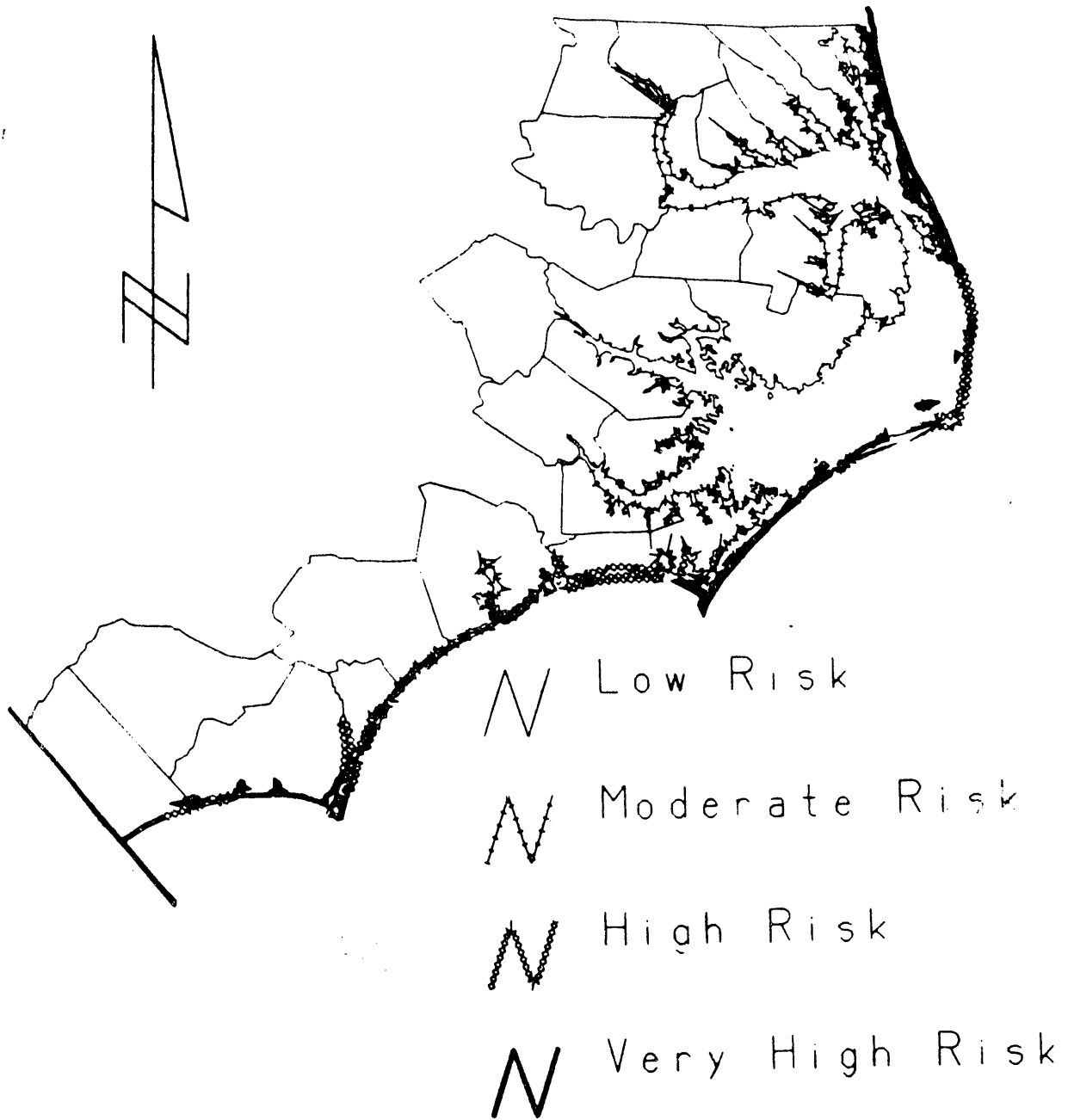


**Fig. 3.2g** Map showing the distribution of low, moderate, high, and very high risk shorelines (South Carolina and North Carolina).



# APPLICATION OF THE SEA-LEVEL SCENARIOS ON THE U.S. SOUTHEAST

## 4.1 METHODS AND DATA SOURCES

The goal of this study is to determine the potential impact that sea-level rise (SLR) may have on the U.S. Southeast. Before an estimation of these impacts could be made, land use data and digital elevation models (DEM) for each study area were needed, along with an estimation of the subsidence rate being experienced within each study area. To construct and calculate this information, U.S. Geological Survey (USGS) 7.5-min topographic maps; Defense Mapping Agency (DMA) 1° by 1° DEMs; USGS Land use and land cover maps; National Aerial Photography Program (NAPP) or National High Altitude Photography Program (NHAP) air photos; and data from the Permanent Service for Mean Sea Level, Bidston Observatory, England, were utilized (Pugh et al. 1987). (A listing of the maps used in this study is contained in Sect. 7.)

### 4.1.1 Land Use Data

The land use maps constructed for each study area are derived from 1:250,000 scale, USGS land use and land cover maps. These USGS land use maps were compiled in the early 1970s and use 4 ha (10 acres) as the minimum mapping unit in urban areas, and 16 ha (40 acres) for rural areas, for each land use category. The classification system used in the USGS land use maps, and by extension the land use maps derived for each study area, is based on the standard definitions outlined by Anderson et al. (1976) in USGS Circular 671. To update the USGS land use maps, it was necessary to overlay them onto newer and more accurate maps [i.e., 1:24,000 USGS 7.5-min topographic map of each study area (photorevised 1973-1988)].

The modified land use maps for each study area, now on a 1:24,000 base, were then checked, and modified as necessary, using 1:80,000 or 1:40,000 NAPP and NHAP air photos (taken in the period 1985-1990). The final 1:24,000-scale land use maps were then digitized and entered into a geographic data base. From this information, the final land use maps were constructed for each study area.

The study areas contained a total of 21 different land use categories. These categories are based on the two-level classification system defined in USGS Circular 671 (Anderson et al. 1976). The first level (i.e., Level I) contains nine general, all-encompassing land cover categories, whereas Level II provides a more detailed description of how the land is being used (e.g., Level I = urban and Level II = residential). What follows is a definition of the Level I, and a listing of the Level II, categories that occurred in the case study areas.

Urban or built-up land consists of areas under intensive use, with much of the land covered by man-made structures. This class includes cities; towns; villages; strip developments; transportation routes; power and communications facilities; and such areas as shopping centers, industrial and commercial complexes, and institutions (e.g., universities

or correctional facilities) that may be isolated from urban areas. Level-II subdivisions are in the following categories: residential; commercial and services; industrial; transportation, communications, and utilities; industrial and commercial complexes; mixed residential and services; and other urban lands (e.g., cemeteries).

Agricultural land comprises land used primarily for the production of food and fiber. The number of structures is low, and the density of the road network is much less in the agricultural lands than in the urban or built-up land. The two Level-II subdivisions are (1) cropland and pasture and (2) orchards, groves, vineyards, nurseries, and ornamental horticulture.

Rangeland is land that is predominantly covered by naturally occurring grasses, grasslike plants, or shrubs. These lands have been influenced by extensive grazing by naturally occurring herbivores and domesticated animals. The Level-II subdivisions are (1) herbaceous rangeland and (2) shrub and brush rangeland.

Forest land is any land that has a crown closure percentage of 10% or more, is stocked or contains trees capable of producing timber or other wood products, and exerts influence on the climate or water regime of the area. Lands from which trees have been removed to less than 10% crown closure, but which have not been developed for other uses, are also included. The Level-II subdivisions are (1) deciduous forest land, (2) evergreen forest land, and (3) mixed forest land.

The delineation of the Water class depends on the scale of the data used; in this case, 1:24,000 scale USGS 7.5-min topographic maps were used. All areas on the map that are persistently water covered, which if linear, are at least 100 m long and, if extended, cover at least 4 ha, have been classified as water. The land use maps derived for this study make no distinction between inland and ocean water bodies, though Level-II categories for these classes exist.

Wetland is defined as an area where the water table is at, near, or above the land surface for a significant part of the year. The hydrological regime is such that aquatic or hydrophytic vegetation is established, although alluvial and tidal flats may be nonvegetated. Wetlands as a rule are associated with topographic lows or the margins of large water bodies. Examples of wetlands include marshes, mud flats, and swamps situated on the shallow margins of bays, lakes, ponds, streams, and man-made impoundments. The Level-II subdivisions are (1) forested wetland and (2) nonforested wetland.

Barren land is any land with limited ability to support life and in which less than one-third of the area is covered by vegetation. Vegetation, if present, is widely spaced and scrubby (more so than that found in rangelands). This class includes transitional areas produced by human activities. However, if it may be inferred from the data source that the land will be returned to its former use, it is not included in the barren land class and will be classified on the basis of its site and situation. The Level-II subdivisions include (1) beaches, (2) sandy areas other than beaches, (3) quarries and gravel pits, and (4) transitional areas.

#### **4.1.2 Digital Elevation Models**

The DEMs used in this study were extracted from DMA 1° by 1° elevation models. The elevations are in meters, and the spacing of the elevations along and between each profile is 3 arc-seconds ( $\approx 90$  m). The elevation data were presented as integer data; as a result, all elevations were rounded to the nearest integer—in the DMA 1° DEMs. This integer representation of the data resulted in DEMs that were unable to accurately locate the coastline. To resolve this problem, supplementary data points were added to the DEM used for each case study area. The supplementary data points were obtained from the coastlines digitized for the land use map of each study area. These coastlines were then "densified" so that a point occurred every 100 m along the coast (or inland water body). These points were given an elevation value of 0 m. These points were added to the DEMs and all 0-m elevation points inland from the coast that did not fall within an inland water body were deleted and all 0-m elevations seaward from the newly added coast were given a value of -1.0 m.

The land use data and the DEM for each study area were then used to determine the amount of land that would be lost to the sea for each SLR scenario, based on elevation alone. To do this the relative SLR (which includes the actual SLR plus local vertical movements) for each study area was applied to its respective DEM. From these DEMs, six predicted coastlines were obtained for each scenario, for each study area. These coastlines were applied to the land use data. This method, analogous to using a cookie cutter, pared away portions of the land use map (for each study area) that would be inundated for each scenario. This allowed the amount of land, by land use type, remaining above mean sea level, for each scenario and study area, to be calculated (assuming that land uses remain constant over time).

#### **4.1.3 Subsidence Rates**

The subsidence rates calculated for the six study areas were obtained using data obtained from the Permanent Service for Mean Sea Level, Bidston Observatory, England (Pugh et al. 1987). A mean relative sea-level trend was calculated by least-squares linear regression for each long-term tide-gauge station with 20 or more years of data that exists in the U.S. Southeast. By subtracting from these rates the global sea-level trend of 1.5 mm/year, derived in Sect. 2, an estimated subsidence rate for each gauge station was obtained. The Galveston, Texas; Caminada Pass, Louisiana; and Daytona Beach, Florida, study areas happen to have one of these stations located within 10 km of them. As such, the subsidence rates used for these study areas have been taken from these nearby gauge stations.

The Bradenton Beach, Florida; McClellanville, South Carolina; and Nags Head, North Carolina study areas do not have a tide-gauge station located within 10 km of them. For these areas the subsidence rates were estimated using a four-step process. The methodology used was adapted and modified from the procedure for averaging temperature time series (Hansen and Lebedeff 1987). Both temperature and sea-level time series share a number of similar characteristics, such as variable record length, data gaps, high interannual variability, and, in general, an increasing trend over time.

The first step was to evaluate the size of the surrounding area for which a given tide-gauge station's record can provide significant information on sea level. For this purpose correlation coefficients have been calculated for all combinations of pairs of stations, with common years of data, in two groups: (1) Gloucester Point, Virginia, to Pensacola, Florida (n=13), and (2) Bayou Rigaud, Louisiana, to Port Isabel, Texas (n=6). These two groups reflect distinct regional differences in sea-level trends. The tide gauge stations along the Gulf coast of Florida have sea-level trends highly correlated with those along the Atlantic Coast; therefore, they have been combined with Group 1. The correlation coefficients calculated between pairs within each group decline with distance. At a distance of 525 km, for example, an  $r^2$  of 0.667 was obtained. However, this distance allowed too much overlap among regional station averages. Therefore, a cutoff radius of 350 km was adopted; this distance corresponds to an  $r^2$  of 0.717.

The next step was to determine the regional average of each tide station. The distance to all stations lying within 350 km of each tide-gauge station was calculated, and a weight (W) was assigned based on this distance as shown in Eq. 4-1.

$$W = 1 - (\text{Distance} / 350) \quad (4-1)$$

A weighted trend was then obtained for each station within the 350-km circle by taking the product of the distance weight (W) and the sea-level trend (SLT) as calculated by linear regression. The average distance-weighted trend (DWT) for all the stations lying within such a circle would be as follows.

$$DWT = \frac{\Sigma(W * SLT)}{\Sigma W} \quad (4-2)$$

The raw sea-level trend, regional trend, and number of contributing stations are shown in Table 4.1.



**Table 4.1 Raw sea-level trend and regional-weighted trend for each long-term tide-gauge station, and the number of stations within the 350-km circles contributing to the average (including center station)**

Gauge station name	Raw sea-level trend (mm/year)	Regional trend (mm/year)	Number of stations in circle
Group 1			
Gloucester Point, VA	3.340	3.734	3
Hampton Roads, VA	4.274	3.740	4
Portsmouth, VA	3.629	3.717	4
Wilmington, NC	2.046	2.498	4
Charleston, SC	3.480	3.017	4
Savannah, GA	2.887	2.915	4
Mayport, FL	2.396	2.258	6
Daytona Beach, FL	2.013	1.968	5
Miami Beach, FL	2.293	2.278	3
Key West, FL	2.320	2.312	2
St. Petersburg, FL	1.647	1.667	5
Cedar Key, FL	1.291	1.691	4
Pensacola, FL	2.439	--	1
Group 2			
Bayou Rigaud, LA	9.387	9.498	2
Eugene Island, LA	9.680	9.468	3
Galveston, TX	6.390	6.093	3
Rockport, TX	4.133	4.387	4
Padre Island, TX	4.975	4.082	3
Port Isabel, TX	3.153	4.067	3

The third step is to interpolate a sea-level trend for the three study areas lying between two adjacent tide stations, by taking the distance-weighted average between the station and the two nearest stations, and using the regional average trends as shown in Table 4.1. For example, in Table 4.2, Bradenton Beach, Florida, lies at a distance of 36.18 km from St. Petersburg and 334.98 km from Key West. The regional-average trend is 1.667 mm/year for St. Petersburg and 2.313 for Key West. The interpolated sea-level trend, weighted by distance, for Bradenton Beach is 1.73 mm/year. Finally, to obtain the projected subsidence rate for the study areas, the eustatic sea-level trend (1.5 mm/year) is subtracted from the interpolated sea-level trend (e.g., Bradenton Beach has a local subsidence rate of 0.23 mm/year).

**Table 4.4 Number of hectares within each land use category for Galveston, Texas, in 1990**

Land use category	Hectares	
I. Urban or built-up land		
Residential	1714.61	
Commercial and services	150.70	
Industrial	333.53	
Transportation and utilities	1104.01	
Industrial and commercial complexes	53.65	
Mixed residential and services		
Other urban lands (e.g., cemeteries)	33.26	
Total urban/built-up lands		3389.76
II. Agricultural land		
Cropland and pasture		
Orchards		
Total agricultural lands		----
III. Rangeland		
Herbaceous (i.e., grass) rangeland		
Shrub and brush rangeland	339.06	
Total rangelands		339.06
IV. Forest land		
Deciduous forest land		
Evergreen forest land		
Mixed forest land		
Total forest lands		----
V. Wetland		
Forested wetland		
Nonforested wetland	1298.08	
Total wetlands		1298.08
VI. Barren land		
Beaches	155.00	
Sandy areas other than beaches		
Quarries and gravel pits		
Transitional areas	838.35	
Total barren lands		<u>993.35</u>
Total number of hectares above mean sea level		6020.25

The subsidence rate was multiplied by the number of years to 2050 and 2100 and combined with SLR scenarios A, B, and C to obtain the relative change in sea level that will be applied to the study area for each scenario (Table 4.5).

**Table 4.5 Sea-level-rise scenarios used for Galveston, Texas. Present subsidence rate for Galveston is 4.89 mm/year**

	1990	2050	2100
Current*	0	29.4	53.9 cm
A. Low	---	43.4	84.9 cm
B. Moderate	---	61.4	119.9 cm
C. High	---	79.4	163.9 cm

\*The current SLR scenario reflects local subsidence only.

#### 4.2.1.2 Predicted coastlines based on elevation

The values in Table 4.5 for SLR were applied to the DEM of the study area, and the impact of each scenario for 2050 and 2100 was determined. The amount of land that is predicted to be lost to SLR for each scenario using this DEM is based on elevation alone (Table 4.6). These values give a general indication of the possible impact that SLR may have on the Galveston area. However, structures such as the Galveston seawall, will impede the inland advance of the sea and will act to reduce the actual amount of land that will be lost.

**Table 4.6 Land above mean sea level at Galveston, Texas, based on sea-level-rise scenarios A, B, and C and current conditions (values in hectares)**

	1990	2050	2100
Current	6020.25	4358.833	3771.727
A. Low	---	4010.334	3098.819
B. Moderate	---	3600.491	829.493
C. High	---	3212.856	728.849

To allow for a more detailed determination of the type of lands that would be lost to the sea, Figs. 4.5, 4.6, and 4.7 were constructed. These figures show the amount of land, by land use type, that will remain in 2050 and 2100 for each SLR scenario. Table 4.7 gives this same information expressed as the percentage of land, by land use type, that will still

be above mean sea level for each scenario. These percentages are based on the values shown in Table 4.4 and help identify the land use types that are actually in danger within this study area.

**Table 4.7 Total land in 1990 (ha) and the percentage of land still above mean sea level for each sea-level-rise scenario for the Galveston study area**

Land use category	Total 1990	Scenario A		Scenario B		Scenario C	
		2050	2100	2050	2100	2050	2100
Residential	1714.6	84.3	72.2	79.9	30.2	73.8	25.1
Commercial and services	150.7	76.2	60.3	70.5	21.6	62.3	19.1
Industrial	333.6	28.8	17.0	23.8	4.6	18.2	3.4
Transportation, communications, and utilities	1104.0	58.4	47.0	53.8	0.1	48.2	0.0
Industrial and commercial complexes	53.6	77.8	36.9	61.1	0.0	40.9	0.0
Other urban lands	33.2	82.9	48.9	70.1	17.8	52.5	14.0
Shrub and brush rangeland	339.0	90.2	81.2	87.1	62.6	82.6	53.0
Nonforested wetland	1298.0	56.8	31.1	46.5	1.1	34.0	0.2
Beaches	155.0	2.4	0.7	1.7	0.0	0.9	0.0
Transitional areas	838.3	64.5	52.5	59.9	2.3	54.0	1.6
Total lands	6020.2	66.6	51.5	60.0	13.8	53.4	12.1

Note: Only land use classes that actually occur within this study area are included in this table.

## 4.2.2 Caminada Pass, Louisiana

The Caminada Pass study area, defined as an undeveloped study area, includes a portion of the town of Grand Isle, which is located predominantly in LaFourche Parish, however, the majority of the study area is in Jefferson Parish. These parishes have the lowest per capita incomes of all the study areas (Fig. 4.8). The population increases that have been experienced within these parishes have been concentrated in the few areas that are not subject to temporary inundation. This constraint has resulted in an unusually high population density on the barrier island within the study area. The land use map derived for this study area, shown in Fig. 4.9, contain Level-I and Level-II land use categories. Table 4.8 shows the amount of land, in hectares, within each category under current conditions (i.e., as of 1990).

The Caminada Pass, Louisiana, quadrangle is near the Wisner State Wildlife Management Area, located within the 30-mile-wide belt of marshlands that borders the Gulf of Mexico, and is bisected by Louisiana State Route 1. The area is located  $\approx 70$  km south of New Orleans and is composed primarily of a series of undeveloped marsh islands. The marsh and barrier islands provide a habitat for a variety of threatened and endangered species. The area also provides temporary habitat for several migratory birds. The only developed area within the quadrangle is located on Grand Isle, the largest barrier island. Grand Isle supports a small resort/fishing community that is mainly located on the stabilized dunes of the island.

### 4.2.2.1 Subsidence

The study area is in the transition zone between the Monroe Uplift and the Mississippi Embayment and is experiencing a mean annual subsidence of 7.9 mm/year (Fig. 4.1). This rate, derived from the tide-gauge records for Bayou Rigaud, Louisiana, reflects subsidence from sediment compaction and fluid withdrawal (i.e., groundwater, oil, and natural gas) that has occurred within the study area. This subsidence rate was multiplied by the number of years to 2050 and 2100 and combined with the SLR scenarios to obtain the relative change in sea-level that will be applied to the study area for each scenario (Table 4.9).

**Table 4.8 Number of hectares within each land use category for Caminada Pass, Louisiana, in 1990**

Land use category	Hectares	
I. Urban or built-up land		
Residential	193.36	
Commercial and services	27.65	
Industrial		
Transportation and utilities		
Industrial and commercial complexes		
Mixed residential and services	21.31	
Other urban lands (e.g., cemeteries)	9.80	
Total urban/built-up lands		252.12
II. Agricultural Land		
Cropland and pasture		
Orchards		
Total agricultural lands		----
III. Rangeland		
Herbaceous (i.e., grass) rangeland		
Shrub and brush rangeland		
Total rangelands		----
IV. Forest land		
Deciduous forest land		
Evergreen forest land		
Mixed forest land		
Total forest lands		----
V. Wetland		
Forested wetland	26.80	
Nonforested wetland	3602.99	
Total wetlands		3629.79
VI. Barren land		
Beaches	93.83	
Sandy areas other than beaches	11.55	
Quarries and gravel pits		
Transitional areas	67.58	
Total barren lands		<u>172.96</u>
Total number of hectares above mean sea level		4054.91

**Table 4.9 Sea-level-rise scenarios used for Caminada Pass, Louisiana. Present subsidence rate for Caminada Pass is 7.9 mm/year**

	1990	2050	2100
Current*	0	47.4	86.9 cm
A. Low	---	61.4	117.9 cm
B. Moderate	---	79.4	152.9 cm
C. High	---	97.4	196.9 cm

\*The current SLR scenario reflects local subsidence only.

#### 4.2.2.2 Predicted coastlines based on elevation

The values in Table 4.9 for SLR were applied to the DEM of the study area, and the impact of each scenario for 2050 and 2100 was determined. The amount of land that is predicted to be lost to SLR for each scenario (Table 4.10) using this DEM is based on elevation alone. These values give a general indication of the possible impact that SLR may have on Caminada Pass. Beach dunes and built structures, such as seawalls, on the developed barrier island may be used to protect the developed areas within the study area. However, the majority of the study area is made up of wetlands that will be subject to both inundation and increased erosion rates. The erosion that would be instigated by SLR (in combination with subsidence) within the wetlands may result in the separation of the barrier islands from the mainland by open water.

**Table 4.10 Land above mean sea level at Caminada Pass, Louisiana, based on sea-level-rise scenarios A, B, and C and current conditions (values in hectares)**

	1990	2050	2100
Current	4054.91	883.09	241.17
A. Low	---	575.88	52.03
B. Moderate	---	287.32	1.64
C. High	---	179.41	0.16

To allow for a more detailed determination of the types of lands that would be lost to the sea, Figs. 4.10, 4.11, and 4.12 were constructed. These figures show the amount of land, by land use type, that will remain in 2050 and 2100 for each scenario, while Table 4.11 shows the amount of land, in percent, that will remain above mean sea level for each

scenario. These percentages are based on the values shown in Table 4.8 and may be used to identify the type of land that is actually in danger within each study area.

**Table 4.11 Total land in 1990 (ha) and the percentage of land still above mean sea level for each sea-level-rise scenario for the Caminada Pass study area**

Land use category	Total 1990	Scenario A		Scenario B		Scenario C	
		2050	2100	2050	2100	2050	2100
Residential	193.3	58.9	1.0	45.3	2.2	17.0	0.0
Commercial and services	27.6	43.0	>0.0	28.8	0.0	3.2	0.0
Mixed residential and services	21.3	10.9	3.1	8.4	0.0	5.4	0.0
Other urban lands	9.8	9.9	0.0	6.7	0.0	1.2	0.0
Forested wetlands	26.8	70.6	14.4	59.2	0.0	52.2	0.0
Nonforested wetlands	3602.9	8.0	0.6	4.2	0.0	2.0	0.0
Beaches	93.8	1.8	0.0	0.5	0.0	0.0	0.0
Sandy areas other than beaches	11.5	6.6	0.0	0.0	0.0	0.0	0.0
Transitional areas	67.5	27.9	0.1	15.7	0.0	4.1	0.0
Total lands	4054.9	21.8	5.9	14.2	1.3	4.4	>0.0

Note: Only land use classes that actually occur within this study area are included in this table.



### **4.2.3 Bradenton Beach, Florida**

The Bradenton Beach study area, a resort-type study area, includes a portion of the city of Bradenton and is near St. Petersburg in Manatee County. This county is experiencing the greatest increase in per capita income and population of any of the Gulf Coast study areas (Fig. 4.13). This population increase has been concentrated in the inland portions of the study area, while the barrier islands have been developed for recreational uses. The land use map derived for this study area, shown in Fig. 4.14, contains Level-I and Level-II land use categories. Table 4.12 shows the amount of land within each category in hectares under current conditions (i.e., as of 1987).

Bradenton Beach, Florida, is in one of the most popular and fastest-growing vacation areas on the Gulf Coast. The resorts within the study area have been expanding over the last decade as visitors discovered the relatively uncrowded beaches, in comparison to those on the east coast of Florida. This area still contains agricultural land, however, that is slowly being converted to residential uses as nearby St. Petersburg grows. The area also contains several forested wetlands within the lagoons created by the coastal barrier islands. The wetlands are on secluded islands or shores within Sarasota Bay, Palma Sola Bay, and Anna Maria Sound.

#### **4.2.3.1 Subsidence**

The study area is in the transition zone between the Ocala Arch and the South Florida Basin. Because no long-term tide-gauge stations occur within 10 km of the study area, the subsidence rate for this area was derived based on the weighted average of the two closest tide-gauge stations. The value obtained, based on the St. Petersburg and Key West, Florida, tide gauge stations, is 0.23 mm/year. This subsidence rate was multiplied by the number of years to 2050 and 2100 and combined with the SLR scenarios to obtain the relative change in sea level that will be applied to the study area for each scenario (Table 4.13).

**Table 4.12 Number of hectares within each land use category for Bradenton Beach, Florida, in 1987**

Land use category	Hectares
<b>I. Urban or built-up land</b>	
Residential	1553.25
Commercial and services	85.50
Industrial	
Transportation and utilities	
Industrial and commercial complexes	29.02
Mixed residential and services	53.19
Other urban lands (e.g., cemeteries)	60.44
<b>Total urban/built-up lands</b>	<b>1761.40</b>
<b>II. Agricultural Land</b>	
Cropland and pasture	732.26
Orchards	
<b>Total agricultural lands</b>	<b>732.26</b>
<b>III. Rangeland</b>	
Herbaceous (i.e., grass) rangeland	75.30
Shrub and brush rangeland	
<b>Total rangelands</b>	<b>75.30</b>
<b>IV. Forest land</b>	
Deciduous forest land	
Evergreen forest land	175.32
Mixed forest land	
<b>Total forest lands</b>	<b>175.32</b>
<b>V. Wetland</b>	
Forested wetland	407.68
Nonforested wetland	
<b>Total wetlands</b>	<b>407.68</b>
<b>VI. Barren land</b>	
Beaches	54.11
Sandy areas other than beaches	30.65
Quarries and gravel pits	
Transitional areas	13.72
<b>Total barren lands</b>	<b>98.48</b>
<b>Total number of hectares above mean sea level</b>	<b>3270.49</b>

**Table 4.13 Sea-level-rise scenarios used for Bradenton Beach, Florida. Present subsidence rate for Bradenton Beach is 0.23 mm/year**

	1987	2050	2100
Current*	0	1.4	2.5 cm
A. Low	---	15.4	33.5 cm
B. Moderate	---	33.4	68.5 cm
C. High	---	51.4	112.5 cm

\*The current SLR scenario reflects local subsidence only.

#### 4.2.3.2 Predicted coastlines based on elevation

The values in Table 4.13 for SLR were applied to the DEM of the study area, and the impact of each scenario for 2050 and 2100 was determined. The amount of land that is predicted to be lost to sea-level rise for each scenario (Table 4.14) using this DEM is based on elevation alone. These values give a general indication of the possible impact that SLR may have on the Bradenton Beach area. The beach dunes and man-made structures, such as seawalls, will protect the developed areas within the study area. However, the small islands within the lagoons are made up of wetlands that will be subject to both inundation and increased erosion rates. The erosion that would be instigated by the SLR (in combination with subsidence) within the wetlands may result in the gradual widening of the lagoon and thinning of the barrier islands.

**Table 4.14 Land above mean sea level at Bradenton Beach, Florida, based on sea-level-rise scenarios A, B, and C and current conditions (values in hectares)**

	1987	2050	2100
Current	3270.49	2263.58	2254.05
A. Low	---	2149.72	2010.04
B. Moderate	---	2010.79	1763.30
C. High	---	1880.00	1410.58

Figures 4.15, 4.16, and 4.17 show the amount of land, by land use type, that will remain in 2050 and 2100 for each scenario. Table 4.15 shows the percentage of land still above mean sea level for each scenario. These percentages are based on the values shown in Table 4.12 and reflect the types of lands that are actually in danger within the study area.

**Table 4.15 Total land in 1987 (ha) and the percentage of land still above mean sea level for each sea-level-rise scenario for the Bradenton Beach study area**

Land use category	Total 1987	Scenario A		Scenario B		Scenario C	
		2050	2100	2050	2100	2050	2100
Residential	1553.2	79.0	71.9	71.9	59.6	66.6	44.9
Commercial and services	85.5	68.6	55.9	55.9	36.5	47.4	7.3
Industrial and commercial complexes	29.0	100	100	100	100	100	96.6
Mixed residential and services	53.1	76.3	54.1	54.1	19.1	38.0	0.0
Other urban lands	60.4	100	100	100	100	100	100
Cropland and pasture	732.2	89.8	87.6	87.6	81.6	85.2	61.9
Herbaceous rangeland	75.3	99.8	99.2	99.2	97.3	98.3	94.7
Evergreen forest land	175.3	56.6	55.6	55.6	52.1	54.7	32.6
Forested wetland	407.6	22.4	13.8	13.8	5.6	9.4	0.3
Beaches	54.1	33.2	23.8	23.8	9.5	17.3	0.0
Sandy areas other than beaches	30.6	16.9	7.0	7.0	0.0	2.4	0.0
Transitional areas	13.7	100	100	100	100	100	100
<b>Total lands</b>	<b>3270.4</b>	<b>73.4</b>	<b>67.0</b>	<b>67.0</b>	<b>56.9</b>	<b>62.6</b>	<b>42.5</b>

Note: Only land use classes that actually occur within this study area are included in this table.

### 4.3 THE EAST COAST (SOUTHERN HALF)

The relative risk from SLR for coastal areas on the East Coast have been estimated using the Coastal Hazards Data Base. In the East Coast (southern half)  $\approx 15.6\%$  is at very high risk to increased erosion or inundation from SLR. The long-term subsidence trend that is being experienced on the southern portion of the Atlantic Coast makes this area particularly vulnerable to SLR. The amount of land that coastal counties will lose to the sea as a result of global change, combined with information on population and incomes, is an indicator of how (or if) steps will/should be taken to protect the present coastline within a given area.

The East Coast portion of the U.S. Southeast study area is part of the Atlantic Coastal Plain, the largest geologic province within the United States. The general dip of the Atlantic portion of this province is eastward toward the Continental Shelf. However, up-warping within the region has created two major basins and two major arches (Fig. 4.1). The eastward dip of the coastal plain is a result of the seaward-dipping layers of terrestrial and marine sediments that have accumulated during past periods of submergence.

Each of the basins and arches on the East Coast, identified in Fig. 4.1, have their own unique depositional and erosional histories. These structures are known as the Chesapeake Basin, Savannah Basin, and the Cape Fear and Ocala Arches. Both of the basins are large; the Chesapeake Basin extends north from Cape Hatteras past Cape May and the Savannah Basin extends along the South Carolina-Georgia coast. The Cape Fear Arch is located between the two basins with its crest nearly coinciding with the North Carolina-South Carolina border. The uplift within this arch has resulted in the prominent capes, shoals, and cusped bays that have developed along this portion of the coast. The Ocala Arch extends from southern Georgia to central Florida. This arch, in contrast to the Cape Fear Arch, was sufficiently high during Cretaceous times so that only a thin sedimentary cap has developed over the Paleozoic sedimentary rocks (Walker and Coleman 1987).

It is important to recognize that a geologic basin tends to be an area of sediment accumulation (e.g., the Savannah Basin) and an arch tends to be an area of net erosion or sediment deficit (e.g., the Cape Fear Arch). The accumulation of sediments within a basin results in the compaction of the underlying sea floor materials from the weight of the overlying sediments. This compaction process causes higher subsidence rates to occur within coastal zones in a basin than within neighboring coasts on an arch.

The East Coast portion of the U.S. Southeast study area is made up of the coastal counties of the following states: North Carolina, South Carolina, Georgia, and the Atlantic coast of Florida. Figure 4.18 shows the population density of the coastal counties that would be affected if the predicted changes in sea level actually occur. The data in the figure were obtained from the U.S. Population Census for 1970, 1980, and 1990. The state values shown include only the coastal counties located within each state, and the values shown for 2000 through 2100 were predicted with a linear regression line developed with the use of the census data.

### **4.3.1 Daytona Beach, Florida**

Daytona Beach, an urban/residential study area, includes the city of Daytona Beach and is located in Volusia County. This county is experiencing the fastest population growth of any of the East Coast study areas, while its per capita income is near the norm. Figure 4.19 shows the population and income for this study area. This population increase is evenly spread throughout the study area, with more than 90% of the region being developed. The land use map derived for this study area, shown in Fig. 4.20, shows the extent of this development and Table 4.16 shows the amount of land within each category, in hectares, under current conditions (i.e., as of 1988).

Daytona Beach, Florida, was incorporated in the early 1900s. Prior to the 1950s, however, it was more of a speedway than beach (i.e., The Daytona International Speedway). After 1950, however, Daytona Beach became a popular destination for students during spring break. The increased visitation of the area, especially in the 1960s and 70s, resulted in the explosive development of retail and resort-type activities in Daytona Beach and surrounding communities. This development has resulted in the overdevelopment of Daytona's barrier islands. These barrier islands form a continuous front more than 23 miles long and are fronted by beaches that are  $\approx 150$  m wide at low tide. At most locations these beaches are reduced in width to  $< 15$  m, and in some locations are completely inundated, during high tide.

#### **4.3.1.1 Subsidence**

This study area is on the Ocala Arch and is experiencing a mean annual subsidence of only 0.513 mm/year (Table 4.3). This rate was derived from the long-term tide-gauge records for Daytona Beach (Pugh et al. 1987). This rate reflects long-term downwarping, with additional contributions from sediment compaction, residual glacio-isostatic effects and fluid withdrawal (i.e., groundwater). The subsidence rate was multiplied by the number of years to 2050 and 2100 and combined with the SLR scenarios to obtain the relative change in sea level that will be applied to the study area for each scenario (Table 4.17).

**Table 4.16 Number of hectares within each land use category for Daytona Beach, Florida, in 1988**

Land use category	Hectares	
<b>I. Urban or built-up land</b>		
Residential	4202.80	
Commercial and services	847.81	
Industrial	3.06	
Transportation and utilities	315.19	
Industrial and commercial complexes	329.29	
Mixed residential and services	77.88	
Other urban lands (e.g., cemeteries)	276.21	
<b>Total urban/built-up lands</b>		<b>6052.24</b>
<b>II. Agricultural Land</b>		
Cropland and pasture		
Orchards	90.24	
<b>Total agricultural lands</b>		<b>90.24</b>
<b>III. Rangeland</b>		
Herbaceous (i.e., grass) rangeland	719.96	
Shrub and brush rangeland		
<b>Total rangelands</b>		<b>719.96</b>
<b>IV. Forest land</b>		
Deciduous forest land		
Evergreen forest land	1198.36	
Mixed forest land		
<b>Total forest lands</b>		<b>1198.36</b>
<b>V. Wetland</b>		
Forested wetland	479.34	
Nonforested wetland		
<b>Total wetlands</b>		<b>479.34</b>
<b>VI. Barren land</b>		
Beaches	71.70	
Sandy areas other than beaches	11.40	
Quarries and gravel pits	42.30	
Transitional areas	114.15	
<b>Total barren lands</b>		<b><u>239.55</u></b>
<b>Total number of hectares above mean sea level</b>		<b>8779.75</b>

**Table 4.17 Sea-level-rise scenarios used for Daytona Beach, Florida. Present subsidence rate for Daytona Beach is 0.513 mm/year**

	1988	2050	2100
Current*	0	3.1	5.6 cm
A. Low	---	17.1	36.6 cm
B. Moderate	---	35.1	71.6 cm
C. High	---	53.1	115.6 cm

\*The current SLR scenario reflects local subsidence only.

#### 4.3.1.2 Predicted coastlines based on elevation

The values in Table 4.17 for SLR were applied to the DEM of Daytona Beach to determine the impact of each scenario on the study area for 2050 and 2100. The amount of land that may be lost to SLR for each scenario (Table 4.18) using this DEM is based on elevation alone. These values give a general indication of the possible impact that SLR may have on the Daytona Beach area. However, the presence of manmade structures (at the beach-backshore interface) and beach nourishment projects may protect the current coast from the adverse effects of SLR. The erosion that would be instigated by the increase in sea level (in combination with subsidence) within the few remaining wetlands may result in the barrier islands being reduced in size and the wetlands within the lagoon being inundated.

To allow for a more detailed determination of the types of lands that would be lost to the sea, Figs. 4.21, 4.22, and 4.23 were constructed. These figures show the amount of land, by land use type, that will remain in the years 2050 and 2100 for each SLR scenario. Table 4.19 shows the percentage of land (in relation to present) that will still be above mean sea level, by land use type. These percentages are based on the values shown in Table 4.16 and reflect the types of lands that may be in danger within the study area.

**Table 4.18 Land above mean sea level at Daytona Beach, Florida, based on sea-level-rise scenarios A, B, and C and current conditions (values in hectares)**

	1988	2050	2100
Current	8779.75	8525.56	8504.77
A. Low	---	8414.37	8273.27
B. Moderate	---	8283.55	8051.21
C. High	---	8166.20	7558.91



**Table 4.19 Total land in 1988 (ha) and the percentage of land still above mean sea level for each sea-level-rise scenario for the Daytona Beach study area**

Land use category	Total 1988	Scenario A		Scenario B		Scenario C	
		2050	2100	2050	2100	2050	2100
Residential	4202.8	96.8	94.6	94.6	91.6	92.8	83.5
Commercial and services	847.8	93.2	90.3	90.8	84.8	87.6	63.1
Industrial	3.0	100	100	100	100	100	100
Transportation, communications, and utilities	315.1	94.0	93.1	93.1	91.5	92.2	88.3
Industrial and commercial complexes	329.2	100	100	100	100	100	100
Mixed residential and services	77.8	100	99.7	99.7	98.7	99.1	65.0
Other urban lands	276.2	71.8	71.8	71.8	71.8	71.8	71.6
Orchards	90.2	100	100	100	100	100	100
Herbaceous rangeland	719.9	99.8	99.7	99.7	99.5	99.6	99.4
Evergreen forest land	1198.3	99.7	99.1	99.1	97.3	98.1	93.6
Forested wetland	479.3	79.9	78.1	78.1	77.3	77.9	76.7
Beaches	71.7	87.0	71.7	71.6	34.2	50.8	2.6
Sandy areas other than beaches	11.4	0.0	0.0	0.0	0.0	0.0	0.0
Quarries and gravel pits	42.3	98.5	92.4	92.4	76.3	83.8	52.3
Transitional areas	114.1	88.8	86.3	86.3	84.0	84.7	84.7
Total lands	8779.7	95.4	93.5	93.5	90.7	91.9	83.3

Note: Only land use classes that actually occur within this study area are included in this table.

### **4.3.2 McClellanville, South Carolina**

McClellanville, an undeveloped study area, includes the small town of McClellanville and is located in Charleston County. This county is experiencing moderate growth in both population and per capita income. This growth is primarily occurring on the barrier islands within the county. Fig. 4.24 shows the population and income for this study area. The study area itself is relatively sparsely populated because the barrier islands along this portion of the coast are part of the Cape Romain National Wildlife Refuge (thus reducing development potential). The land use map derived for this study area, shown in Fig. 4.25, shows the extent of this development. Table 4.20 shows the amount of land in hectares within each category, under current conditions (i.e., as of 1989).

A significant portion of the McClellanville quadrangle is part of the Cape Romain National Wildlife Refuge, founded in 1934. The refuge consists of a series of undeveloped barrier islands and saltwater marshes that lie between the Atlantic Ocean and the Intracoastal Waterway. The marsh and barrier islands provide a habitat for a variety of threatened and endangered species. The area also offers temporary habitat for several migratory species of birds. The portion of the McClellanville quadrangle inland from the Intracoastal Waterway is primarily agricultural, forested, and residential in nature, and it has several small areas of forested wetland. The forested wetlands are in depressions between prehistoric dune lines.

#### **4.3.2.1 Subsidence**

The study area is within the transition zone between the Cape Fear Arch and the Savannah Basin. As no long-term tide-gauge stations occur within 10 km of the study area, the subsidence rate for this area was derived on the basis of the weighted average of the two closest tide-gauge stations. The value obtained, based on the Wilmington, North Carolina, and Charleston, South Carolina, gauge stations, is 1.40 mm/year (Table 4.3). This subsidence rate was multiplied by the number of years to 2050 and 2100 and combined with the SLR scenarios to obtain the relative change in sea level that will be applied to the study area for each scenario (Table 4.21).

**Table 4.20 Number of hectares within each land use category for McClellanville, South Carolina, in 1989**

Land use category	Hectares
I. Urban or built-up land	
Residential	106.52
Commercial and services	
Industrial	
Transportation and utilities	
Industrial and commercial complexes	
Mixed residential and services	
Other urban lands (e.g., cemeteries)	
Total urban/built-up lands	106.52
II. Agricultural Land	
Cropland and pasture	1016.34
Orchards	
Total agricultural lands	1016.34
III. Rangeland	
Herbaceous (i.e., grass) rangeland	
Shrub and brush rangeland	
Total rangelands	----
IV. Forest land	
Deciduous forest land	8.24
Evergreen forest land	
Mixed forest land	3157.51
Total forest lands	3165.75
V. Wetland	
Forested wetland	373.02
Nonforested wetland	8080.82
Total wetlands	8453.84
VI. Barren land	
Beaches	295.15
Sandy areas other than beaches	
Quarries and gravel pits	25.93
Transitional areas	
Total barren lands	<u>321.08</u>
Total number of hectares above mean sea level	13063.57

**Table 4.21 Sea-level-rise scenarios used for McClellanville, South Carolina. Present subsidence rate for McClellanville is 1.40 mm/year**

	1989	2050	2100
Current*	0	8.4	15.4 cm
A. Low	---	22.4	46.4 cm
B. Moderate	---	40.4	81.4 cm
C. High	---	58.4	125.4 cm

\*The current SLR scenario reflects local subsidence only.

#### 4.3.2.2 Predicted coastlines based on elevation

The values in Table 4.21 for SLR were then applied to the DEM of the study area, and the impact of each scenario for 2050 and 2100 was determined. The area of land that is predicted to be lost to SLR for each scenario (Table 4.22) using this DEM is based on elevation alone. The majority of the study area is made up of wetlands that will be subject to both inundation and increased erosion rates. The erosion that would be instigated by the SLR (in combination with subsidence) within the wetlands could result in the separation of the barrier islands within this area from the mainland by open water.

**Table 4.22 Land above mean sea level at McClellanville, South Carolina, based on sea-level-rise scenarios A, B, and C and current conditions (values in hectares)**

	1989	2050	2100
Current	13063.57	8436.51	7754.53
A. Low	---	7147.97	5640.83
B. Moderate	---	5934.51	5107.03
C. High	---	5340.35	4522.50

To allow for a more detailed determination of the types of lands that would be lost to the sea, Figs. 4.26, 4.27, and 4.28 were constructed. These figures show the amount of land, by land use type, that will remain in 2050 and 2100 for each scenario. Table 4.23 shows the percentage of land that will remain at mean sea level for each scenario. These percentages are based on the values shown in Table 4.20 and reflect the land uses that are in danger within the study area.

**Table 4.23 Total land in 1989 (ha) and the percentage of land still above mean sea level for each sea-level-rise scenario for the McClellanville study area**

Land use category	Total 1989	Scenario A		Scenario B		Scenario C	
		2050	2100	2050	2100	2050	2100
Residential	106.5	92.9	91.1	91.5	87.3	89.7	76.4
Cropland and pasture	1016.3	98.8	97.1	97.4	94.7	96.0	87.5
Deciduous forest land	8.2	12.1	0.0	0.0	0.0	0.0	0.0
Mixed forest land	3157.5	98.9	97.2	97.6	95.7	96.5	90.9
Forested wetland	373.0	100	100	100	100	100	98.7
Nonforested wetland	8080.8	32.8	13.9	16.9	6.8	8.9	2.4
Beaches	295.1	54.8	42.8	45.1	26.7	35.8	2.7
Quarries and gravel pits	25.9	94.8	86.3	88.2	69.9	80.1	12.3
Total lands	13063.5	57.0	44.4	46.5	39.0	40.9	33.8

Note: Only land use classes that actually occur within this study area are included in this table.

### **4.3.3 Nags Head, North Carolina**

Nags Head, an resort-type study area, is located within Dare County and includes the resort and fishing communities of Nags Head and Manteo. This county has the lowest permanent population of the three East Coast study areas. Figure 4.29 shows the population and per capita income for this study area. The population of this area is concentrated on the barrier islands, and the entire region has some form of recreational development under way. The land use map derived for this study area, shown in Fig. 4.30, shows the extent of this development and Table 4.24 shows the amount of land within each category, in hectares, under current conditions (i.e., as of 1983).

The Nags Head, North Carolina, study area covers a segment of the Outer Banks and contains portions of Roanoke Island, Bodie Island, and the northern terminus of Cape Hatteras National Seashore. The Outer Banks consists of a string of barrier islands and peninsulas that lie between the ocean and the sounds along 125 miles of North Carolina's coast. The islands that form the Outer Banks are constantly shifting due to storm winds and wave action, and some evidence has been found that suggests that the barrier islands may be migrating landward.

The two communities within the study area, Manteo (on Roanoke Island) and Nags Head (on Bodie Island), have been populated continuously since the 17th century. The earliest recorded effort to colonize the area occurred in 1585 on Roanoke Island, the site of the first English colony established in North America. Though this colony was unsuccessful, the area was resettled and developed a strong maritime economy centered on fishing. In the last 40 years, however, Nags Head (along with many other towns on the Outer Banks) have been transformed into resort communities that cater to the people who visit Cape Hatteras National Seashore.

#### **4.3.3.1 Subsidence**

This study area is in the southern end of the Chesapeake-Delaware Basin. Because a long-term tide-gauge station does not exist within 10 km of this study area, the subsidence rate for this study area was derived based on the weighted average of the two closest tide-gauge stations. The value obtained, based on the Wilmington, North Carolina, and Portsmouth, Virginia, gauge stations, is 1.87 mm/year (Table 4.3). This subsidence rate has been multiplied by the number of years to 2050 and 2100 and combined with the SLR scenarios to obtain the relative change in sea level that will be applied to the study area for each scenario (Table 4.25).

**Table 4.24 Number of hectares within each land use category for Nags Head, North Carolina, in 1983**

Land use category	Hectares	
<b>I. Urban or built-up land</b>		
Residential	737.58	
Commercial and services	216.39	
Industrial	81.96	
Transportation and utilities	30.44	
Industrial and commercial complexes	27.84	
Mixed residential and services		
Other urban lands (e.g., cemeteries)		
<b>Total urban/built-up lands</b>		1094.21
<b>II. Agricultural Land</b>		
Cropland and pasture		
Orchards		
<b>Total agricultural lands</b>		----
<b>III. Rangeland</b>		
Herbaceous (i.e., grass) rangeland	262.14	
Shrub and brush rangeland	266.50	
<b>Total rangelands</b>		528.64
<b>IV. Forest land</b>		
Deciduous forest land		
Evergreen forest land	168.99	
Mixed forest land	522.63	
<b>Total forest lands</b>		691.62
<b>V. Wetland</b>		
Forested wetland	115.40	
Nonforested wetland	1327.75	
<b>Total wetlands</b>		1443.15
<b>VI. Barren land</b>		
Beaches	59.58	
Sandy areas other than beaches	167.70	
Quarries and gravel pits		
Transitional areas	433.22	
<b>Total barren lands</b>		<u>660.50</u>
<b>Total number of hectares above mean sea level</b>		4418.20

**Table 4.25 Sea-level-rise scenarios used for Nags Head, North Carolina. Present rate of subsidence for Nags Head is 1.87 mm/year**

	1983	2050	2100
Current*	0	11.2	20.5 cm
A. Low	---	25.2	51.6 cm
B. Moderate	---	43.2	86.6 cm
C. High	---	61.2	130.6 cm

\*The current SLR scenario reflects local subsidence only.

#### 4.3.3.2 Predicted coastlines based on elevation

The values in Table 4.25 for SLR were applied to the DEM of the study area, and the impact of each scenario for 2050 and 2100 was determined. The amount of land that may be lost to SLR for each scenario is shown in Table 4.26 —these estimations are based on elevation alone. These values give a general indication of the possible impact that an increase in sea level may have on the Nags Head area, but the construction of erosion control structures in the future may reduce the impact of SLR on this study area.

**Table 4.26 Land above mean sea level at Nags Head, North Carolina, based on sea-level-rise scenarios A, B, and C and current conditions (values in hectares)**

	1983	2050	2100
Current	4418.20	2875.51	2783.98
A. Low	---	2738.15	2486.22
B. Moderate	---	2565.38	2166.48
C. High	---	2396.90	1569.83

Figures 4.31, 4.32, and 4.33 show the amount of land, by land use type, that will remain in 2050 and 2100 for each scenario. Table 4.27 shows the amount of land, in percent, that will remain above mean sea level for each scenario. These percentages are based on the values shown in Table 4.24 and reflect the land uses that are in danger within the study area.



**Table 4.27 Total land in 1983 (ha) and the percentage of land still above mean sea level for each sea-level-rise scenario for the Nags Head study area**

Land use category	Total 1983	Scenario A		Scenario B		Scenario C	
		2050	2100	2050	2100	2050	2100
Residential	737.5	89.9	82.3	83.9	69.1	78.5	38.3
Commercial and services	216.3	60.2	29.7	34.8	13.2	22.4	2.9
Industrial	81.9	99.8	97.4	98.2	90.0	95.7	33.8
Transportation, communications, and utilities	30.4	69.0	63.9	64.9	56.7	62.0	37.3
Industrial and commercial complexes	27.8	0.0	0.0	0.0	0.0	0.0	0.0
Herbaceous rangeland	262.1	0.0	0.0	0.0	0.0	0.0	0.0
Shrub and brush rangeland	266.5	84.3	79.3	80.2	71.4	77.1	42.9
Evergreen forest land	168.9	91.7	87.9	89.1	76.8	85.1	64.8
Mixed forest land	522.6	99.0	97.5	97.9	94.3	96.7	82.0
Forested wetland	115.4	98.2	95.8	96.4	90.7	94.5	79.5
Nonforested wetland	1327.7	20.0	16.0	16.8	11.5	14.7	2.5
Beaches	59.5	53.5	24.1	29.2	7.4	16.5	0.0
Sandy areas other than beaches	167.7	87.5	80.5	81.9	68.9	77.3	42.4
Transitional areas	433.2	86.8	85.2	85.7	75.9	84.0	56.0
Total lands	4418.2	61.8	56.2	57.3	48.6	54.0	32.1

Note: Only land use classes that actually occur within this study area are included in this table.

#### 4.4 CONCLUSIONS

In the six case studies discussed in this Sect., the amount of land, by land use type, that would be inundated from four SLR scenarios was determined. The SLR used for each scenario included both an estimated long-term subsidence rate for the given study area and a "global" SLR component (the current scenario only considered the local subsidence rate of each study area). Thus, the actual increase in relative sea level varies, depending on the study area in question. Several of the figures in this Sect. depict predicted future coastlines (e.g., Fig. 4.5). These figures were derived from contour lines generated from digital elevation models of each study area. The minimum contour interval obtainable in the models was 5 cm. Because of this, the future coastline for each scenario shown in the figures in this Sect. (i.e., there are three for each study area) may differ from those indicated by the SLR scenarios by  $\pm 2.5$  cm. The areas shown in the tables were calculated, based on elevation, from digital elevation models correct to the nearest centimeter.

The amount of land lost to the sea varies by study area because of differences in each area's relative relief, mean shore slope, and the presence or absence of coastal stabilization structures (e.g., seawalls). Heavily developed areas, such as Daytona Beach, Florida, and Galveston, Texas, tend to have abrupt increases in elevation as one travels inland from the beach, and may not experience significant change in the shape of the coast in response to the low and moderate SLR scenarios used in this project; however, they will experience increased rates of coastline recession.

In the absence of hard erosion-prevention structures (e.g., seawalls), the natural process of shoreline recession will insure the continued existence of a beach in study areas with sand lithologies (Brunn 1962; Hands 1976; Dean 1991). In areas with limited sand-sized sediment supplies, such as Caminada Pass, Louisiana, the beaches may be completely removed as has been predicted in this Sect. Thus, the total land lost to the sea for each scenario should provide a good first guess of the possible impact of SLR on each study area; the amount of land lost to the sea by land use type is less precise, as the impact that variations in coastal lithologies may have on beach recession or wetland migration rates were not addressed.

By disregarding the possible migration of land use types in response to SLR, this Sect. has assumed that land use is immobile over time. Because of this, the amount of beach lost to SLR may be overestimated. As the Bruun rule predicts, if left alone and with adequate sediment supplies, a beach will try to maintain a constant profile (and, by extension, size) as sea levels increase. Thus, the amount of land in the "beach" land use class may stay relatively constant over time, whereas the amount of land inland from the beach "lost" from its present land use may actual be greater than predicted in this Sect. (i.e., as the foundations of structures formerly hundreds of meters inland are undermined as the beach is displaced inland). Sect. 5 deals with the question of how physical processes will influence the extent to which the shoreline may migrate inland in response to SLR versus the role that the presence of limiting factors (e.g., seawalls or roads) may have on the ability of the shore to respond to an increase in sea level.

## **4.5 FIGURES**

**Fig. 4.1** Location of geologic basins and arches within the U.S. Southeast.

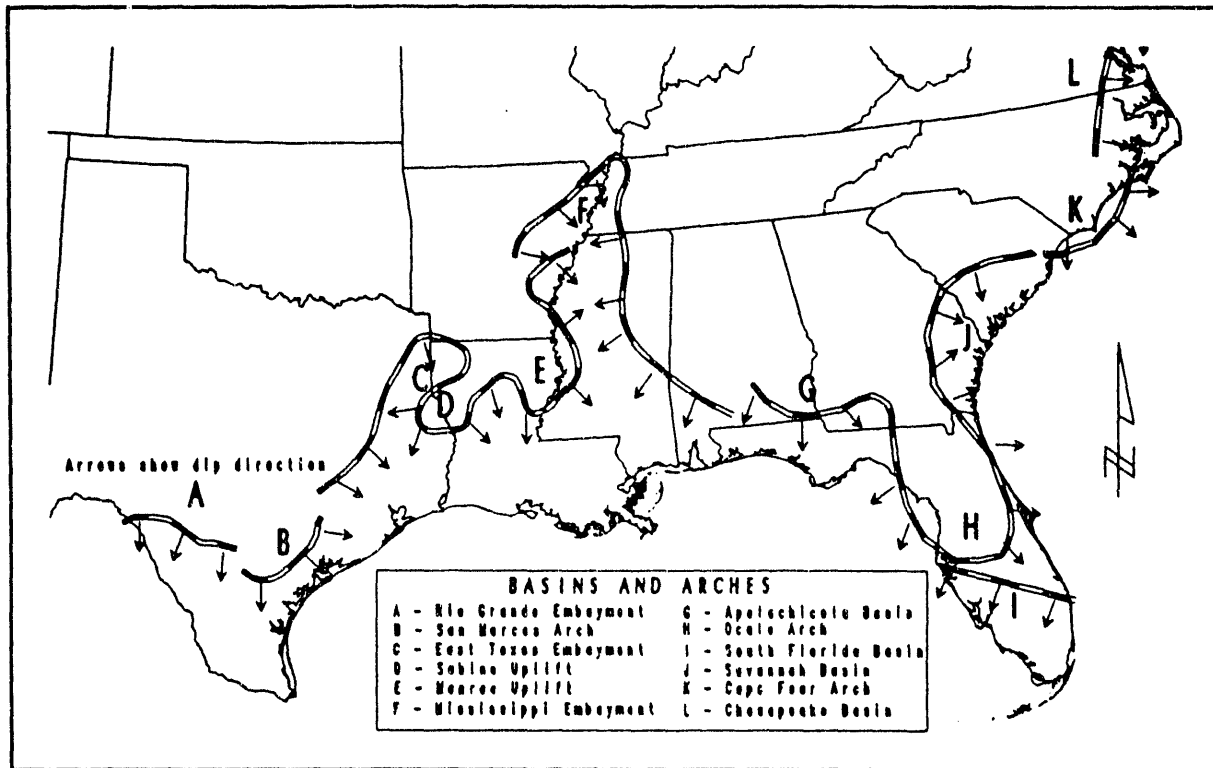


**Fig. 4.2** Population per square kilometer in the coastal counties of Texas, Louisiana, Mississippi, Alabama, and the Gulf coast of Florida (values after 1990 were estimated using linear regression).

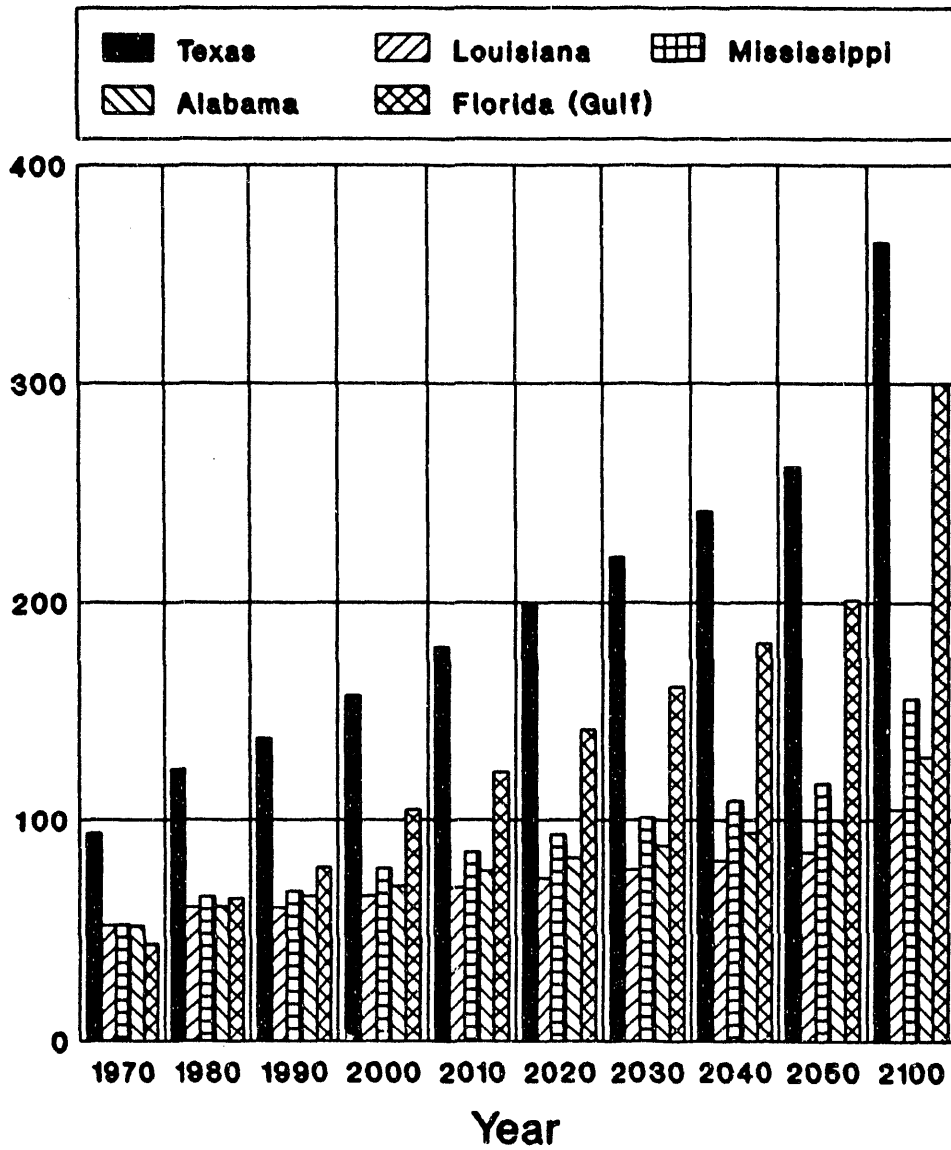


**Fig. 4.3 Galveston County, Texas: population and per capita income (values after 1990 were estimated using linear regression).**

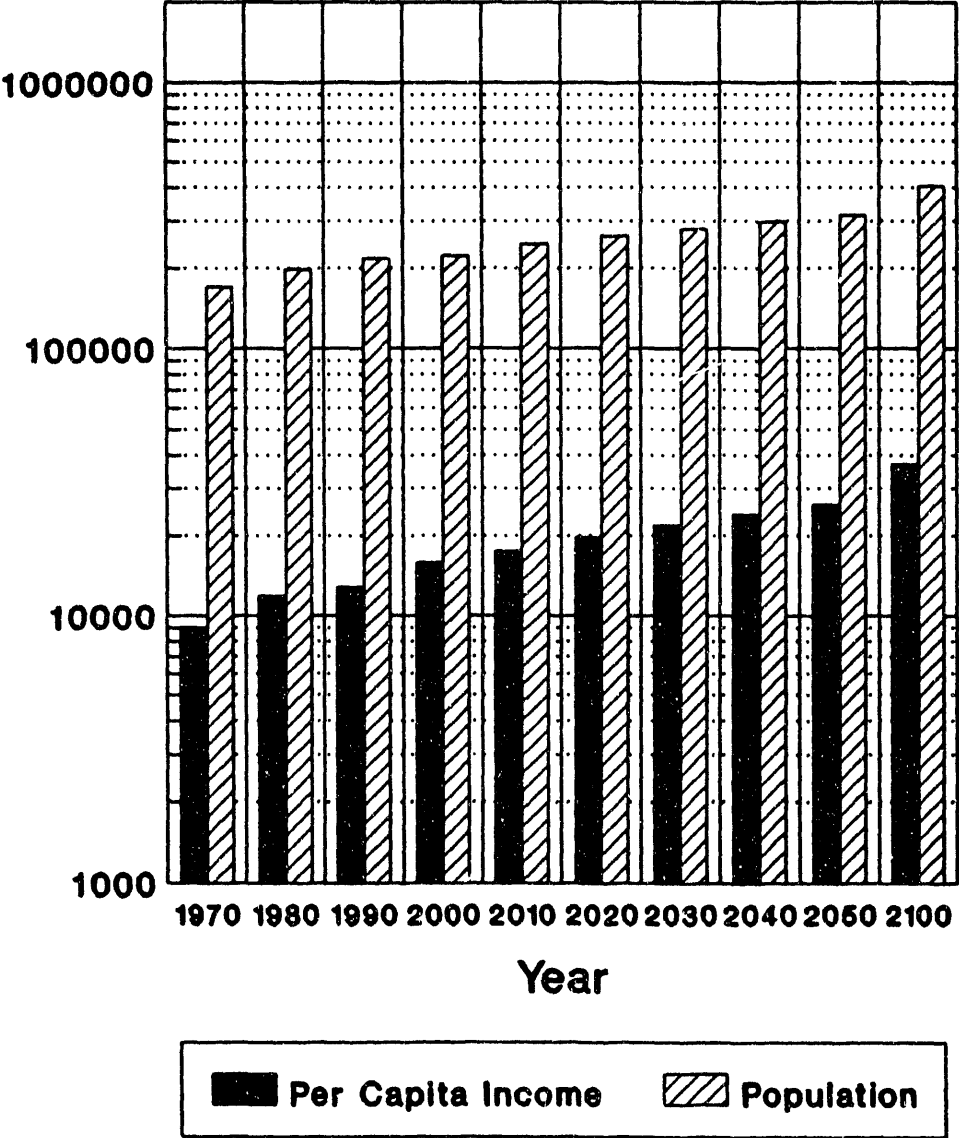


Fig. 4.4 Galveston study area land use map.

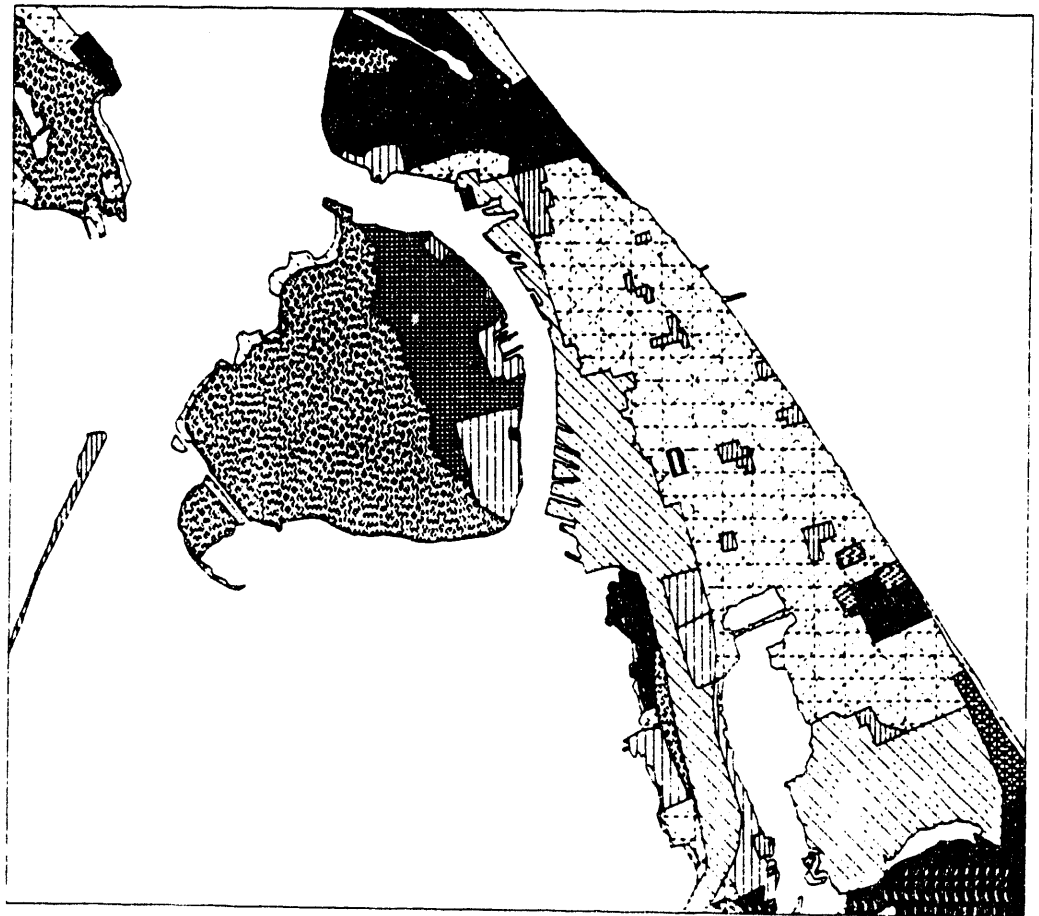
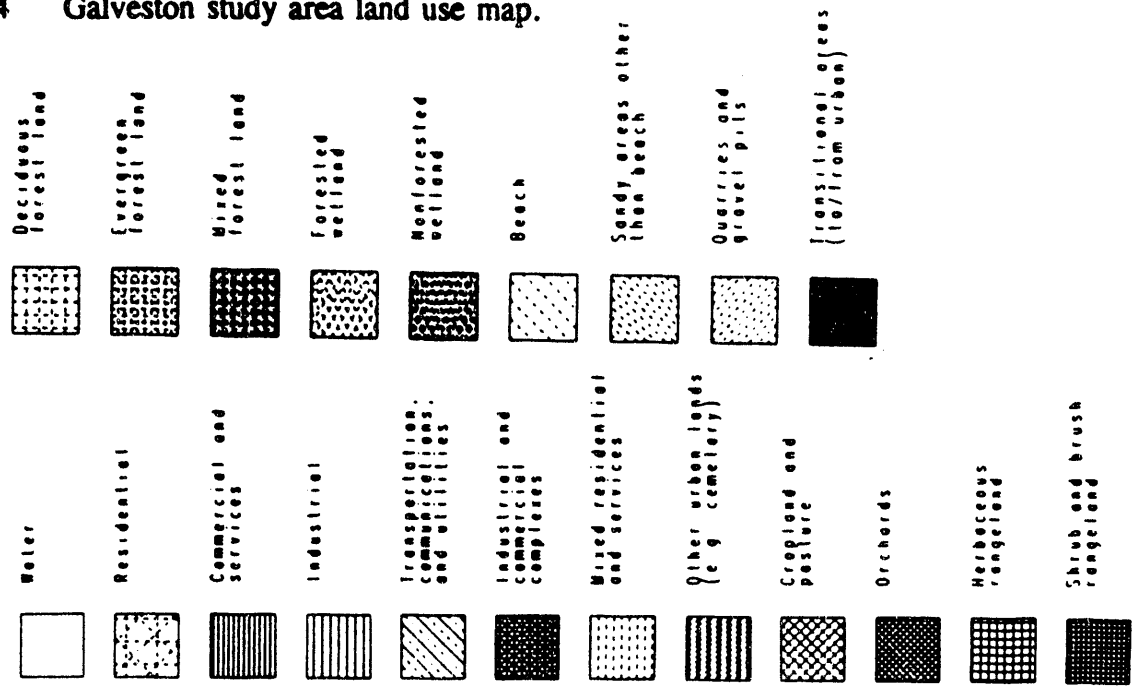


Fig. 4.5 Application of the low sea-level-rise scenario on the Galveston study area. Coastlines shown are for the year 2050 and 2100.

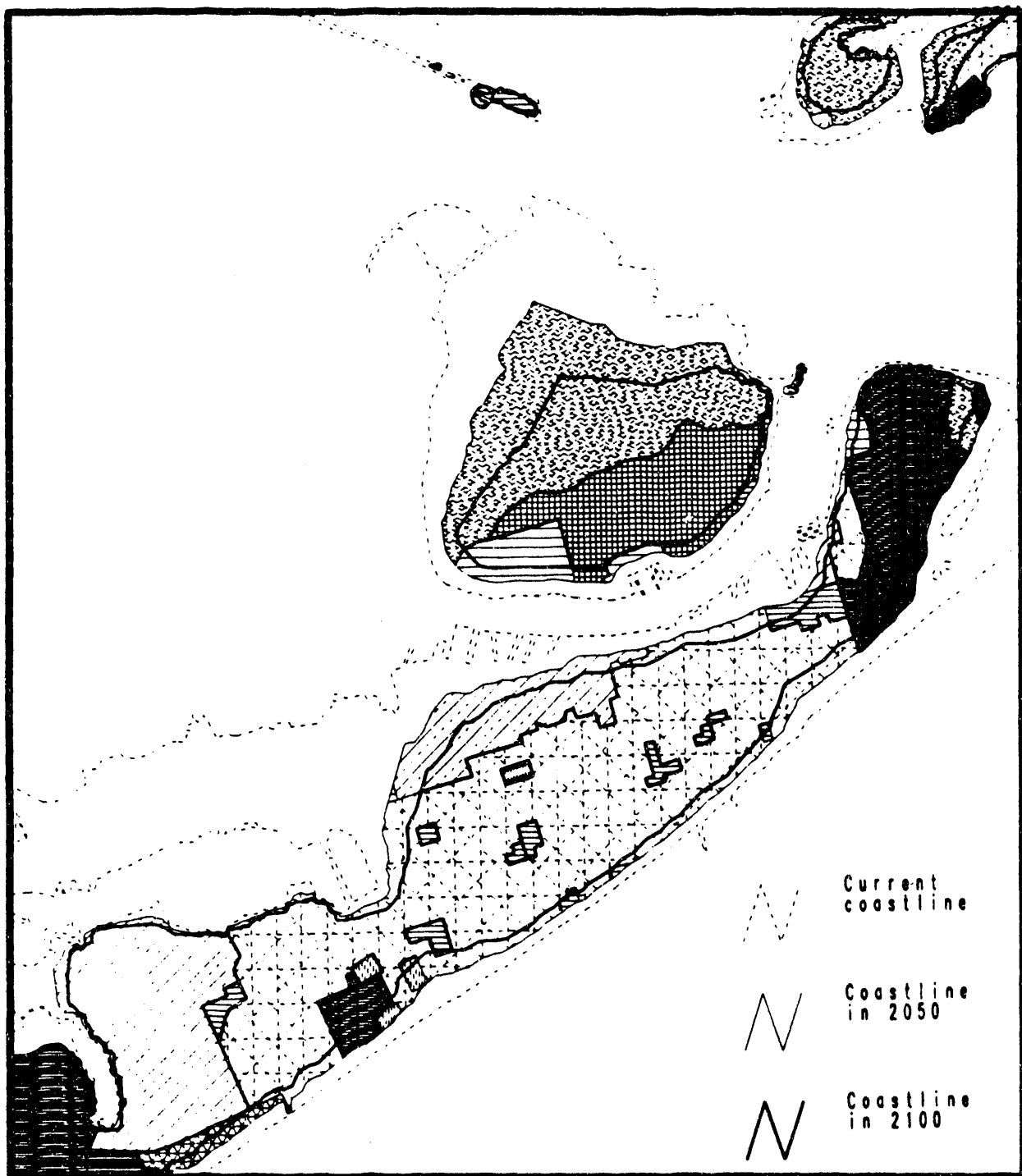




Fig. 4.6 Application of the medium sea-level-rise scenario on the Galveston study area. Coastlines shown are for the year 2050 and 2100.

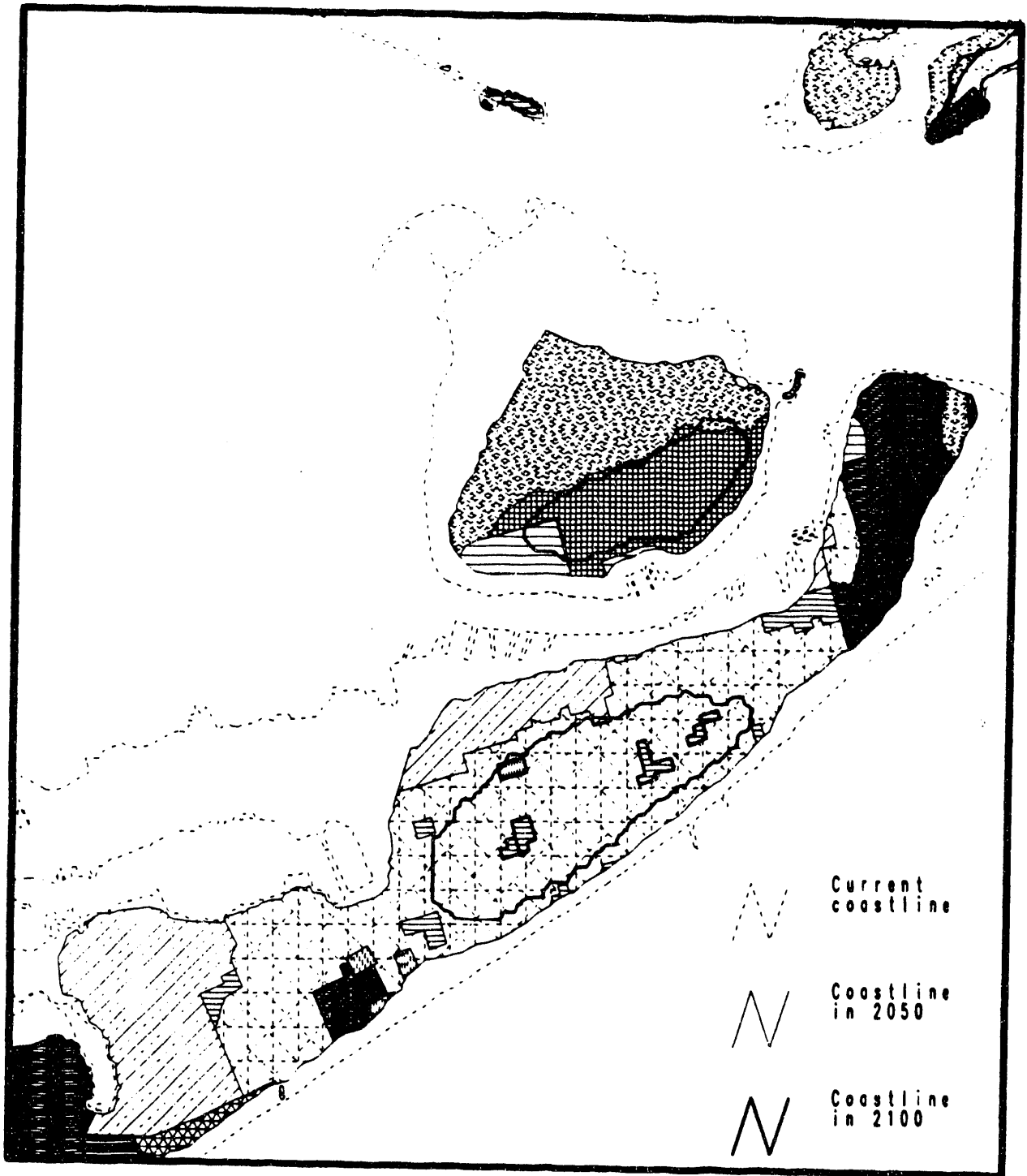
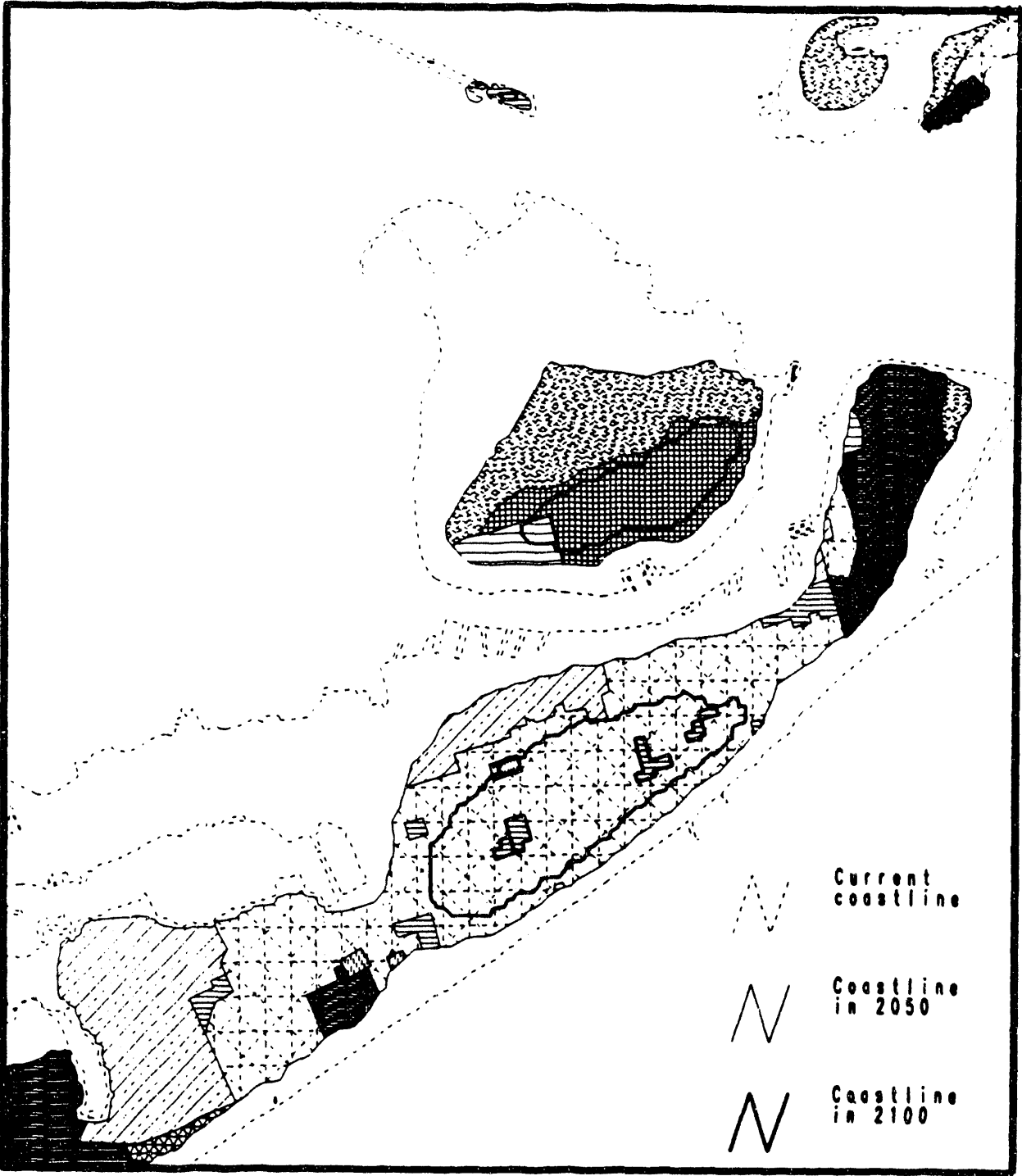


Fig. 4.7 Application of the high sea-level-rise scenario on the Galveston study area. Coastlines shown are for the year 2050 and 2100.



**Fig. 4.8 Jefferson Parish, Louisiana: population and per capita income (values after 1990 were estimated using linear regression).**

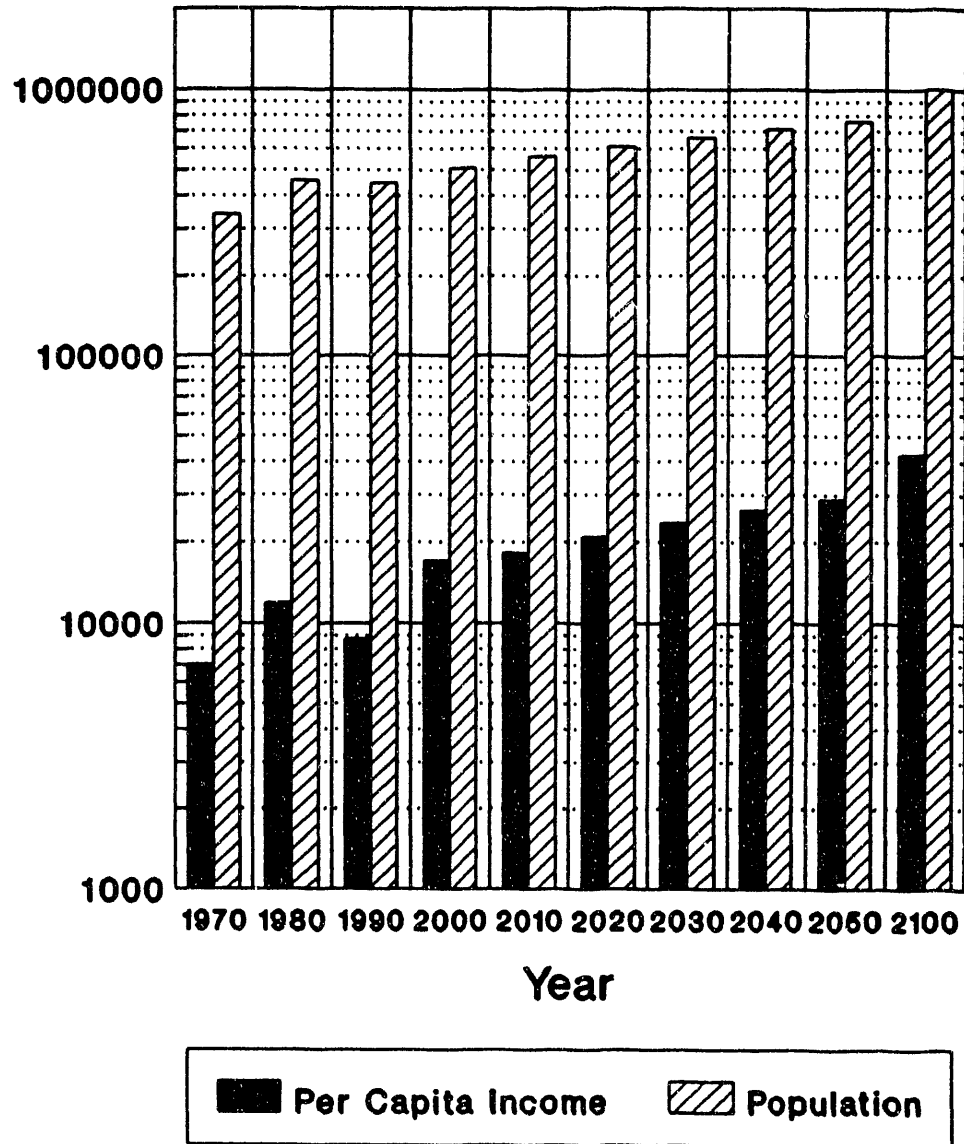


Fig. 4.9 Caminada Pass study area land use map.

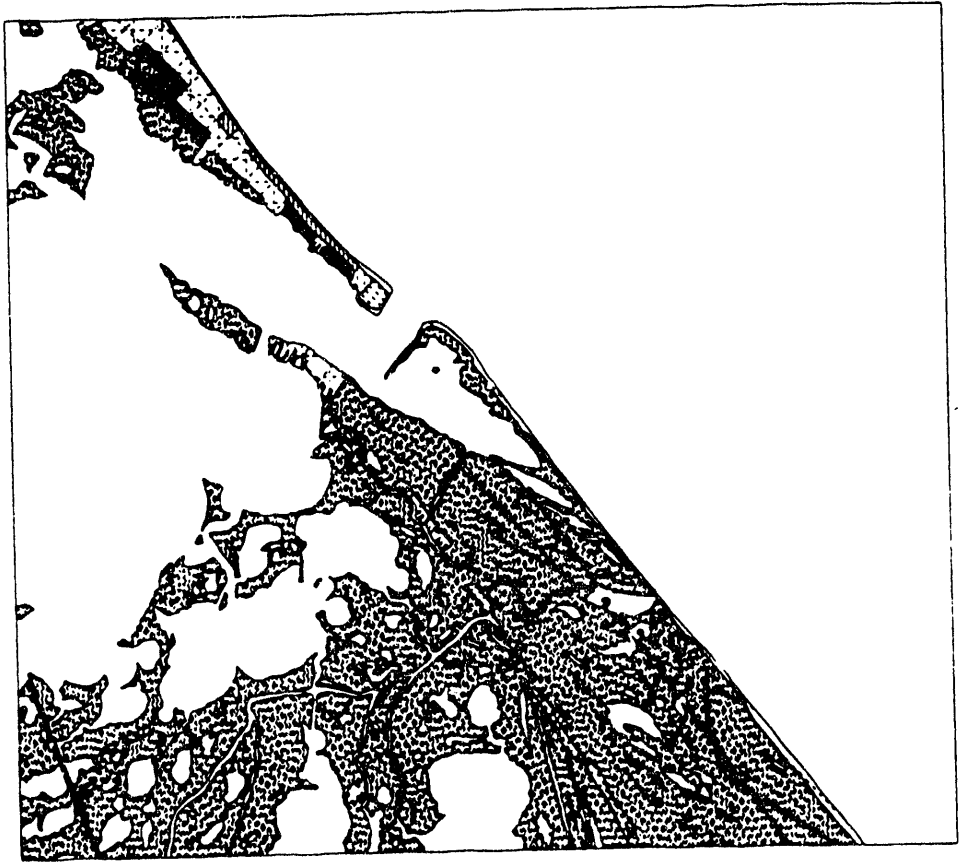
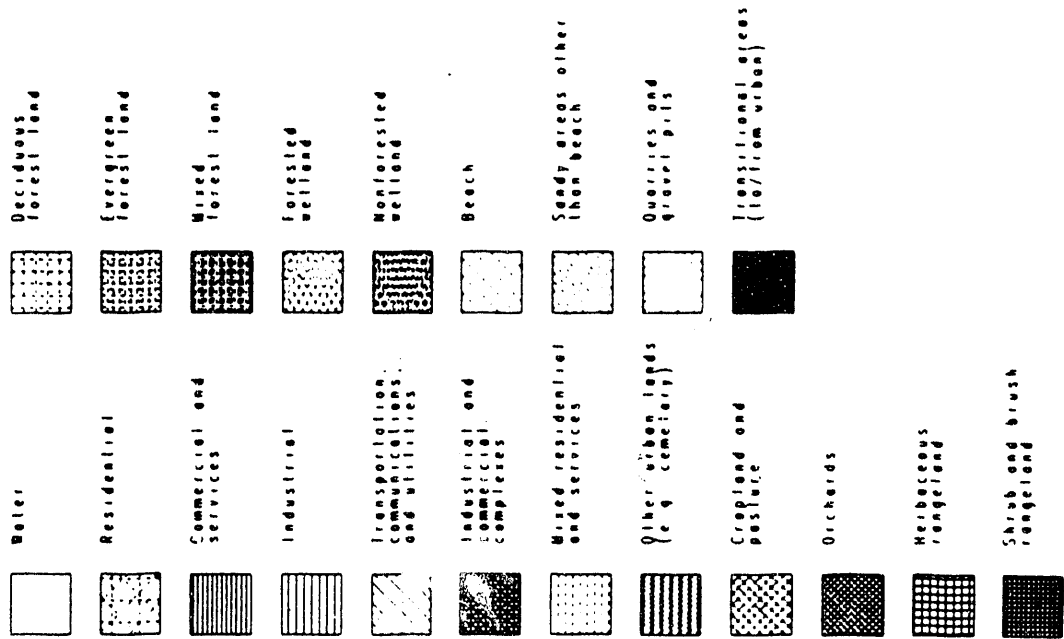


Fig. 4.10 Application of the low sea-level-rise scenario on the Caminada Pass study area. Coastlines shown are for the year 2050 and 2100.

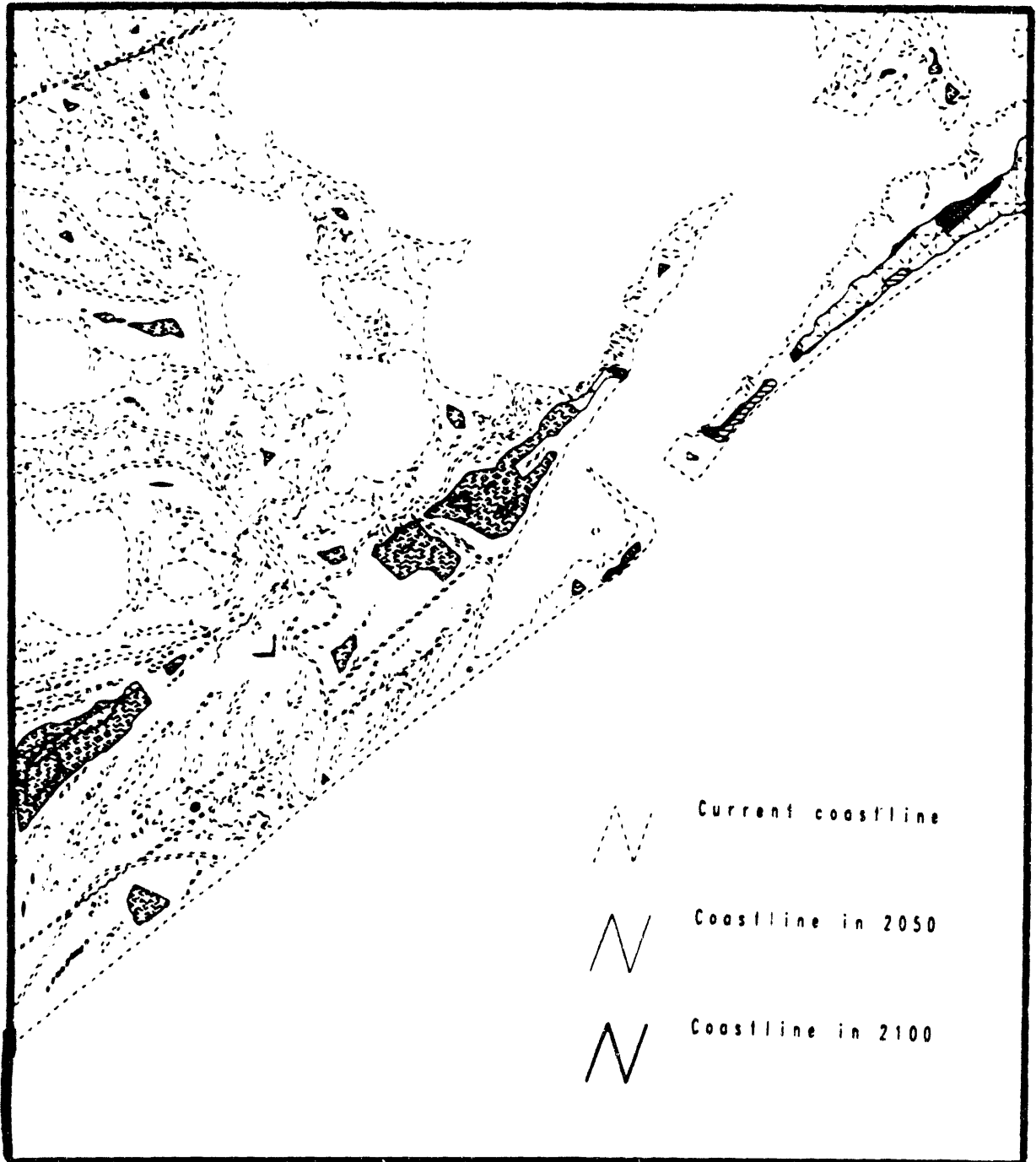


Fig. 4.11 Application of the medium sea-level-rise scenario on the Caminada Pass study area. Coastlines shown are for the year 2050 and 2100.

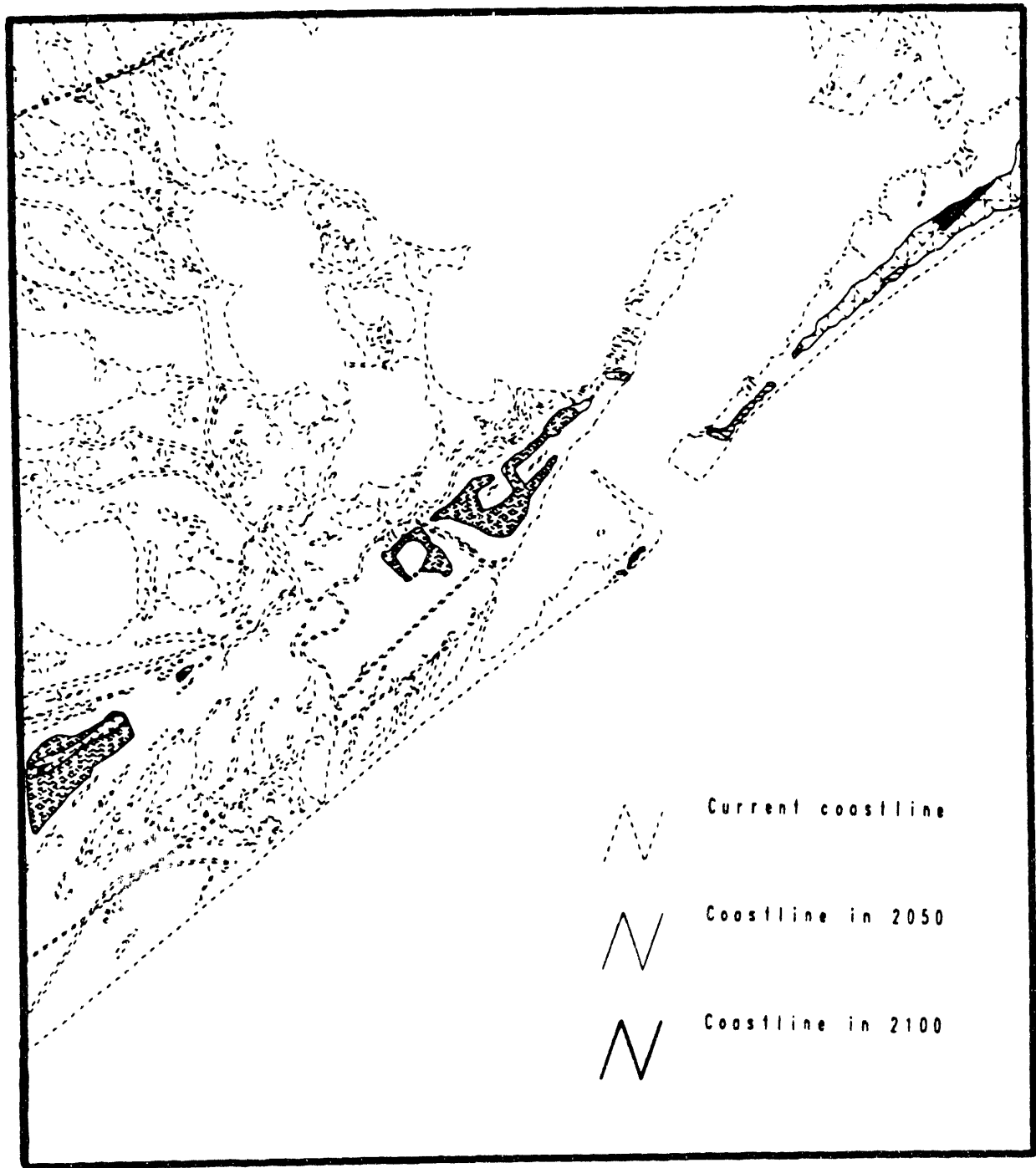
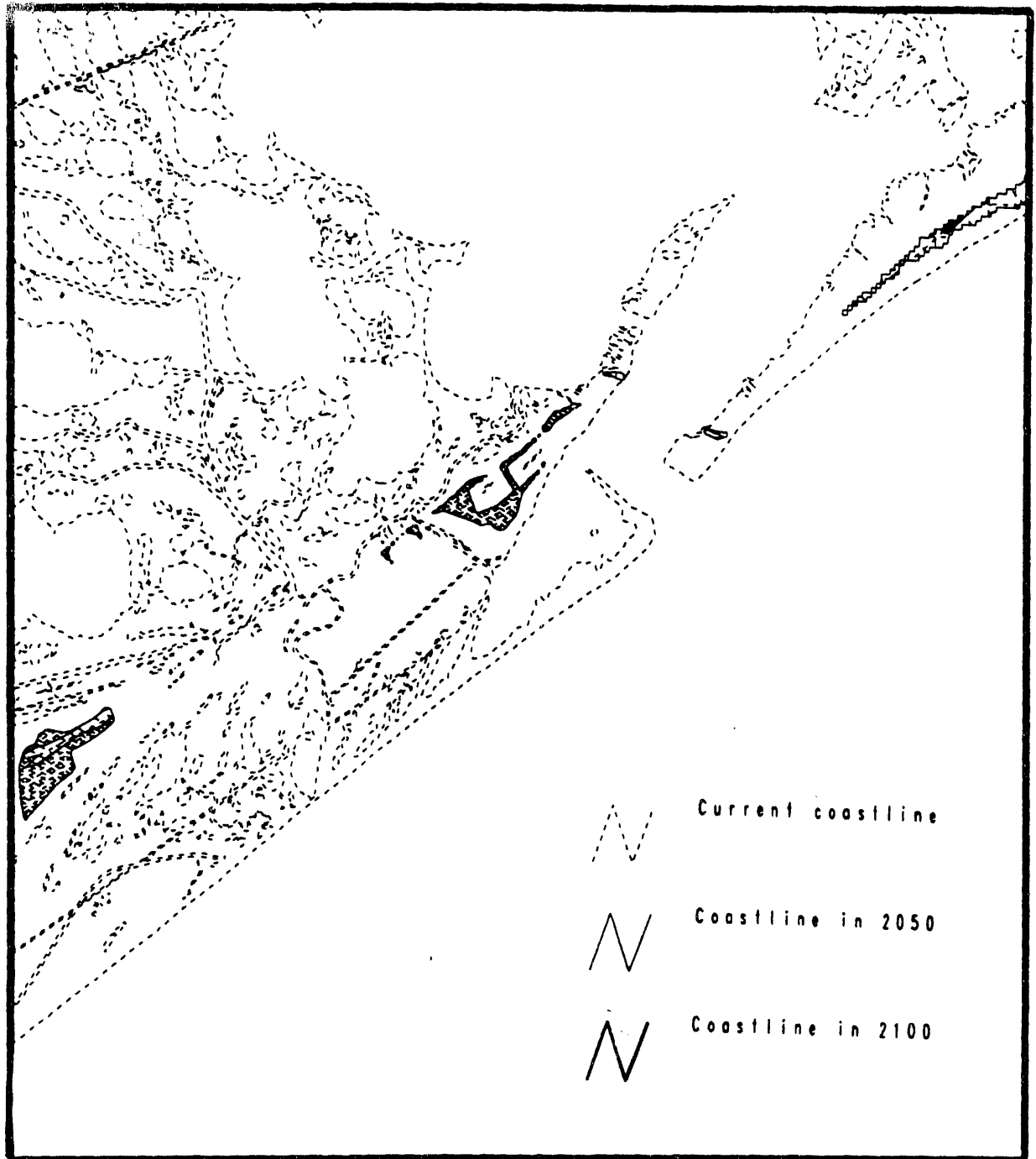


Fig. 4.12 Application of the high sea-level-rise scenario on the Caminada Pass study area. Coastlines shown are for the year 2050 and 2100.



**Fig. 4.13 Manatee County, Florida: population and per capita income (values after 1990 were estimated using linear regression).**

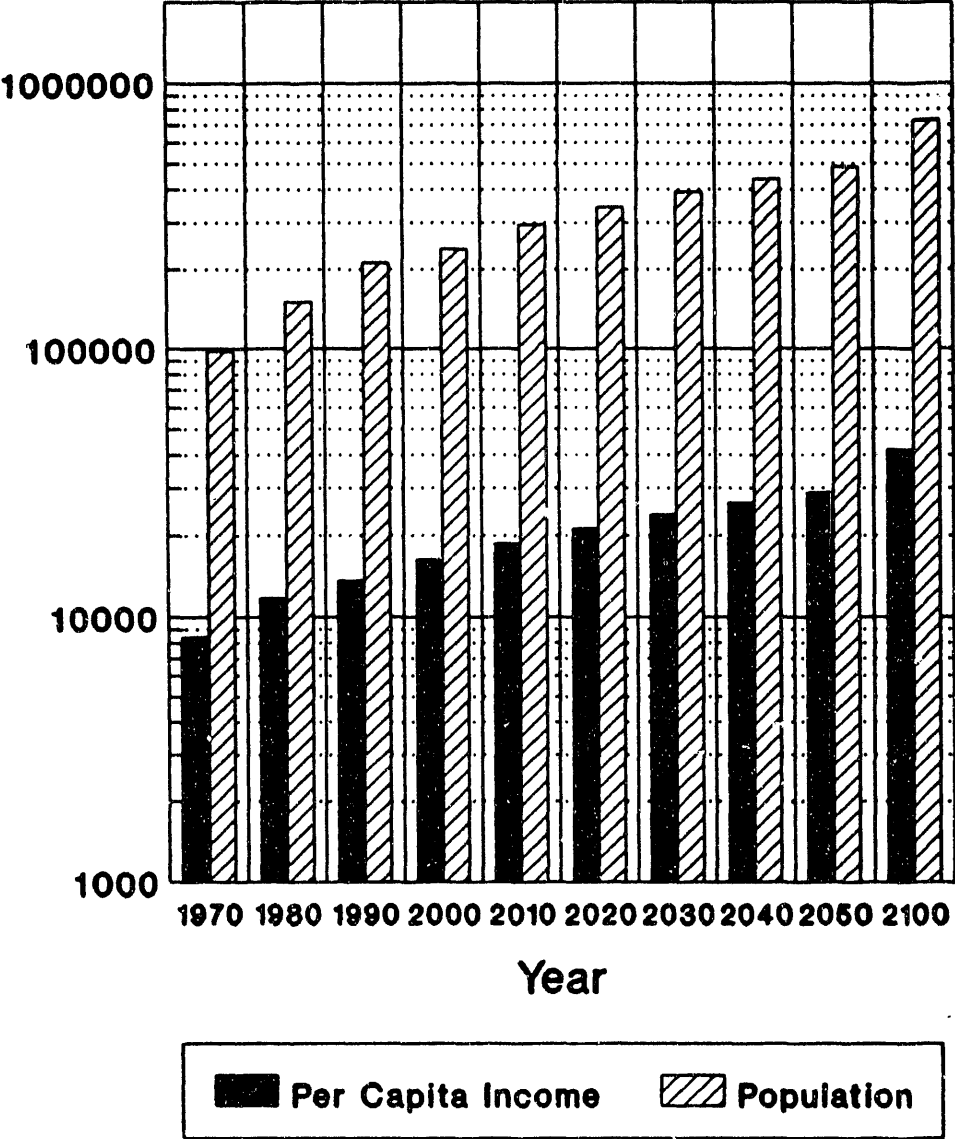




Fig. 4.14 Bradenton Beach study area land use map.

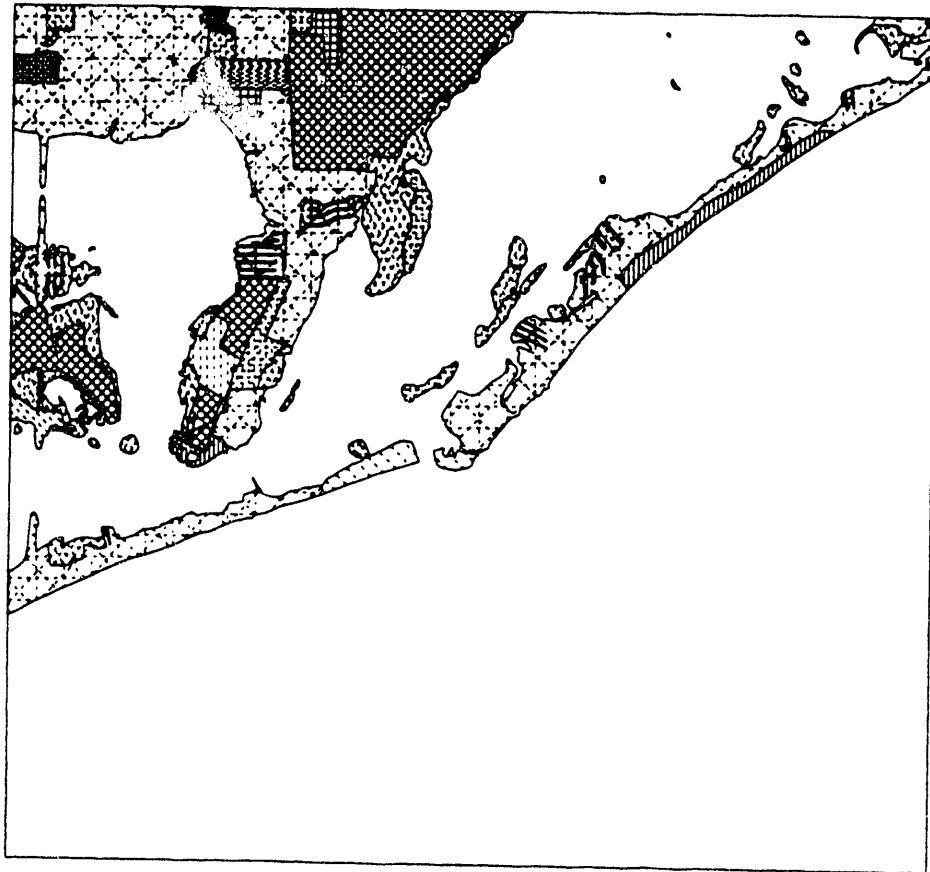
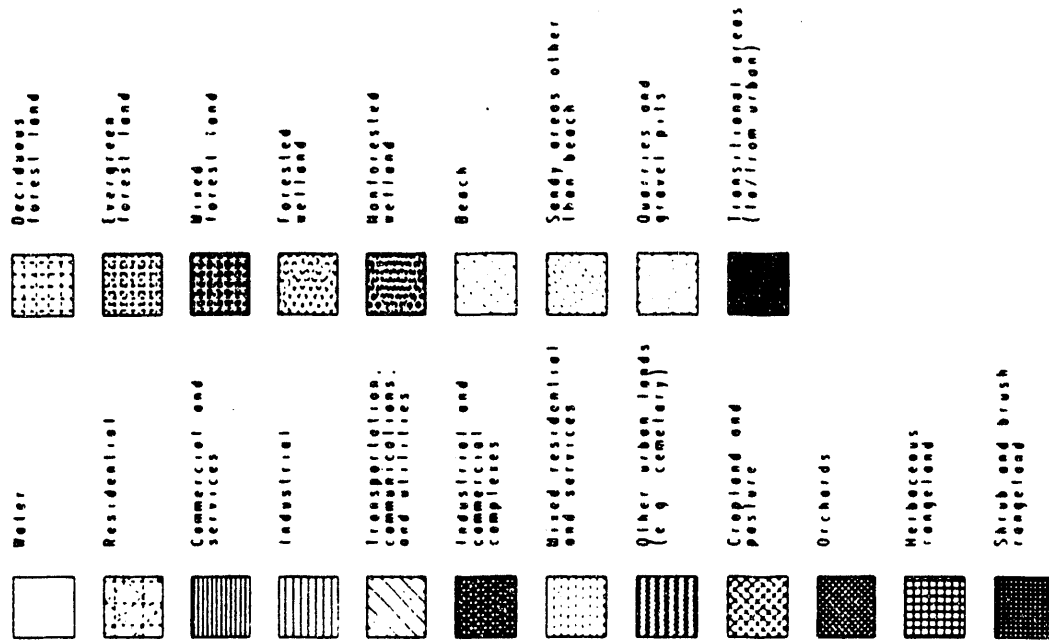


Fig. 4.15 Application of the low sea-level-rise scenario on the Bradenton Beach study area. Coastlines shown are for the year 2050 and 2100.

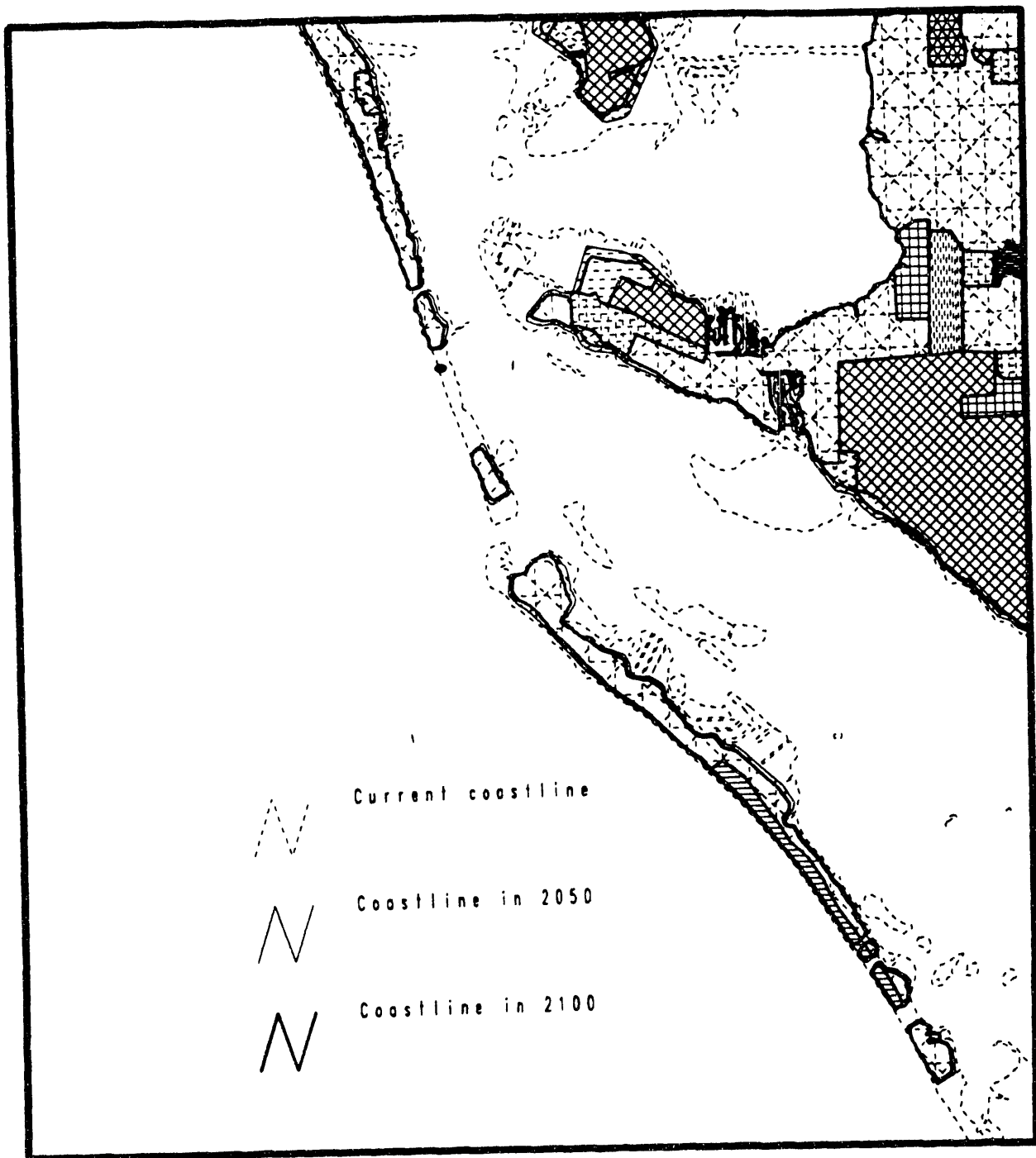


Fig. 4.16 Application of the medium sea-level-rise scenario on the Bradenton Beach study area. Coastlines shown are for the year 2050 and 2100.

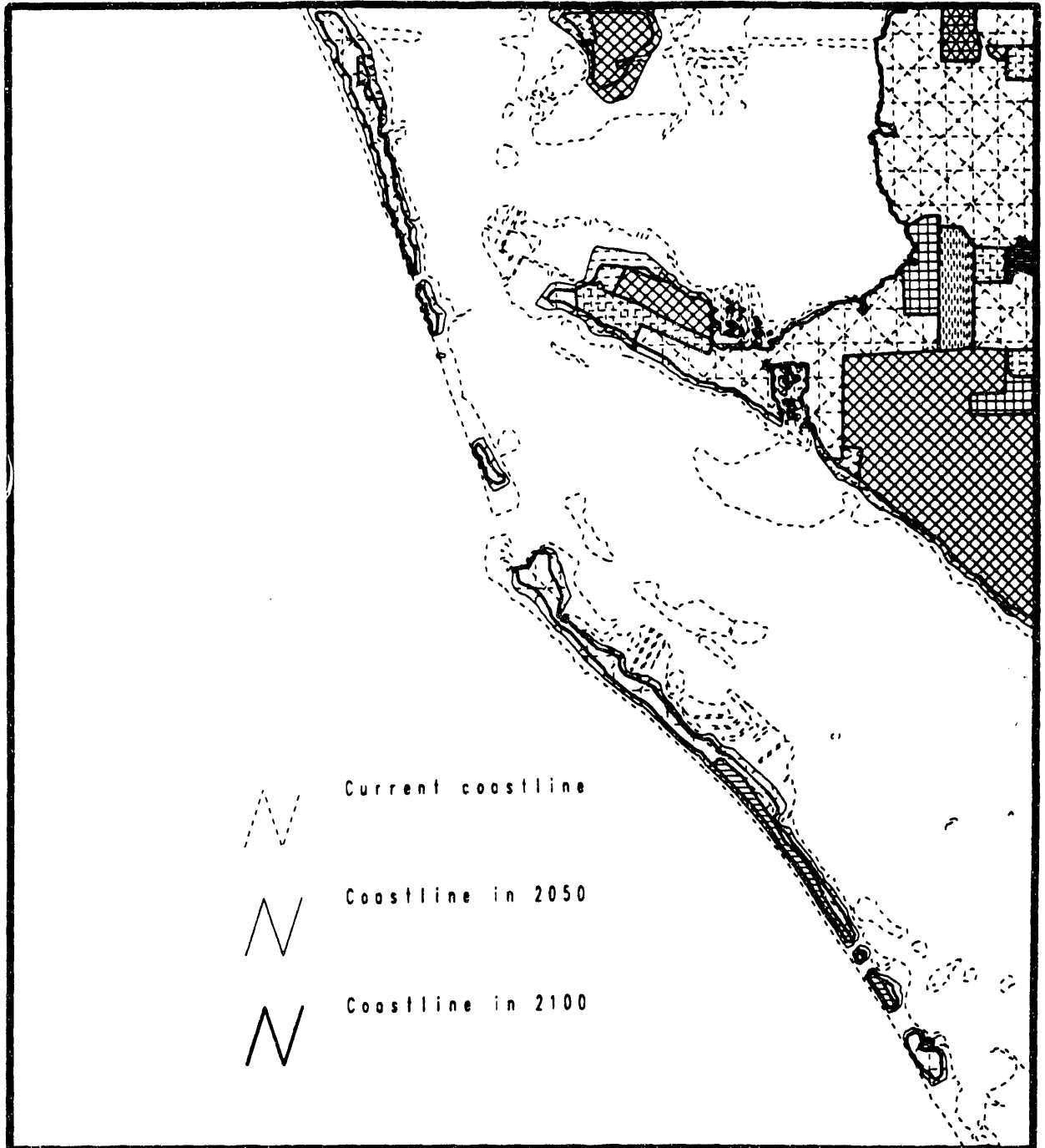
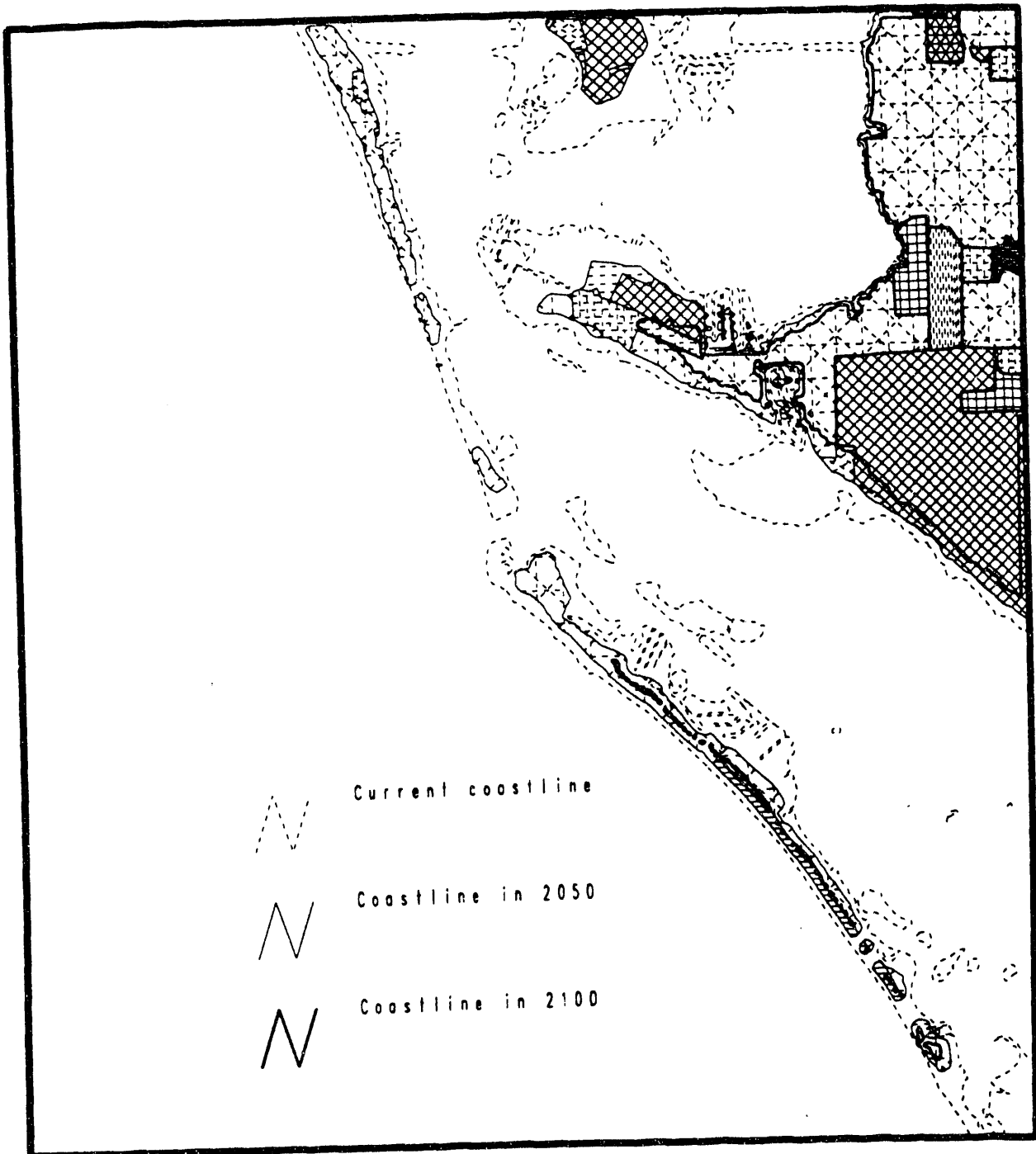
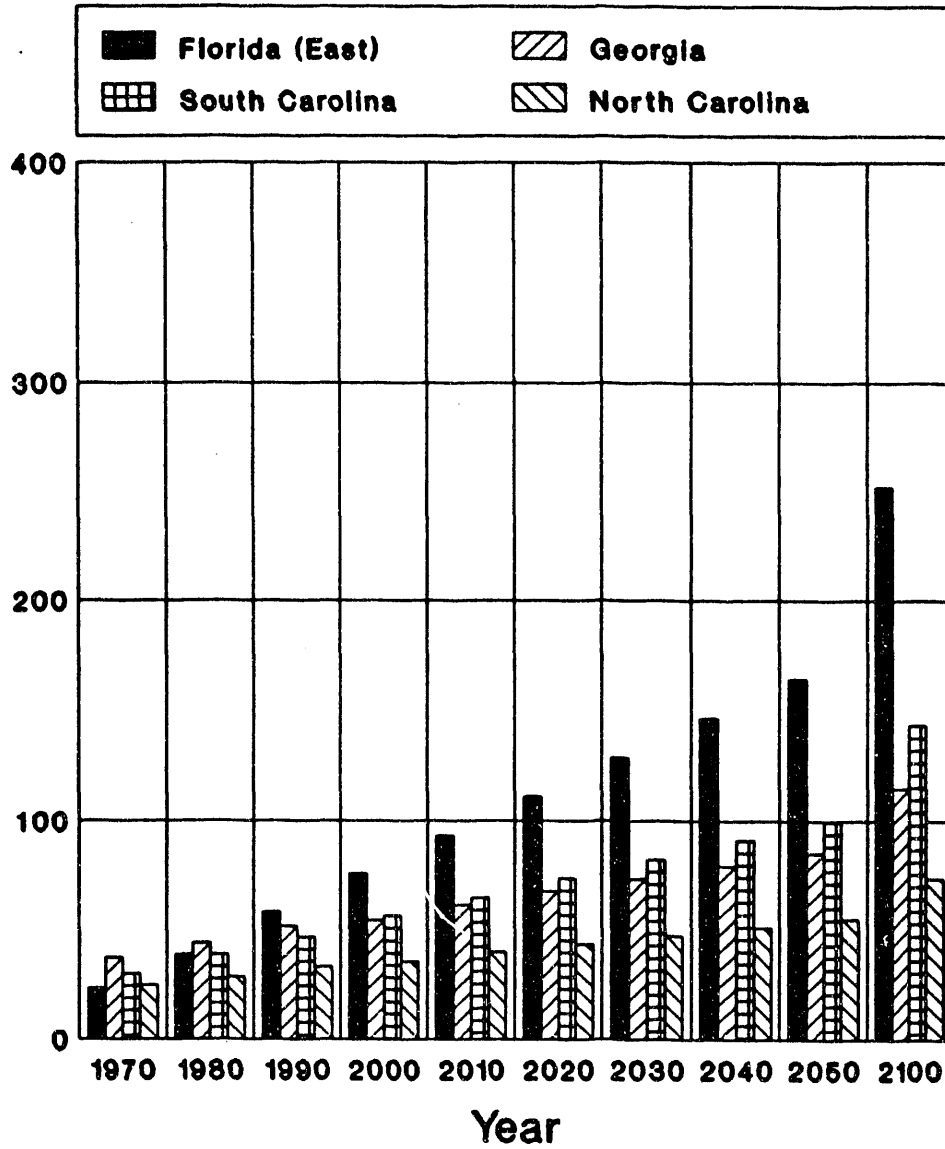


Fig. 4.17 Application of the high sea-level-rise scenario on the Bradenton Beach study area. Coastlines shown are for the year 2050 and 2100.



**Fig. 4.18** Population per square kilometer in the coastal counties of North Carolina, South Carolina, Georgia, and the Atlantic coast of Florida (values after 1990 were estimated using linear regression).



**Fig. 4.19 Volusia County, Florida: population and per capita income (values after 1990 were estimated using linear regression).**

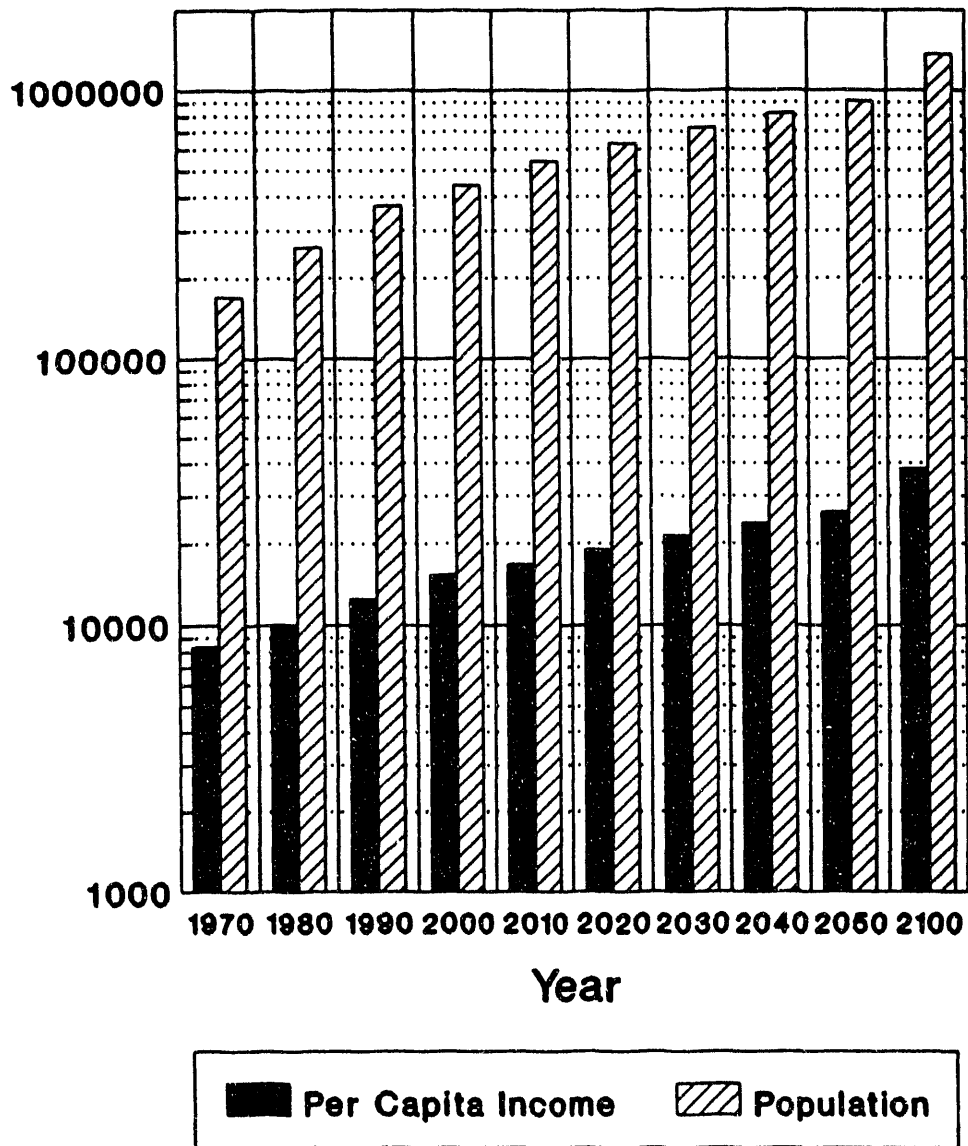


Fig. 4.20 Daytona Beach study area land use map.

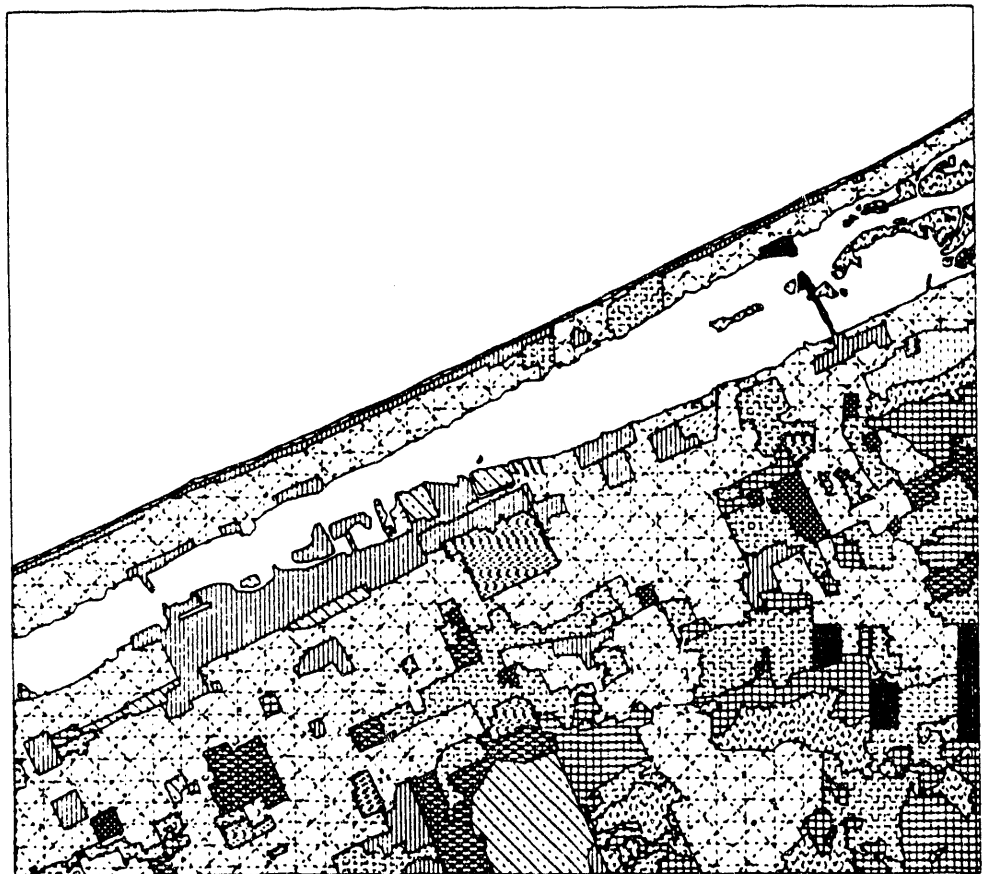
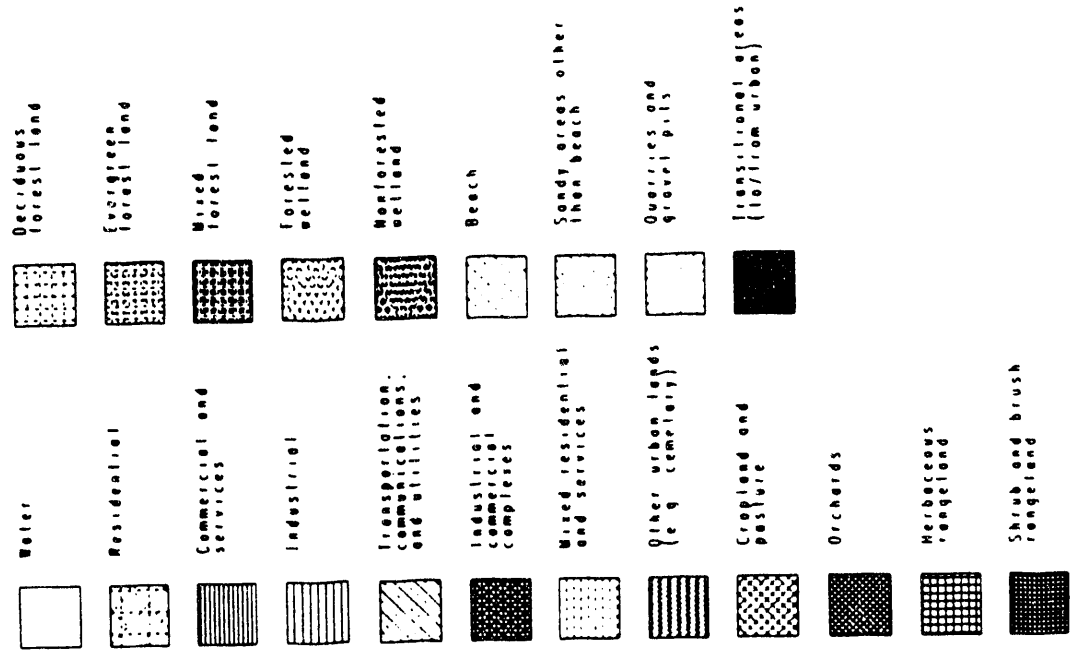


Fig. 4.21 Application of the low sea-level-rise scenario on the Daytona Beach study area. Coastlines shown are for the year 2050 and 2100.

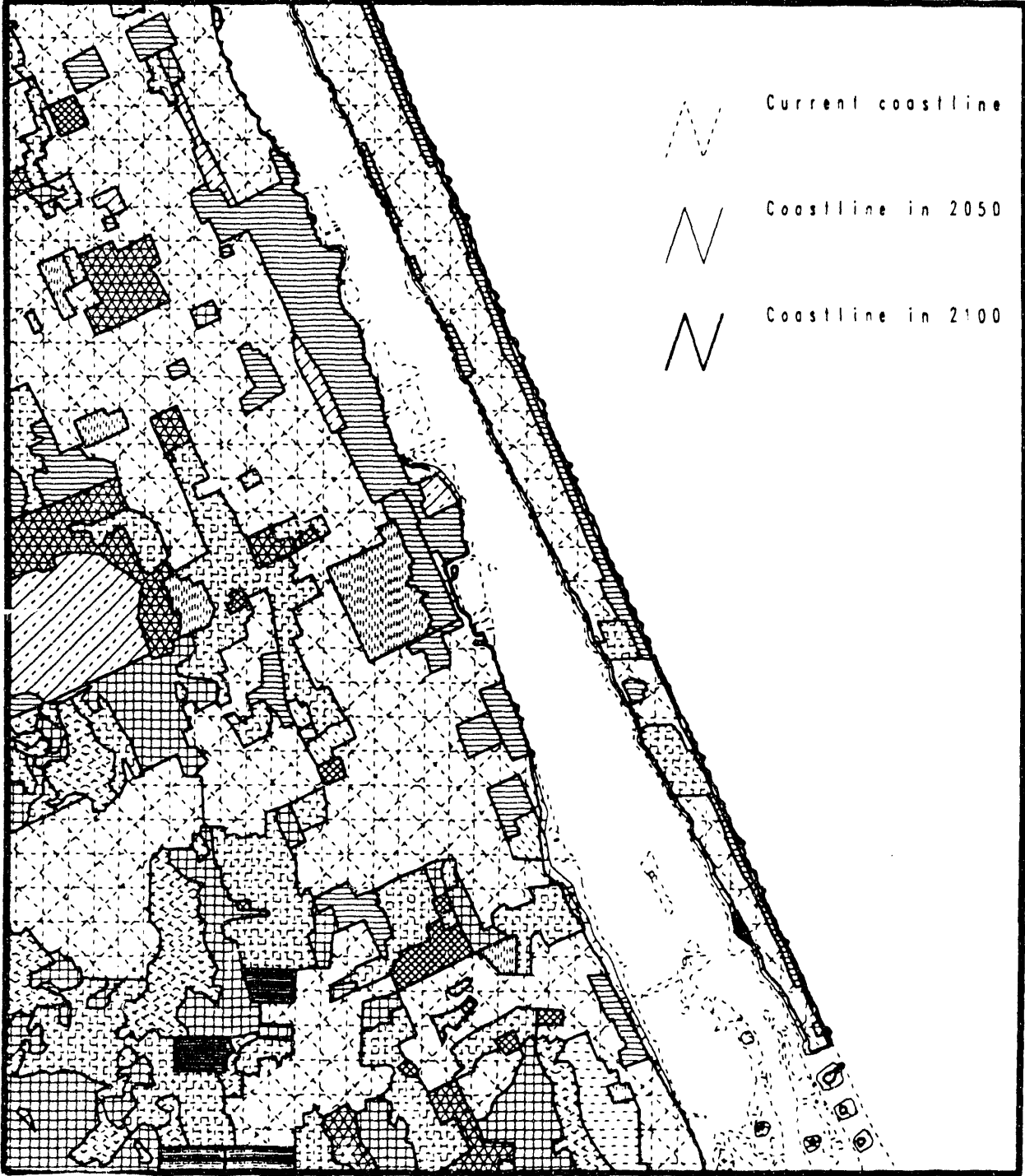




Fig. 4.22 Application of the medium sea-level-rise scenario on the Daytona Beach study area. Coastlines shown are for the year 2050 and 2100.

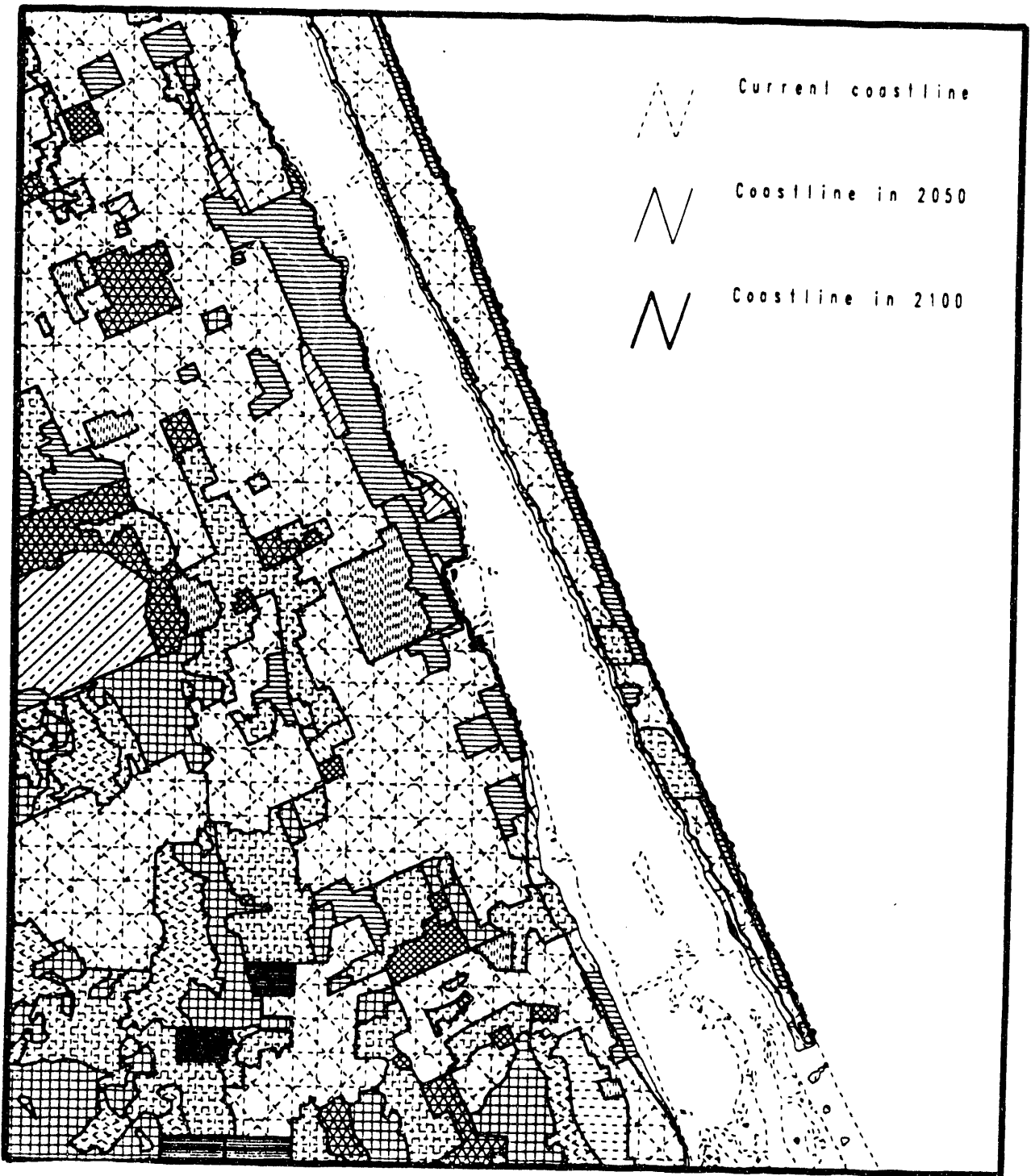
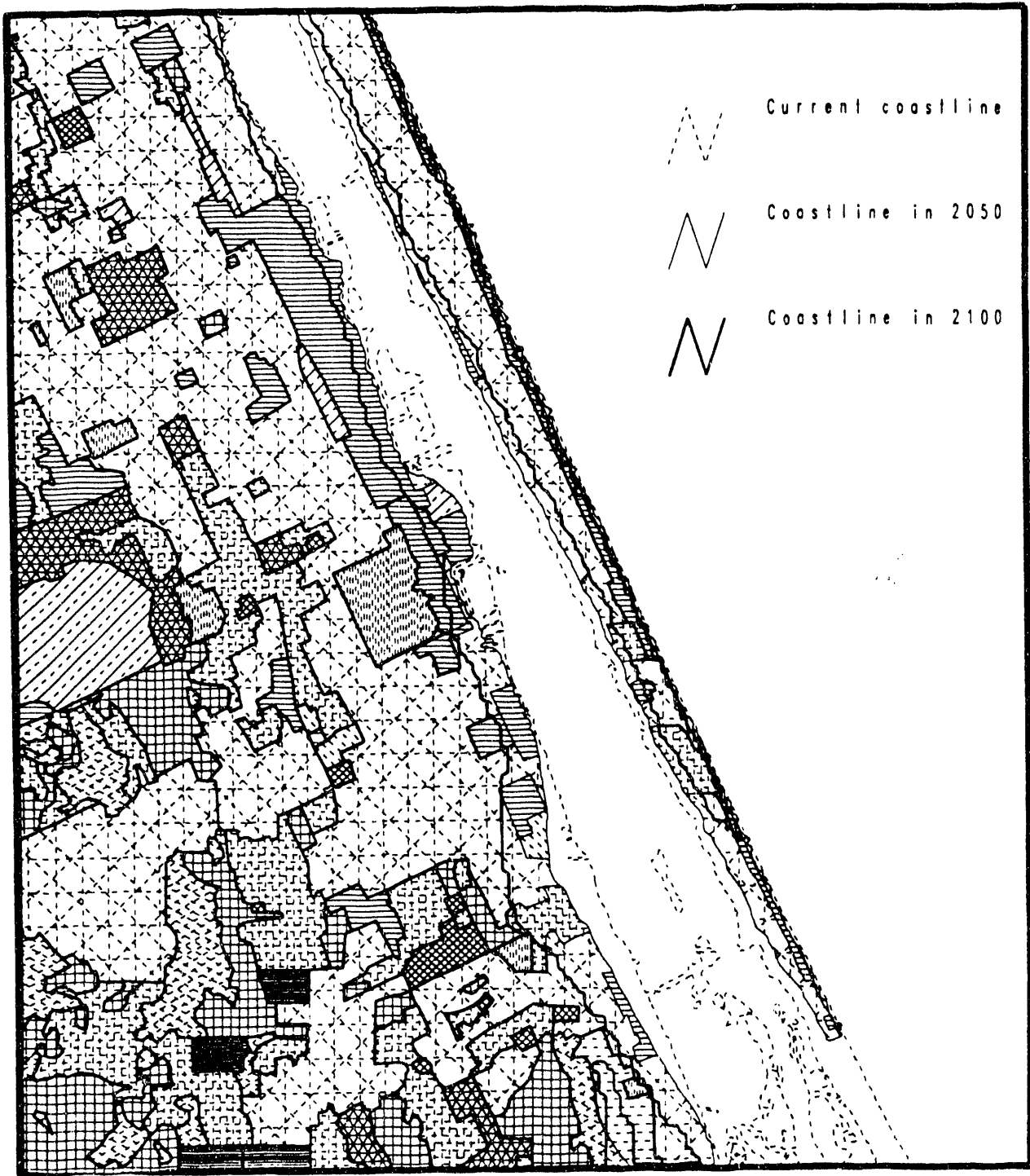


Fig. 4.23 Application of the high sea-level-rise scenario on the Daytona Beach study area. Coastlines shown are for the year 2050 and 2100.



**Fig. 4.24 Charleston County, South Carolina: population and per capita income (values after 1990 were estimated using linear regression).**

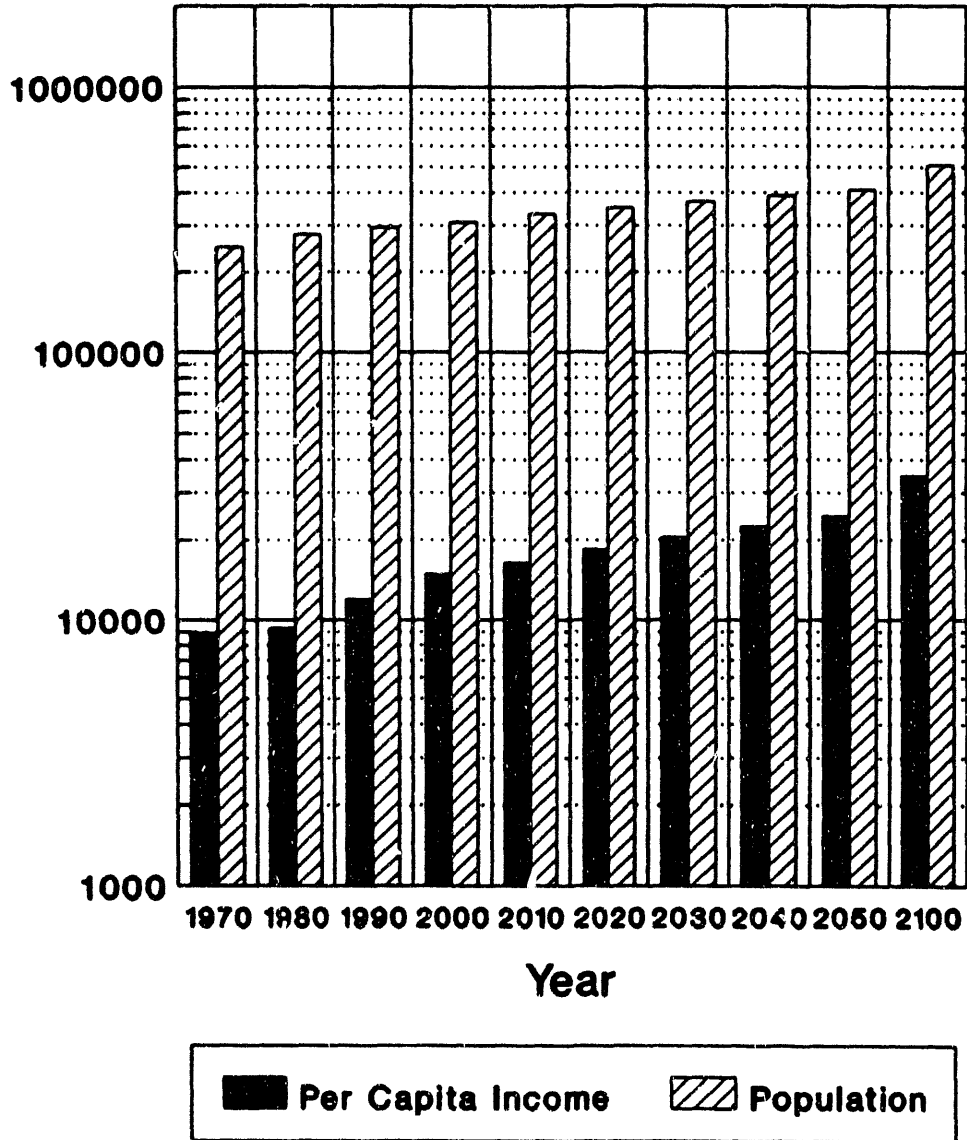


Fig. 4.25 McClellanville study area land use map.

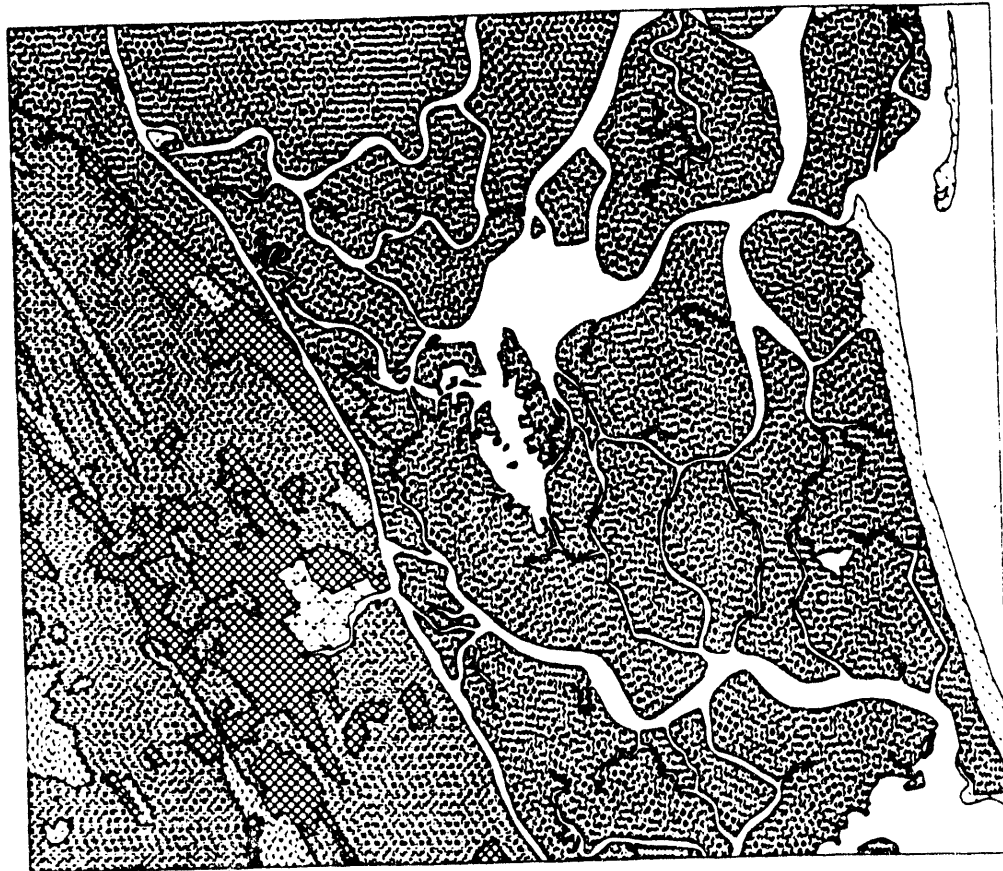
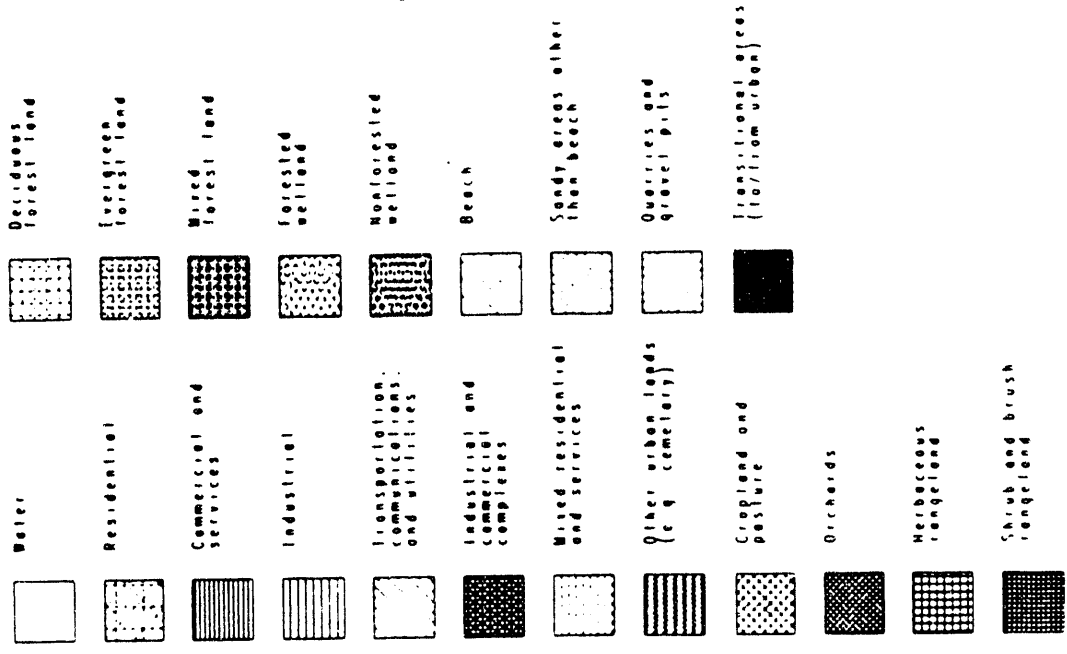


Fig. 4.26 Application of the low sea-level-rise scenario on the McClellanville study area. Coastlines shown are for the year 2050 and 2100.

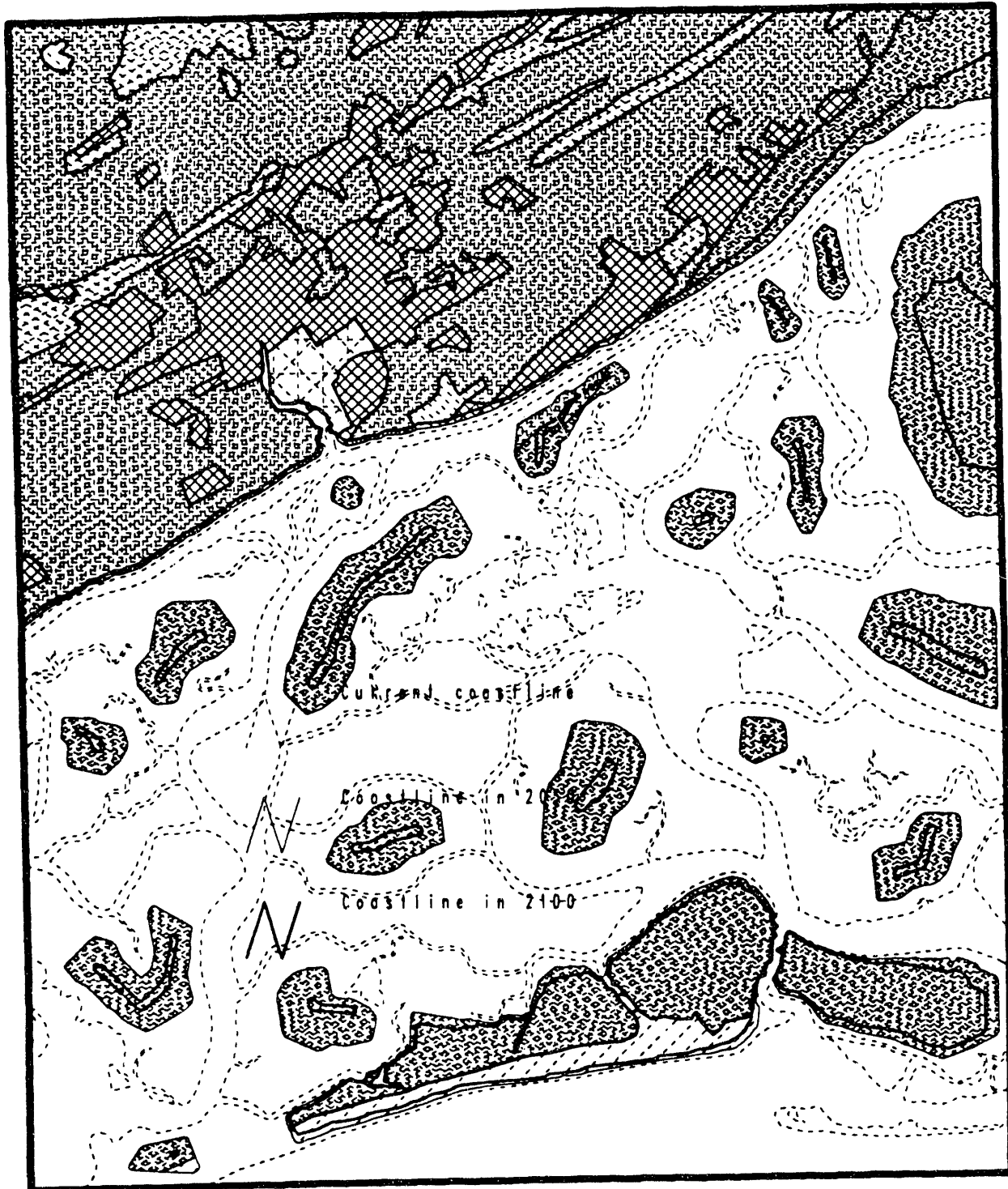


Fig. 4.27 Application of the medium sea-level-rise scenario on the McClellanville study area. Coastlines shown are for the year 2050 and 2100.

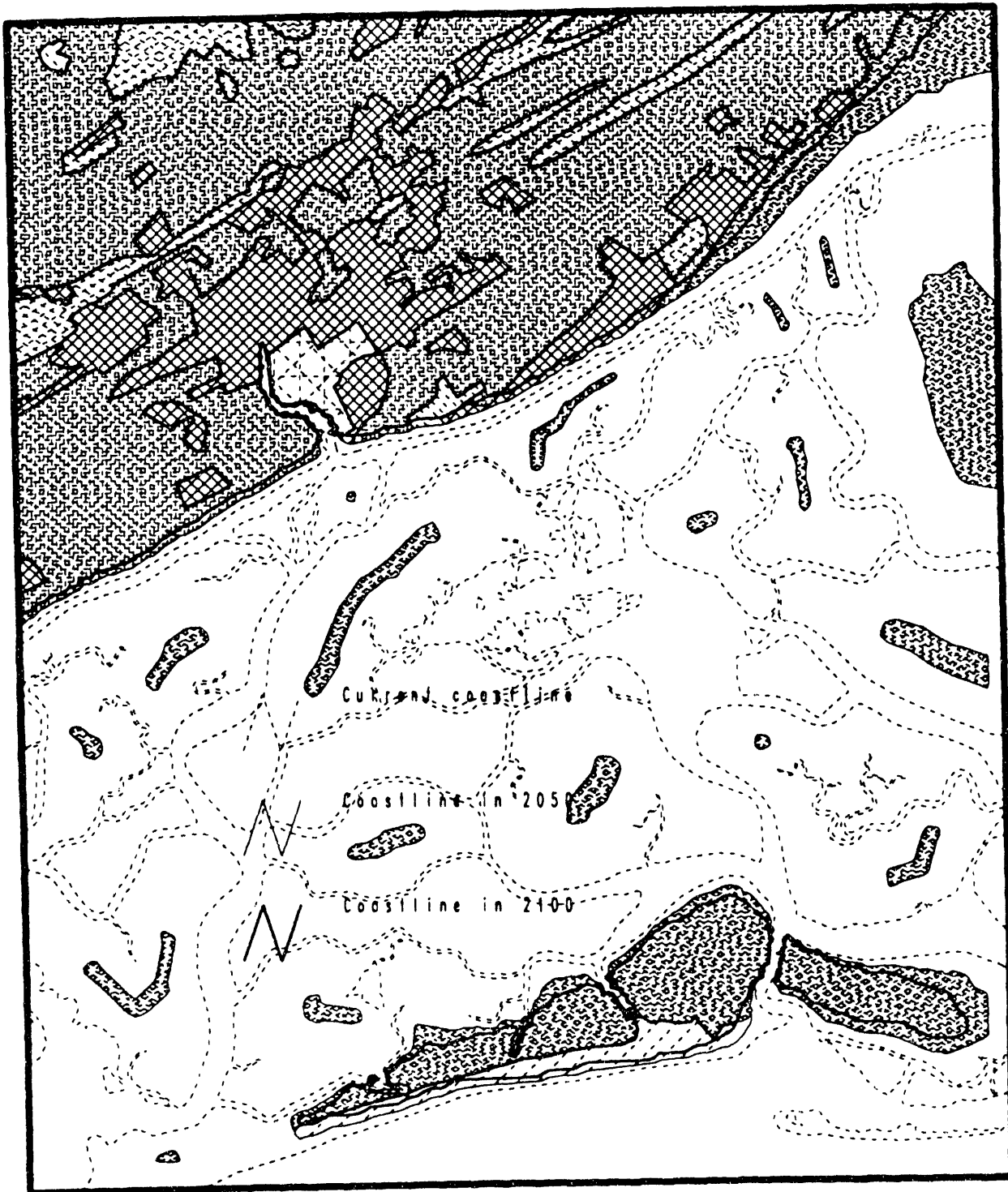
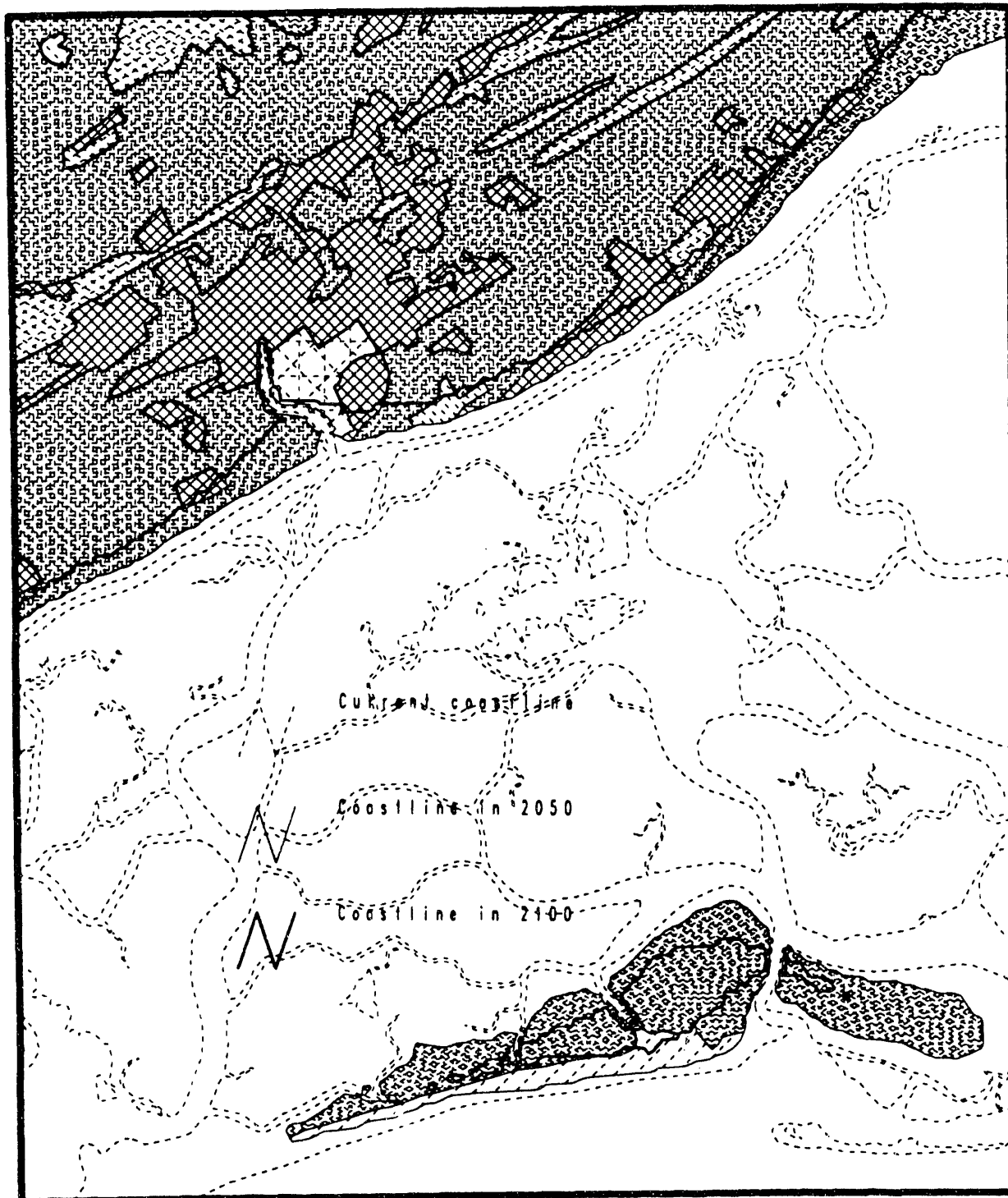


Fig. 4.28 Application of the high sea-level-rise scenario on the McClellanville study area. Coastlines shown are for the year 2050 and 2100.



**Fig. 4.29** Dare County, North Carolina: population and per capita income (values after 1990 were estimated using linear regression).

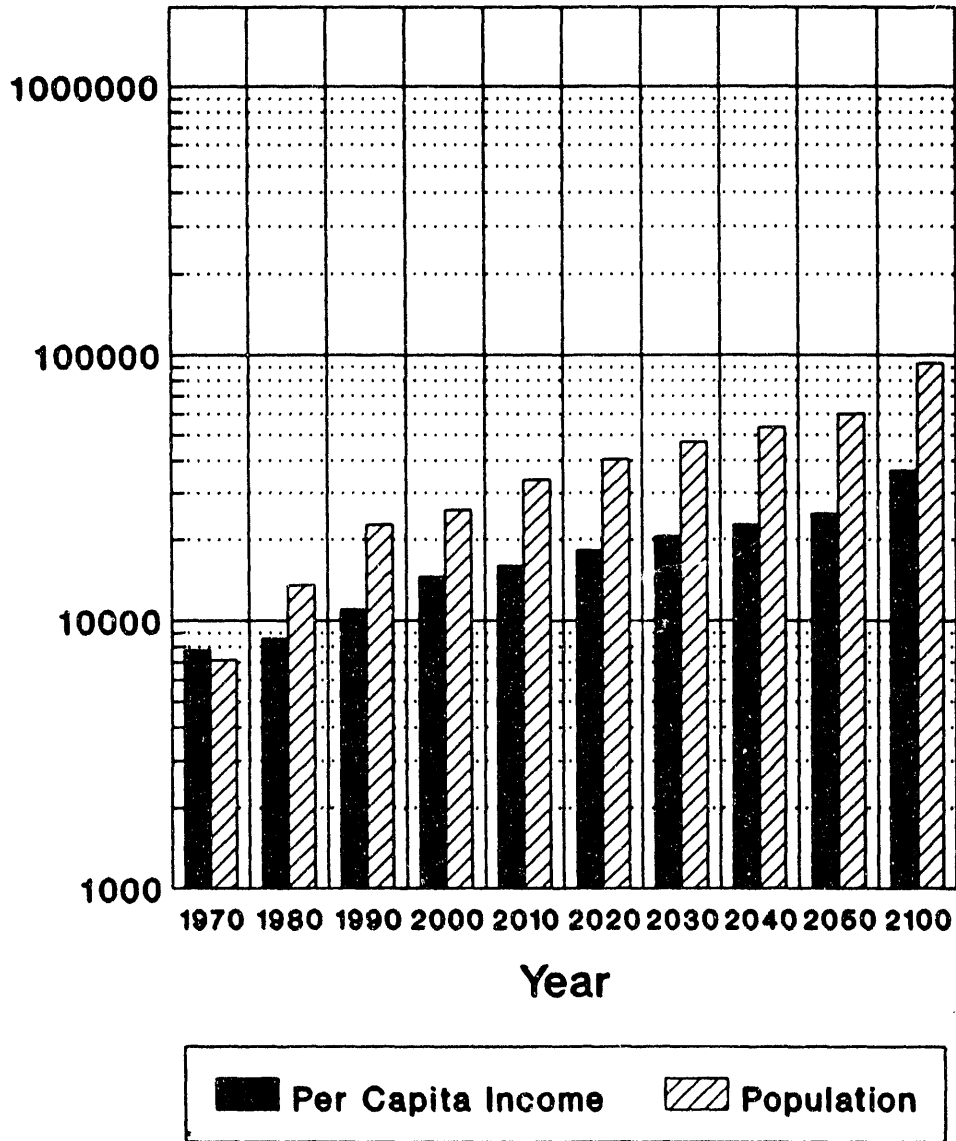




Fig. 4.30 Nags Head study area land use map.

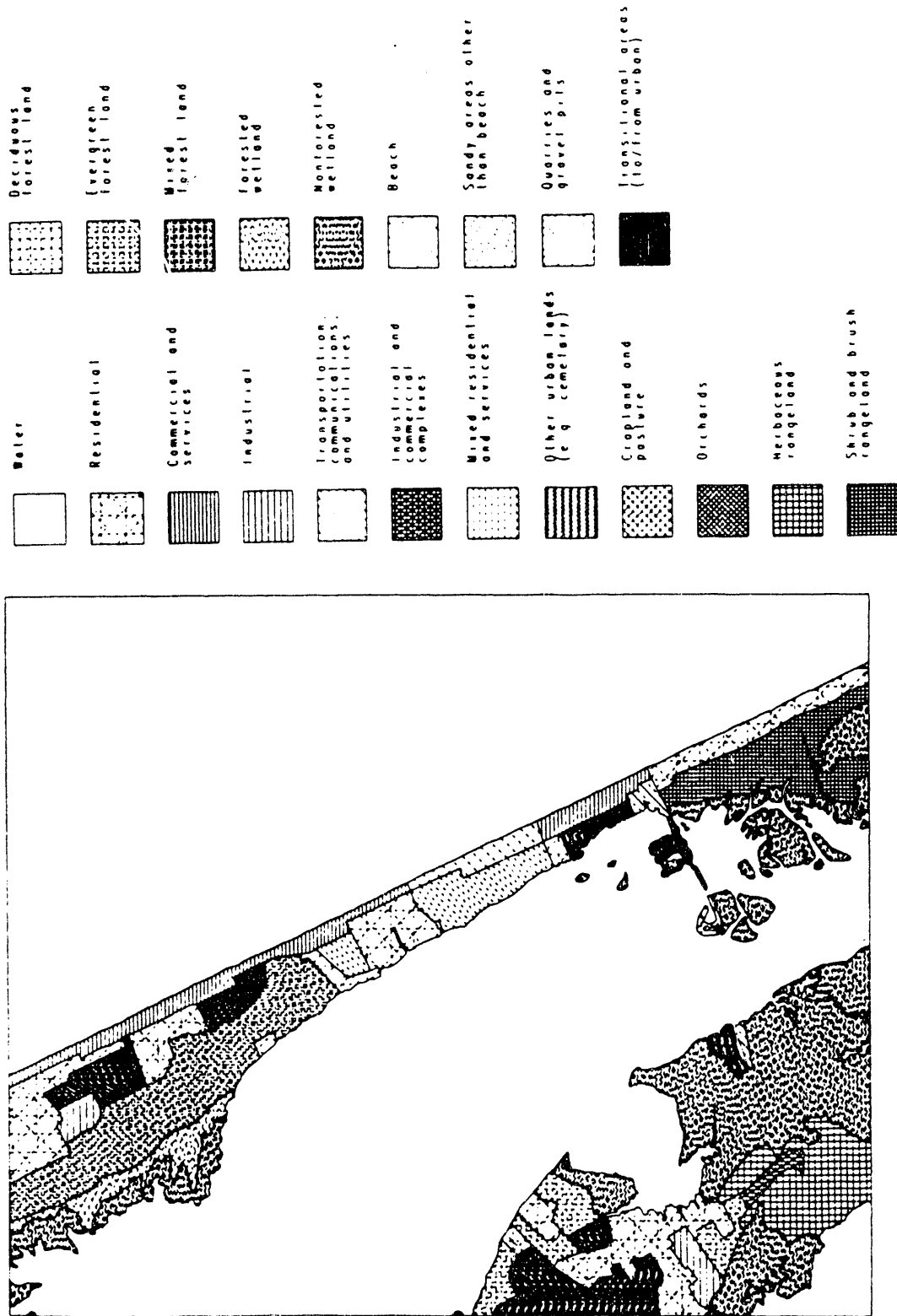


Fig. 4.31 Application of the low sea-level-rise scenario on the Nags Head study area. Coastlines shown are for the year 2050 and 2100.

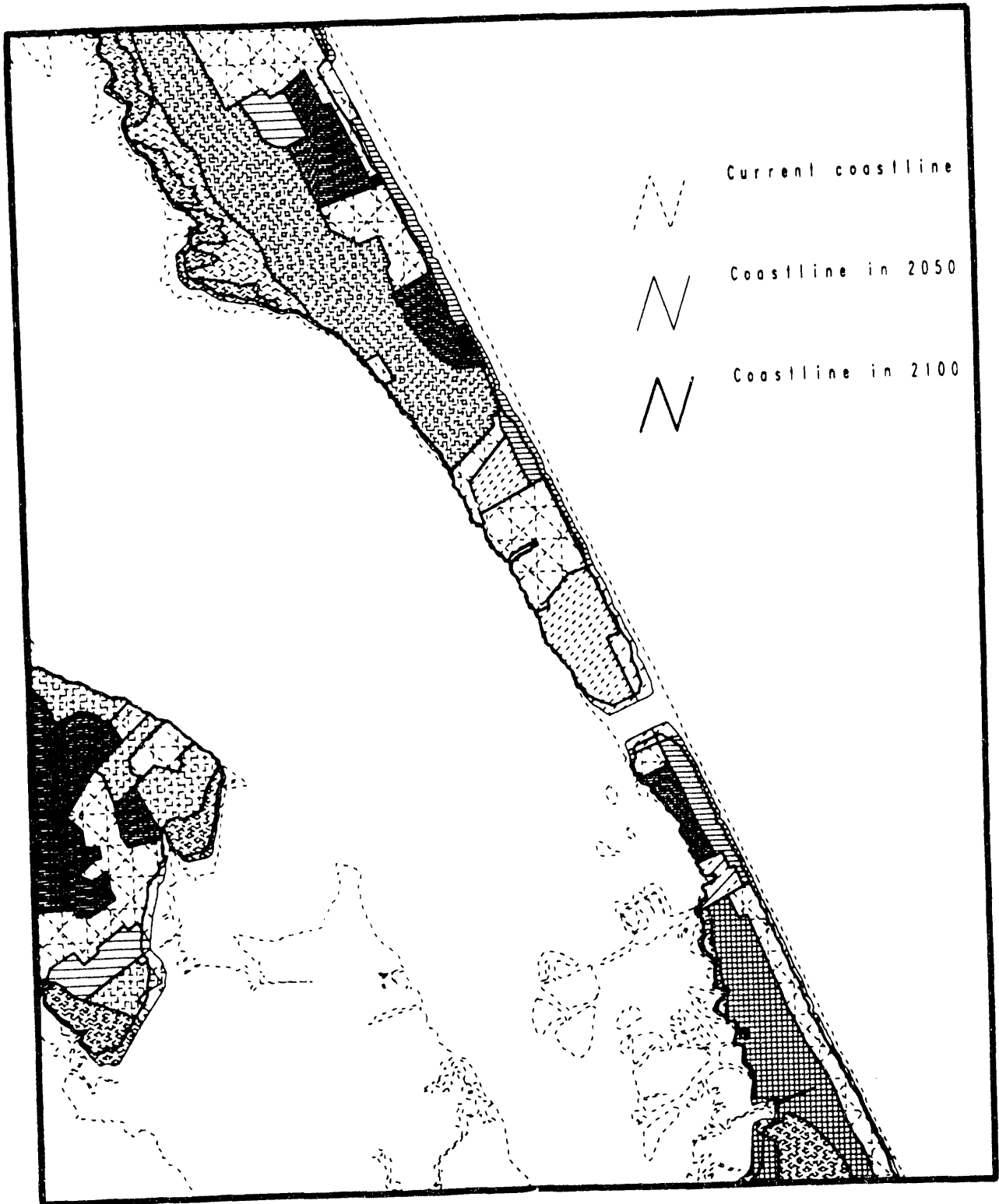


Fig. 4.32 Application of the medium sea-level-rise scenario on the Nags Head study area. Coastlines shown are for the year 2050 and 2100.

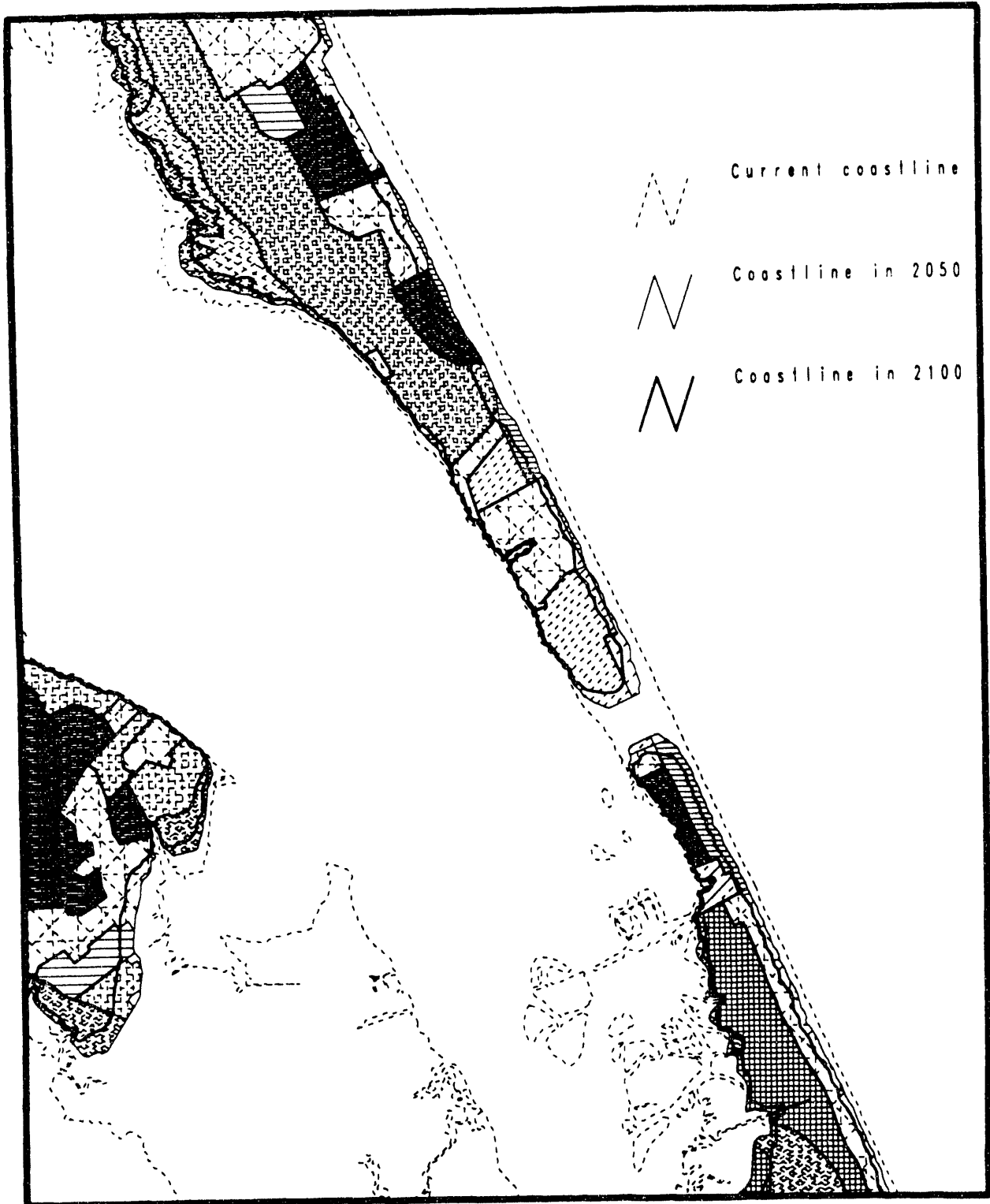
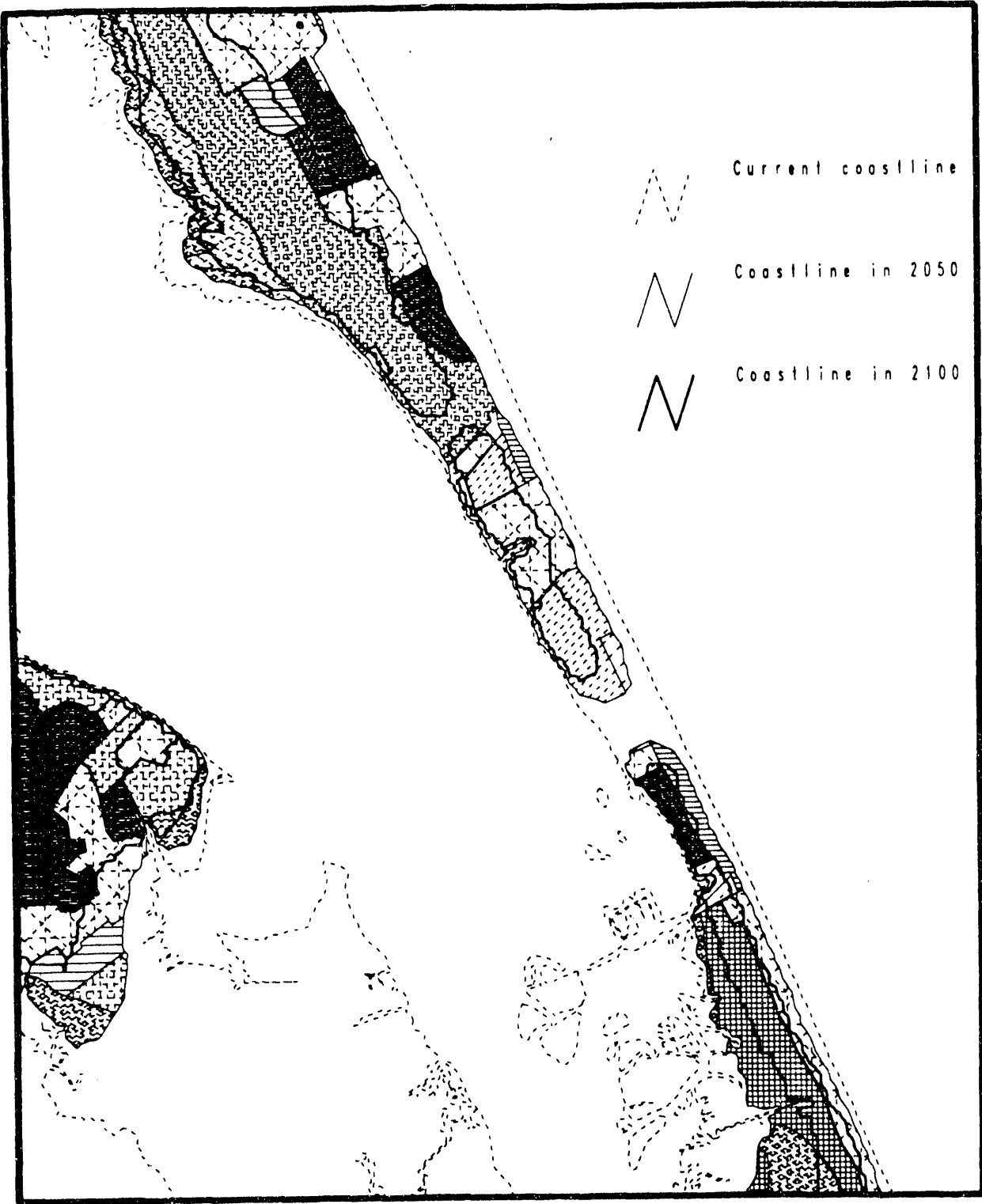


Fig. 4.33 Application of the high sea-level-rise scenario on the Nags Head study area. Coastlines shown are for the year 2050 and 2100.



# **ANALYSIS OF THE EFFECTS OF BIOPHYSICAL FACTORS ON THE EXTENT OF COASTAL INUNDATION**

## **5.1 INTRODUCTION**

The objective of this section is the identification of biophysical (e.g., longshore currents) and physical factors (e.g., roads or seawalls) that could potentially interfere with the inland advance of the sea in response to sea-level rise (SLR) in each of the six study areas. Towards this end, the following tasks were conducted:

1. identification of coastal landforms and structures that could potentially interfere with the inland advance of the sea or modify coastal processes, such as sediment transport and erosion/accretion rates;
2. estimation of the possible changes in shoreline position for transects in each study area, for three SLR scenarios, as a result of the limiting factors identified in task (1); and
3. revision of the inundation estimates made in Sect. 4, that are based on static inundation models, using the results of task (2).

The investigation conducted herein is designed to identify the future land-water interface under different SLR scenarios. Tropical and extratropical storms are capable of inundating large areas. The analysis of the effects of these storms falls outside the scope of this study. It should be noted, however, that the frequency and intensity of tropical and extratropical storms may increase in response to global warming, thus placing many coastal areas at greater risk to episodic inundation than would be expected based on the SLR scenarios alone.

## **5.2 METHODOLOGY**

### **5.2.1 Generic Methods in Use for Sandy Coasts**

Various methods of estimating shoreline response to changes in water levels have been proposed by researchers, based on their individual perception of the dominant processes involved in coastal erosion. Perhaps the most complete summary and evaluation of these methodologies is contained in a report produced by the National Research Council (1987). Briefly, the report lists four generic approaches whereby the erosional potential of SLR may be used to predict future shoreline recession:

1. extrapolation from historical trends (Leatherman 1984),

2. the Bruun Rule (Bruun 1962),
3. the sediment budget method (Everts 1985), and
4. the dynamic equilibrium method (Dean 1983).

Method 1 involves the use of information on the historic response of a coast to past changes in local sea level to make projections of shoreline change based on a given SLR scenario. Although this method is only partially quantitative, it encompasses the interplay of the various in situ factors such as waves, currents, and time, on shoreline formation and response. The primary assumption in this approach is that the past response pattern is solely attributable to sea-level change and, by extension, that the future shoreline position may be extrapolated for any given sea level. This is a tenable assumption provided the shoreline materials encountered in the future, as the sea encroaches landward, remain largely unchanged.

As originally put forth, Method 2, which represents the sediment balance within the entire active profile area, is mathematically represented as follows:

$$R = S \frac{W_*}{(h_* + B)} \quad (5-1)$$

where

- R = shoreline recession,
- S = SLR,
- W<sub>\*</sub> = width of active profile,
- h<sub>\*</sub> = depth of closure,
- B = dune height.

The depth of closure is the offshore depth at which beach and nearshore sediments, taken over time, cease to be reworked by wave agitation. Beyond this depth, wave- and current-induced sediment transport does not result in a significant change in the mean water depth. The essence of the Bruun Rule is schematically represented in Fig. 5.1.

Several criticisms have been made on the validity of the Bruun Rule, even though some of its opponents find the concept on which it is based "intuitively appealing" (Hands 1976). The main drawbacks of the Bruun Rule are that it does not allow for the onshore transport of sediments, it omits longshore transport, and it assumes a constant dune level over which the rising sea will not breach. At a more fundamental level, the association of shoreline retreat with a SLR, which is the premise of the Bruun Rule, has also been called into question. In a study that covers the entire east coast of Florida for the period 1897-1989, during which time concurrent sea-level-change (at Fernandina Beach, Mayport, and Miami, Florida) and shoreline-change data are available, Grant (1992) concluded that there is only a weak, but positive, correlation between a rise in sea level and shoreline position as a whole. Grant (1992) obtained a mean long-term accretion rate of +0.08 m/year

for the period concerned. This trend, at least for the sandy east coast of Florida, indicates that shorelines are accreting in the face of known increases in sea level, in direct contradiction of the negative correlation postulated in the Bruun Rule. This lack of correlation may put the validity of the Bruun Rule into question; however, more data of a similar nature, from other shores, are needed to put Grant's (1992) findings into the proper perspective.

Since the introduction of the Bruun Rule, various correction factors have been developed to account for the non-sand fraction (in the sediments) as well as for losses of sediment due to longshore transport. In a subsequent paper, Bruun (1983) has added two correction factors to account for sediment loss from the nearshore sediment budget: one deals with the sediment fraction finer than 0.06 mm in the form of  $(1 + r/100)$ , and the other accounts for the loss of sediments to a submarine canyon in the form of  $(1 + L/100)$ , where  $r$  and  $L$  are the respective percentage fractions. Hands (1981) has also introduced the factor  $G_s$ , defined as the overfill ratio, to account for the difference in textural properties between the materials of the eroding beach and the abutting bluff. Other losses such as longshore sediment transport gradients, if known, can also be incorporated as formulated by Kriebel and Dean (1985) in the following manner:

$$R_T = R + \left[ \frac{1}{B+h_*} \right] \frac{V_1}{P} \quad (5-2)$$

where

$R_T$  = total projected shoreline recession,

$B$  = dune height,

$h_*$  = depth of closure,

$V_1$  = net gains or losses of sediment per linear length known over some time period,

$p$  = percentage of sand-sized material.

In the above formulation, expressing the net sand volume change in terms of a quantity per linear length of shoreline facilitates its incorporation into the erosion analysis of a beach profile with a known unit width. Hence, the net gain or loss to the profile is reflected as a linear accretion or erosion of the profile over the total depth given by  $(B + h_*)$ . In the same manner, other avenues of sediment gain or loss, such as, beach nourishment, overwash, aeolian transport, or offshore loss in deep water, in addition to longshore transport gradients, can be accounted for.

The simplicity of Eq. (5-1) is obvious, as only three field-based parameters,  $W_s$ ,  $h_*$ , and  $B$  are required. However, the estimation of these parameters, especially  $h_*$ , commonly termed the pinch-out depth, is empirically-based. It was not until recently that efforts to peg estimates of  $h_*$  to wave and sediment characteristics have begun to yield useful results. In addition, the estimation of correction factors in order to improve the predictive capability of the Bruun Rule may push the amount of data required, and analysis effort required, toward that of Method 3.

The Bruun Rule has been applied to the Great Lakes Area (Hands 1976) and the

results obtained were found to be reasonable. Weggel (1979) also applied the Bruun Rule to the case of an exponential offshore profile and recommended the following approximate estimating procedure:

$$R = \left[ \frac{S}{\alpha (B+h_*)} \right] \ln \left( \frac{S}{h_*} \right) \quad (5-3)$$

where  $\alpha$  is the empirical coefficient describing the exponential rate of increase in water depth with distance offshore. The similarity to the Bruun Rule is immediately apparent from the equality of  $W_*$  and  $(1/\alpha)\ln(S/h_*)$ , whereby Eq. (5-3) reduces to the Bruun Rule.

As mentioned above, several improved versions of the Bruun Rule that account for non-sand fractions and longshore transport gradients as well as for other sources and sinks in the form of correction factors have emerged in the literature. The latest addition is one that incorporates the effects of these deviations by introducing a site-specific deviation factor,  $G_i$  (Dean 1991; Mehta et al. 1991). It assumes that the present recession rate,  $R_1$ , is related to the present SLR rate,  $S_1$ , in accordance with the Bruun Rule plus the site-specific deviation,  $G_i$ , due to unknown causes:

$$R_1 = S_1 \frac{W_*}{h_* + B} + G_i \quad (5-4)$$

For a different SLR rate in the future,  $S_2$ , it is assumed that  $G_i$  will remain unchanged. Thus, the resulting new recession rate,  $R_2$ , becomes this:

$$R_2 = R_1 + [S_2 - S_1] \left[ \frac{W_*}{h_* + B} \right] \quad (5-5)$$

The addition of the  $G_i$  term can be viewed as calibrating or *Adjusting* the Bruun Rule to site-specific conditions. In this manner, it is very similar to the approach of Leatherman, projecting future recession from historical trends, but in a more quantitative way.

The *Shore Protection Manual* (Coastal Engineering Research Center 1984) contains some useful guidance, both qualitative and quantitative, for determining the closure depth (i.e.,  $h_c$ ). The qualitative methods include examining the offshore profile for a break either in geometric pattern or subaqueous sediment characteristics, the interpretation of which is not a clear-cut task. On the other hand, the quantitative methods are based on wave-based zonation. For quartz sand, the following approximate relationships are recommended based on linear wave theory:

$$d_1 \approx 2H_{s50} + 12\sigma_H \quad (5-6)$$



$$d_i \approx H_{s50} \bar{T}_s \left[ \frac{g}{5000 d_{50}} \right]^{0.5} \quad (5-7)$$

where

- $d_i, d_s$  = limiting depth of sediment motion,
- $H_{s50}$  = mean annual significant wave height,
- $\sigma_H$  = annual standard deviation of significant wave height,
- $\bar{T}_s$  = annual average significant wave period,
- $d_{50}$  = medium diameter of subaqueous sediment,
- $g$  = acceleration due to gravity.

Eq. (5-6) is appropriate for estimating the seaward limit to extreme surf-related effects through a typical year, while Eq. (5-7) is recommended for determining the seaward limit to sand agitation by the median annual wave conditions. The original approximation method proposed by Hallermeier (1981), on which Eq. (5-6) is based, appears in a slightly different form:

$$h_s = (\bar{H}_s - 0.3 \sigma_H) \bar{T}_s \left[ \frac{g}{5000 d_{50}} \right]^{0.5} \quad (5-8)$$

where  $\bar{H}_s$  is the average wave height. However, the modified exponential distribution for nearshore wave height shows that  $H_{s50}$  and  $\bar{H}_s$  are related (Coastal Engineering Research Center 1984):

$$H_{s50} = \bar{H}_s - 0.3 \sigma_H \quad (5-9)$$

whereby the identity between Eq. (5-7) and Eq. (5-8) becomes apparent. Another wave-based relationship is suggested by results obtained from the Great Lakes area by Hands (1983), who proposed the use of twice the significant wave height as the "depth of limiting motion." In the case of sediment budget calculations with time spans on the order of decades, typical values of the closure depth along the U.S. continental coast range from 4 to 8 m (National Research Council 1987). Given the uncertainty associated with interpreting geometric and sediment breaks in offshore profiles and the increasing availability of well-documented wave hindcast data, it seems that the use of a wave-based relationships to estimate closure depth should prove helpful.

Method 3 makes use of the concept of a sediment budget. Within a proscribed control volume, all losses and gains of sediments in and out of the control volume are quantified and tallied to yield the resulting profile. Similar to the Bruun Rule, the underlying assumptions here are that the shore face will remain in equilibrium with the sea surface and

move vertically upward as SLR. In addition, the profile shape is assumed to remain unchanged during the rise. The sediment balance required to maintain an equilibrium shore face profile is this:

$$kV_e + V_o - V_d = 0 \quad (5-10)$$

where

- $V_e$  = volume eroded as the shore face profile translates landward and/or upward,
- $V_d$  = accretional volume of sand-sized sediment to satisfy continuity,
- $V_o$  = sediment additions to or subtractions from the shore face by transport across the boundaries of the control volume,
- $k$  = portion of  $V_e$  that is sand size or larger.

When the initial shore face and back beach profiles are known, Eq. (5-10) can be solved by numerically integrating it from the seaward limit of the equilibrium shore face profile to the landward limit of sediment transport on the back beach, to yield the shoreline change rate. These boundaries of integration, which also include internal boundaries such as the landward limit of the shore face, are estimated from field data, as are the values of  $k$  and  $V_o$ . In his application of the approach to Ocean City, Maryland, Everts (1985) included seven different conduits of sediment additions and subtractions: net sediment volume contributed to or lost from the control volume by longshore sediment transport; net sediment volume as a result of shore-normal transport at the base of the shore face; net sediment volume occurring behind the foredune as a result of overwash; aeolian transport; net sediment volume occurring landward of the foredune as a result of inlets; gain as a result of addition of fill and from outside the control volume; and, lastly, loss as a result of sand mining. As pointed out in the National Research Council Report (1987) this approach is straightforward in concept, but its application requires accurate data and subsequent proper interpretation to yield valid results. Furthermore, there are major differences in sediment budgets from site to site, and each area must be evaluated individually with respect to the existing sediment budget and the effects of present and future rates of SLR.

Method 4 employs the concept of equilibrium beach profile, which was first developed by Per Bruun in 1954 in an empirical form:

$$h = Ay^{\frac{2}{3}} \quad (5-11)$$

where

- $h$  = water depth,
- $y$  = seaward distance from the shoreline,
- $A$  = profile scale parameter.

Based on the analysis of 502 beach profiles along the U.S. Atlantic and Gulf coasts,

Dean (1977) found that the exponent 2/3 was indeed correct on an average basis. The parameter A was found to correlate well with sediment characteristics. On a theoretical basis, Dean (1977) also showed that the monotonic equilibrium profile of the form expressed in Eq. (5-11) is consistent with the concept of a uniform wave energy dissipation per unit of water volume. The net offshore sediment flux,  $Q_s$ , is then approximated according to the excess energy per unit volume at each point within the surf zone as follows:

$$Q_s = K(D - D_e) \quad (5-12)$$

where

- K = rate constant,
- D = wave energy dissipation rate/unit volume,
- $D_e$  = equilibrium wave energy dissipation rate/unit volume.

Coupled with the sediment continuity equation in the cross-shore direction, these equilibrium beach concepts form the basis for a two-dimensional numerical erosion model that may be solved for the evolution of a shoreline in the cross-shore direction.

In the present investigation an analytical approach for estimating shoreline response of the equilibrium profile to a rise in sea level has been adopted. As in the case of the Bruun Rule, it is assumed that the associated storm events will last long enough to attain a new equilibrium profile. In this regard, an implicit equation that describes shoreline change induced by SLR has been derived (Dean 1990):

$$\Delta y + \frac{3}{5} \frac{h_e W_e}{B} \left[ 1 + \frac{\Delta y}{W_e} \right]^{\frac{5}{3}} = \frac{3}{5} \frac{h_e W_e}{B} - \left[ \frac{S}{B} W_e \right] \quad (5-13)$$

where

- $\Delta y$  = shoreline change,
- $W_e$  = width of the active profile ( $= [H_b/(\kappa A)]^{3/2}$ ),
- $H_b$  = water depth at breaking.

The other parameters are as defined earlier. In defining  $W_e$ , both Eq. (5-11) and the spilling breaker assumption ( $H_b = \kappa h_e$  and  $\kappa \approx 0.8$ ) have been invoked. In its present form Eq. (5-13) only considers cross-shore transport. Another major assumption here is that landward transport of sediment by overwash and/or aeolian transport processes occur in sufficient quantities to cause the dune and berm to grow vertically as the profile retreats (Kriebel and Dean 1985). However, it does take into account the decreasing height of the dune in the face of SLR, thereby yielding a greater shoreline recession than predicted by the Bruun Rule. In fact, for a small relative ratio of  $\Delta y$  to  $W_e$ , Eq. (5-13) reduces to the Bruun Rule. Equation (5-13) requires an iterative approach for its solutions, which is shown in a

nondimensional plot in Dean (1990).

Other than the method of trend lines, which is more generic in nature, the methods enumerated above are expressly formulated for mainland sandy coasts. On the other hand, Holocene evidence indicates that barrier islands tend to retreat in a translational fashion while attempting to maintain a constant width through overwash and filling in on the bay side. Dean and Maurmeyer (1983) have modified the Bruun Rule (a.k.a., Double Bruun Rule) to simulate barrier island retreat by accounting for the fact that the entire island is now active in upward elevation while the corresponding yield of material comes only from the differential closure depth between the ocean and the bay. The retreat is calculated as follows:

$$R = S \left[ \frac{W_{*b} + W_I + W_{*o}}{(B_o + h_{*o}) - (B_b + h_{*b})} \right] \quad (5-14)$$

where the subscripts b, I and o denote bay, island, and ocean, respectively as indicated in Fig. 5.2.

### 5.2.2 Wetlands

For wetlands, which characteristically consist primarily of fine-grained cohesive materials, a physically based process model that is able to simulate wetland response to a rise in sea level to the same degree of success as for sandy coasts has not emerged (Mehta and Cushman 1989). Furthermore, the precise nature of chemical and biological variables, which can be as important as physical processes in cohesive sediment dynamics, is not clearly known. The state of wetland modeling has not substantially changed since the above sentiment was expressed and the plea made for more studies to be conducted on fine sediment transport.

Orson et al. (1985) have identified three possible modes of response of salt marshes to rising sea level, depending on the relative abundance of sediment supply for marsh accretion, as follows:

1. marsh drowning if the sediment supply and rate of accretion are less than the rate of coastal submergence (e.g., due to relative SLR),
2. marsh expansion if sedimentation exceeds coastal submergence, and
3. marsh maintenance if sedimentation balances coastal submergence.

Therefore, most study efforts in this respect apply these basic modes of response and consider wetland drowning to occur when a marshes rate of vertical accretion does not keep up with the future rise in sea level.

Similarly, wetland loss may be caused by a combination of mechanisms; shoreline

erosion at the seaward fringe being the most obvious. However, shoreline erosion probably accounts for only 1% of all marsh losses annually —on a nationwide basis (National Research Council 1987). A more probable catastrophic mechanism for wetland loss with a large increase in sea level will be the formation of extensive interior ponds allied with general tidal creek bank erosion and headword growth as tidal prisms increase (National Research Council 1987). The subsequent rapid enlargement and coalescence of interior ponds will convert wetlands to open water habitats. This process has been documented in the Mississippi Delta (DeLaune et al. 1983) and the Blackwater Wildlife Refuge (Stevenson et al. 1986).

The variability of local vertical accretion rates can be large, as evident from Table 5.1, which covers a wide geographical area along the Atlantic and Gulf coasts. In reviewing studies of vertical marsh accretion rates, Wolaver et al (1988) noted that marshes along the East Coast are actively accreting between 1.5 and 51.8 mm/year, which in some places is well above the local rate of SLR. As pointed out by Orson et al. (1985), the ability of salt marshes to maintain surface elevation with respect to the mean high water level is influenced to a large degree by local submergence rates, sedimentation rates, density and composition of the indigenous flora, and type and intensity of cultural modifications. At a more local level, Wolaver et al. (1988) suggested that the ability of the vegetated marsh to keep pace with SLR is a function of sediment deposition during tidal inundation, and material resuspension and its consequent export from the marsh through runoff during low-tide exposure. Hence, these authors have further suggested that the marsh can keep pace with SLR by a dynamic interaction of deposition and resuspension processes that are controlled by the height of the marsh with respect to mean sea level. An attempt at using a simplified form of this process model has been made by Krone (1985), who demonstrated the utility of the approach in predicting the response of marshes to SLR in the San Francisco Bay area. The dominant process modeled is one of deposition represented by the following equation, which is based on a consideration of the mass balance involved:

$$(y_w - y_m) \frac{dC}{dt} + w_s C - C_o \frac{dy_w}{dt} = 0 \quad (5-15)$$

where

- $y_w$  = elevation of the water surface relative to a selected datum,
- $y_m$  = elevation of the marsh surface relative to the same datum,
- $w_s$  = settling velocity of the suspended fine sediment flocs,
- $C$  = concentration of suspended sediments,
- $C_o$  = concentration of suspended solids in the flooding waters,
- $t$  = time.

**Table 5.1 Rates of marsh accretion and relative sea-level rise**

Location	Mean tidal range (m)	Relative SLR (mm/year)	Salinity (ppt)	Accretion rate	
				range (mm/year)	mean (mm/year)
Barnstable, Massachusetts	2.9	0.9	20-30	3-8	5.5
Prudence Island, Rhode Island	1.1	1.9	28-32	2.8-5.8	4.3
Farm River, Connecticut	1.8	1.9	<sup>a</sup>	<sup>a</sup>	5.0
Fresh Pond, New York	2.0	2.2	26	<sup>a</sup>	4.3
Flax Pond, New York	2.0	2.2	26	4.7-6.3	5.5
Lewes, Delaware	1.3	2.0	25-30	<sup>a</sup>	4.7(> 10) <sup>b</sup>
Nanticoke, Maryland	0.7	3.2	2-6	4.9-7.2	6.1
Blackwater, Maryland	0.3	3.9	1-5	1.7-3.6	2.6
North River, North Carolina	0.9	1.9	<sup>a</sup>	2-4	3.0
North Inlet, South Carolina	1.6	2.2	30-35	1.4-4.5	2.5
Savannah River, Georgia	3.0	2.5	<sup>a</sup>	<sup>a</sup>	11.0
Sapelo Island, Georgia	2.1	2.5	30-35	3.5	4.0
Barataria, Louisiana <sup>c</sup>	0.5	9.5	<1->15	5.9-14.0	7.2
Fourleague, Louisiana	0.3	8.5	10-20	<sup>a</sup>	6.6
Lake Calcasieu, Louisiana	0.6	9.5	15	6.7-10.2	7.8

<sup>a</sup> Not reported.

<sup>b</sup> Lower value obtained by dating with lead-210, higher with cesium-137.

<sup>c</sup> Values based on fresh, brackish, intertidal, and water marshes.

Source: Mehta and Cushman 1989 and Stevenson et al. 1986.

As boundary conditions,  $C_o = C$  during the rising phase and  $C_o = 0$  during the falling phase of the daily tide.

The settling velocity is computed on the basis of an empirical relation that is usually derived from laboratory tests and has the following general form:

$$W_s = kC^{\frac{4}{3}} \quad (5-16)$$

where  $k$  is a constant specific to the type of sediment. Knowing the ambient concentration of  $C_o$ , which may be obtained with a calibration formula, with measured values of  $y_m$ , and the density of the marsh, the rate of marsh growth can be obtained through a numerical solution of the governing equation.

Admittedly, this simple model, which is essentially a "zero-dimensional" model, does omit such relevant considerations as wave-induced motion and tidal creek hydrology. For example, in studying the late Holocene sedimentation and erosion of estuarine fringing marshes located on the York River, Virginia, Finkelstein and Hardaway (1988) suggested that the exposure to storm waves was also of significance in the maintenance or erosion of the fringing marshes. Nonetheless, a means of predicting marsh vertical growth, however simple its formulation may be, is a valuable addition to our limited tool kit in this respect.

On a more pessimistic note, at the present time it is practically impossible to separate these multifarious processes, which are interlinked in very complex ways. Hence, in the effort to evaluate the likely impacts of a SLR on wetlands, individual site-specific assessments directed at addressing specific problems have been the dominant modus operandi of investigators in this field; relegating research aimed at clarifying and identifying the physics, chemistry, and biological processes that interact and influence wetland processes, to secondary importance.

The site specificity of this problem-oriented approach has had other adverse consequences, in that the application of the findings to other sites and, by extension, of generalizing them for regional- and national-scale assessments may be rather limited. However, although not directly transposable, the experience and results obtained for similar studies, at other localities, may serve to shed some light on likely responses of wetlands to a rising sea. It is with this premise that the following attempts at generalizing wetland response are documented; with a view of applying some of them to our wetland study areas to arrive at a preliminary assessment. Further refinements of this method may be instituted as the learning curve is extended through focused research.

It has been claimed that when SLRs at a rate greater than 1 cm/year, the inland reestablishment rate of wetland may not keep pace with the outer-edge die back because of drowning (Zimmerman et al. 1991). In fact, the above threshold rate has been termed as catastrophic, in which case substantial reduction in wetland area and a corresponding increase in open water habitats are projected (Orson et al. 1985). Also, the percentage of open water in a Gulf coastal marsh has been directly related to the rate of coastal submergence for the last 85 years (Mitsch and Gosselink 1986), thus establishing a close link between accumulated aggradation deficit (vertical accretion rate minus local SLR) and wetland loss.

These results underline the delicate position of our coastal wetlands, between survival and demise. A change in the rate of SLR or sedimentation of as little as 1 to 2 mm/year can determine whether the a marsh will survive (Mitsch and Gosselink 1986). In the horizontal direction, Phillips (1986) suggested that along the Atlantic and Gulf coasts, marsh shoreline erosion rates of more than  $\approx 0.3$  m/year (and perhaps much less) will result in a loss of wetlands at a greater rate than new marshes can be created.

In spite of the formidable hurdles mentioned above, two notable attempts at determining the potential impact of accelerated SLR on wetlands have been reported in the literature (Kana et al. 1988a; 1988b). Essentially the methodology employed involves the following steps:

1. Develop a composite transect representing an average profile of the area that links wetland species to substrate elevations from field data. The result is a species zonation pattern that is elevation dependent.
2. Develop a conceptual model for changes in marsh under different scenarios of SLR. The resulting model of future wetland zonation should include projected rates of SLR and the rate of sedimentation and peat formation (vertical accretion) that raises the substrate in tandem with SLR.
3. Apply the conceptual model to the study area. It is assumed that if the rate of vertical accretion, which in turn is a function of the rate of sedimentation, can keep pace with the rise in sea level, no wetland drowning will occur. On the other hand, if sea levels increase faster than the vertical accretion rate, wetland zones will migrate landward. The extent of this landward retreat hinges on whether the landward shift would be halted by human intervention in the form of bulkheads, seawalls, and the like. At any rate, because of the generally concave upward nature of nearshore profiles, it is likely that a net reduction in wetland acreage will occur during the landward shift of the wetlands.

As elaborated above, this methodology is field-based, requiring accurate wetland transects and estimation of the rate of sedimentation and the degree of human intervention. With improved understanding of the fundamental relationship between substrate elevation and wetland habitats, extension of the use of remote sensing techniques and aerial photography to demarcate wetland elevations based on plant species becomes a worthwhile proposition. Park et al. (1989) have applied this technology in conjunction with geometric map-based models that consider the dominant terrestrial/marine processes in evaluating wetland conversion and shoreline reconfiguration along the continental coasts of the United States. Mean annual vertical accretion rates measured for tidal wetlands range from 2 to 10 mm for salt marshes and 5 mm for mangrove swamps. In the two studies previously cited (Kana et al. 1988a; 1988b), the rate of sedimentation adopted was 5 mm/year.



### 5.2.3 Previous Applications

Several of the methods enumerated above (Leatherman 1984; Bruun 1962; Everts 1985; Dean 1983) have been applied to a common site —Ocean City, Maryland (Titus et al. 1985). The Ocean City study remains to date the only comparative study of shoreline response to SLR using these different evaluation methods in the open literature. The SLR scenarios adopted for this comparative study, which indicate absolute rise over the 1980 level, are shown in Table 5.2. Figure 5.3 compares the results derived based on the methods used by Bruun, Everts, Leatherman, and Kriebel and Dean (1985). All the methods predict shoreline recession, but of differing magnitudes. The original Bruun Rule consistently underpredicts for all the scenarios by as much as a factor of three. This appreciable divergence has been explained on the basis of the longshore transport gradient, which has been altered significantly at Ocean City as a result of jetty construction (Titus et al. 1985).

**Table 5.2 Relative sea-level-rise scenarios for Ocean City, Maryland**

Year	Current trend	Mid-range low rise	Mid-range high rise
	(cm)	(cm)	(cm)
2000	7	12	17
2025	16	34	47
2050	25	65	92
2075	34	108	154

For this particular site, Evert's method always yields the greatest shoreline recession followed closely by Dean's method. The Adjusted Bruun Method is seen to yield a prediction very close to that based on the approach of Leatherman.

### 5.2.4 Adopted Approaches for Sandy Coasts

There is no absolute benchmark whereby the performances of the methods can be compared. Evaluation on theoretical considerations is also unlikely to prove meaningful, with the exception of perhaps the Bruun Rule, which has been shown to be overly simplistic, given the present state of understanding of littoral processes. Under these constraints, it seems logical to base the choice of methodology on the availability of data and prior studies. Depending on the availability of data, some or all of the methods of Bruun Rule based on Eq. (5-1), Adjusted Bruun Rule based on Eq. (5-5), Dean (analytical approach), and

Leatherman will be employed in this investigation. The method of Everts is deemed too data-demanding to be appropriate for the present investigation.

### **5.2.5 Sea-Level-Rise Scenarios**

The generic SLR scenarios that will be applied to each of the six study sites are based on a composite of several published SLR projections. These scenarios also take into consideration the recent downward shift in the projected SLR scenarios based on improved understanding of the underlying processes affecting SLR and refined modeling of continental glaciers, as discussed in Sect. 2. The scenarios adopted for this study are classified into four categories: current (a site-specific subsidence scenario), low, intermediate, and high. These scenarios are tabulated in Table 2.4 (Sect. 2) and are depicted in Fig. 2.7. The scenarios actually applied to each site were arrived at by combining the low, moderate, and high global SLR scenarios with the values given for the current scenario for each study area.

## **5.3 GALVESTON, TEXAS**

### **5.3.1 Site Description**

Galveston study area consists of Galveston Island, a long barrier island on the southeast shore of Texas facing the Gulf of Mexico. The study area contains the eastern part of the barrier island and all of Pelican Island, which is separated from Galveston Island by Galveston Channel, a narrow navigation channel, as indicated in Fig. 5.4. The eastern extremity of the study area borders the navigation channel (Bolivar Roads), which extends into Galveston Bay. The relief is generally low, the highest elevation being  $\approx 5$  m above National Geodetic Vertical Datum (NGVD) based on the USGS 7.5-min topographic map for Galveston (AMS 7042 IV SE Series V882, scale 1:24,000).

On the Gulf side, the offshore profile slopes gently seaward as shown in Fig. 5.5. The profile was generated from the USGS 7.5-min topographic map, U.S. Nautical Charts No. 11324 (Galveston Bay Entrance, scale 1:25,000) and 11323 (Approaches to Galveston Bay, scale 1:80,000) of the area. The locations of these offshore transects are shown in Fig. 5.6 and cover a shore distance of  $\approx 7.2$  km along the open Gulf Coast. The offshore profile steepens in a westward direction from the west jetty, partly a consequence of the trapping of eastward-bound sediments by the west jetty, which builds up the nearshore profile. The offshore profile is generally concave upward until about the 5.0 to 6.0 m water depth where the sea floor bulges slightly (except at transect No. 3) before dropping off nearly uniformly. The bottom contours are generally straight and parallel to the shoreline. The shore face sands grade gently seaward into mud and silt.

On the bay side, extensive shoreline modification in the form of jetties and wharfs has yielded an artificial shoreline along the channel. On the other hand, the northern half of Pelican Island remains undeveloped, and there is evidence of westward sediment transport at its northern tip. The part of Galveston Bay abutting the bay side of Galveston Island is

shallow. It is crisscrossed by numerous navigation channels that have a maximum depth of  $\approx 2.5$  m at  $\approx 5.5$  km from the bay shoreline.

Figure 4.3 depicts the land use pattern within the Galveston study area. The western two-thirds of the study area is highly urbanized; residential and commercial development dominate the Gulf side and Bay side, respectively. The only pristine areas are a pocket of nonforested wetland on the eastern tip and two areas of beaches: one on the tip, which is wedge-shaped (East Beach), and the other on the linear beach which fronts the seawall along the western portion of the study area. The wider beaches on the eastern tip may have benefitted from a bay entrance jetty that has halted loss of sediments into the navigation channel. The remaining area facing the Gulf Coast, which is protected by a seawall, has been shorn of a fronting beach. Pelican Island is largely undeveloped, being covered by wetland to the north and brush land to the south. Two pockets of industrial areas and one residential area line its southern shore, perhaps a spillover of the heavily developed area on the opposite side of the channel. A narrow beach fringes the wetland area on the eastern side of the navigation channel.

### **5.3.2 Sea-Level-Rise Scenarios**

The SLR scenarios for this project were developed in Sect. 2 and are summarized for this study area in Table 4.5. The present rate of subsidence for Galveston is 4.9 mm/year and was used to determine the future SLR for the current scenario. Based on the assumption of static inundation, the area of submergence under each scenario of future SLR was calculated in Sect. 4. Section 4's estimates for inundation will be modified here, if necessary, as outlined in Sect. 5.1.

### **5.3.3 Previous Studies**

The effects of SLR on the land surrounding Galveston Bay have been previously studied (Leatherman 1983; 1984) using the trend-line method discussed in Sect. 5.2.1. Essentially, the method entails the empirical determination of a future shoreline based on shoreline responses to local sea level changes in the historical past (i.e., historical trends). Since the completion of these studies, a downward revision in the projection of SLR has occurred, as discussed previously. This reduction is evident from Fig. 5.7, which depicts the various SLR scenarios adopted by Leatherman for his study, presumably after appropriate modification of the eustatic SLR rate for site specific conditions. As indicated, the two sets of scenarios begin to diverge measurably during the years 2025-2030, with those adopted by Leatherman increasingly higher than those used in this study. In reducing the two sets of scenarios to a common base line for comparison, the average projected rate of SLR for the period 1990-2050 for the current study was used to extrapolate backward in time to obtain the sea level for the base year 1980.

The opposite trend for the current scenario results from the smaller rate of rise used by Leatherman (30 cm/century, where he removed an estimated amount due to local

subsidence from the historical trend), whereas the rate adopted here (49 cm/century) includes land subsidence. His rationale for his SLR scenario is premised on the findings of Thompson (1982), who determined that the estimated rate of future subsidence for this area is insignificant and that Galveston Island is essentially stable. This conclusion is surprising, and seems to contrast sharply with the ongoing episodes of subsidence occurring within Mississippi's Atchafalaya delta, at the reported rate of 10 mm/year (McAnally et al. 1984), which is attributed mainly to sediment consolidation. Portions of the Mississippi delta have recorded subsidence rates as high as  $\approx 18$  mm/year. The rates quoted above refer to actual subsidence caused by factors other than SLR.

At the Atchafalaya delta, the deeper layers are subsiding at slower rates than the newly deposited sediments. It is probable that the subsidence rate sustained by these deeper layers is also affecting Galveston, since they both lie at the fringes of the Gulf Coast basin. Galveston Island developed from the coalescing of several exposed offshore sand bars that grew seaward by shore face deposition about 4500 years ago (Fisher et al. 1972). Remnants of relic beach ridges that have not been obliterated by human settlement and subsequent development testify to a slow seaward growth or accretion by sand from longshore and onshore currents. On the other hand, the Atchafalaya delta has grown by the continued accumulation of fluvial sediments from the Mississippi River. This difference may help to account for the disparities between the observed subsidence rates in each area.

#### **5.3.4 Results and Discussion**

A study similar to this one was conducted for Galveston by Leatherman in 1984. Therefore, one possible approach is to modify the results of Leatherman's work using the new SLR scenarios. Implicit in the modification effort would have been the assumption that future shoreline retreat is linearly correlated with future SLR in the same proportion as that which was obtained on the basis of historical data. For example, a threefold increase in SLR will increase the recession rate by a factor of 3, with the provision that lag effects in shoreline response are small compared with overall extrapolation accuracy. The adoption of the approach of Leatherman in the current study is particularly attractive in light of the difficulty in obtaining site-specific data, thereby warranting recourse to a simple extrapolation of historical trends for projection purposes.

The adjusted Bruun Rule may also be used in this context, whereby the depth of closure,  $h$ , is estimated on the basis of annual wave statistics available from a Wave Information Study (WIS) (Hubertz and Brooks 1989), whereas, the width of the active profile,  $W$ , is measured from the offshore profile from the relevant bathymetric/nautical charts. For this purpose, several offshore profiles were constructed, with transect No. 2 being assumed to be representative of the project site. These transects are shown in Fig. 5.5 and 5.6. The dune height,  $B$ , was estimated from the contours in the relevant USGS 7.5-min topographic map series mentioned earlier. Since the same parameter inputs are required for Eq. (5-13), the method based on Dean's approach to equilibrium beach profile offers another means of estimating shoreline retreat.

Out of the 50 stations covered in the WIS Report for the Gulf of Mexico, Station 11

is the closest to the study site. The relevant positional characteristics of Station 11 are Lat. 29.0° N, Long. 94.5° W, and 18.2 m water depth. The wave characteristics reported are based on 20 years (1956-1975) hindcast wave data in which the significant wave height,  $H_s$ , is an energy-based estimate, represented by  $4\sqrt{E}$ , where E is the total energy of the wave spectrum. The following values were extracted for use:

$$\begin{aligned}\bar{H}_s &= 1.1 \text{ m,} \\ \bar{T}_p &= 5.6 \text{ s,} \\ \sigma_H &= 0.4 \text{ m,}\end{aligned}$$

where  $\bar{T}_p$  is the mean peak wave period (associated with spectral peak). In this case,  $\bar{T}_p$  is taken to be equal to  $\bar{T}_s$  and the value of  $H_{s50}$  is obtained from Eq. (5-9).

When these values are plugged into Eq. (5-6) and Eq. (5-7), the calculated closure depth obtained was 6.8 m and 19.8 m, respectively. The sediment size,  $d_{50}$ , has been assumed to be 0.15 mm in the above computation. Also implicit in the above computation is the assumption of insignificant refraction and shoaling effects on waves traversing into the nearshore zone away from the wave shadow zone of the inlet jetty, which may be partly justified on the basis of a gradually varying sea floor slope and bottom dissipation. Bearing in mind that Eq. (5-7), and hence the value of 19.8 m, is based on the seaward limit of wave agitation, which can be viewed as the upper bound of  $h_*$ , and given that there is no apparent reason to go either way, it seems that an in-between value that is commensurate with the present extent of uncertainty associated with the other inputs to the study should suffice.

On the basis of linear wave theory, Komar (1976) has ventured a Shields type of criterion for the threshold of sediment motion under waves. For sediment grains  $<0.5$  mm in diameter, the relevant relation reads as follows:

$$\frac{\rho u_t^2}{(\rho_s - \rho) g D} = 0.21 \left[ \frac{d_o}{D} \right]^{\frac{1}{2}} \quad (5-17)$$

where  $u_t$  and  $d_o$  are the near-bottom threshold velocity and orbital diameter of the wave motion, respectively. Both  $u_t$  and  $d_o$  are related to the wave height H, water depth h, and wave period, T, by Eq. (5-18).

$$u_t = \frac{\pi d_o}{T} = \frac{\pi H}{T \sinh\left(\frac{2\pi h}{L}\right)} \quad (5-18)$$

The density of water is  $\rho$ , while  $\rho_s$  and  $D$  are the density and diameter of the sediment grains, respectively. For the same site conditions as before,  $h_c$  was computed to be 16.3 m.

An examination of Fig. 5.5 (transect No. 2) reveals that a sea-floor break occurs at about the 5-m depth, at which point the upward concave profile changes to a convex one. Further seaward, another break occurs at  $\approx 7.5$ -m water depth, signifying the termination of the convex feature. Yet further seaward, another break seems to occur at  $\approx 9$  m bottom contour, even though it is more apparent on one profile than the other. All these features could serve as the geometric limits of significant sediment motion, depending on the prevailing wave climate. Hence, all the three depths of 5 m, 7.5 m, and 9 m have been used in the subsequent analysis in order that the resulting projections can be treated as reasonable bounds of the likely changes in the depth of closure. The corresponding widths of the active profile are extracted from Fig. 5.5; they are 1.5, 3.0, and 5.4 km, respectively.

Without actual field survey, the berm height,  $B$ , was estimated to be the highest elevation shown in the topography sheet in the vicinity of the shoreline, which equals 5 m at mean sea level. The above information then enabled the computation of projected shoreline retreats using the Bruun Rule and the equilibrium beach profile method (Dean 1990).

To be able to apply Leatherman's trend line method the historical rate of shoreline response to local sea-level change must be known. In this study the value determined by Leatherman was used (1983). For the period 1850 to 1960, the average rate of SLR,  $S_b$ , was 3 mm/year whereas the corresponding shoreline retreat rate,  $R_b$ , was 0.65 m/year for unprotected shoreline within the bay. Hence, if the future SLR is  $3S_b$ , then the future shoreline retreat rate will be  $3R_b$ .

In Leatherman's study (1984), no retreat was forecast for the Gulf side of Galveston Island because of human intervention in the form of seawalls. It was further assumed that this massive engineering structure would remain intact. In the current study, this assumption was relaxed so that the results are consistent with the prediction based on static inundation for comparison purposes. Hence, two scenarios covering both conditions of fixed (with seawall) and mobile (without active intervention by seawall) Gulf shoreline were adopted. Tables 5.3 and 5.4 summarize the results of the three approaches discussed above for the case of mobile Gulf shoreline at the vicinity of the most westward groin for the milestone years 2050 and 2100, respectively. For this particular analysis, it is assumed that the bay side of the barrier island is anchored by Pelican Island, and the erosion will proceed as would a mainland coastline. In addition, the tendency for the eastern end of Galveston Island to rotate bayward and, hence, impart additional retreat to the Gulf shoreline in the event of SLR-induced geomorphic change was ignored. This simplistic approach was taken in order to compare the projected shoreline changes with those based on static inundation so that some initial inferences can be made as regards the need and feasibility of increasing the sophistication of approach.

The rows of values in Table 5.3 for the Bruun Rule, Adjusted Bruun Rule, and Dean's method correspond to, from top to bottom, the closure depths of 5.0 m, 7.5 m and 9.0 m, respectively. The Adjusted Bruun Rule was cast in the form of Eq. (5-5), and the values of  $R_1$  and  $S_1$  correspond to the historical rates established by Leatherman.

**Table 5.3 Predicted shoreline recession for the year 2050, Galveston, Texas**

Method	Mobile Gulf shoreline			
	Current scenario	Low scenario	Moderate scenario	High scenario
	(m)	(m)	(m)	(m)
Leatherman	64	94	133	172
Bruun Rule	44	65	92	119
	71	104	147	191
	113	167	237	306
Adjusted Bruun Rule	56	77	104	131
	66	99	143	186
	83	136	206	276
Dean	45	66	93	121
	72	105	150	192
	113	167	238	308
Static Inundation	-	105	165	210

It can be seen in this table that Dean's approach consistently predicts more recession than that predicted by the original Bruun Rule, which is expected as previously explained. However, the difference is very minor because of the small ratio of  $\Delta y/W_*$ , which varies from 0.021 to 0.169. As mentioned earlier, Eq. (5-13) approaches the original Bruun Rule for small values of  $\Delta y/W_*$ .

If the pair of  $(h_*, W_*)$  is taken to be (7.5 m, 3 km), the predictions of all the methods enumerated agree well with one another as well as with the projected shoreline retreats based on static inundation, bearing in mind that the digitation error in using a 1:24,000 base map is in the region of 10 to 20 m corresponding to 0.5 mm on the map. In this regard, and taking into account the uncertainties inherent in the analysis, it seems reasonable, at least for preliminary planning, that a first-cut estimate of shoreline recession in the absence of human intervention can be made on the basis of static inundation for Galveston Island due to the flat offshore profile and the generally low land topography.

**Table 5.4 Predicted shoreline recession for the year 2100, Galveston, Texas**

Method	Mobile Gulf shoreline			
	Current scenario	Low scenario	Moderate scenario	High scenario
	(m)	(m)	(m)	(m)
Leatherman	117	184	260	355
Bruun Rule	81	127	180	246
	129	204	288	393
	208	327	462	632
Adjusted Bruun Rule	103	149	202	268
	122	196	280	385
	152	272	407	576
Dean	81	129	183	254
	130	207	294	405
	211	329	470	648
Static Inundation	-	225	344	405

The above analysis presupposes that the shoreline is allowed to respond freely to environmental forcing. However, in the case of highly urbanized barrier islands such as Galveston, efforts will be made to improve the seawall as the sea-level rises to protect the billions of dollars of investment that have already been poured into establishing the present-day city of Galveston. This sentiment has been echoed repeatedly in published reports (National Research Council 1987; Leatherman 1984; Smith and Tirpak 1989). Hence, it is highly improbable that the Gulf shoreline will be permitted to respond freely to SLR.

On the bay side, the absence of the mobilizing agent, in this case storm events, due to the semi-enclosed nature of the bay, is unlikely to significantly effect the transition to a new equilibrium profile in the event of a SLR. The semi-enclosure formed by the Texas City Dike on the northeast, Pelican Island, and the causeway crossing East Bay and the mainland proper in a clockwise direction. Hence, the bay side shoreline, even if it is mobile, is apt to retreat as a result of direct submergence rather than the redistribution of sediment. As indicated in Fig. 5.6, the heavily built-up bay shore is dotted with pier facilities lining both sides of the Galveston Channel. Again, economic considerations do not seem to support the abandonment of these facilities.

Hence, the only shoreline that is likely to be permitted to shift landward on the basis of economic considerations is the northern shoreline of Pelican Island. As a result of its



relatively secluded location, the future shoreline can be traced using the static inundation approach. The land area lost will consist of wetlands. The effect of wetland drowning on other economic activities such as the fishing industry, and on environmental quality in general is difficult to quantify, but it is unlikely to garner a large enough lobby for it to be protected, given the current economic paradigm.

The case of the East Beach is more complicated. The beach may be raised to protect the shore end of the west jetty from being outflanked. At the same time, it also functions to protect the seawall on this part of the island, and offers recreational benefits, which may become scarce as beaches are lost to the rising sea. In the future, it may make economic sense to hold this line of defense in place, in addition to a phased shoring up of the seawall. Hence, for the case of Galveston, it may be argued, at least on economic grounds, that protection efforts in the form of profile nourishment, shoring up of seawall, extension of ring dikes, raising of land levels, and the like are likely to be forthcoming such that the only land loss will be limited to the northern part of Pelican Island.

To summarize the above findings, and to obtain point responses with reference to specific locations, several points were selected that are located on the three transects shown in Fig. 5.6. The likely dispositions of the points on each transect, lettered A through H, are depicted graphically in Fig. 5.8, 5.9, and 5.10 and tabulated in Table 5.5. With this analysis, the revised estimates of land area lost under different SLR scenarios have been recomputed from the projected shoreline change maps based on static inundation using a square-counting technique as shown in Table 5.6. The figures in parentheses represent percentage loss of land area relative to the present land area.

The values contained in Table 5.5 assume that the northern half of Pelican Island will be allowed to retreat up to the projected shoreline in year 2050 under the high scenario, which is the assumption in the estimation of land area eroded. It is seen that obstructions, from built infrastructure, play a significant role in determining the projected land area that will be lost as a result of accelerated SLR due to the heavily developed nature of the coastal margin. On a percentage reduction basis and depending on the SLR scenario for each milestone year (2050 or 2100), it can be stated that structural obstructions, if they are held in place, may reduce the projected area lost to the sea by 33 to 70%.

### **5.3.5 Conclusions**

For Galveston, preliminary analysis indicates that static inundation models yield projected shoreline retreats that are in close agreement with simple physical process models, assuming that the shoreline is allowed to respond freely to SLR. The percentage loss of area within the study area ranges from 33% to 47% at the year 2050 and 49% to as much as 88% at the year 2100 based on the three SLR scenarios adopted. The only land areas left at the turn of the next century would be the two high portions at the center of Galveston and the southern part of Pelican Island.

**Table 5.5 Predicted changes in shoreline position, Galveston, Texas. Reference point locations are shown in Figs. 5.8, 5.9, and 5.10**

Reference Point	Predicted change
A	East Beach is likely to shift to the location of the lagoon and to be artificially raised by nourishment to serve as protection for seawall and jetty
B	The shoreline may be allowed to retreat up to the projected 2050 shoreline under the high scenario. However, due to the comparatively less developed nature of old Fort San Jacinto, the entire transect 1 may be foregone if dictated by the high costs of building ring dikes for protection
C	Shoreline is likely to be fixed at the seawall by human intervention
D and E	Pier facilities are likely to be raised in elevation to continue their functions, while land may be artificially raised to keep pace with the rising sea
F	This is the most undeveloped area within the study area, and current economic practice is unlikely to prevent wetland loss as predicted by static inundation. Initially, the wetlands will shift landward, though in ever-reducing acreage, until it is halted in its path by landward levees followed by its total demise
G	Same as for C
H	Same as for D and E

**Table 5.6 Revised estimates of land area lost (ha) for Galveston, Texas**

SLR scenario	Year 2050		Year 2100	
	Static inundation	Structural obstruction	Static inundation	Structural obstruction
Low	2010 (33%)	1340 (22%)	2921 (49%)	1600 (27%)
Moderate	2420 (40%)	1410 (23%)	5191 (86%)	1600 (27%)
High	2807 (47%)	1560 (26%)	5291 (88%)	1600 (27%)

However, it is unlikely the above scenario will be allowed to proceed because of the sheer economic value of the infrastructure on Galveston Island. In view of the high property values and the enormous cost of replacing infrastructure, it would seem prudent to protect the coast through the increased use of engineering structures. Hence, at least for the case of Galveston, it may be argued that the majority of the central Galveston Island and the southern part of Pelican Island is unlikely to be lost to the rising sea. It is probable that the seawall will be shored up, pier and land elevations raised, and new bulkheads built, where

necessary, to protect upland properties. This "staking a claim" response through shoreline armoring is also consistent with the projection of Leatherman (1984) in which no shoreline retreat is predicted for the open Gulf Coast, whereas the marsh shoreline of the northern part of Pelican Island is predicted to erode by about 0.72 to 2.54 m/year.

Obstruction due to structures plays a significant role in determining the projected land area that will be lost as a result of accelerated SLR due to the heavily developed nature of the coastal margin. Depending on the SLR scenario and the milestone year in question (2050 or 2100) structural obstructions, if they are held in place, may reduce the amount of land lost to SLR by 33 to 70%.

## **5.4 CAMINADA PASS, LOUISIANA**

### **5.4.1 Site Description**

The entire Louisiana coastal zone, within which the Caminada Pass project quadrangle is located, is the result of deltaic deposition, specifically that of the Mississippi River, in geologically recent times. The largest wetland community in the United States is located within this zone. However, conversion of these marshes and swamps to open water habitat to the tune of  $\approx 80 \text{ km}^2$  a year as a result of various cultural practices has placed the continuing existence of this diverse ecosystem in question (Louisiana Wetland Protection Panel 1987). The SLR projected by the IPCC (1990) could further accelerate the destruction of the remaining coastal wetlands.

The project site lies within Bayou Lafourche, which is one of the four barrier shoreline systems in Louisiana. Specifically, it is composed of the eastern half of the Caminada-Moreau headland and the western one-third of Grand Isle, as shown in Fig. 5.11. Caminada Pass, which separates Caminada Spit to the west and Grand Isle to the east, links Caminada Bay to the Gulf of Mexico. The seaward fringing beaches curve smoothly westward, whereas the leeward shoreline is irregular and highly indented, characteristic of barrier coasts.

The study area is generally of low relief with a series of parallel beach ridges occupying the southeast portion of the area. Elevations range from a maximum of 1.2 to 1.8 m on the crests of sandy beaches, to a minimum of  $\approx 0.5$  m in the marshes (U.S. Army Corps of Engineers 1971). The bottom topography is depicted in Fig. 5.12, which was prepared with the use of the USGS 7.5-min topographic map of Caminada Pass, Louisiana (DMA 7942 II NE-Series V885) and U.S. Nautical Chart 11358 (40th Ed., 4/13/91). The locations of the three transects that were drawn through the study area are shown in Fig. 5.13. Generally, the three transects exhibit similar offshore profiles with two breaks in slope, which occur at water depths of  $\approx 6$  m and 10 m. The slightly shallower depths after the first break in slope along transect A may be due to the ebb-tidal shoal complex associated with Caminada Pass, which tends to skew toward the northeast. However, this ebb shoal is dwarfed by the one associated with Barataria Pass to the northeast, as evident from the undulations in the depth contours in Fig. 5.11. In the same figure, it is also noted that the offshore region within the project quadrangle is relatively free of the many offshore oil

platforms and the associated submarine pipelines that dominate the seascape in this part of the Gulf.

Figure 4.8 (Sect. 4) shows the land use pattern within the project quadrangle. Most of the land area is covered with nonforested wetlands, and a narrow strip of sandy beach that fronts the entire project coastline. The only developed area within the project quadrangle is on Grand Isle, which supports a small resort/fishing community.

#### **5.4.2 Sea-Level-Rise Scenarios**

The SLR scenarios for the study area were developed in Sect. 2 and are summarized for this study area in Table 4.9. The present rate of subsidence for Caminada Pass is  $\approx 8.20$  mm/year and was used to determine the future SLR for the current scenario. Based on the assumption of static inundation, the amount of land that may be inundated under each SLR scenario has been generated. In this section these estimates will be modified, if necessary, as outlined in Sect. 5.1.

#### **5.4.3 Previous Studies**

In the National Shoreline Study (U.S. Army Corps of Engineers 1971), the Gulf shoreline along Grand Isle was listed as suffering critical erosion and that Caminada Spit was experiencing noncritical erosion, based on historical shoreline changes. Specifically, within the period 1812-1954, the shoreline west of Caminada Pass (to East Timbalier Island) receded an average distance of  $\approx 19$  m a year, while the corresponding figure for the shoreline east of Caminada Pass (to Sandy Point) ranges from 4.6 m to 7.6 m. These are regionally averaged figures that may introduce unnecessary bias for our small area of interest. Between 1853 and 1935, the western end of Grand Isle retreated 5.6 m/year on the average. During the subsequent period until 1955, the same area accreted  $\approx 15$  m/year. Hence, the western end of Grand Isle has been described as in a cyclic state of accretion and erosion.

In a more recent study (Penland and Boyd 1981), the erosion rates for Caminada-Moreau headland ranged between 10 to 20 m/year for the period 1934-1974. It was also reported that more than 70% of the total annual erosion experienced there is attributable to hurricanes. Along the Caminada Pass spit, rates of shoreline erosion vary from 5 m/year at the west to stable and slightly accretional adjacent to the pass. Prior to 1972, however, Grand Isle had historically eroded on its western end at Caminada Pass and accreted down drift at its eastern end at Baratavia Pass. In order to reconcile this latter trend with the previous results, it is suggested that within the period from 1955 to 1972, a reversal of shoreline change occurred due to the construction of a jetty system on the western shore of Caminada Pass. Since this system of jetties was constructed the shoreline change pattern at the western end of the island has reversed into an accretional trend of  $\approx 5$  m/year. The erosion along the central Gulf coast of Grand Isle persisted at rates  $< 5$  m/year. The overall accretion/erosion pattern suggests that within the study area, the predominant littoral

transport is in the easterly direction.

The above shoreline change pattern is consistent with an evolutionary model advanced by Penland et al. (1981), which is based on the premise that deltas of different ages produce barrier islands in all stages of development. The evolutionary process, which commences from an abandoned delta complex, occurs in three phases:

1. erosional headland with flanking barrier islands,
2. transgressive barrier island arcs, and
3. sandy inner shelf shoals.

The transition from phase 1 to 2 is facilitated through subsidence, marine reworking, and the offshore movement of sediments. The primary mechanism for the subsequent evolution to phase 3 is a net sediment deficit that occurs when the internal sand supply is exhausted by shore face retreat/subsidence processes, which may result in the total disappearance of the subaerial portion.

Phase 1 evolution may be seen on the Lafourche Delta, which comprises an erosional headland, the Caminada-Moreau coast, and two nearly symmetrical sets of barrier island chains: Caminada Pass spit and Grand Isle to the east and the Timbalier Islands to the west. The project quadrangle falls within the former island chain. In this case, the Caminada-Moreau coast serves as the erosional headland and is a nodal point in the sediment transport system; sediments emanate from here and move eastward and westward. The east-directed portion of the littoral drift contributes to accumulation down drift in the Caminada Spit/Grand Isle system and the subsequent lateral migration of the latter in the direction of longshore sediment transport. This eastward growth is amply borne out by the beach ridge development and recurved spit position on Grand Isle (Penland et al. 1981).

The most comprehensive data source on historic barrier island erosion in Louisiana is a 5-year cooperative effort between the USGS and Louisiana Geological Survey, which began in 1987 (Sallenger et al. 1987). One of the major goals of the 5-year study was the compilation and quantification of changes in shoreline position along Louisiana's barrier coast, from the mid-1850s to 1989. The compilation technique is based on a computer mapping system that quantifies shoreline change data derived from cartographic data sources and near-vertical aerial photography (McBride et al. 1991). The shoreline change data, which cover 880 shore-normal transects at  $\approx 15$  second intervals of latitude or longitude along both the Gulf-side and bay-side shorelines, are presented in terms of magnitude, direction, and rate of change. The results that are relevant to this project were extracted and are shown in Table 5.7.

**Table 5.7 Barrier shoreline change statistics, Caminada Pass, Louisiana**

Parameter			Caminada-Moreau Headland and Grand Isle	Caminada-Moreau Headland	Grand Isle
Gulf-side shoreline change rate (m/year)	Long term	Average	-7.9	-13.3	0.9
		Std. dev.	8.4	5.6	3.1
		Range	6.2/-20.0	-2.9/-20.0	6.2/-3.4
	Short-term	Average	-6.5	-13.6	5.2
		Std. dev.	11.5	7.8	5.7
		Range	16.7/-42.0	-2.8/-42.0	16.7/-2.5
Bay side shoreline change rate (m/year)	Long-term	Average	-0.1	4.1	-1.0
		Std. dev.	2.4	1.9	1.3
		Range	7.0/-2.8	7.0/1.9	2.8/-2.8
	Short-term	Average	-3.0	-1.8	-3.2
		Std. dev.	4.3	1.4	4.6
		Range	5.5/-13.0	0.4/-3.7	5.5/-13.0
Island area Change rate	Long-term	-	-	-	-1.0 ha/year
	Short-term	-	-	-	1.1 ha/year
Projected date of disappearance	Long-term	-	-	-	Year 2148
	Short-term	-	-	-	-

Source: McBride et al. 1991.

In Table 5.7 a plus (+) sign denotes shoreline movement in a seaward direction, whereas a negative (-) sign denotes shoreline movement in a landward direction (toward the mainland) for the Gulf side. For the bay side the sign conventions are opposite. Also, *long-term* implies shoreline record covering more than 100 years, whereas the past 10-15 years are considered to be *short-term*. There are significant differences in the shoreline behavior of the Caminada-Moreau headland and Grand Isle, which constitute two separate phases of deltaic evolution as noted previously. While the Caminada-Moreau headland, which is an eroding abandoned feature, clearly exhibits an erosional trend with an average

rate of -13.3 m/year, Grand Isle, which is a down drift flanking barrier island, remains relatively stable and even slightly accretionary (+0.9 m/year). The change in the areal extent of Grand Isle also indicates relative stability, no doubt a consequence of beach nourishment efforts over the years. Overall, there is a noticeable increase in the short-term shoreline erosion rate over the long-term rate, which implies an acceleration in shoreline retreat in recent years.

On a local scale within the project quadrangle, the spatial distribution of shoreline change in the longshore direction, as derived from the relevant published shoreline change plot (McBride et al. 1991), indicates that the average long-term rate of shoreline erosion on the Gulf side decreases from about 12 m/year at the western extremity to  $\approx 2.5$  m/year just before Caminada Pass in a roughly linear manner. Across the pass, the erosional trend persists at about the same magnitude for  $\approx 3$  km along the Grand Isle, after which the rate tapers off to near zero at the eastern extremity. Beyond and outside the project quadrangle in the eastward direction, accretion occurs.

On the bay side, Caminada Spit displays shoreline advance at a rate slightly less than the rate at which its counterpart on the Gulf side has been retreating. The resulting landward movement of both the bay-side and Gulf-side shorelines experienced here implies that the spit is moving as a whole toward the mainland, a process characterized as landward rollover. On the other hand, the western portion of Grand Isle shows shoreline retreat at roughly the same rate as its counterpart on the Gulf side. This condition leads to island narrowing, which is characterized as in-place breakup, as a result of the converging shorelines. Both conditions result in a net loss of land area, though the latter mode is definitely more alarming. In Louisiana, landward rollover can occur only where an adequate supply of sediment exists for the barrier to respond to the high rates of relative SLR (McBride et al. 1991). In contrast, in-place breakup is a consequence of either/both insufficient sediment supply or/and incomplete overwash process if the island is too wide. Hence, the eastern portion within the project quadrangle will likely experience relatively rapid deterioration.

Prompted by the increasing concern for potentially extensive wetland loss due to the projected acceleration in the rate of SLR, various projections of the future shoreline of Louisiana have been made. From one such report, cited by the Louisiana Wetland Protection Panel (1987), it was shown that given a SLR of 55 cm by the year 2033, most of the wetland currently forming the main bulk of the land area within the project quadrangle would be replaced by open water, leaving behind two adjacent linear subaerial strips, which are the remnants of the Caminada-Moreau headland and a much narrowed Grand Isle.

In a newer study covering the 48 conterminous states (Park et al. 1989), the percentage loss of vegetated wetlands in Louisiana as a whole by the year 2100 has been estimated to be 47% with a 0.14-m rise in sea level (based on the historical rate of SLR), 49% with a 0.5-m rise, 57% with a 1-m rise, 97% with a 2-m rise, and 99% with a 3-m rise under the scenario of standard protection of areas with residential and commercial development. The study approach has been outlined in Sect. 5.2.2. The projection is based on the extension of studies on seven sample sites that cover both interior and ocean marshes, which constitute  $\approx 13.7\%$  of the Louisiana coast (only two sites, one at Pelican Pass at the western extremity of the Caminada-Moreau headland and the second at Golden Meadow in the interior of the headland, can be considered to be in the vicinity of the project

drowned as SLR, because of the net negative accretion deficit.

As discussed in Sect. 5.4.3, the erosion phenomenon at Grand Isle can be characterized as in-place breakup. Such a characterization lends itself to the application of the Bruun Rule on both the Gulf side and the sound side independently of each other. On the Gulf side, the various input values based on a 20-year wave hindcast study for Station 20 (Long. 28.5° N, 90.5° W, 38-m water depth), which is located closest to the study area, are  $\bar{H}_s = 1.1$  m,  $\bar{T}_p = 5.6$  s, and  $\sigma_H = 0.4$  m (Hubertz and Brooks, 1989). Substituting these values into Eq. (5-8) yields  $h_c = 15.4$  m, assuming  $d_{50} = 0.25$  mm. Extrapolating uniformly from Fig. 5.12 yields  $W_c = 9,400$  m at this closure depth. These values compare well with those used by List et al. (1991), which they applied to the western half of Caminada Moreau headland ( $h_c = 15.0$  m and  $W_c = 9,600$  m). Because of the large closure depth involved, the value of B, the dune height, which is unavailable from the limited published literature reviewed, was assumed to be small in comparison with the closure depth, as was the case in the study by List et al. (1991). For the bay side, the distance from the bay shoreline to the mid-point of the bay water body (780 m), as measured from the relevant USGS Quadrangle sheet, was taken as  $W_c$ , while the corresponding  $h_c$  and B were taken as 1.5 m and 1.0 m, respectively.

For transect B, which is characterized by landward rollover as the erosion mechanism, the use of the Double Bruun Rule would be feasible if not for the fact that the bay-side marshes would be drowned, thereby contributing to barrier narrowing as opposed to a constant  $W_1$  assumed in the approach. Hence, the projected rate of erosion here was tracked using the method of trend lines. Table 5.8 lists the input values used, and the results of computation are given in Tables 5.9 (year 2050) and 5.10 (year 2100). In these tables, R and S denote the magnitudes of shoreline retreat and SLR, respectively, while the subscript h denotes "historical."

In Tables 5.9 and 5.10, the predictions based on the Bruun Rule are greater than those based on the trend-line method for transect A under all SLR scenarios. For all other situations, the reverse is the case. The excessive prediction for transect A may be because too large a closure depth was used. Changes in sea floor elevation over the past 100 years, as determined by bathymetric comparisons led to the discovery by List et al. (1991) of a major depositional body east of the Bayou Lafourche headland between Caminada Pass and Quatre Bayou Pass, the eastern entrance to Barataria Bay. This mostly sand-sized accumulation is located at shore face depth (defined by the authors as water depths of 4 to 8 m). Only transect A traverses this bathymetric shallow.

On the other hand, the underprediction of the Bruun Rule for all other cases, using the results of the trend lines as the basis for comparison, can be explained by the presence of a substantial longshore sediment transport gradient, which renders the use of the Bruun Rule (Eq. 5.1) inoperative as discussed in Sect. 5.2.1. List et al. (1991) also reached this conclusion when they conducted a hindcasting of shoreline retreat along the eastern portion of the Bayou Lafourche headland. Even with a maximum SLR rate of 12 mm/year, they found that less than half the shoreline retreat could be attributed to SLR alone.



**Table 5.8 Input values used in the various approaches, Caminada Pass, Louisiana**

transect	Approaches			
	Bruun Rule		Trend lines	
	h. + B	W.	dR <sub>s</sub> /dt	dS <sub>s</sub> /dt
	(m)	(m)	(m/year)	(mm/year)
A (Gulf)	15.2	9,400	3.5	9.0
A (Bay)	2.5	780	3.0	9.0
B (Gulf)	x	x	5.5	9.0
C (Gulf)	15.2	9,400	8.5	9.0

Note: "x" implies that a value was not calculated for the given method.

**Table 5.9 Comparison of projected shoreline retreat for the year 2050, Caminada Pass, Louisiana**

Sea-level-rise scenario	transect	Projected shoreline retreat (m)			
		Bruun Rule		Trend lines	
		Gulf side	Bay side	Gulf side	Bay side
Low (dS/dt = 10.53 mm/year)	A	391	197	246	211
	B	x	x	386	x
	C	391	x	597	x
Moderate (dS/dt = 13.53 mm/year)	A	502	253	316	271
	B	x	x	496	x
	C	502	x	767	x
High (dS/dt = 16.53 mm/year)	A	613	310	386	331
	B	x	x	606	x
	C	613	x	937	x

Note: "x" implies that a value was not calculated for the given method.

**Table 5.10 Comparison of projected shoreline retreat for the year 2100, Caminada Pass, Louisiana**

Sea-level-rise scenario	transect	Projected shoreline retreat (m)			
		Bruun Rule		Trend lines	
		Gulf side	Bay side	Gulf side	Bay side
Low (dS/dt = 11.02 mm/year)	A	750	378	471	404
	B	x	x	741	x
	C	750	x	1,145	x
Moderate (dS/dt = 14.20 mm/year)	A	966	487	607	521
	B	x	x	955	x
	C	966	x	1,475	x
High (dS/dt = 18.20 mm/year)	A	1,238	625	779	667
	B	x	x	1,223	x
	C	1,238	x	1,891	x

Note: "x" implies that a value was not calculated for the given method.

The adjusted Bruun Rule (Eq. 5-5), which incorporates a correction factor that calibrates the rule to site specific conditions, was applied to the study area using the input values shown in Table 5.8. The results obtained using this method are given in Table 5.11. These erosion predictions are very close to the results obtained using the trend-line method.

**Table 5.11 Projected shoreline retreat based on the Modified Bruun Rule, Caminada Pass, Louisiana**

Sea-level-rise scenario	transect	Projected shoreline retreat (m)			
		Year 2050		Year 2100	
		Gulf side	Bay side	Gulf side	Bay side
Low	A	267	209	522	400
	B	x	x	x	x
	C	567	x	1,072	x
Moderate	A	371	265	739	508
	B	x	x	x	x
	C	678	x	1,281	x
High	A	489	321	1,011	646
	B	x	x	x	x
	C	789	x	1,561	x

Note: "x" implies that a value was not calculated for the given method.

The width of the island strip at transect A is only about 300 m. This transect will be completely inundated even under the low SLR scenario. For transect B, the spit may be breached, as it has been in the past century during the landfall of hurricanes Flossy in 1956 and Betsy in 1965 (Penland and Boyd 1981), and disintegrate. Under other circumstances, the spit may weld to the mainland shoreline. However, one should remember that the interior shoreline is composed of marsh. Since the estimated rate of vertical accretion for the marsh lands is below the projected rate of SLR, the marsh lands will tend to be drowned and converted into open water, primarily through coalescence of interior ponds triggered by a sediment deficit, as discussed in Section 5.2.2.

For transect C, the situation is similar to transect B, except that here the marsh is contiguous but dotted by various-sized interior ponds. These ponds are the precursors of an enlarged water body that would eventually engulf the marsh. Hence, while the sandy fringes may be pushed as thin sand wedges over the back-barrier sediments and afford, at best, nominal protection at the Gulf edge, the marsh dieback from the bay side will simply convert the subaerial sand deposits to underwater sand shoals. While historic trends predict substantial shoreline retreat, the magnitude of these changes were estimated base on assumptions about the mechanisms at work. In this case, the causative agent is considered to be hydrodynamic forces. Missing from consideration here is the sediment supply that is the cause of the entire deltaic formation in the first place.

Put in this perspective, and assuming that the present trend of sediment deprivation to the coastal reaches continues, very little land will be left within the project quadrangle by the year 2100. This is because nearly 90% of the land is wetland marsh that is vulnerable to inundation by SLR. This is also true for the static inundation model, where even under the low SLR scenario, the percentage of land above mean sea level is only 11% by the year 2050. By the year 2100, over 96% of the land within the study area will be lost to the sea.

Unlike the other study sites, where coastal erosion is primarily caused by long-term SLR, anthropogenic causes may be responsible for some of the problems being experienced in Caminada Pass's wetlands. Currently, several measures have been proposed for curtailing wetlands loss; the measure with the highest priority has been the restoration of Louisiana's barrier islands. Storm protection, the ability to limit wave erosion of interior marshes, and maintenance of the salinity level of the brackish estuarine waters are the primary motivations. Viewed in this light, it may be tempting to consider that protection efforts to ensure the longevity of Grand Isle through beach nourishment are likely to be forthcoming, given that Grand Isle is one of only two recreational beaches in Louisiana. However, as pointed out in the report by the National Research Council (1990), the economics (i.e., the relative high cost of sand fill versus the value of property to be protected) could make such projects uneconomical.

As for Caminada Spit, which is undeveloped, it may be allowed to migrate toward the mainland by landward rollover, while still maintaining its integrity as a first line of defense for the marsh from waves. The same can be said of the mainland coastline, which will continue to erode as in the geological past but at a much greater rate. The estimates of land loss made here are not unlike those made by the Louisiana Wetland Protection Panel in 1987. The Louisiana Wetland Protection Panel, while acknowledging that global warming currently does not play an important factor in wetland loss in Louisiana, strongly emphasized that the possibility of a rise in sea level of 1 m or so is not a reason to give up on efforts to protect coastal wetlands. But, just another reason to implement measures to restore the delta's former ability to keep pace with subsidence and SLR. However, the possible future implementation of these remedial measures, and the resulting change in the amount of land that would be inundated, is beyond the scope of this work.

#### **5.4.5 Conclusions**

Within the Caminada Pass project quadrangle, the high rates of erosion threaten established development. More importantly, the rapid disintegration of the Grande Isle barrier island will remove the marshes first line of defense —against incoming storm surges. Although the use of analytical methods with a rudimentary consideration of biophysical factors predicts progressive degradation with finite land area remaining at the milestone years considered here, a total land loss is entirely possible from other processes triggered by a deficit in sediment supplies. This is already an acknowledged problem and the projected increase in the rate of SLR is going to accelerate the destruction of the study area. Human actions may, at least partially, prevent some of the predicted damage to the inland wetlands. Thus far, however, no plan of action has been undertaken to nourish or protect the coastal

wetlands of Louisiana. Hence, these potential actions and the changes in land loss consequent upon their implementation have been excluded from this analysis.

## **5.5 BRADENTON BEACH, FLORIDA**

### **5.5.1 Site Description**

The Bradenton study site is within Manatee County, which is on the west coast of Florida near the middle of the peninsula, immediately south of the entrance to Tampa Bay, as shown in Fig. 5.14. The project quadrangle includes the southern half of Anna Maria Island and the northern half of Longboat Key, separated by Longboat Pass. This pass, which was added to the system of federal navigation channel projects in 1977 (Harvey 1982), connects Sarasota Bay with the Gulf of Mexico.

Both Anna Maria Island and the northern part of Longboat Key are low beach ridge, barrier islands. The islands generally having a northwesterly-southeasterly orientation, vary in width from  $\approx 120$  m near the south end of Anna Maria Island and south of the Manatee/Sarasota County boundary in Longboat Key, to  $\approx 650$  m near Holmes Beach on Anna Maria Island and 1,200 m at about the midpoint of the portion of Longboat Key in Manatee County. Elevations along the barrier ridges are generally below 3 m (U.S. Army Corps of Engineers 1972). The Gulf beach is generally low and narrow. For Anna Maria Island, the average grain size of surficial sediments shows a progressive seaward fining, being  $\approx 0.58$  mm at the low water mark to  $\approx 0.15$  mm at a depth of  $\approx 5.5$  m (U.S. Army Corps of Engineers 1972). The corresponding values for Longboat Key are 0.16 mm and 0.51 mm, respectively, which indicates a reverse trend of seaward coarsening. The large mean diameters reported may have resulted from grain-size distributions that are skewed toward the larger sizes because of the presence of shell fragments.

The offshore profiles generally exhibit a relatively steep nearshore slope ( $\approx 1$  in 30) followed by a much flatter offshore gradient as shown in Fig. 5.15. The locations of these offshore transects, two each on Anna Maria Island and Longboat Key, respectively, are shown in Fig. 5.16. The point of transition typically occurs at water depths ranging from 3.5 to 5 m. Inter-transect comparison reveals that the profiles closer to Longboat Pass (transects B and C, especially the latter) are generally shallower than those further away, which may reflect the influence of the ebb-tidal delta located seaward of the pass. Also, the submarine bar formation tends to be much subdued at transects close to the Pass. According to Harvey (1982), tidal flushing at Longboat Pass, in the presence of a weak wave climate, has built a large ebb-tidal delta that recurves to the south around the north end of Longboat Key. However, the inlet receives sufficient tidal prism to stay open and will undoubtedly continue to do so in the future if the size of the bay is not reduced by fill as the islands are developed, which would decrease the tidal prism (Bruun 1966).

Longboat Pass had a wave-dominated, mixed-energy (straight), configuration during the latter part of the 19th century, but changed to a mixed-energy (offset) type in the early 1900's. At present (1990), the inlet is tide-dominated (Davis and Gibeau 1990). It has been

suggested that the gradual switch in the inlet regime may have been in response to a decrease in wave energy and sediment supply. Storm activity apparently has left its legacy in the form of multiple flood-tidal shoals. However, there are no indications that these multilobed sediment accumulations, which have been colonized by vegetation, have been active during the past 100 years (Davis and Gibeaut 1990). Similarly, the inlet channel here has maintained a fairly constant size and shape over the past several decades. It is  $\approx$  6 to 7 m deep at the throat and is between 100 to 200 m wide.

Overall this is a low wave energy coastline with an average wave height of  $\approx$  0.3 m (Harvey 1982). The corresponding mean significant wave height is  $\approx$  0.8 m (Foster and Savage 1989). Nevertheless, the prevailing higher energy pattern due to waves emanating from the northwest, as modified by the local physiography (nearshore and underlying limestone topography), and the occasional passage of tropical storms nearby, is the primary episodic force controlling shoreline change within the study area over the past 100 years.

Figure 4.13 depicts the land use pattern within the Bradenton Beach Quadrangle. The Gulf shoreline is intensively developed by residential and service-oriented development, except for the portions immediately north and south of Longboat Pass, which remain as sandy beaches. The bay shoreline reflects the same dominance of human development, except for some isolated patches of forested wetlands. On the other hand, the mainland shoreline, which is sheltered by the barrier islands, shows a good mix of the various major categories of developed and undeveloped land uses.

### **5.5.2 Sea-Level-Rise Scenarios**

The SLR scenarios for this project were developed in Sect. 2 and are summarized for this study area in Table 4.13. The present rate of subsidence for Bradenton is  $\approx$  0.23 mm/year and was used to determine the future SLR for the current scenario. Based on the assumption of static inundation, the total area inundated under each SLR scenario has been generated in Sect. 4. Section 4's estimates of inundation will be modified here, if necessary, as outlined in Sect. 5.1.

### **5.5.3 Previous Studies**

In an engineering study conducted in 1972, the Army Corps of Engineers determined that the problem along the Gulf shoreline of Manatee County was one of erosion and lowering of the beach profiles, where protected by seawalls, and recession of the shoreline, where unprotected by seawalls. These changes appeared to result from severe storms, which occasionally swept across the Gulf. On the basis of the past position of the mean high waterline, from surveys by U.S. Coast and Geodetic Survey and by the Corps of Engineers, it was determined that from 1874-1883 to 1968 the northern two-thirds of Anna Maria Island advanced an average of 64 m while the southern one-third receded an average of 129 m. However, the retreat along the southern shoreline has been offset by a shoreline advance of 10 m measured for the entire Gulf shoreline during the period 1939-1946, and a much

smaller erosion of 1.8 m for the period 1946-1968. This reversal in shoreline movement could likely have resulted from the construction of a crib jetty along the north shore of Longboat Pass (Walton 1977). The 230-m long jetty, which was completed in 1959, immediately trapped sand moving south along southern Anna Maria Island, causing a 180-m accretion by 1960 (Harvey 1982).

For the total period of 1883-1968, the shoreline change for Longboat Key exhibited the same general trend where the northern two-thirds advanced by an average of 108 m and the southern one-third receded an average of 53 m. Similarly, there were both advances and retreats during the subperiods noted above, with a similar overall advance (4.9 m) during the period 1939-1946. In terms of volume, the annual rate of erosion based on the 90-year span was 106,000 m<sup>3</sup> for Anna Maria Island and 18,000 m<sup>3</sup> for Longboat Key.

In a subsequent study on Longboat Key, Harvey (1982) found that Longboat Key, on the whole, was an eroding barrier island that averaged 0.45 mm/year of erosion between 1940 and 1980. However, there was substantial spatial variation. As expected, Longboat Pass exerts an appreciable control over beach changes in its vicinity. Thus, for instance, the greatest erosion was at Whitney Beach (6.2 m/year) located  $\approx$  1.4 km south of Longboat Key. Approximately 3 km south of the Pass, shoreline change reversed into accretion, with a high of  $\approx$  1.5 m/year occurring at  $\approx$  4 km south of the Pass.

In conclusion, Harvey (1982) stated that a single, average beach erosion rate cannot summarize the diversity of erosion conditions present on Longboat Key. In a similar vein, the same can also be said for Anna Maria Island. This spatial variation reflects subtle differences in the orientation of the beach segments and the relative influence of Longboat Pass. For example,  $\approx$  37 m of erosion purportedly occurred on North Longboat Key after the 1977 dredging, which removed  $\approx$  161,000 m<sup>3</sup> of dredged material with one-third of the dredged volume disposed along 1,280 m of North Longboat Key shore. Erosion occurred directly adjacent to the Pass, soon after dredging took place (Harvey 1982). Table 5.12 sums up the spatial and temporal shoreline change patterns along North Longboat Key, which can be considered to be representative of the varied behavior of the entire project shoreline. The location of the respective beach segments are shown in Fig. 5.17.

Part of the temporal variability can be attributed to the construction of a near-continuous mixture of seawalls, revetments, and groin fields starting in the 1950's with a major development of the barrier islands, which obscured the "natural" rate of shoreline change. If left alone, according to Foster and Savage (1989), the shoreline would have been expected to continue to evolve in a curved orientation to face the northwest waves, with some anchoring by submerged outcroppings of bedrock.

**Table 5.12 Trends in shoreline change, North Longboat Key, Florida. Beach segment numbers refer to Fig. 5.17**

Beach segment	Rate of change		Change in trend after 1968
	1940-1980 (m/year)	1968-1980 (m/year)	
1 Beercan Island	-2.3	-0.3	decelerated erosion
2 Whitney Beach	-6.2	+0.5	trend reversal: erosional to stable/accretional
3 Gulfside Road	-0.4	+0.3	trend reversal: erosional to stable/accretional
4 Cannon's Beach	+1.1	-2.1	trend reversal: accretional to erosional
5 Silver Sands	+1.5	+0.4	decelerated accretion
6 Golden Beach	+0.9	+1.2	accelerated accretion
7 Holiday Beach	+0.4	-0.1	trend reversal: accretional to stable/erosional
8 Harbor Beach	-0.3	-1.4	accelerated erosion
9 Bayport Beach	-0.3	-0.3	no change in erosional trend

*Source: Harvey 1982.*

However, irrespective of the agents of change, the major cause of shoreline recession on Longboat Key has been a deficit in the nearshore sand supply. This is apparent from the increasing sediment deficit being experienced by reaches further south from the primary sand source -the ebb-tidal delta at Longboat Pass (Curtis 1984). In a study spanning the three adjacent county shorelines in Southwest Florida (Manatee, Sarasota, and Charlotte), Foster and Savage (1989) concluded that the shoreline changes and evolving shoreline orientations in their study area over the past 100 years are consistent with net southward littoral transport. However, they also noted the occurrence of net littoral drift reversals, which are particularly apparent on the south side of inlets, such as Longboat Pass, where the associated ebb-tidal shoal refracts incoming waves in such a way that the resulting sediment transport is generally directed into the area from the south during all seasons. The change in refraction pattern, the sheltering from high storm wave activity, and the occasional merging



of the shoals onto the shoreline all combine to form a fluctuating bulbous-shaped accretion area on the south side of Longboat Pass.

In inventorying the beach conditions in Florida, Clark (1990) identified three stretches of the shoreline within the project quadrangle as critically eroding. Of the three, one is further classified as Category I (high erosion rate or recent significant erosion condition with or without adjacent development), whereas the remaining two are classified as Category II (moderate or low erosion rates, but with a narrow beach fronting a highly developed area). Thus, continuing concern about the consequences of coastal erosion, expressed by Clark (1990) and Smith (1991), coupled with a long-term recession of offshore contours and a rising sea level, suggest that the study areas historical rate of erosion may continue, or even accelerate, in the future.

#### **5.5.4 Results and Discussion**

The preceding account has underscored the highly variable nature of shoreline position within the project quadrangle. This variability puts into question the temporal period over which to calculate the average rate of shoreline change. More importantly, there are doubts as to the validity of Bruun Rule in this respect; since, as evident from the discussion in Sect. 5.5.3, and more generally from Fig. 5.17, the shoreline along the southwest coast of Florida in general and within the project quadrangle in particular shows both accretionary and erosional trends in the face of SLR.

Following the same argument that will be discussed for the Daytona study site (Sect. 5.6.4), the modified Bruun Rule as expressed by Eq. (5-5) was used in the subsequent analysis. In this case, the historical rate of shoreline change for each transect were obtained from Fig. 5.18. The profiles in Fig. 5.18 have been prepared based on the recent Florida Department of Natural Resources (FDNR) coastal survey monument and beach profile set, which is part of an overall data base of historical shoreline changes in Florida constructed using all U.S. Coast and Geodetic Survey, National Ocean Survey, and U.S. Geological Survey coastal topographic maps from 1850 to 1987, and supplementing them with beach profile surveys by FDNR for the period 1972 to 1988 (Foster and Savage, 1989). The physical survey monuments are identified as "R" monuments, and are spaced at  $\approx 300$  m intervals. These survey map data are relative to the approximate mean high waterline, and include offshore soundings, which extend  $\approx 1,000$  m seaward along the profiles.

Subjective judgement was used in determining the end years to be used in computing the respective historical rates of shoreline change. In this case, since the respective shoreline change curves for transects A and B show a general downward (erosional) trend, except for some minor perturbations after the 1950s, the starting and ending years of the record were used. The accretionary trends around the 1960s and in 1977 in these two curves are likely to be the result of shore armoring works, which started in the 1950s, and the disposal of dredged material from Longboat Pass on the shore in 1977, respectively. Subsequently, maintenance dredging was carried out in 1982 (154,000 m<sup>3</sup>) and 1985 (114,000 m<sup>3</sup>) (Dean and O'Brien 1987). Dredged material from the 1982 dredging was placed on adjacent islands, whereas that from the 1985 dredging was placed only on the shore of Anna Maria

Island, which manifested itself in the shoreline change curve for transect B as an upward climb (accretion).

Both transect C's and D's curves exhibit a reversal at about 1943, but in the opposite sense. Since transect D is situated downdrift of transect C, the opposite trend could be explained on the basis of mutual interaction: when transect C accretes, less sediment is made available to the downdrift area, which responds by eroding to the (unchanged) wave-induced sediment transport potential. On the other hand, when transect C erodes, the eroded material moves downdrift to benefit transect D. In this explanation, it is implicit that changes at transect C are more influenced by inlet processes. However, it may be possible that the nodal zone (the area in which the predominant direction of the longshore sediment transport changes direction) may be shifted by the change in wave refraction over the ebb-tidal shoal such that transect D erodes and the local reversal in drift brings the eroded material to benefit transect C. Regardless of the local mode of transport, the shoreline change patterns at both the transects are still consistent with each other. For transect C, the slight "hump" around 1977 is likely to be the result of the same mechanism that was operative at transects A and B; the disposal of the dredged material from Longboat Pass.

It is difficult to pinpoint the cause(s) of the major reversal occurring in the 1940's, which seems pretty much an event exclusive to Longboat Key as there was no corresponding reversal on Anna Maria Island. These forcing mechanisms may have included a change in wave approach/shoreline orientation, which seems unlikely as it would have manifested itself in a more regional manner, and the uncovering/outcropping of the underlying limestone/beachrock formations, which offer localized areas with higher resistance to wave forcing. The latter mechanism has also been suggested by Foster and Savage (1989), although they pointed out the need for further research in order to definitively identify the role that bedrock geology may play the areas long-term erosion trend.

Cycles of beach erosion and accretion by tidal inlet dynamics is a well-known phenomenon along barrier coasts. This phenomenon may be invoked to explain the observed erosion/accretion reversal at transects C and D. Figure 5.19 shows the bathymetry in the vicinity of Longboat Pass in three different years: 1883, 1940, and 1977 (Harvey 1982). The 1883 bathymetry shows no significant offset and the ebb-tidal shoal was largely symmetrical, even though the channel was recurved to the south. It appears that during this time period the sand that eroded north of the Pass slowly bypassed the channel toward the south as dictated by the regional southward drift pattern. The bypassed material was retained on the south side of the Pass, thereby nourishing the beaches there. This sand retention may have been aided by a local reversal in drift direction (northward) to eventually build-up a substantial downdrift offset as evidenced by the bathymetry in 1977. Within the same time period, the tidal channel migrated northward  $\approx 275$  m. Of the three mechanisms suggested by Aubrey and Speer (1985) that are responsible for tidal inlet migration in an updrift direction, it seems that attachment of distal ebb-tidal delta bars to the downdrift barrier spit, and storm-induced breaching and subsequent stabilization to form a new inlet, are plausible propositions here.

By 1940, the seaward offset at Longboat Key had grown to almost 900 m relative to south Anna Maria Island (Fig. 5.19), and the Pass had widened, and was 900 m across. After 1939, however, navigation and beach protection activities began to reverse these

natural processes (Harvey 1982). As a result, the Pass narrowed to  $\approx 240$  m, mainly due to a fast growing spit from Longboat Key that encroached into the Pass, which was fed by eroding beaches to the south. Consequently, the seaward offset also receded. However, a more significant morphological change was the appearance of a long, narrow, moon-shaped bar flanking the north side of the Pass. It is suggested that this geomorphic feature may have acted as a shore-normal littoral barrier that prevented, to a large degree, the natural bypassing of southward drift that had benefitted north Longboat Key prior to the 1940s. However, outside the shadow zone of this shore-normal feature, natural bypassing was restored, which benefitted the more southern reaches. Hence, the major reversal in shoreline change in the 1940s could be explained on the basis that transect C lies within the shadow zone mentioned, while transect D lies beyond in the southern direction.

For the present purpose, it was felt that the changes after 1943 would be more reflective of the current and future behavior of the shoreline. Assuming that these external factors will remain unchanged or respond in like manner as observed after 1943, the year 1943 and the end year of the record (1986) were used in computing the historical rates of shoreline change for transects C and D. Hence, the historical rates of shoreline change ( $R_1$ ) for transects A, B, C, and D were taken to be -0.70 m/year, -1.70 m/year, -4.41 m/year, and +1.48 m/year, respectively, where a positive sign denotes accretion and vice versa.

The respective values of  $h$ ,  $B$  and  $W$  were estimated from Fig. 5.15. The results of computation are summarized in Table 5.13 (year 2050) and Table 5.14 (year 2100). Also given in the same tables are the predictions on the basis of static inundation for comparison purposes where a negative sign within parentheses denotes accretion. Although there are noticeable differences among the offshore bathymetries for the four transects, it was decided that a uniform set of input values based on averages be used since it is likely that the ebb-tidal delta may be actively reworked and smoothed out by the expected increase in wave influence as a result of SLR, resulting in a more uniform regional offshore bathymetry. In this case, the values used were  $h = 4.5$  m,  $B = 2$  m, and  $W = 300$  m.

**Table 5.13 Comparison of projected shoreline retreat for the year 2050, Bradenton Beach, Florida**

Sea-level-rise scenario	transect	Projected shoreline retreat		
		Double Bruun Rule		Static Inundation
		dR <sub>2</sub> /dt	R <sub>2</sub>	
		(m/year)	(m)	(m)
Low (dS/dt = 2.6 mm/year)	A	0.7	42	30
	B	1.7	102	submerged
	C	4.4	264	24
	D	(-1.5)	(-90)	15
Moderate (dS/dt = 5.6 mm/year)	A	0.9	54	40
	B	1.9	114	submerged
	C	4.6	276	33
	D	(-1.3)	(-78)	24
High (dS/dt = 8.6 mm/year)	A	1.0	60	75
	B	2.0	120	submerged
	C	4.7	282	60
	D	(-1.2)	(-72)	60

**Table 5.14 Comparison of projected shoreline retreat for the year 2100, Bradenton Beach, Florida**

Sea-level-rise scenario	transect	Projected shoreline retreat		
		Double Bruun Rule		Static Inundation
		$dR_2/dt$	$R_2$	
		(m/year)	(m)	(m)
Low ( $dS/dt = 3.0$ mm/year)	A	0.8	88	45
	B	1.8	198	submerged
	C	4.5	495	36
	D	(-1.4)	(-154)	21
Moderate ( $dS/dt = 6.2$ mm/year)	A	0.9	99	105
	B	1.9	209	submerged
	C	4.6	506	90
	D	(-1.3)	(-143)	70
High ( $dS/dt = 10.2$ mm/year)	A	1.1	121	submerged
	B	2.1	231	submerged
	C	4.8	528	135
	D	(-1.1)	(-121)	105

It is generally believed that the retreat of a barrier island from long-term SLR occurs through a roll-over mechanism. This mechanism has been modeled by the Double Bruun Rule. The width of transect A, B, C, and D is currently 530 m, 200 m, 890 m, and 380 m, respectively. This width is particularly important for transect B, where any projected shoreline recession close to the present width can be considered as leading to total inundation. In this case, the predicted shoreline recession for each SLR scenario is greater than the width of transect B (Table 5-14). Table 5-14 shows that the static inundation and Double Bruun Rule predictions of future shoreline change for the two transects on Anna Maria Island (A and B) agree reasonably well, except perhaps for transect A under the high scenario for milestone year 2100. Both methods project that transect A will be severely impacted, and that transect B will likely be breached through, even under the low SLR scenario.

For transect C, the method of static inundation severely underestimates the future erosional stress, principally because it fails to take into account the highly dynamic nature

of inlet-controlled processes. To the extent that transect D is closely influenced by what happens at transect C, the opposite trend predicted by static inundation is also understandable. However, the relative stability of transect D, when compared to the other three transects, was also borne out by the predictions of static inundation as evidenced from the least retreat predicted, primarily due to the higher ground elevations prevailing here. Hence, at places where morphological changes induced by inlet processes are dominant, the use of static inundation would be highly unreliable. However, it would have erred on the conservative side by underestimating future shoreline recession in an overall sense. Nonetheless, it may be prudent to view the expected losses based on static inundation as yielding the lower bound of projected land loss, assuming no human intervention.

The static inundation model shows that the land loss within the project quadrangle would range from 33% (10.1 km<sup>2</sup>) to 57% (18.6 km<sup>2</sup>), as seen in Table 4.15, the bulk of which comprises residential development (3.3 km<sup>2</sup> to 8.6 km<sup>2</sup>) and wetlands (3.2 km<sup>2</sup> to 4.0 km<sup>2</sup>). These loss values would increase based on the projections of the adjusted Bruun Rule, assuming that nature is allowed to take its own course. This destructive process could also be accelerated by the disintegration of barrier islands due to storm-induced breaching. The removal of this first line of defense against oceanic forces would render the mainland fully exposed to the brunt of sea encroachment and hence, enhanced erosional stress.

Given the intensive urban development that has occurred on the barrier islands in this study area, it is highly probable that technology will be invoked to hold back the sea. According to Smith (1991), coastal erosion is threatening over \$66 million worth of structural improvements along the southern 6.8 km shoreline of Anna Maria Island, a major portion of which is within the project quadrangle. The value quoted above does not consider the cost of public infrastructure and land values. In fact, the Corps of Engineers estimates that property values in the area have gone down \$36 million because of the severe erosion being experienced in portions of the study area. To reduce these potential losses, the Corps has formulated a protection plan that features beach nourishment. Similar beach restoration work has also been planned for Longboat Key (L. Ryder, personal communications). Furthermore, if the protection to the mainland coast that is afforded by these barrier islands is taken into account, the proposal that human intervention will be called for is even more credible.

However, justification for protection, given the present economic framework that values the tangible and quantifiable, is unlikely to be extended to wetlands in the foreseeable future. Hence, retreat and even drowning of the isolated patches of wetlands and fringing forests would proceed unabated, if natural vertical accretion were to lapse behind the rate of SLR. Given such a scenario, the percentage of land loss may be reduced from the projection on the basis of static inundation to a level ranging from about 14% (milestone year 2050 under the low scenario) to 25% (milestone year 2100 under the high scenario).

### 5.5.5 Conclusions

For the Bradenton study area, previous studies indicated that it is largely an eroding barrier shoreline. However, there is substantial temporal and spatial variability in shoreline position, especially along Longboat Key. Analysis of bathymetric changes in the vicinity of Longboat Pass reveals that tidal inlet dynamics exert a substantial control on previous episodes of shoreline changes along the northern half of Longboat Key. Economic arguments and the fact that plans are afoot to address the problem of coastal erosion at Anna Maria Island, and by extension, Longboat Key, suggest that the projected percent of land loss within the project quadrangle on the basis of static inundation may be reduced by 50% as a result of human intervention.

## 5.6 DAYTONA BEACH, FLORIDA

### 5.6.1 Site Description

The Daytona Beach study area lies within the northeast part of Volusia County, which is on the northeast coast of Florida, as shown in Fig. 5.20. The coastline of Volusia is a continuous and rather straight barrier beach, broken only at Ponce de Leon Inlet, which serves as the outlet for the Halifax River. The area is generally low and flat with a well-developed coastal ridge along the shoreline. It is separated from the mainland by a narrow tidal estuary that provides drainage through Ponce de Leon Inlet for most of the interior area. Water depths in the river range generally from 0.9 to 1.8 m, except along the channel of the Intracoastal Waterway, which is maintained to a depth of 3.6 m.

The beaches in Volusia county vary in width from 9 m to 90 m, with an average width of  $\approx 52$  m at mean sea level (Chiu 1989). The beach sediment typically consists of fine, well-sorted quartz sand that produces a hard-packed profile that is ideal for driving vehicles (Hine 1989). The beach is wide at low tide, which implies that the beach slope is very flat.

Ponce de Leon Inlet has had a significant influence on the shoreline in its vicinity since the construction of jetties at the inlet entrance in the 1970s (Jones and Mehta 1978). Using an even-odd analysis, which breaks down the shoreline change into an even (symmetric) component and odd (anti-symmetric) component. The boundaries of the erosional influence for Ponce de Leon Inlet is  $\approx 2.7$  km north of the inlet, which is  $\approx 2.5$  km south of the southern boundary of the study area. Hence, the shoreline change pattern within the study area can be taken to be outside the zone of erosional influence of the inlet.

Figures 5.21(a), (b), and (c) show offshore profiles along three representative cross-shore transects —the relative locations of which are shown in Fig. 5.22, which have been developed using the compiled survey data base of FDNR as discussed in Sect. 5.5.4. Note that the transect profiles tend to be parallel in nature, indicating that on the seaward side of the barrier islands that the shoreline contours are generally straight and parallel to the coastline.

Two beach profiles are shown in each plot to give an indication of the changes that

have taken place during the intervening period (16 years in this case). Other than some changes in the nearshore portion due to bar formation, which is usually a manifestation of seasonal changes. It is seen that there is very little change between the two profiles for transects A and B. Transect C shows shoreline recession, while its offshore portion seems to be stable. All three transects exhibit an almost linear offshore slope starting at an elevation of -3 to -4 m. When superposed, transects A and C overlap over almost the entire measured profile, whereas transect B is slightly deeper offshore. The mean nearshore profile slope is 1 to 75, which steepens to a mean offshore profile slope of 1 to 60. The average grain size of beach sediments north of Ponce de Leon Inlet, which can be taken to be representative of that within the project quadrangle, is  $\approx 0.2$  mm (Hine 1989).

Figure 4.19 depicts the land use pattern within the Daytona Beach quadrangle. The entire length of ocean shoreline within the project quadrangle is fringed with a continuous stretch of sandy beach. Other than the two discrete parcels of natural landscape (evergreen forests) located midway along the barrier island strip, the remaining land space is taken up by either service/commercial or residential development, which attests to the intensive development that has occurred in this region. Several small islands within the Halifax River, at the southern boundary of the project quadrangle, contain forested wetlands.

### **5.6.2 Sea-Level-Rise Scenarios**

The SLR scenarios for this project were developed in Sect. 2 and are summarized for this study area in Table 4.17. The present rate of subsidence for Daytona Beach is  $\approx 0.51$  mm/year and was used in determining the current scenario. Based on the SLR scenarios in Sect. 4 the total area that would be inundated has been calculated. Sect. 4's estimates of inundation will be modified here, if necessary, as outlined in Sect. 5.1.

### **5.6.3 Previous Studies**

The entire coastline of Volusia County has been evaluated by Hine (1989) from the perspectives of dominant processes, shoreline change, and stabilization efforts. His study revealed that the Volusia County coastline is a Holocene barrier island and lagoon-estuarine system that is broken only by one tidal inlet (Ponce de Leon). There is no evidence of overwash fans or storm-surge platforms. Neither is there geomorphic evidence of past inlet activity except in the Ponce de Leon Inlet area itself (the name used prior to 1926 was Mosquito Inlet) and in a former inlet in the Bethune Beach area south of the Ponce de Leon Inlet.

The present barrier-island system was most likely formed within the past 5,000 years in response to the varying sea-level stands that have occurred since the end of the Wisconsin glaciation. The decline in the rate of SLR 5,000 years ago, enabled the barrier island system to stabilize through vegetation-augmented, accretional widening, and upward vertical building. Presently, it appears that this building phase has ceased and that the barrier island may be entering a new phase of erosion. However, considerable complication is likely to



result from the subtle geological control exerted by the Anastasia Formation, which is erosion-resistant. While there appears to be no control or obvious presence of the Anastasia Formation in Volusia County, it is not unreasonable to suggest that portions of this formation, buried in the subsurface, may subtly control barrier island stability or even locally supply sands when exposed (offshore, for example).

Based on the calculations of Walton (1976), who used shipboard wave observations, the net annual sand transport for the coastal reach between Matanzas Inlet and Ponce de Leon Inlet, which includes the project quadrangle, is  $\approx 78,000 \text{ m}^3/\text{year}$  to the south. It has been speculated that since a similar calculation shows a reduced net southward transport ( $22,000 \text{ m}^3/\text{year}$ ) at the coastal reach immediately to the south (Ponce de Leon Inlet to Cape Canaveral), much of the balance of the sand transport has gone into dune building and contributed to the relative stability of this shoreline (Hine 1989).

Indeed, beach profile measurements based on FDNR monument survey for the period 1972-1984 indicate that little change has occurred over this time frame (Hine 1989). However, the widest swings of beach behavior are located near Ponce de Leon Inlet. In an update of the beach conditions in Florida, Clark (1990) identified two stretches of coast within the Volusia County as critical erosional areas where substantial development of recreational interests are threatened. One of them, which stretches from FDNR monuments R-117 to R-148 ( $\approx 9 \text{ km}$  in length), includes the southern portion of the project quadrangle (the southern boundary of the project quadrangle is located at R-125; numbers increase in the southward direction). Hence, the southern 2.1 km (from R-117 to R-125) of the project shoreline falls within the critically eroding category. Since the entire coastline within the project quadrangle is intensively developed, and in the absence of such a classification for the remainder of the project coastline, it can be construed as being stable.

Perhaps the most comprehensive analysis of historical shoreline change along the coastline of Florida to date is Grant (1992). The results of Grant's analysis are all the more relevant since he also investigated the correlation between historical shoreline change and the corresponding SLR, which is a direct attempt at examining the very premise of the Bruun Rule that a SLR is invariably associated with shoreline recession as discussed in Sect. 5.2.1. Fig. 5.23 is a graphical summary of his investigation, which indicates that the mode of the three regional frequency distributions of shoreline change rates is approximately zero, and is flanked on both sides by positive (accretion) and negative (erosion) values.

On a county wide basis, the average shoreline change rates up to the 1930's (from 1873) and from the 1930s to the present (1989) are  $+0.32 \text{ m/year}$  and  $+0.43 \text{ m/year}$  (a positive sign denotes accretion), respectively. The slight increase after 1930s may be the results of inlet modification and, perhaps less significantly, beach nourishment efforts. Updrift of the Ponce de Leon Inlet, but still within the influence of the inlet (taken as up to 2,740 m to its north), the average shoreline change rates before and after training (installation of double jetty completed in 1971) are  $+0.67 \text{ m/year}$  and  $+2.1 \text{ m/year}$ , respectively. The corresponding values for the influenced shoreline to the south (up to 2,740 m to the south of Inlet) are  $+0.87 \text{ m}$  and  $-0.83 \text{ m/year}$ , respectively. The substantial changes since installation are a typical consequence of updrift accretion and downdrift erosion expected of changes induced by shore-normal littoral barriers.

For the period after the completion of the jetties at Ponce de Leon Inlet, the averaged

shoreline change rates on a county wide basis with and without the influenced shoreline in the vicinity of Ponce de Leon Inlet removed are +0.42 m/year and +0.44 m/year, respectively. It can then be inferred that the influence of the Ponce de Leon Inlet is a relatively localized effect and does not affect the averaged shoreline behavior of the Volusia County shoreline to a substantial degree. Hence, for all intents and purposes, the shoreline of the Volusia County can be taken to have exhibited an average shoreline accretion of about 0.36 m/year (1873-1989). The county wide discussion here serves merely to draw attention to the fact that the Volusia County shoreline has a long history of accretion. Actual site-specific data will be used in the subsequent analysis of shoreline change within the project quadrangle.

Historically, sea level along the Volusia County coastline has been rising since its geological past. Since both Volusia and south Florida are situated approximately in the same tectonic setting, Hine (1989) transposed the average rate of SLR based on radiocarbon dating of samples at South Florida to Volusia, yielding a value of  $\approx 3.8$  cm per century. Using tide gauge data recorded in the past 60 years, the compilation efforts of Hicks et al. (1983) indicate that there is an overall rise of  $\approx 16$  cm per century. Hence, the association of a historical rise in sea level and shoreline accretion in this case is not in congruence with the expectations based on the Bruun Rule. In fact, Grant (1992) found that on a county-by-county basis along the east coast of Florida, there is no correlation above  $r=0.41$  between a rise in sea level and a change in shoreline position, and, more importantly, the correlation values, however weak, are positive.

#### 5.6.4 Results and Discussion

The results of Grant's (1992) analysis, which reveal a lack of correlation between shoreline and sea level changes along the east coast of Florida in general and the Volusia County shoreline in particular, immediately put in doubt the validity of applying the Bruun Rule in this region. Similarly, the method of trend lines is also rendered inoperative. This apparent inconsistency underscores the inadequacy of current analytical approaches in predicting shoreline response to a SLR. Its resolution is beyond the purview of the present study and will have to await renewed research on SLR responses.

However, a variation of the Bruun Rule that incorporates a local source term, which takes into account the historical behavior of the shoreline response to sea-level change, is perhaps germane to the problem at hand. In this context, although the parameter  $R_1$  in Eq. (5-5) has been formulated explicitly to account for the present recession rate induced by the present rate of SLR, it can be generalized to include shoreline advance as well since  $R_1$  is assumed as a calibrating parameter to suit local conditions. It is suggested that the low rate of historical SLR has been conducive to a historical trend toward accretion due to the complicated interaction among other factors such as the local production of sediments, longshore sediment transport gradients, and tide range/wave height differences. However, under the accelerated rates of SLR assumed for the future, it is conceivable that the resulting destructive forces may overwhelm the constructive factors to such an extent as to bring about a reversal in shoreline erosion/accretion (e.g., mean wave heights will increase).

In the subsequent computations, the same input values for  $h$ ,  $B$ , and  $W$ , which are estimated from Fig. 5.21(a), (b), and (c), have been used for all three transects since they are all very similar in profile shape; these are 5 m, 6 m, and 450 m, respectively. The historical rates of shoreline change are taken from the same FDNR data set discussed in Section 5.6.3, but now specific to each transect as shown in Fig. 5.24. As indicated, all three temporal shoreline change curves exhibit an increasing trend. Ignoring the pulse-like event around the period 1974-1975, which may be the result of episodic occurrence, it is seen that the rate of shoreline accretion slowed down considerably after the 1930s. This is consistent with the average trend for the Volusia County shoreline discussed in Section 5.6.3. Qualitatively, this may be construed as a response to an increasing rate of SLR in the latter period, which tends to support the argument offered above for generalizing the use of Eq. (5-5). Taking the average of the end values, the historical rates of shore advance for transects A, B, and C have been estimated from Fig. 5.24 to be 0.39, 0.44, and 0.41 m/year, respectively. These values are close to the average value of 0.36 m/year discussed in Section 5.6.3. From Fig. 5.24, it is also apparent that the shoreline at transects A and B seem to have recovered fully from the episodic events around 1974-1975, while transect C apparently has not, hence the shoreline recession shown in Fig. 5.21(c).

Using the current rate of SLR adopted for the study site (2.0 mm/year) as representative of the historical rate of SLR, the projected rates of shoreline recession under different scenarios and at different milestone years are given in Table 5.15 (year 2050) and Table 5.16 (year 2100) where the values enclosed within parentheses denote accretion.

As far as the ocean shoreline is concerned, it is seen that the projected behavior of the shoreline is essentially stable. The small numeric values are actually within the expected bounds of short-term shoreline fluctuations due to seasonal variations and storm events, which can be as much as 20 m (Grant 1992). Except for transect C under the high scenario, the projections based on static inundation are similar. As noted previously, transect C is located very close to a critically eroding area identified by Clark (1989) while Fig. 5.21(c) shows a net recession for the period 1972-1988. Hence, it is not surprising that transect C appears to be the most vulnerable.

Hence, for the present purpose, it may be prudent to use the results from the approach of static inundation, but tempered with subjective judgement based on site-specific considerations. Static inundation figures show that the highest percentage of land loss under the most severe scenario is  $\approx 17\%$ . From the breakdown listed in Table 4.19, the bulk of the land loss consists of residential and commercial development at the southern portion of the project quadrangle (the digital terrain output shows that the southern 4 km of the barrier island strip will be completely lost to the sea). The fronting beach along the seaward margin will also be lost almost completely.

**Table 5.15 Comparison of projected shoreline retreat for the year 2050, Daytona Beach, Florida**

Sea-level-rise scenario	transect	Projected shoreline retreat		
		Modified Bruun Rule		Static inundation
		$dR_2/dt$	$R_2$	
		(m/year)	(m)	(m)
Low ( $dS/dt = 2.9$ mm/year)	A	(-0.35)	(-21)	negligible
	B	(-0.40)	(-24)	negligible
	C	(-0.37)	(-22)	negligible
Moderate ( $dS/dt = 5.9$ mm/year)	A	(-0.23)	(-14)	negligible
	B	(-0.28)	(-17)	negligible
	C	(-0.25)	(-15)	negligible
High ( $dS/dt = 8.9$ mm/year)	A	(-0.11)	(-7)	negligible
	B	(-0.16)	(-10)	negligible
	C	(-0.13)	(-8)	24

While the southern portion of the study area has been categorized as critically eroding (Clark 1990), this classification is also a reflection of the monetary values placed on the on-site economic development. Hence, it is likely that given the high economic stakes, which are dependent on the availability of scenic beaches, there will be continuing efforts to forestall the sea advance through beach nourishment, at least for the low and moderate SLR scenarios.

Although it is highly unlikely that future beach nourishment policies will apply irrespective of the rate of SLR, it has to be borne in mind that the relative prosperity of Daytona Beach hinges heavily on the availability of scenic beaches. This beach-dependence tends to exclude other engineering approaches, such as shore armoring, when efforts are made to preserve the shoreline. In this respect, the current shoreline will be held in place. In order to maintain continuity in the alongshore direction, efforts to prevent the predicted break-through are likely to be made.

**Table 5.16 Comparison of projected shoreline retreat for the year 2100, Daytona Beach, Florida**

Sea-level-rise scenario	transect	Projected shoreline retreat		
		Modified Bruun Rule		Static inundation
		$dR_2/dt$	$R_2$	
		(m/year)	(m)	(m)
Low ( $dS/dt = 3.3$ mm/year)	A	(-0.34)	(-37)	negligible
	B	(-0.39)	(-43)	negligible
	C	(-0.36)	(-40)	24
Moderate ( $dS/dt = 6.5$ mm/year)	A	(-0.21)	(-23)	negligible
	B	(-0.26)	(-29)	24
	C	(-0.23)	(-25)	36
High ( $dS/dt = 10.5$ mm/year)	A	(-0.04)	(-4)	10
	B	(-0.09)	(-10)	42
	C	(-0.06)	(-7)	570 (totally submerged)

It is pertinent here to note that because of the height and width of the foredune ridge, the dense vegetation along the natural stretches of barrier island, and the narrow character of the back-barrier lagoon (Halifax River), it is highly doubtful that storm surges could form new inlets anywhere along the Volusia County coast (Hine 1989). Also, Mehta and Brooks (1973) showed that no breakthrough, either from the ocean or lagoon side, could be sustained and form a relatively stable inlet along a similar elongated semi-enclosed body of water south of the Ponce de Leon Inlet (this finding is based on the assumption that Ponce de Leon Inlet will remain open, an assumption that may be put in question if a new inlet were formed north, or up stream, on the Halifax River).

The same argument regarding protection needs based on economics can also be applied to the development along both shores of the Halifax River. In this case, the balance will be tilted even more toward protection due to the protected nature of the shoreline. Under this scenario of human intervention, the only land loss that will likely be sustained will be that associated with forested wetlands occupying several subaerial shoals within the southern channel of Halifax River, which amounts to about 2% of the total land lost on the basis of static inundation.

### **5.6.5 Conclusions**

A previous study (Grant 1992) conducted in the Daytona Beach area has raised doubts regarding the validity of the Bruun Rule in the present case. Despite a historical pattern of SLR, the shoreline has accreted during the corresponding period. However, a generalization of the modified Bruun Rule did enable computations to be made in this respect. Except for transect C, the projected behavior of the ocean shoreline agrees well with that based on static inundation. This is perhaps expected because of the long history of dune-building and shoreline stability evident along a substantial length of the project coastline. The relative vulnerability of transect C is consistent with the findings of Clark (1989) and a time-separated comparisons of beach profile surveys.

Considerations of dominant physiographic factors and economic concerns lead to discounting of the predicted land loss on the basis of static inundation. The intensive development that has taken place argues for continuing efforts to stabilize the shoreline at its present position. On the other hand, wetlands thriving on subaerial shoals in the waterway may be the only "resources" that may be foregone due to their perceived low economic value. As a result of human intervention, it is likely that the 17% land loss predicted under the most severe conditions on the basis of static inundation will be reduced to less than 5%, and then only if the wetlands are unable to keep pace with the rising sea level.

## **5.7 McCLELLANVILLE, SOUTH CAROLINA**

### **5.7.1 Site Description**

The Cape Romain study area is situated within the Santee River Delta. The Santee Delta was growing until the 1940's from fluvial sediments being deposited by the river. This sediment originated from the piedmont and mountains to the west of the Santee River. However, since the 1940s the delta has experienced high rates of erosion as a result of dam construction and upstream water diversion from the Santee River (these activities reduced the amount of sediment delivered to the coast).

The Cape Romain Wildlife Refuge, which forms a significant portion of the study area, consists of a series of undeveloped barrier islands and saltwater marshes that lie between the Atlantic Ocean and the Intracoastal Waterway and forms the longest uninterrupted stretch of pristine ocean shoreline in South Carolina (Fig. 5.25). As is typical of any ocean shoreline backed by a wide expanse of salt marsh, the project site is generally flat and subjected to tidal inundation. Numerous tidal creeks crisscross the salt marshes. Typical offshore profiles along the project coastline are shown in Fig. 5.26; the positions of these offshore transects are indicated on Fig. 5.27. As evident from Fig. 5.26, the shoreline is fronted by a relatively mild offshore slope, where the 10 m underwater contour is located at about 8,000 to 10,000 m offshore (note that Fig. 5.12 is exaggerated vertically). This gently sloping bottom is a manifestation of the shallow ocean reservoir adjacent to South Carolina's continental shelf, which is bounded by the Gulf Stream about 90 km from the

shoreline. The continental shelf circulation here is a large gyre in which water moves counterclockwise between the coast and the Gulf Stream (South Carolina Water Resources Commission 1970).

On a more local level, the nearshore bottom slope is generally steeper with a slope of  $\approx 0.5^\circ$  (1 to 110), which then gives way to a much gentler slope of about  $0.05^\circ$  ( $\approx 1$  to 1200). This break in slope occurs at 300 to 500 m offshore. Also, Fig. 5.26 shows that the offshore profile along transect A is steeper than the profiles along transects B and C, which are generally similar in profile shape. Figure 5.27 indicates that transect A cuts through the sand spit adjacent to the Key Inlet, which results in a steeper offshore slope seaward of the sand spit (the shoreline for transect A is taken as the seaward water edge of the sand spit).

No information regarding the sediment characteristics of offshore bottom could be procured with the limited search effort conducted. However, in comparison with the offshore profiles at the Galveston site (Fig. 5.5) where the 10 m depth is  $\approx 4,000$  m to 7,000 m offshore, and inasmuch as the sediment size is generally acknowledged to be uniquely related to bottom slope for a given wave environment, it is perhaps not unrealistic to assume that the offshore bottom is underlain by mud (fine-grained sediment) deposits. Of course, the presence of relatively thin sand surficial deposits that occur in discrete linear fringes and bars cannot be excluded. Landward of the mean water line, the association of saltwater marshes with hydric soils that are predominately fine-grained again reflects the predominance of a muddy substrate. In the first update of the National Wetlands Status Report (Dahl and Johnson 1991), only 9.9% of the 2.2 million ha of coastal wetlands remaining in the conterminous United States were found to be associated with unconsolidated sandy/rocky shores. Hence, the entire profile can be treated as a mud profile in which the usual transport mechanisms derived for sand sediments would not be expected to be entirely applicable.

Figure 4.24 depicts the land use pattern within the McClellanville Quadrangle. As indicated, the ocean shoreline consists of a narrow fringe of sandy beaches backed by extensive salt marshes, which are classified as nonforested wetlands in this case. The township of McClellanville, which is basically a fishing village dominated by modest wood-frame houses and mobile homes, is landward of the Intracoastal Waterway and forms the only residential area within the project site. The township is surrounded by a combination of deciduous forest, forested wetland, and cropland and pasture. The only other land use that attests to the presence of anthropogenic influence is the quarries/gravel pits located east of the township.

Generally, a characteristic feature of coastal marshes along the South Atlantic coast is the vast expanse of smooth cordgrass, *Spartina alterniflora*, which covers the soft grey sediments between mean sea level and approximately mean high water (Odum et al. 1974). These broad nearly level expanses of grass and soft sediment developed under the influence of high tidal amplitudes, dendritic creeks and deep tidal channels in vast numbers, giving the marshes a characteristic dissected pattern in plan view. The slow, gentle subsidence of these marshes also contributes to the formation of these intricate creek patterns.

### 5.7.2 Sea-Level-Rise Scenarios

The SLR scenarios for this project were developed in Sect. 2 and are summarized for this study area in Table 4.21. The present rate of subsidence for McClellanville is  $\approx 1.4$  mm/year and was used to determine the future SLR for the current scenario. Based on the assumption of static inundation, the area submerged under each SLR scenario was generated in Sect. 4. Section 4's estimates of inundation will be modified here, if necessary, as outlined in Sect. 5.1.

### 5.7.3 Previous Studies

The portion of the South Carolina coast that is discussed here has not been studied in detail in the past, primarily because of its undeveloped nature. Although the area to the south, including Charleston, have been extensively studied. However, some general comments on the morphology and shoreline change pattern of this chain of relatively inaccessible barrier islands are in the open literature in connection with regional studies of a wider spatial coverage.

In a beach erosion inventory of Charleston County, Stephen et al. (1975), who based their study on aerial photographs from 1941 to 1973, found that Raccoon Key (which encompasses the entire project shoreline) is a transgressive shoreline whose beaches consist of eroding mud, a low sand and shell berm, and washover terraces. Measured erosion rates range from 180 to 460 m, which clearly indicate a long-term erosional trend. On the other hand, the recurved spit on the southeast corner of the project quadrangle (Fig. 4.24) is a propagational feature that is fed by sediments eroded from the eastern side of Cape Romain Island. From 1941 to 1968, the spit grew at an average rate of  $\approx 45$  m/year. The study ascribes the main causes of erosion to the reduction of river-borne sediment supply (which is elaborated further in subsequent paragraphs) and the result of exposure to severe wave attack from large stretches of open water.

In likening the morphological behavior of the Grand Strand, which lies to the north, to that of the Santee Delta, Kana (1989) suggested that the erosional trend of  $\approx 30$  cm/year experienced here is of the order that can be attributed to inundation as a result of a local SLR of  $\approx 24$  cm/century.

In a mapping study that involved 336 km of the open Atlantic coastline from Tybee Island, Georgia, to Cape Fear, North Carolina, for the period 1851 to 1983, Anders and Reed (1989) found that the coastal reach from Bulls Bay to North Inlet, which includes the project site, is erosion-dominated. The maximum erosion rate of  $\approx 12$  m/year was shown to occur in the vicinity of the Cape Romain Wildlife Refuge, where shoreline movement of more than 1,300 m was registered within the study period. It is evident that the long-term erosional trend identified by Stephen et al. (1975) still persists.

In terms of temporal pattern, the shoreline was accretional until the 1940s and primarily erosional during the period 1960-1983. However, the severity of the physical loss has had little economic repercussion. At least that seemed to be the prevailing sentiment in the early 1970s as eloquently borne out by the finding of the South Carolina Tidelands



Report (South Carolina Water Resources Commission 1970) who stated that “an examination of the second major reach, that between Winyah Bay and Charleston Harbor, reveals no serious beach erosion north of Bull Island.” This perceived absence of erosion threat is partly a legacy of couching most physical problems in strictly economic terms and the failure to recognize the intrinsic value of ecological systems that thrive in wetlands and their interlinkages with human economic activities (e.g., fishing).

In attempting to establish the causative agents for shoreline change through regression analysis, Anders and Reed (1989) found that shoreline change is well-correlated with maximum significant wave height,  $H_{s, \max}$ , derived from the hindcast results of the WIS by the U.S. Army Corps of Engineers ( $H_{s, \max} = 4.6$  m for Cape Romain). Hence, they suggested that the long-term erosional history of the coast studied may depend heavily on storm frequency and intensity. However, as Kana (1988, 1989) pointed out, upstream dams and river diversion have triggered episodes of rapid erosion along this stretch of coast. Hence, the above interpretation needs to be considered in light of the known impact that human intervention has had on the region. Unfortunately, Anders and Reed noted, SLR data are not available in sufficiently small spatial increments along the studied coast to permit their direct comparison with measured shoreline change over the period of record.

On a regional basis, an update of the National Wetland Trend Analysis (NWTa) Study (Tiner 1991) indicated that for the period 1974-1983, South Carolina lost  $\approx 460$  ha of estuarine wetlands, which is  $\approx 0.3\%$  of the total acreage. The study used a combination of statistical sampling and photo interpretation techniques and defined estuarine wetlands as encompassing salt marshes, mangrove swamps, and tidal flats. Although the data set does provide some opportunities for a real-time assessment of the effects of recent SLR on estuarine wetlands, Tiner claims these data may not be of much use for site-specific studies, as is the case here, because of the lack of SLR data of sufficient spatial resolution as previously cited.

Inasmuch as the generally higher erosion potential associated with a higher sea level is translated in part through the occurrence of storm events of greater frequency, it may be instructive to examine the response of wetlands to episodic events. Since an analytical treatment will not be possible because of our lack of understanding of the underlying processes, our purposes will be served by examination of field data from an extreme event such as a hurricane. Such an opportunity was afforded by Hurricane Hugo, which swept through the area in September 1989, leaving a swath of destruction in its wake.

Hurricane Hugo, with sustained wind speed in excess of 135 mph, made landfall just north of Charleston, South Carolina, shortly after midnight on Friday morning, September 22, 1989, 1 hour before high tide. Although the resulting economic damages have been well documented, they mostly concern either damages to properties and infrastructure (Wang 1990; Stauble et al. 1990; U.S. Army Corps of Engineers 1990; Macchio 1990) or the extent of water inundation (USGS 1990). While the project site was stricken by the highest storm surge, ranging from 6.1 m on the western border to 3.7 m on the eastern border of the project quadrangle, the damages as gleaned from the reports cited above relate only to the seaward margin where barrier islands exist and to the landward properties. Stauble et al. (1990) reported that many of the narrow barrier islands were breached or completely overwashed, resulting in landward migration of the barriers into the marsh. On the other

hand, Macchio (1990), in describing the aftermath at the hardest hit area, McClellanville, documented, "After Hugo, boats lay stranded everywhere and layers of ocean mud (emphasis added) lay on the road and befouled homes throughout the village." Although there were extensive damages reported on upland forests where a vast majority of the trees were simply sheared off at a height of 3 to 7.5 m above the ground (Macchio 1990), no mention was made of the salt marshes. Although it is tempting to deduce that the salt-marsh vegetation, being of low elevation and having a dense undergrowth that helps to retard the erosive forces of storm surge, may have escaped relatively unscathed from the onslaught, there is a dearth of reports to this effect, and this opportunity to gauge the field response of wetlands to episodic events was lost.

#### **5.7.4 Results and Discussion**

As mentioned previously, of all the assessment methods pertinent to sandy shores discussed in Sect. 5.2.1, only the method of trend lines does not presuppose the type of substrate; it only presupposes that the forcing and response patterns that were operative in the past remain unchanged and continue to operate into the future. Hence, this method is applicable to muddy shorelines fringed with wetlands. More importantly, the change in shoreline position is largely the result of SLR. The assumption of a muddy shoreline (other than the advancing sand spit at the southeast corner of the project quadrangle) in this case is not unrealistic.

When the above premises are considered, the results of applying the method of trend lines are shown in Table 5.17 together with those based on static inundation measured from the digital output maps provided. In this method, the average historical rate of shoreline recession was taken to be 10 m/year, which is the algebraic mean of the two end values of the range of values that Stephen et al. (1975) reported.

On the other hand, the corresponding historical rate of SLR is available from a few sources. The current rate of SLR adopted for the study site (2.9 mm/year) is a potential candidate. Kana et al. (1988a) assumed the current rate of relative SLR in Charleston to be 2.5 mm/year. Hicks and Crosby (1974) reported the value 2.2 mm/year, which is based on trend and variability analyses of yearly mean sea level of tide gauge data at Charleston for the period 1941 to 1972. Stevenson et al. (1986) also used this value as the apparent SLR rate for North Inlet, South Carolina in their attempt to correlate vertical accretion in marshes with SLR. Since the period of data coverage for the above study coincides with that of the erosion inventory study (Stephen et al. 1975), the value of 2.2 m/year was deemed to be representative of the historical rate of SLR in the past for the present purpose.

**Table 5.17 Comparison of projected shoreline retreats for McClellanville, South Carolina**

Scenario	Static inundation		Method of trend lines	
	Year 2050	Year 2100	Year 2050	Year 2100
	(m)	(m)	(m)	(m)
Low	8,450	8,530	1,018	2,109
Moderate	8,660	8,760	1,836	3,700
High	8,720	8,980	2,655	5,700

On the basis of static inundation, it is found that various islands of wetlands manage to remain above the static water level. The number of these individual subaerial land masses reduce drastically with increase in water level (meaning either further into the future or a higher SLR scenario). This may imply that the elevation of these land masses will not be much higher than the static water level and will be subjected to hydraulic stresses from all sides in the future. Hence, it is unlikely that the vegetation, once isolated, will be able to thrive simply because of its reduced size below the level of minimum acreage for viable sustenance. The vegetation dieback will further hasten the disintegration of the isolated land masses. As for the presently growing sand spit, it may be breached and severed from Cape Romain and subsequently migrate shoreward through overwash processes to coalesce with the seaward isolated salt-marsh islands. The inherent assumption here is that the longshore supply of sediment from the east is not sufficient to keep pace with the transporting capacity of the enhanced wave action because of extreme events, as borne out starkly by the impacts of Hurricane Hugo. Once welded to the mud substrate, these sand deposits can be considered an integral part of the island masses and further disintegration should proceed as projected.

Even though the disintegration of the islands over time may slow down the projected rate of shoreline retreat somewhat, it is unlikely that the overall picture as regards the projected shoreline position based on the method of static inundation will be materially altered. Indeed, the previous episodes of shoreline retreat may well occur in the same fashion. Hence, the projected shoreline in the case of static inundation is taken to be the mainland shoreline given by the digital model output without regard to the existence of the island patches shown in them. The values shown are the averaged values based on the individual retreats along transects A, B, and C. It will be evident from the following that the above values are modified by the incorporation of biophysical and sedimentary processes.

It is seen that the projected shoreline recessions are of the order two to eight times those based on the method of trend lines. The approach of static inundation wholly ignores the dynamics of the wetland systems, which can accrete vertically to keep pace with a rise in sea level as well as grow laterally.

An important consideration in assessing the response of wetlands to SLR is the role

of vertical marsh accretion and the concomitant sedimentation. Stevenson et al. (1986) have documented previous studies on marsh development along the Atlantic and Gulf coasts, where in most instances sedimentation and peat formation have kept pace with rising sea level. They found a positive relationship, based on the regression approach, between accretion balance (vertical accretion rate minus local apparent SLR) and the tide range of the following form, which is based on 13 nonriverine marshes ( $r = 0.86$ ):

$$Y = 2.4X - 2.1 \quad (5-18)$$

where

Y = accretionary deficit in mm/year,

X = mean tide range in m.

The ranges of Y and X for their data points are from 0.5 to 3.0 m and from 2 to 4 mm/year, respectively.

Hence, they concluded that both sediment input and the amount of tidal energy (by proxy of the tidal range) are equally important in determining rates of marsh accretion. This implies that a marsh in an area of a smaller tidal range is more likely to drown compared with one in an area of a greater tidal range in the event of a SLR of equal magnitude.

The effects of future SLR on both vertical marsh accretion and tidal range have not been adequately studied. Frequently, correlations in the former case were made with respect to the past rates of SLR and the present rate of vertical accretion is held constant without regard to potential changes in the sedimentation regime. On the other hand, the effect on the latter in the case of inlet-bay systems has been examined, which primarily forecasts an increase in tidal range with rise in sea level (Mehta et al. 1987).

Sedimentation rates in most wetlands amount to only a few millimeters a year (Orme 1990). In the study by Stevenson et al. (1986), the mean vertical accretion rates reported by individual marsh studies documented by them range from 2.5 mm/year (North Inlet, South Carolina) to in excess of 10 mm/year (Lewes, Delaware). The corresponding figures reported by Orme (1990), which are grouped by the type of environment (salt marsh, tidal flats, estuaries, bays and lagoons, deltas, natural lakes, Sabkha evaporites, and peat bogs) are 2.4 mm/year (bays and lagoons) and 10.9 mm/year (tidal flats). In the case study on Charleston, Kana et al. (1988a) assumed a value of 5 mm/year, after taking into account the published rate of 4 to 6 mm/year measured by Ward and Domeracki (1978) in an intertidal marsh 20 km south of Charleston.

In the present study, the rate of vertical accretion was taken as 5 mm/year in an attempt to evaluate the survivability of wetlands under different SLR scenarios. Table 5.18 shows the results. It is evident from Table 5.18 that in other than the low scenario, future SLR will result in the drowning of wetlands and, hence, their conversion to open water. Under these circumstances it is likely that the wetlands will tend to shift landward, provided there is adequate space on the landward side for such a lateral shift. The role of the

migrating sand spit that will merge into the marsh is not known precisely. However, since the sand supply is likely to be source-limited, the sandy sediments may exist only as a surface veneer as a result of wave sorting and may afford limited armoring effect during relatively calm conditions. Hence, the overall retreat pattern is unlikely to be changed appreciably.

**Table 5.18 Annual net accretion deficit of wetlands, McClellanville, South Carolina**

Scenario	End year	Sea-level rise (cm)	Average annual rise (mm)	Annual sedimentation (mm)	Annual net accretion deficit (mm)
Current	2050	8.4	1.4	5	3.6
	2100	15.4	1.4	5	3.6
Low	2050	22.4	3.7	5	1.3
	2100	46.4	4.2	5	0.8
Moderate	2050	40.4	6.7	5	-1.7
	2100	81.4	7.4	5	-2.4
High	2050	58.4	9.7	5	-4.7
	2100	125.4	11.4	5	-6.4

Wetlands follow a zonation pattern that is primarily elevation-dependent, being a reflection of the duration of submergence and, hence, sedimentation and salinity regimes. The more salt-tolerant halophytes predominate on the seaward fringe, whereas the less tolerant species are found in the higher landward area. This elevational grouping manifests in the form of low marsh and high marsh and a transition zone that blends into the upland vegetation. The presence of high and low marsh zones, as is found in the Charleston area (Kana et al. 1988a), is a characteristic of wetlands along submerging coasts, which is one of the six major sedimentary tidal marsh types suggested by Stevenson et al. (1986), based on accretionary relationships.

From Fig. 5.26 it can be seen that the nearshore profile, up to about 5,000 m offshore, is concave upward. Such a topographic makeup implies that the horizontal area of wetlands available on the landward side of the water's edge would be less compared with the case of uniform slope due to the elevation dependency of wetland species. Any human protection measures that seek to halt the encroachment of the sea onto upland properties will further limit the space for a landward shift of the wetlands. The maintenance of the Intracoastal Waterway is a prime example, as the salt marshes are unlikely to be allowed to encroach into this navigable waterway. Therefore, it may well be that the wetlands will be

squeezed out of existence under the moderate and high SLR scenarios on the basis of static inundation. An infrastructure that would be adversely affected is the Intracoastal Waterway, which skirts the landward edge of the study areas wetlands. Although the need for navigation may argue for the continued protected of the waterway, the sheer cost of such a project over the distances in question puts in doubt the ability of the U.S. Government to finance such a project. At any rate, if the forecast based on static inundation is accepted for the study area and the marsh is not allowed to migrate inland, it will be completely inundated.

However, as evident from Table 5.17, the trend-line method predicts that about half of the wetlands will remain, even for the high scenario. Granted that wetlands may drown for the moderate and high SLR scenarios as projected in Table 5.18, it is suggested that the ensuing retreat of the wetlands will follow the horizontal trend predicted in Table 5.17.

For the low scenario, the entire outcome hinges on the accuracy and persistence of the current sedimentation supply. Although previous episodes of shoreline retreat in the study area have been attributed to a sediment deficit caused by the diversion of the Santee River, a conscious effort is currently underway to restore the flow of the river (however, the sediment once carried by this river will still be trapped behind the upland dams). Provided this restored flow is not diverted in the future, and that the flow contains sufficient sediment, it may be concluded for the low SLR scenario that the natural vertical accretion of marshes in the study area will be able to keep pace with the projected rise in sea level. However, episodic retreat will still occur under extreme storm conditions such as hurricanes.

Biophysical factors (in this case, salt marshes) play a significant role in mitigating the extent of projected impacts based on static inundation. For the low scenario where the upward accretion of salt marshes is expected to keep pace with the rise in sea level, the outlook is one of relative stability, bearing in mind the ameliorative effects of the redirection project concerned. On the other hand, while the salt marshes will be progressively drowned under the moderate and high scenarios based on a cut-off accretion rate of 5 mm/year, the extent of retreat, as projected by the trend line method, indicates a 50 to 66% reduction in the projected area of land lost compared with the predictions of static inundation.

The revised projected land areas lost, after taking into account any structural obstruction, are shown in Table 5.19 for various scenarios. These estimates are based on simple proportions of the averaged change in linear lengths computed along transects A, B, and C. The figures in parentheses represent percentages of land area loss relative to the present land area. It is emphasized that the estimates of land area lost to SLR shown in Table 5.19 are tentative. Indeed, the simplicity of the calculations belies the complexity of the issue at hand, and the predicted values, together with the inherent assumptions about marsh accretion rates made for this study area, should be viewed with caution. In addition, the simplified approach used for this case study does not consider the physiological response of wetland plants (e.g., stress) to an accelerated rate of SLR.

**Table 5.19 Revised estimates of land area lost (ha), McClellanville, South Carolina**

Sea-level-rise scenario	Year 2050		Year 2100	
	Static inundation	Biophysical factors	Static inundation	Biophysical factors
Low	5,916 (43%)	Minor	7,423 (56%)	Minor
Moderate	7,129 (54%)	1,510 (12%)	7,957 (61%)	3,370 (26%)
High	7,723 (59%)	2,340 (18%)	8,541 (66%)	5,420 (41%)

The likely increase in salinity associated with a rise in sea level could possibly put additional stress on wetland plants, especially those at the inner (landward) fringe, which thrive on the lower end of the salinity-dependent zonation. The subsequent vegetation dieback may render the substrate more vulnerable to both current- and wave-induced erosion. Inasmuch as the marsh accretion rate is the summed contribution from both inorganic sediments and organic (peat) formation, the demise of interior marsh plants will reduce the biogenous source of sediment production, thereby aggravating the accretion deficit to such an extent that the marsh fringe erosion in the interior would extend outward. Consequently, the wetland may be lost as a result of the spatially varying vertical accretion rates and the ensuing coalescence of interior tidal creeks or ponds.

Because of the complexity of the problem of assessing wetland response to SLR, prudence dictates that any assessment should err on the conservative side. Viewed in this light, it is suggested that the extent of shoreline retreat based on the trend line method be taken as yielding the lower bound and that the static inundation model should then be taken as yielding the upper bound. The wetland response to a rise in sea level in the future may lie somewhere within the boundaries proscribed above.

### 5.7.5 Conclusions

For McClellanville, salt marshes play a pivotal role in determining the spatial extent of projected impacts resulting from SLR. Due to the low, flat elevation characteristic of wetlands, the project site will be submerged up to the Intracoastal Waterway, a cross-shore distance of  $\approx 10$  km from the present shoreline, based on static inundation. However, the dynamic nature of the ecosystem defies such a simple treatment.

The results of analysis indicate that the salt marshes may be able to keep pace with SLR for the low scenario by accreting vertically, thus reducing the land area lost to static inundation. For the faster rates of SLR envisaged under the moderate and high scenarios, the natural accretion rate is expected to be overwhelmed. In these circumstances, the use of the method of trend lines indicates that the projected land area lost will still be appreciably smaller than the predictions of static inundation due to the ability of the wetland vegetation to migrate landward. Because of the wide expanse of wetlands present, created possibly through a span of thousands of years, slightly less than half of the present wetland acreage

is expected to remain by the year 2100, even under the high SLR scenario.

Although hard numbers are usually favored in decision making, it must be stressed that the above scenario is based on a single set of conditions that are assumed to prevail in the future. Coupled with the intrinsic deficiency in our current understanding of wetland response to sea-level change, it is prudent to view the results obtained from the trend-line method as yielding the lower bound whereas that of the method of static inundation as yielding the upper bound of the potential extent of wetland loss to the specified SLR scenarios. Societal response should then be formulated in such a way that it is flexible enough to handle these eventualities, should they arise in the future.

## **5.8 NAGS HEAD, NORTH CAROLINA**

### **5.8.1 Site Description**

The Nags Head study area (Fig. 5.28) is in the northern part of the Outer Banks, which are a long chain of barrier islands rimming the mainland shoreline of North Carolina. They are separated from the mainland by Albemarle Sound to the north and Pamlico Sound to the south. The Outer Banks occupy a 200-km-long segment of the North Carolina shoreline, which has a total length of  $\approx 480$  km. The islands are generally wide, low, and flat. Only certain areas have well-developed dunes, where orientation and sand supply permit dune development. The study area is in the northern arm of the Outer Banks and trends generally in a north-northwest to south-southeast direction. As is typical of barrier systems, the long, narrow strip of land is separated from the mainland by a shallow body of water and has a straight, smooth seaward margin in contrast with the rather irregular sound-side shoreline. Geologically, the genesis of the chain of barrier islands that makes up the Outer Banks is attributed to the drowning of beach ridges due to rising sea level during the Holocene Transgression, according to one of the several theories of barrier island formation in vogue.

The rate of SLR took a measurable dip  $\approx 5,000$  to 6,000 years ago, which may have helped to ensure the relative stability of the island chain by permitting natural colonization by vegetation. However, the barriers continue to respond to SLR and episodic events by lateral migration through the processes of breaching and overwash. However, despite the recognition that these areas are generally unsuitable for permanent habitation, residential development has proceeded apace, thereby exerting substantial developmental pressure on this dynamic environment.

Specifically, the project quadrangle consists of a portion each of Roanoke Island and Bodie Island, the southern part of which merges into the Cape Hatteras National SeaShore. There is no inlet within the project quadrangle. The two islands are linked by a causeway-cum-bridge connection that serves as the only land access route to Roanoke Island within the project quadrangle. North Carolina State Highway 12 runs along the seaward side of Bodie Island.

The relief is generally low with prominent dune features, whereas the bottom topography is as depicted in Fig. 5.29. The locations of the three transects are shown in



Fig. 5.30. Generally the three transects are similar in profile shape out to the 14 m depth contour, which is located at  $\approx 1,500$  m offshore. Further seaward, all transects exhibit a break-in-slope to a flatter gradient. The location of this break in bottom slope agrees well with the common observation that "on the coast of the Carolinas, where waves have intermediate values, the slopes commonly flatten at about 45 ft (13.7 m)" (Shepard 1960). The two northernmost transects have generally the same bed gradient up to the 20-m depth contour after which the bottom profile along transect B eases into a subaqueous mound. This low-elevation underwater mound is seen to be part of a spurlike bathymetric feature extending from the north, as evident in Fig. 5.30. On the other hand, the offshore profile along transect C, the southernmost transect, shows a much flatter and more uniform bed gradient. The relative uniformity of the nearshore profiles indicates that the southern portion of the project quadrangle is beyond the lateral influence of the ebb-tidal shoal development at Oregon Inlet, which is located  $\approx 10$  km south of the project quadrangle, notwithstanding the statement that "Oregon Inlet is causing accelerated erosion 8 miles (15 km) away in south Nags Head" (North Carolina Department of Natural Resources and Community Development 1984). The widths of Bodie Island at the three transects are  $\approx 2.7$  km, 1.0 km, and 2.3 km from north to south, respectively. About half of the width at transect C consists of salt marshes, which occupy the sound side of the island. The narrowest width of  $\approx 0.5$  km is slightly north of the bridge link to Roanoke Island.

The mean height of the dunes within the study area was deduced from general statements quoted in published literature (elevations are generally less than 3 m) as well as published beach profiles. Published beach profiles show that the dune profile generally terminates at  $\approx 2.1$  m from the mean water level at Nags Head (Dolan et al. 1967) and  $\approx 7.0$  m at Duck where the Coastal Engineering Research Center Field Research Facility is located (Howd and Birkemeier 1987).

The tide here is semidiurnal, and the average range is  $\approx 0.9$  m. The beaches are moderately steep (1:15 to 1:30) and are composed mainly of quartz sand and gravel (size ranges from 0.10 to 25 mm) (Dolan et al. 1969). The mean sediment size computed from the data tabulated in Dolan et al. (1969) is  $\approx 0.2$  mm. In a later study, the mean grain size of the sediments at the vicinity of Nags Head Pier on land and in the sea has been reported to be 0.35 and 0.37 mm, respectively (Dolan et al. 1980). The locations of these referenced points on the profiles are not clear from the report. The difference between the two measurements could thereby be the result of seasonal changes or just spatial variation along a beach profile.

Figure 4.29 depicts the land use pattern within the Nags Head Quadrangle. On the ocean side, the entire project shoreline is heavily developed except for a short stretch in the middle where sandy beaches exist. On the sound side, the shoreline is vegetated by wetlands and deciduous forests along the northern and southern one-thirds, while the middle one-third is occupied by relic sand dunes interspersed with discrete parcels of residential development. In addition to the natural dunes, a line of artificial dunes has been built by the National Park Service along the barrier reach from Nags Head southward, which extends all the way to Ocracoke Inlet (Pierce and Colquhoun 1970). The occurrence of extensive overwash-adapted grasslands on the barrier flats, which are dominated by *Spartina patens*, reflects the characteristics of the Outer Banks vegetation (Godfrey 1976).

As for the portion of Roanoke Island in the project quadrangle, it is mainly vegetated with wetlands and evergreen forest at the outer fringe with a core of residential and commercial development. The salt marshes here are situated on sediments supplied almost exclusively from old inlets and storm overwash.

### **5.8.2 Sea-Level-Rise Scenarios**

The SLR scenarios for this project were developed in Sect. 2 and are summarized for this study area in Table 4.25. The present rate of subsidence for Nags Head is  $\approx 1.86$  mm/year and was used to determine the future SLR for the current scenario. Based on the assumption of static inundation, the area submerged in each SLR scenario has been generated in Sect. 4. Sect. 4's estimates of inundation will be modified here, if necessary, as outlined in Sect. 5.1.

### **5.8.3 Previous Studies**

It has been suggested that erosion of barrier coasts may be caused by the continuing evolution of the coastal zone in response to the postglacial transgression (Leontyev 1965). Since barrier islands are relic forms that originated under hydrodynamic conditions that are different from those of the present day, these features are still undergoing reconstruction and erosion associated with the above phenomenon. Superimposed on this long-term adjustment is the shorter term recessions of human time scales, which further complicate matters when attempting to predict future changes in barrier island location. In the following subsection we review the available literature for relevant information that can aid in minimizing the uncertainty associated with the inundation assessment for this study area.

A limited search for relevant reports revealed a dearth of historical information on coastal erosion for the project site after the 1970s. On the basis of the measurements conducted using time-separated aerial photographs, Langfelder (1971) has computed the composite mean annual rates of shoreline change (by proxy of both the dune line and high water line) along the entire ocean shoreline of North Carolina. The spatial coverage was every 305 m. The time periods dated from the 1940s-1950s to 1970. The coastline north of Oregon Inlet, which includes the project site, was described as exhibiting small to moderate erosion rates at both the dune line and high water line. When scaling was done from the relevant shoreline change map, the rate of erosion for the project site were found to be between 0.8 and 0.3 m/year, respectively.

On a regional scale, the University of Virginia, Charlottesville, initiated an effort to collect and combine the shoreline change data that, at that time, was fragmented among various agencies and repositories. This effort culminated with the establishment of the Coastal Erosion Information System (CEIS) (Dolan et al. 1989). CEIS is an information storage and retrieval system consisting of structured data sets for each of the coastal states, statistical subroutines, and a bibliography of source data. These widely disparate historical data on erosion rates then forms the basic information that led to the publication of the

Coastal Erosion and Accretion Map in the National Atlas in 1989. For North Carolina, the CEIS data indicate that 72% of the states shorelines have been eroding (Dolan et al. 1990). The mean rate of erosion on a statewide basis is 0.7 m/year (Dolan et al. 1989). Although the map cited above provides an overview of the national coastal recession situation, it has limited utility because of its coarse resolution (National Research Council 1990).

For the Outer Banks, the most recently published analysis of shoreline change was completed by Dolan et al. in 1991. Unfortunately, the coverage ends just short of the project quadrangle, as shown in Fig. 5.31. However, a data base with a finer resolution (50 m intervals) does exist under the name COASTS (Dolan et al. 1978). Because of time constraints it was not feasible to acquire this data set, to obtain relevant shoreline change information for the project site, and it was not pursued further. Fig. 5.31 was included here to highlight the alternating and often wavy shoreline change pattern even within a short shoreline reach and, hence, the uncertainty involved in using statewide average rates for site-specific analysis. Therefore, only the published erosion data by Langfelder (1971) was available, and used in the subsequent analysis.

Historically, the coast of North Carolina has always faced the threat of catastrophic damage from hurricanes, northeasters, and other major storms, even though there has been a comparative lull in these episodic activities in the past 30 years. One ferocious storm of particular notoriety is the gigantic northeaster known as the Ash Wednesday Storm of 1962 that caused erosion and destroyed kilometers of protective dunes on the coast from Cape Hatteras northward—greater than any previously known storm. Therefore, it is understandable that considerable efforts have been expended in conducting studies aimed toward hazard mitigation, studies of this nature are exemplified by the report by McElyea et al. (1984). On the other hand, no known site-specific study on the potential impacts of future SLR have been reported for this study area. The only reference to this effect, albeit of a generic nature, is the general statement that “the horizontal island-migration rate in North Carolina should be 100 to 1,000 times the rate of sea level rise.” This result is based on a model describing the simple bed slope dependence of island migration (a distance of 80 km across the Continental Shelf) during the previous 15,000 years in which the sea level rose by about 76 m, assuming the cross-shore profile remained unchanged (Pilkey et al. 1978).

Outside the confines of the project quadrangle, several engineering studies such as those on Oregon Inlet (south of the project) and at the vicinity of the Coastal Engineering Research Center Pier at Duck (north of the project) have been conducted. Understandably, the application of these results to the project site is not always straightforward because of likely differences in the physiographic and sedimentary regimes. On the other hand, the likely impacts of “external” actions on the project site are equally contentious, as raised by the controversy over the proposed stabilization of Oregon Inlet [see Mehta and Montague (1991)]. Pilkey (1980) has argued that the unstabilized Oregon Inlet acts as a “safety valve” that can quickly release back into the ocean huge volumes of water built up by storms in the sounds behind the barrier. If this safety valve function is tampered with through jetty construction, which reduces its discharge capacity, the dammed water may seek a new escape route through a weakened section of the barrier, a prime candidate being the low area at Nags Head. This reversal of the usual mode of barrier rupture (i.e., from the ocean side versus bay side) is consistent with a theory of inlet formation expounded by Leatherman

(1987a). Leatherman believed that the water trapped behind a barrier system, after a hurricane had passed, could breach the barrier island chain from the bay-side, thus creating a new inlet.

On the other hand, the Outer Banks as a whole have been a haven for geomorphological studies, which offer insights, albeit qualitative, into the evolution of the barrier system in the past and possibly into the future as a result of anthropogenic perturbations. While these studies appear in a wide range of reports, papers, and books they have been summed up in a condensed format in the *Final Environmental Statement for Undeveloped Coastal Barriers* (U.S. Department of the Interior 1983), which covers both a generic treatment of coastal barriers and specific documentation on the Outer Banks. A major portion of the relevant information, though, has been extracted from Leatherman (1979b).

In terms of generic responses, it is noted that with a rise in sea level, a coastal barrier migrates landward up the gradual sloping bottom of the very broad surface of the coastal shelf that extends into the sea. This migration distance is usually about two or three orders of magnitude larger than the vertical rise of the sea, which is consistent with the results of the simple model mentioned above. This notion of landward movement, whereby the barrier moves as an "ecological unit", departs from the traditional concept associated with the erosion of a mainland coast. Whereas the latter phenomenon connotes a net disappearance of land, the former may be manifest as the barrier moving landward onto marsh and lagoonal deposits without significant loss in plan area.

Although a barrier may move in response to a steadily rising sea, the rate of its migration is basically unsteady, being dictated by episodic events that give rise to overwash and inlet formation and, to a lesser extent, aeolian dune migration. These three processes combine to transport sediment landward: inlets provide conduits for landward movement of sediments into flood-tidal shoals that later become new marshes, while the overwash process facilitates the roll-over of the barrier. The last process, which is self-explanatory, is especially pertinent when dunes are oriented across prevailing winds.

The key to the ultimate fate of a coastal barrier is its ability to respond to the rising sea level by migrating landward. If this natural migration is slowed down or halted, then the entire barrier will be threatened with submergence. Implicit in this dynamic response pattern is the adequacy of sediment supply. Without a relatively continuous supply of sediments, a coastal barrier would not exist. In the same vein, Leatherman (1981) has suggested two major theories for landward barrier migration with SLR, which are based on his review of an extensive set of published papers on barrier evolution. These theories involve shore face retreat and in-place drowning, and the vast majority of the papers Leatherman reviewed support the first principle of continuous shore face retreat with SLR. This, however, depends on the rate of SLR. Drowning would inevitably occur if water level rises rapidly.

Inlets are vital to the migratory process of a coastal barrier because of the development of flood tidal shoals, which serve as sinks for longshore sediment transport. These shoals provide the substrate for marsh growth as well as an accretionary bases for deposition of overwash and wind-blown sands. The end result is the landward displacement of barrier ecosystems. However, overwash as a sediment transport mechanism becomes

effective only when the barrier width is less than some critical value. Above that value the barrier migration is dominated by inlet dynamics. Historically, several inlets have opened and closed along the Outer Banks as shown in Fig. 5.32, one of which (Roanoke Inlet) was located within the project quadrangle.

The above processes are relevant to the Outer Banks and, more specifically, the project quadrangle, as evidenced from the following considerations:

1. the Outer Banks may have migrated impressive distances since their initial formation,
2. the location of a historical inlet at the barrier coast that corresponds to about the middle of Bodie Island, and the presence of sandy materials underlying the salt marshes of Roanoke Island, indicate that these wetlands are built on relic tidal shoals, a conclusion which is consistent with the inlet processes just described,
3. overwash is a regular event on the Outer Banks, which can be characterized as having a low tidal range and high storm frequency, except at places with man-made dunes, and
4. overwash deposits are quickly colonized by buried grasses as the plants push up through the new overlying sand, a process that can take less than 2 years.

Ecological data show that the major vegetation zones on barrier islands, in particular the grasslands, are adapted to overwash and inlet dynamics and follow the barriers back (Godfrey 1976). Hence, barrier islands are capable of surviving an increase in sea level provided their basic response mechanisms, as mentioned above, are not compromised by permanent human development, which often leads to a forced stabilization of the island in place, and eventually in its inundation from the bay (sound) and ocean side. Therefore, their survival will, in part, hinge on the extent to which man interferes with nature's survival mechanisms. Thus, only when past errors need to be corrected and when future actions that could imperil the natural recovery capabilities of barrier islands occur, should people become involved in "island protection projects".

#### 5.8.4 Results and Discussion

The experiences described, indicates that the migration of the coastal barrier system could be simulated, at least to the first order, by the use of the Double Bruun Rule (Eq. 5.14). This rule is amenable to describing the rolling-over process, sidestepping for the moment the question of potential drowning at the higher rates of SLR.

The relevant wave statistics, based on a 20-year hindcast study (1956-1975) (Jensen 1983), are  $\bar{H}_s = 0.71$  m,  $\sigma_H = 0.65$  m,  $\bar{T}_p = 5.6$  s for Station 83 (Nags Head). Taking the mean grain size as 0.30 mm and plugging these values into Eq. (5-9) and then (5-6) and (5-7), the values of  $d_1$  and  $d_2$  were computed to be 8.8 m and 7.4 m, respectively. These

values envelop the closure depth computed by Hallermeier (1981) for Nags Head (7.95 m), which is defined as the maximum water depth for nearshore erosion by extreme (12 hr/year) wave conditions. From Sect. 5.8.1, it is known that the offshore bottom slope uniformly flattens out at  $\approx 14$  m water depth. Hence, the closure depth for all the three transects can be taken as 10 m, which is an intermediate value within the bounds of values cited, and occurs at an offshore distance of  $\approx 900$  m, as seen in Fig. 5.29.

On the basis of limited dune height information available as discussed in Sect. 5.8.1, the seaward dune height is taken as 2 m. Because of the lack of dune information on the sound side the same dune height as for the seaward side has been assumed for this analysis, though these dunes generally tend to be higher in elevation, unless they have been flattened by human encroachment, as they are relic features that were formed during past periods of higher sea level.

For ease of computation of the sound-side closure depth ( $h_{\text{so}}$ ), which is much shallower than on the ocean side, was taken as the greatest depth available from the relevant nautical charts for each transect, which is assumed to be located at the midpoint of the intervening water space. Using this information Eq.(5-14) was calculated and used to obtain the ratio of shoreward recession to SLR (R/S) for each transect. The results of these calculations are shown in Table 5.20.

**Table 5.20 Projected ratios of R/S based on the Double Bruun Rule, Nags Head, North Carolina**

transect	$W_{\text{so}}$ (m)	$W_1$ (m)	$W_{\text{so}}$ (m)	$B_o = B_b$ (m)	$h_{\text{so}}$ (m)	$h_{\text{so}}$ (m)	R/S
A	5,880	2,700	910	2	3	10	1,356
B	2,200	1,000	910	2	0.9	10	452
C	840	2,300	910	2	0.6	10	431

From Table 5.20, it is seen that the R/S ratio for transects B and C fell within the bounds 100 to 1,000, which is in line with values obtained using historic data for the geological past, at which time the average SLR rate was  $\approx 5.1$  mm/year. The much larger R/S ratio for transect A is a consequence of the greater width of both the barrier island (i.e., strip) at this point and the water body separating the strip from the mainland. However, it is difficult to visualize that the whole barrier island system will retreat as a connected whole while subjected to such a disparity in the magnitude of shoreward retreat. Hence, it is likely that the strip will be breached at a narrow section in between transect A and transect B after which inlet dynamics will dominate over overwash as the primary mechanism for landward migration. It is noted that based on the static inundation model, that the barrier strip will be cut into two separate portions at a location just south of transect B under all SLR scenarios because of the low elevation prevailing at this site. Under the high scenario, another severance will occur about midway between transects A and B. These potential gaps

are evident in Figs. 4.30, 4.31, and 4.32. Once disintegration of the barrier strip starts, erosion will likely occur in the direction of the longitudinal axes of the islands due to inlet widening as a result of increased tidal prism following the rise in sea level. Static inundation predicts the loss of large tracts of coastal wetlands abutting the sound shoreline at the southern part of Bodie Island and those located across the waterway within the project quadrangle. The anchoring effect of Bodie Island on the sound side of transects B and C is also consistent with the lower rate of retreat to be expected there.

When the relationship between the historical rate of SLR and shoreline erosion/accretion is known, the method of trend lines could also be applied. In this case, the nearest permanent tide gauge station operated by the National Ocean Survey, with analyzed long-term sea-level trend data, is located at Portsmouth/Norfolk, Virginia, which is  $\approx 80$  km to the north of the project quadrangle. The mean rates of SLR for the periods 1936-1972 and 1940-1972 are 3.81 and 3.87 mm/year, respectively (Hicks and Crosby 1974). Since the historical rate of shoreline change discussed in Sect. 5.8.3 is for the period 1940s-1950s to 1970s, the historical rate of SLR used is 3.87 mm/year. In this case, two sets of values were computed, one corresponding to each of the historical rates of retreat for the high water line (0.3 m/year) and dune line (0.8 m/year).

The results of both methods are tabulated in Tables 5.21 (year 2050) and 5.22 (year 2100) together with those from static inundation, which were calculated from the relevant outputs from the digital terrain model of the area.

**Table 5.21 Projected shoreline retreat along the seaward margin for the year 2050, Nags Head, North Carolina**

Sea-level-rise scenario	transect	Projected shoreline retreat (m)			
		Static Inundation	Double Bruun Rule	Trend lines	
				$(dR/dt)_h = 0.3$ m/year	$(dR/dt)_h = 0.8$ m/year
Low	A	90	342	20	52
	B	48	114	20	52
	C	45	109	20	52
Moderate	A	180	586	33	89
	B	90	195	33	89
	C	84	186	33	89
High	A	270	830	47	127
	B	147	277	47	127
	C	123	264	47	127

Note: The subscript h denotes historical.

**Table 5.22 Projected shoreline retreat along the seaward margin for the year 2100, Nags Head, North Carolina**

Sea-level-rise scenario	transect	Projected shoreline retreat (m)			
		Static inundation	Double Bruun Rule	Trend lines	
				$(dR/dt)_h = 0.3 \text{ m/year}$	$(dR/dt)_h = 0.8 \text{ m/year}$
Low	A	225	700	40	107
	B	120	233	40	107
	C	102	222	40	107
Moderate	A	405	1,174	73	196
	B	210	391	73	196
	C	180	373	73	196
High	A	810	1,771	101	270
	B	435	590	101	270
	C	234	563	101	270

From Tables 5.21 and 5.22, it is obvious that the predictions based on the use of the R/S ratio (1,356) for transect A is way above the results obtained using the other approaches; the results of the trend line method, using  $(dR/dt)_h = 0.3 \text{ m/year}$  are the lowest, while those using  $(dR/dt)_h = 0.8 \text{ m/year}$  are close to the results of static inundation for transects B and C, but not transect A. The trend of these predictions seems to suggest that the rate of shoreline retreat increases northward within the project quadrangle. Of all the methods considered here, only the use of the Double Bruun Rule results in sound-side accretion for the barrier strip, which is consistent with the assumption of island rolling-over inherent in the method. On the other hand, the method of static inundation predicts barrier narrowing from both sea and sound sides, which may hasten the disappearance of these islands. Considering that the premise of form preservation during the roll-over process may not always be valid, irrespective of the rate of SLR and, hence, disregarding the extreme predictions of this approach, it seems that the prediction based on static inundation is in reasonable agreement with the analytical methods attempted here, except perhaps for transect A.

It must be remembered that the above analysis is based on the premise that the barrier islands will respond freely to the natural forces without human intervention. It has been argued that along the Outer Banks, where the development is spread out and the traditional building is a wooden single-family house that could be readily moved, retreating from the shore would be more attractive than beach stabilization (National Research Council 1990).



However, the disrupting processes of overwash and inlet dynamics may lead to total abandonment of some developed barrier islands.

It has been claimed, however, that many communities on this barrier chain have existed for decades or centuries and that they are important in terms of their historic heritage (Denison 1981). Recognizing that these developed properties represent a complex web of private property ownerships and some of these individual property rights are protected under the constitution, it may not be too farfetched to suggest that funds will be appropriated to forestall the occurrence of the projected erosion impacts. Since no erosion control devices designed to harden or stabilize the ocean beach's location are allowed in North Carolina, effective January 1985 (National Research Council 1990), this protection would most likely be in the form of beach nourishment. This scenario may be true for transects A and C, which are located along the developed portion of the shoreline reach. On the other hand, transect B traverses an "undeveloped" sandy beach and dune area (Fig. 4.29). As mentioned earlier, this is also in the vicinity of the low-elevation area that is most vulnerable to breaching during a storm event. Since it may be cost-prohibitive to protect the entire reach, especially at places where no development is at risk, and also since it may be prudent to incorporate a safety flood release to reduce undue bay-side stress on the developed portions of the barrier, it is projected that transect B may be permitted to erode and ultimately breach to serve as an additional inlet that could handle the augmented tidal prism in the future.

**Table 5.23 Predicted changes in shoreline position, Nags Head, North Carolina. Reference point locations are shown in Fig. 5.30**

Referenced point	Predicted change
A	Shoreline is likely to be fixed at the present position by human intervention
B	Existing wetlands are likely to keep up with the rising water under the low scenario, but will likely drown under medium and high scenarios in which case shoreline retreat will follow the prediction of static inundation
C	Shoreline is likely to be permitted to erode and an inlet formed at the vicinity of the relic Roanoke Inlet along transect B (see Fig. 5-30)
D	Same as for C
E	Same as for B
F	Same as for A
G	Same as for B
H	Same as for B

On the sound side, the projected loss of coastal wetlands is linked to the marsh

vertical accretion rate. Adopting the same cut-off rate as that used for the McClellanville project site, which is 5 mm/year, it can be assumed that the wetlands within the study area will keep pace with the rising sea for the low SLR scenario. For both the medium and high scenarios, where the projected rate of SLR is in the range 7.2 to 11.9 mm/year, the wetlands will disappear as projected. With these caveats in mind, the likely location of the land-water interface for each transect (as indicated in Fig. 5.30) are given in Table 5.23.

After generalizing from wetland erosion rates shown in Table 5.23 new land loss estimates were made. These revisions were based on the shoreline change maps and digital terrain models provided, and are given in Table 5.24.

**Table 5.24 Revised estimates of land area lost (ha), Nags Head, North Carolina**

Sea-level rise scenario	Year 2050			Year 2100		
	Static inundation	Structural obstruction	Percentage difference	Static inundation	Structural obstruction	Percentage difference
Low	1,680	200	-88%	1,930	210	-89%
Moderate	1,855	1,500	-19%	2,250	1,850	-18%
High	2,020	1,620	-20%	2,850	2,000	-30%

From Table 5.24, it is seen that the assumed need to protect “development” would reduce the projected land losses as a result of SLR by nearly 90% for the low SLR scenario. The losses in this case are from the sound-side shoreline as well as from the new inlet through the barrier. On the other hand, the wetlands are projected to be drowned as a result of the high rate of SLR under the medium and high scenarios. Under these circumstances, the percentage of reduction in land loss drops to 20-30%, the bulk of which consists of salt marshes.

### 5.8.5 Conclusions

For Nags Head, the Double Bruun Rule yields excessive results (when the effects of human intervention are considered), whereas the trend-line method yields projected shoreline recessions that are in reasonable agreement with those based on static inundation, provided the shoreline is free to respond without human intervention. However, it is argued that since the landward migration process is primarily accomplished in quantum leaps by overwash and sand transport via possible breakthrough in the form of inlets, it is highly improbable that the seaward fringe, which has seen intense real estate and property development, will be left to the vagaries of the sea. Hence, it is foreseen that the local populace will mobilize funds to protect the existing coastline where it is developed. In

regard to the relatively undeveloped area along transect A, if any area was to be foregone to act as a relief for the enhanced tidal prism anticipated in the future, this would be it.

If a cut-off rate of 5 mm/year is used for the natural vertical accretion rate for marshes, the projected land loss is reduced substantially for the low SLR scenario. For the medium and high scenarios, the reduction comes only in the seaward fringe by virtue of shoreline protection works.

## **5.9 CONCLUDING COMMENTS**

On the basis of the various analytical shoreline change models discussed in Sect. 5.2, potential adjustments to the first order estimates of inundation effects due to SLR for each of the six selected sites were made. This concluding section attempts to summarize the above findings and relate them to some identifiable physical characteristics with a view to evaluating the degree to which such relationships may be useful for regional applications.

Table 5.25 compares the six sites in terms of selected physical characteristics. It is to be noted that the list of dominant physical traits, with an evident element of subjectivity, includes most of the factors considered in the formulation of the Coastal Vulnerability Index presented in Sect. 3. The exceptions are dominant land use and shore protection status. The values of the mean and the highest significant wave height for each site are taken from the relevant wave hindcast studies quoted in the preceding sections. All the sites can be characterized, at least in part, as barrier islands that may be broken by an inlet. Also, all the sites have been previously established as being at very high risk according to the Coastal Vulnerability Index criteria.

Erosion history, subsidence rate and future SLR, and mean/highest significant wave height are closely related in the sense that the latter two combine to influence erosion, unless modified by human intervention, which is expressed through shore protection status. Similarly, the type of land use is also intertwined with shore protection status; the higher the economic value of land use, the more extensive the shore protection in place.

**Table 5.25 Physical characterization of the study areas**

Study site	Geomorphologic characterization	Dominant land use	Erosion history	Subsidence rate; future SLR	Shore protection status	Mean/Highest significant wave height (m)
Galveston, Texas	Barrier islands with an inlet	Urbanization (residential and commercial)	Stable where protected by seawalls, 0.65 m/year otherwise	4.9 mm/year; 29.4 - 163.9 cm	Massive seawall, groins	1.1/4.0
Caminada Pass, Louisiana	Barrier shoreline with an inlet (Mississippi Delta)	Nonforested wetlands (small resort/fishing community on Grand Isle)	East of inlet: long-term erosion; > 5 m/year to 20 m/year West of inlet: variable; < 5 m/year to stable	8.2 mm/year; 49.2 - 200.2 cm	inlet jetty and some beach restoration work on Grand Isle	1.1/5.8
Bradenton Beach, Florida	Barrier islands with an inlet	Residential and service-oriented development	Classified as critically eroding	0.2 mm/year; 1.4 - 112.5 cm	individual seawalls, beach restoration	0.8/3.2
Daytona Beach, Florida	Unbroken barrier chain	Urbanization (resort and commercial development)	Generally accretional at 0.4 m/year; however, southern portion classified as critically eroding	0.5 mm/year; 3.1 - 115.5 cm	individual seawalls, groin fields	0.8/5.0
McClellanville, South Carolina	Barrier islands and salt marshes (Santee Delta)	Wildlife preserve (nonforested wetlands)	Long-term erosion; > 5 m/year	1.4 mm/year; 8.4 - 125.4 cm	Largely pristine	0.7/3.8
Nags Head, North Carolina	Unbroken barrier island	Resort development	About 0.5 m/year	1.9 mm/year; 11.2 - 130.6 cm	Individual seawalls, dune stabilization	0.7/5.9

While Table 5.25 is a characterization of the present status, Table 5.26 is a prediction of the physical impacts of future SLR in terms of land loss, from which the effects of biophysical factors and built infrastructure may be identified. Here the connotation of built infrastructure should be stretched to include future human intervention, which is based on a subjective evaluation of the future need for such an action. As indicated, the two sets of percent figures refer to the situations at years 2050 and 2100, respectively, and correspond to low, moderate, and high SLR scenarios from top to bottom for each relevant cell entry.

On the basis of static inundation, it is seen that the percent land loss is the lowest for Daytona Beach and the largest for Caminada Pass, the others being intermediate between these two extremes. While the high subsidence rate that typifies, and the wetlands that dominate the Caminada Pass site combine to contribute to the worst predicted status, the relative stability of Daytona Beach may have been biased inordinately by the preponderance of relatively high hinterland area found within the project quadrangle.

**Table 5.26 Predicted land loss, in percent, and the relative influences of biophysical factors and built infrastructure on inundation**

Study site	Static inundation (S.I.) alone @ yr 2050 : 2100	Biophysical factors (B.F.) only	B.F. plus built infrastructure @ 2050 : 2100	Influence of biophysical factors	Influence of biophysical factors + built infras.	Influence of built infrastructure
Galveston, Texas	33% : 49% 40% : 86% 47% : 88%	Similar to S.I. due to the flat off-shore profile and low topography	22% : 27% 23% : 27% 26% : 27%	Small	Percent reduction ranges from 33% to 70%	High
Caminada Pass, Louisiana	87% : 99% 93% : 100% 96% : 100%	Similar to S.I.	Similar to B.F.	Small due to the high rate of subsidence	Small due to the high rate of subsidence	Small to medium
Bradenton Beach, Florida	34% : 39% 39% : 46% 43% : 57%	Similar to S.I. but greatly enhanced where influenced by inlet processes	14% to 25%, consisting of wetlands and fringing forest	Large within the zone of influence of inlet	About 50% reduction due to human intervention	Medium to high
Daytona Beach, Florida	5% : 6% 6% : 9% 8% : 17%	Similar to S.I.	< 5% consisting largely of wetlands	Small	High	High
McClellanville, South Carolina	43% : 55% 54% : 61% 59% : 66%	Minor 12% : 26% 18% : 41%	Similar to B.F.	Large (percent reduction ranges from 38 to 100%)	Large (percent reduction ranges from 38 to 100%)	Low
Nags Head, North Carolina	38% : 44% 42% : 51% 46% : 64%	Similar to S.I.	5% : 5% 34% : 42% 37% : 45%	Small	Percent reduction ranges from 18 to 89%	High

The biophysical factors alone generally play a substantial role along wetland-fringed coasts by offsetting the potentially adverse impacts of SLR through the natural phenomenon of vertical marsh growth. However, this ameliorative effect is soon overwhelmed along rapidly subsiding coasts, as exemplified by Caminada Pass in this study, where the rate of vertical marsh growth is unable to keep pace with the high rate of subsidence, and hence relative SLR. Thus, incorporation of biophysical factors in the assessment of potential land loss along wetland-fringed coasts can result in either substantial or no substantial change to the predictions based on static inundation, depending on site-specific factors such as the rates of subsidence and the natural vertical growth of marshes.

Generally speaking, the amount of land lost to the sea (from SLR) on sandy coastlines is not affected by the presence, or absence, of biophysical factors. However, biophysical factors may play a strong role when inlet processes dominate, as is the case for Bradenton Beach. Hence, the predicted land loss may be roughly sketched by interpolating between zero elevation (mean sea level) and the elevation given by the magnitude of the vertical rise of future sea level, as shown on a contour map, only under certain circumstances. The areas where static inundation models may be suitably applied to assess the potential land loss based on static inundation include sandy shores that have relatively low rates of subsidence, low projected future SLR, and that are not directly influenced by inlet processes. Based on these

six case studies, there does not seem to be a strong correlation between the role of biophysical factors in influencing the predicted land loss based on static inundation, and land use intensity.

As expected, the role of built infrastructure is related strongly to land use intensity. When the prevailing land use consists of high-valued economic activities, such as urban and resort development, the predicted land loss (from static inundation) is strongly discounted because of the great likelihood of human intervention through beach nourishment or other coastal protection efforts. Conversely, when the predominant landscape is one of pristine wetlands, the impetus for human intervention is much less, at least as dictated by the prevailing resource valuation paradigm in use.

In summary, the following conclusions were reached based on the information derived from the six case studies:

1. The results of predicted land loss in the event of a future SLR based on static inundation can be used as a first-order estimate under certain circumstances: when the coast is sandy, when the rate of relative SLR (subsidence plus future SLR) is relatively low, and where the reach in question is beyond the dominant effects of inlet processes.
2. For wetland-fringed coasts, the method of static inundation severely overestimates the amount of potential land loss, principally because the method completely ignores the ability of marsh land to accrete vertically, when there is adequate sediment supply for such a natural process to outstrip the rate of SLR. Otherwise, the results based on static inundation can be viewed as the upper bound of potential land loss in the event of a rate of SLR that outpaces the natural vertical accretion rate of marsh land.
3. The role of built infrastructure in influencing the results of potential land loss based on static inundation is strongly correlated with the intensity of land use. The more intensely the coastal zone is developed, the greater the probability that human intervention will limit the projected sea advance through beach nourishment and, perhaps, with other shoreline-hardening measures. This is primarily an economic decision. Under this scenario, the projected land loss will be confined to areas that have little perceived economic value, such as wetlands.
4. Since inlet processes are local phenomena in the sense that they have finite zones of influence on either side, it may not be prudent to extrapolate the findings here to regional applications over the entire U.S. Southeast coast without considering inlet locations.
5. Finally, it would be oversimplifying to suggest that all developed shores will be protected against the impacts of SLR. Hence, it is conceivable that from a national or regional context, some sort of prioritization criteria will have to be invoked to channel limited resources to selected coastal reaches.

## **5.10 FIGURES**

**Fig 5.1**

**Schematic representation of the Bruun Rule (National Research Council 1987).**

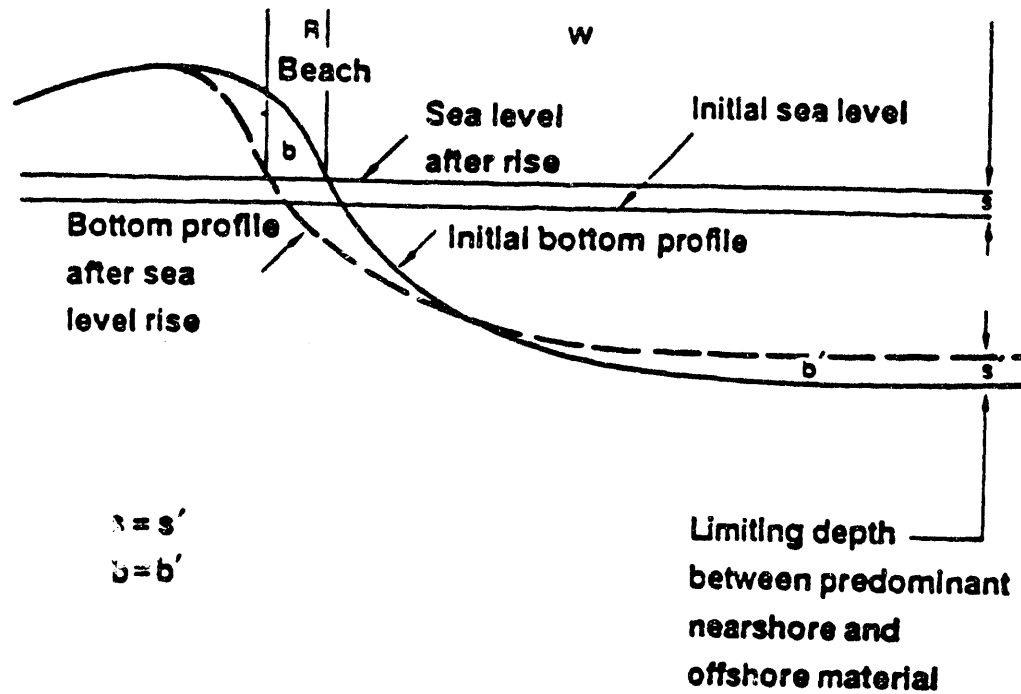


*FIGURE REPRINTED WITH PERMISSION*



**Fig 5.2** Barrier island equilibrium response (Dean and Maurmeyer 1983).

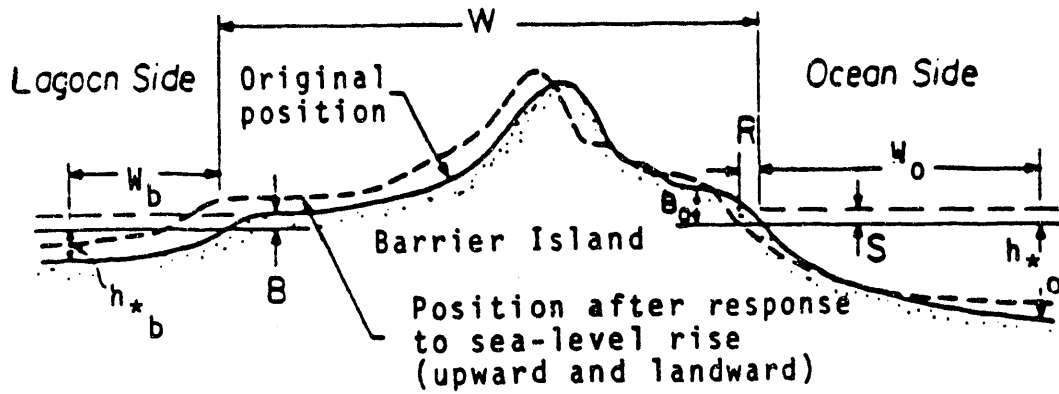


*FIGURE REPRINTED WITH PERMISSION*

Fig 5.3

Comparison of projected shoreline retreat, Ocean City, Maryland.

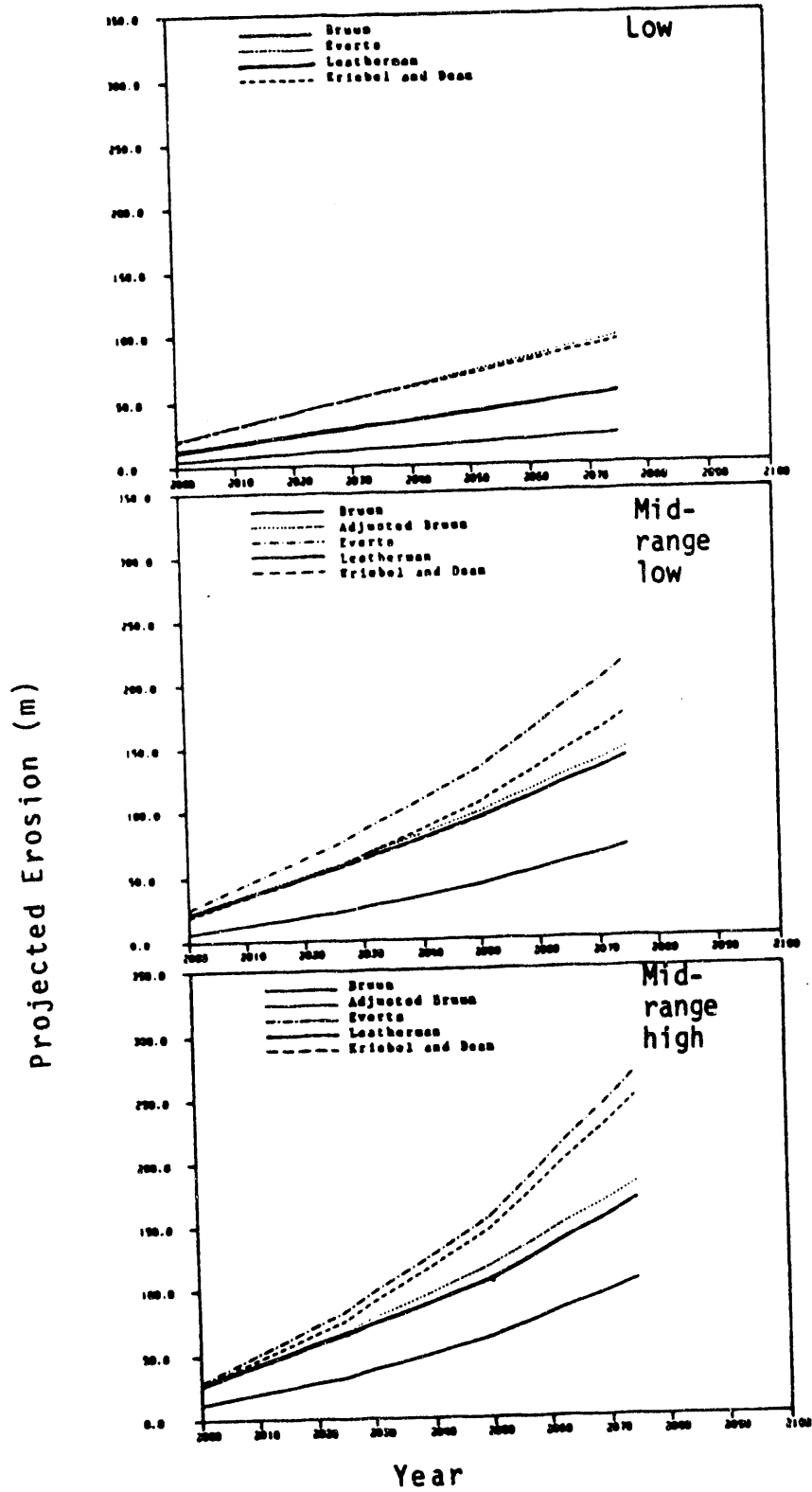


Fig 5.4 Study area, Galveston, Texas.

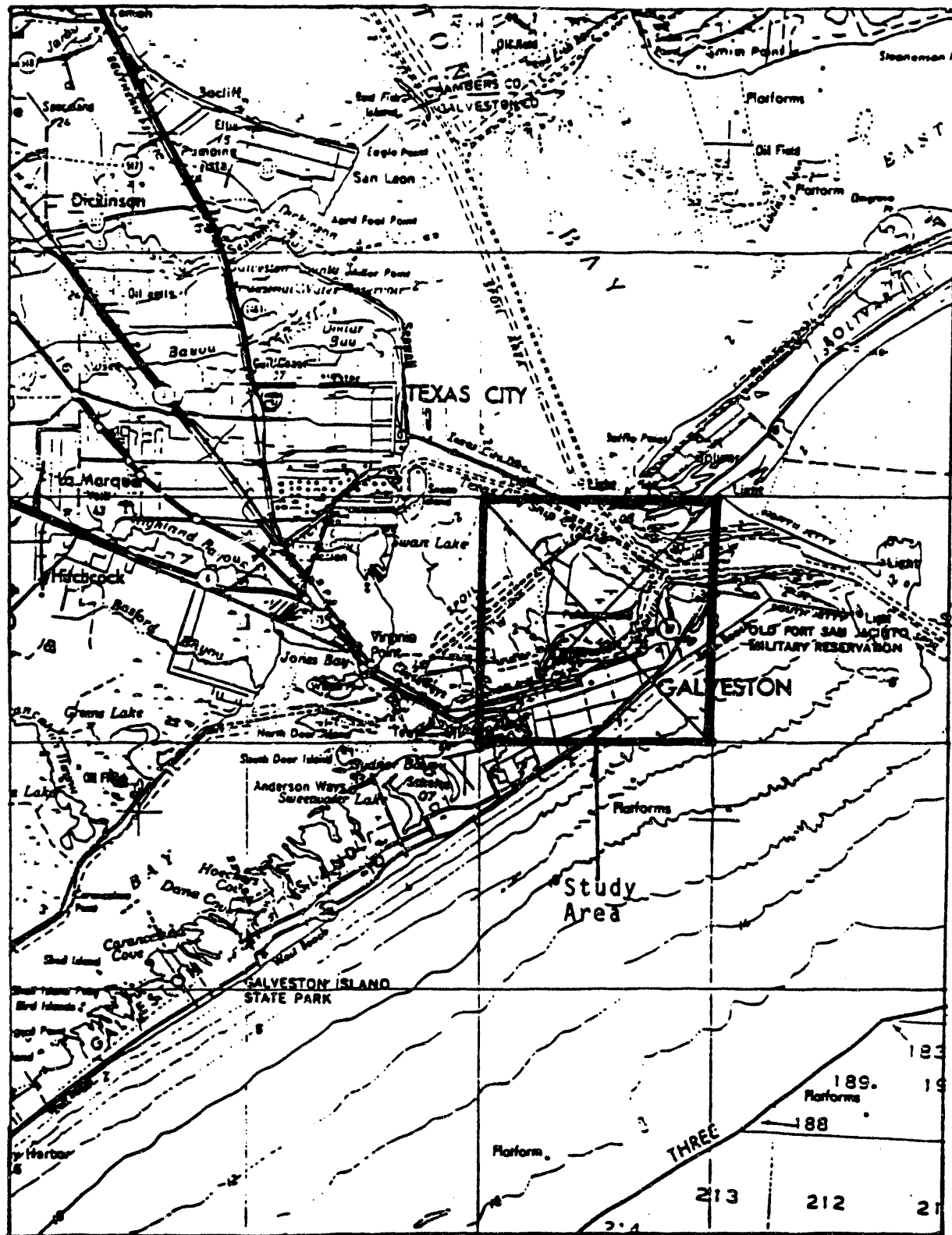


Fig 5.5 Offshore profiles, Galveston, Texas (based on U.S. Nautical Charts).

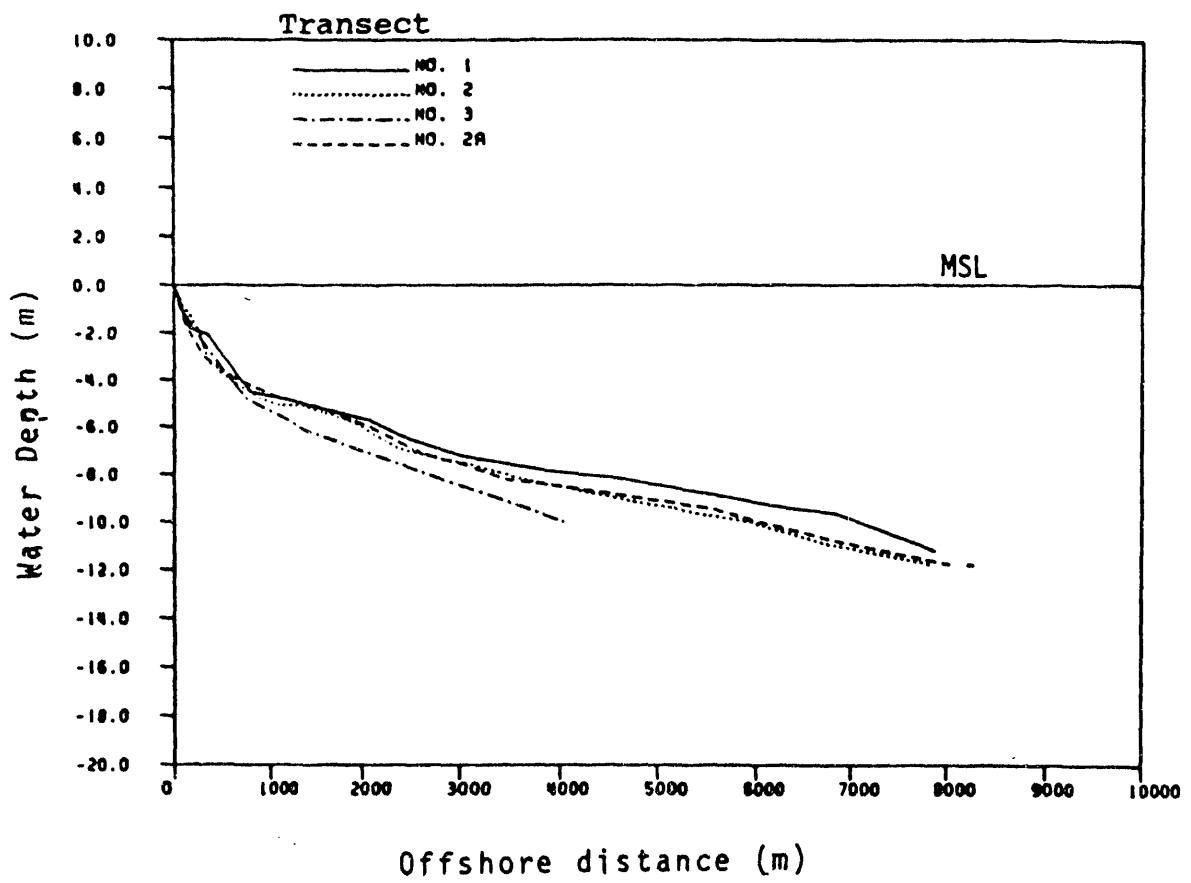


Fig 5.6 Location of cross-shore transects, Galveston, Texas.

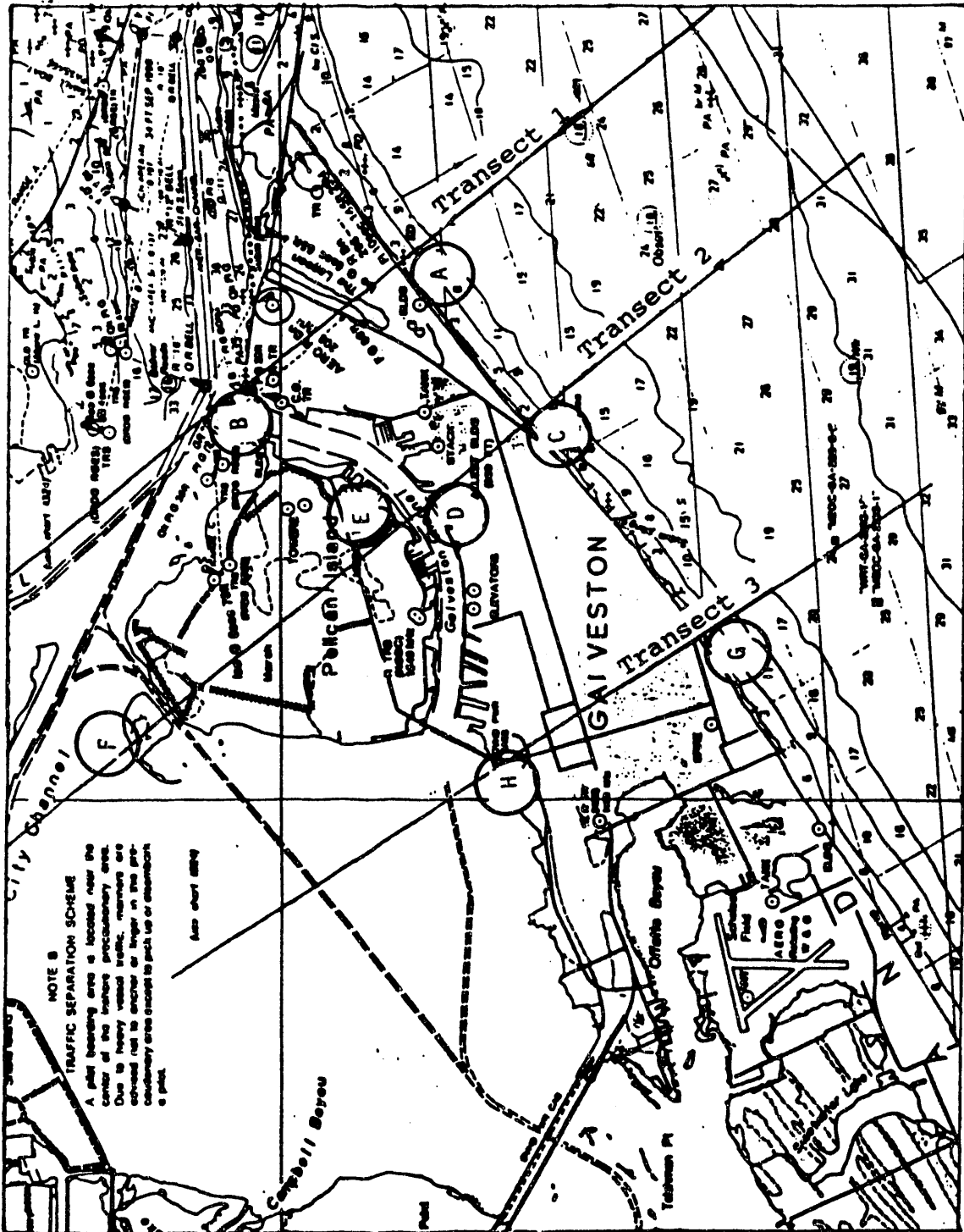
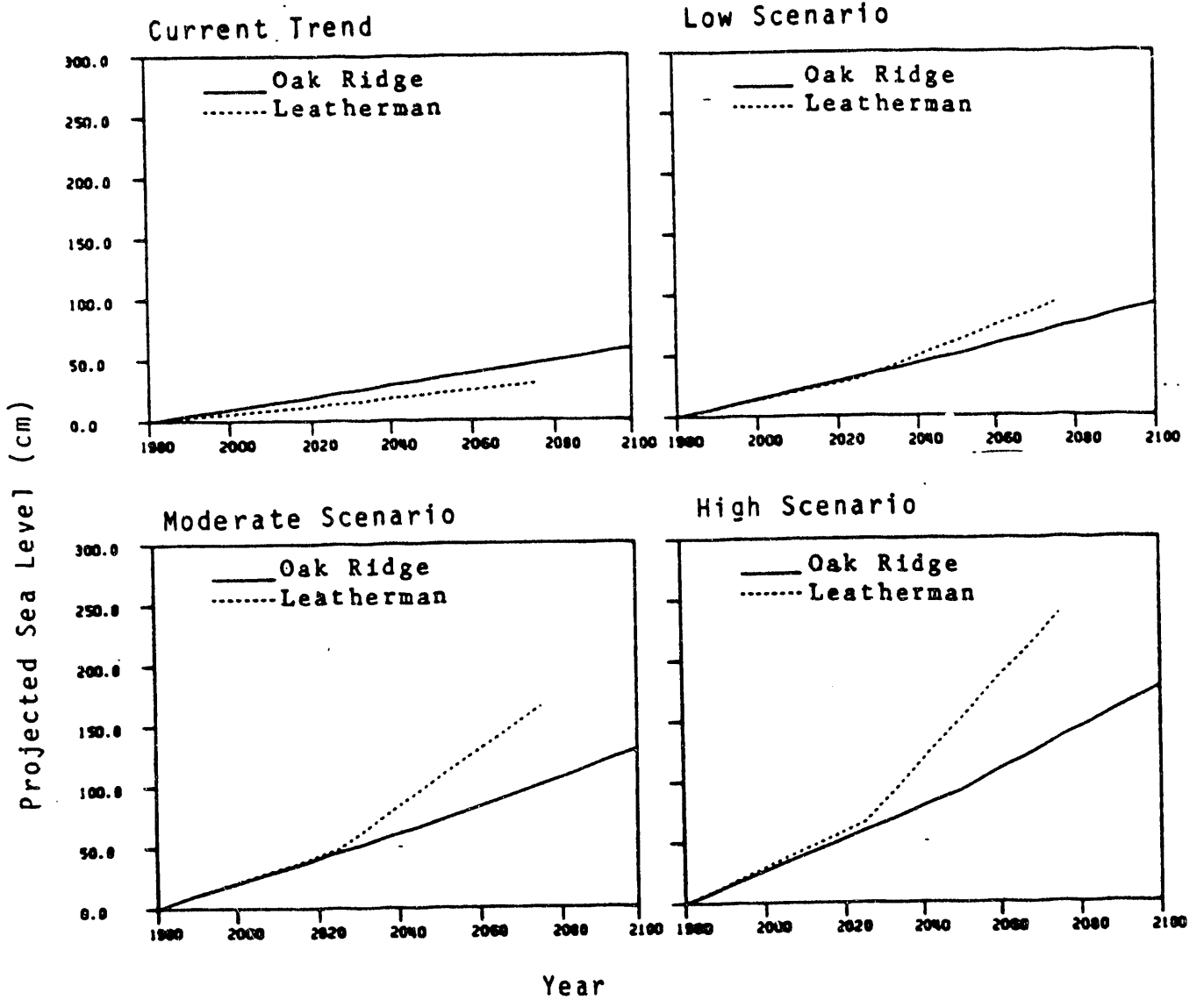
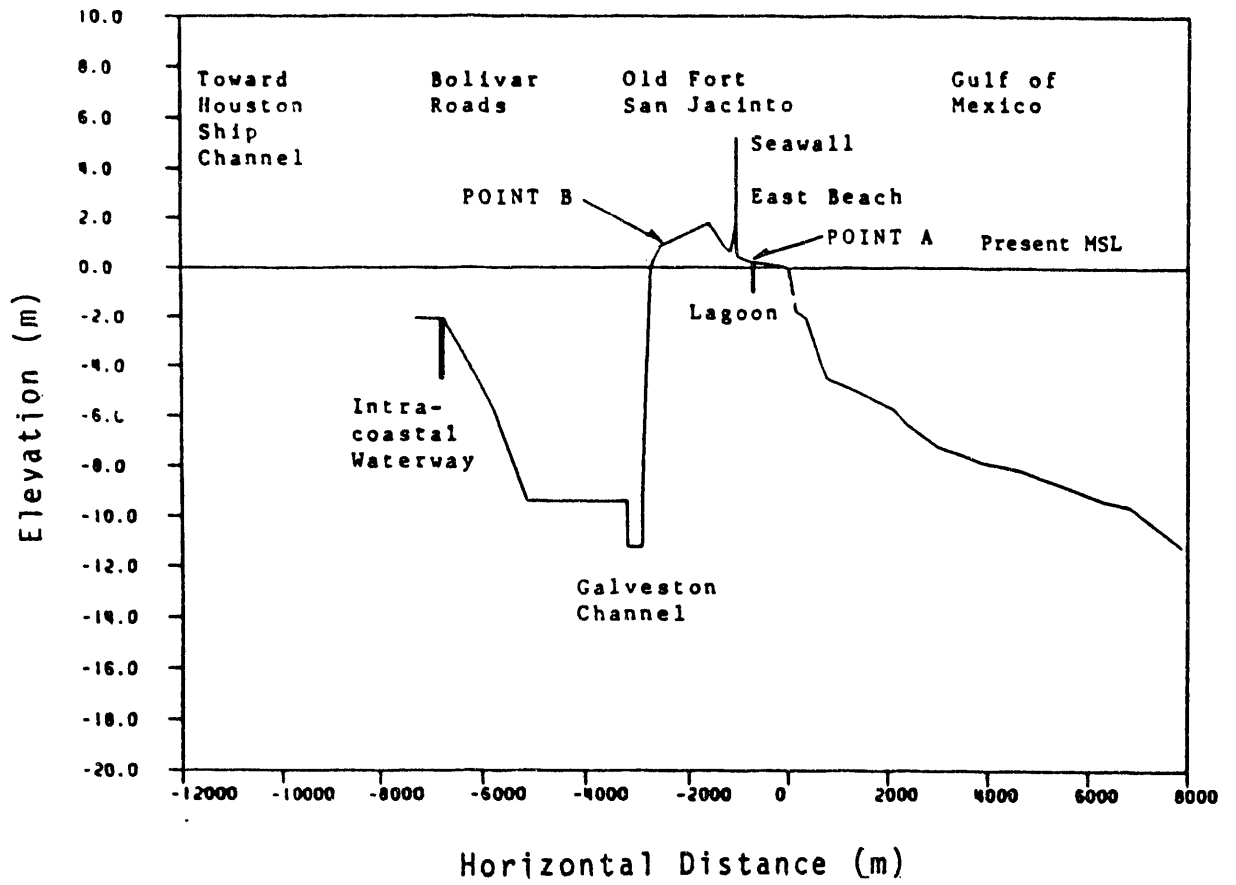


Fig 5.7

Sea-level-rise scenarios for Galveston, Texas.



**Fig 5.8** Projected locations of waterline for the year 2100 at transect 1, Galveston, Texas.



**Fig 5.9** Projected locations of waterline for the year 2100 at transect 2, Galveston, Texas.

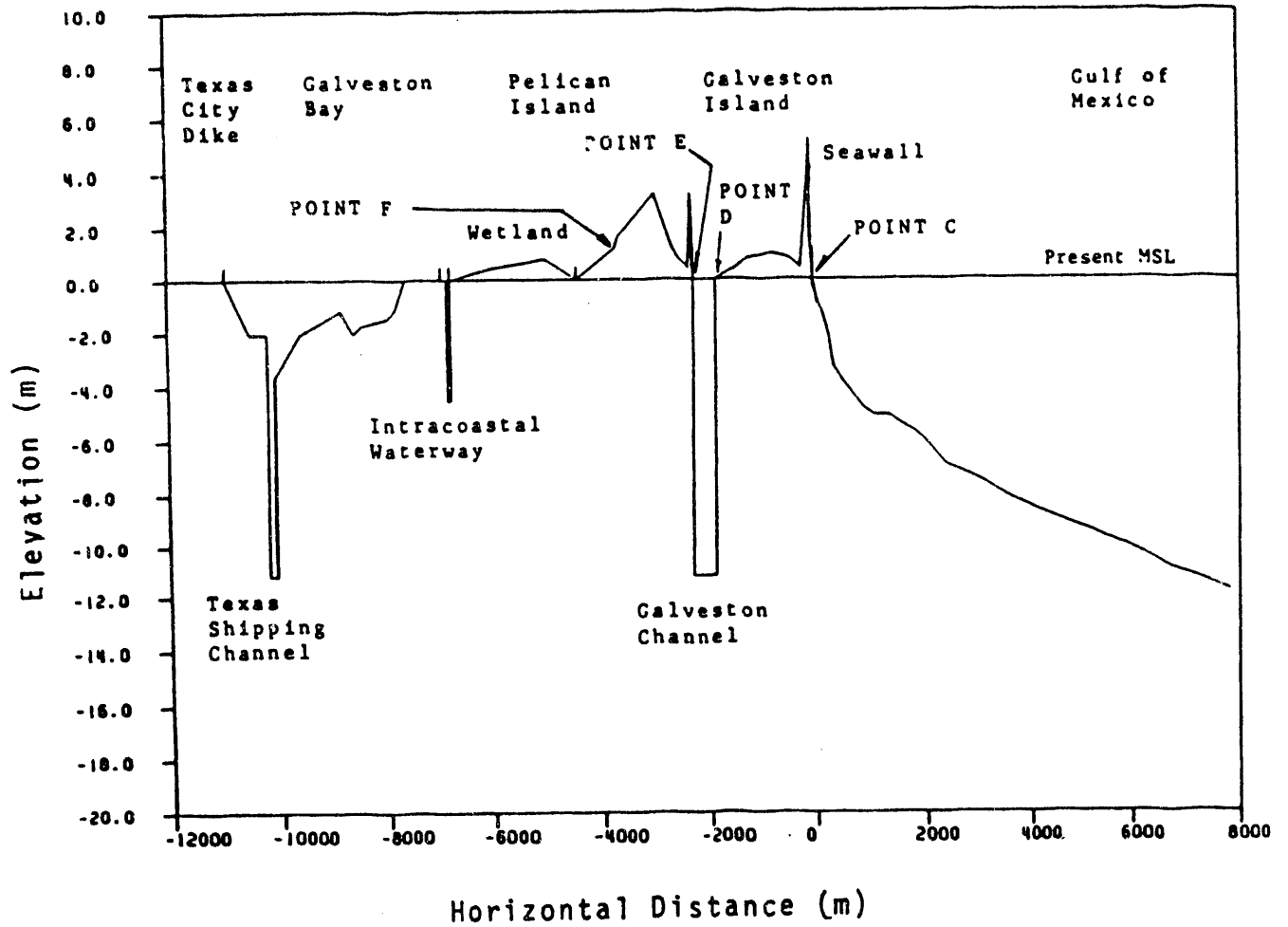




**Fig 5.10** Projected locations of waterline for the year 2100 at transect 3, Galveston, Texas.

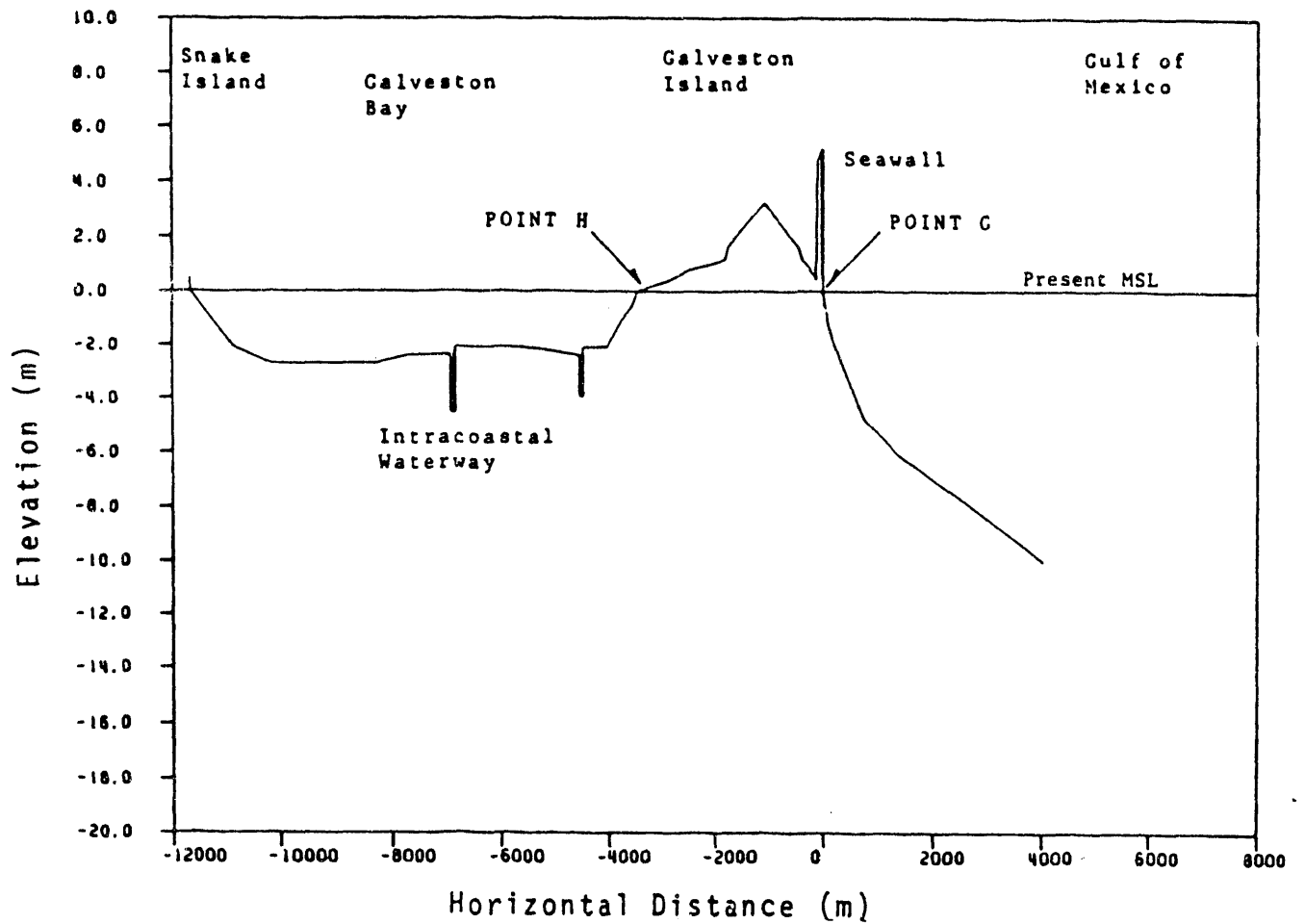




**Fig 5.12** Offshore profiles, Caminada Pass, Louisiana (based on U.S. Nautical Charts).

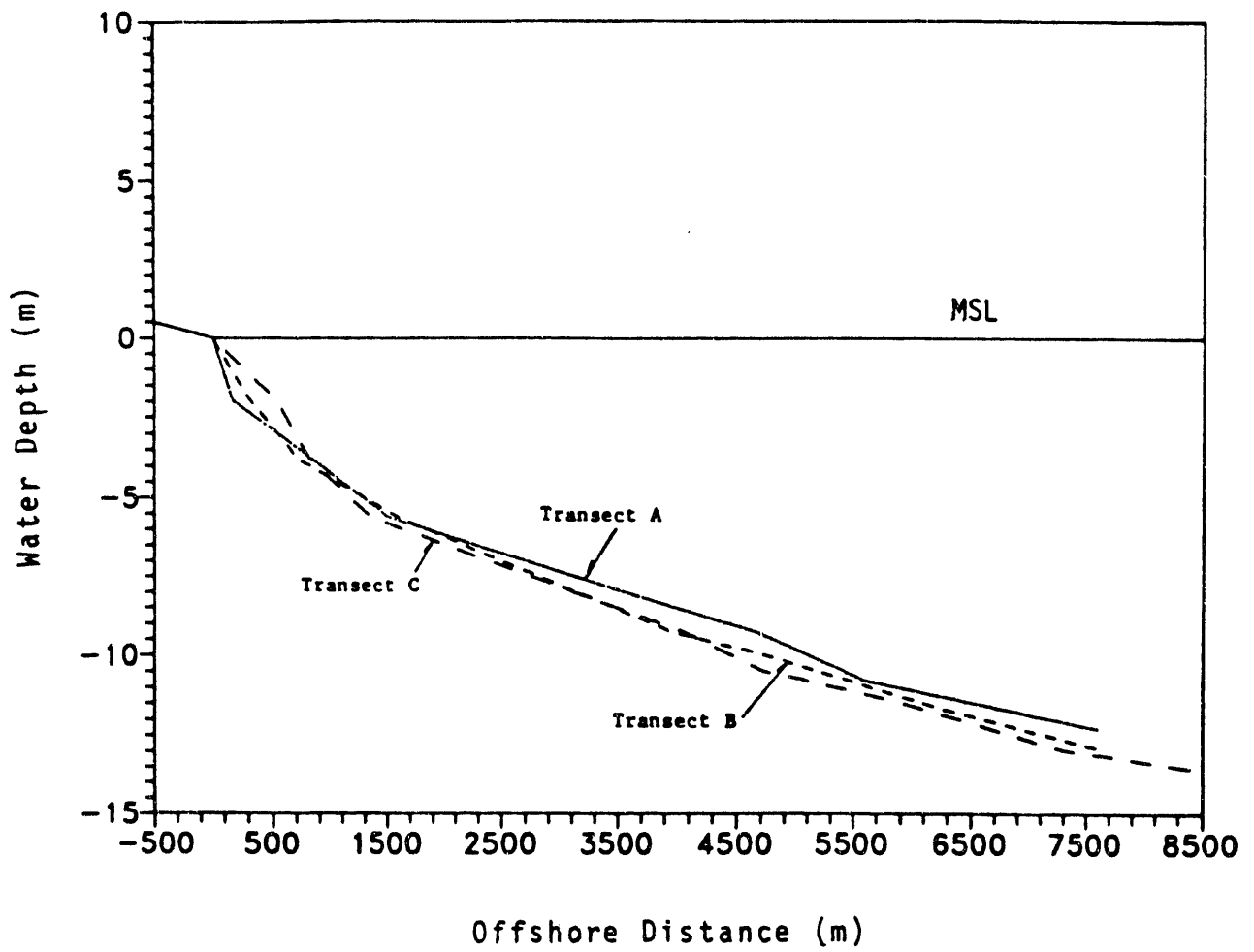


Fig 5.13 Location of cross-shore transects, Caminada Pass, Louisiana.

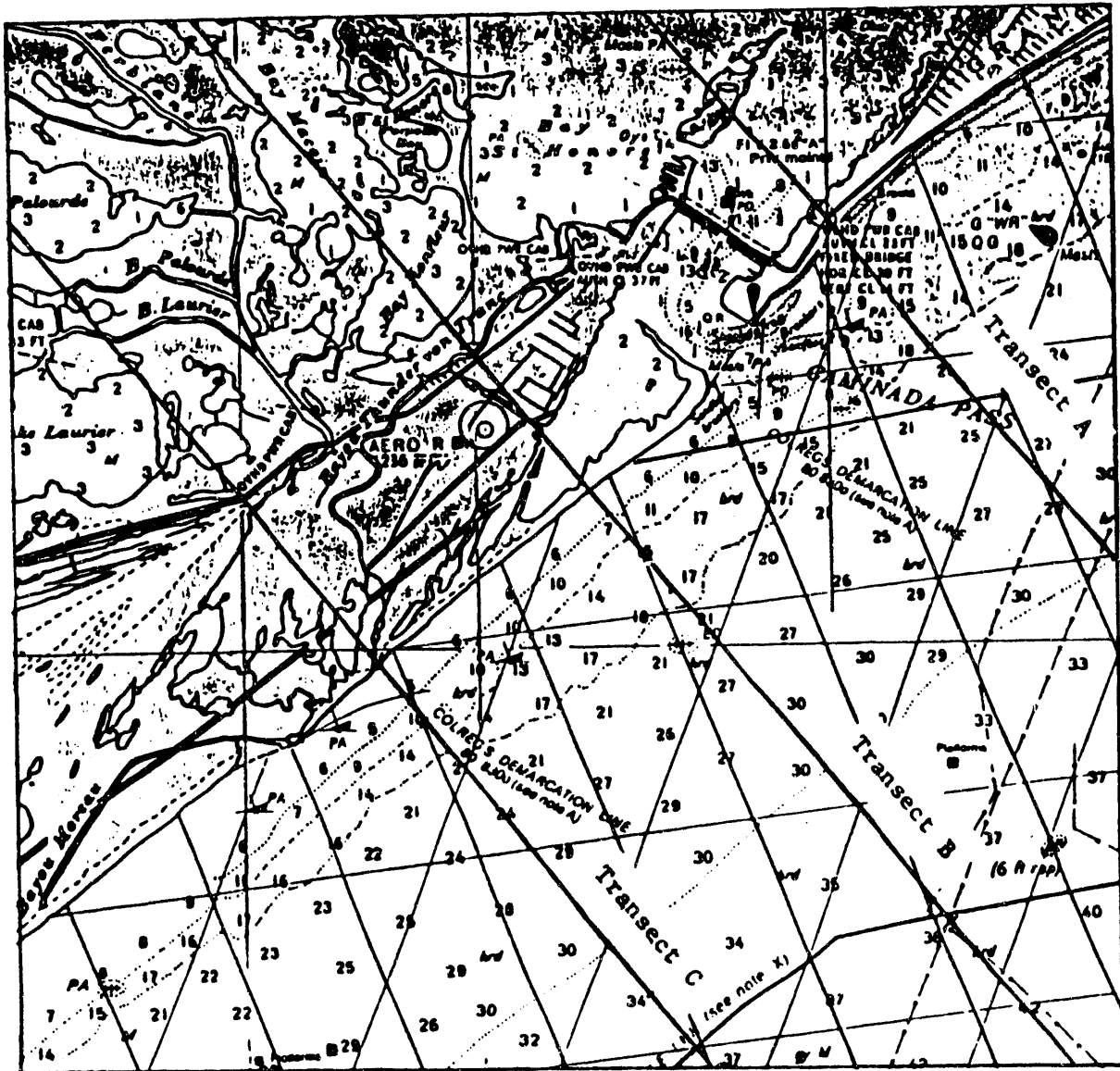


Fig 5.14 Study area, Bradenton Beach, Florida.

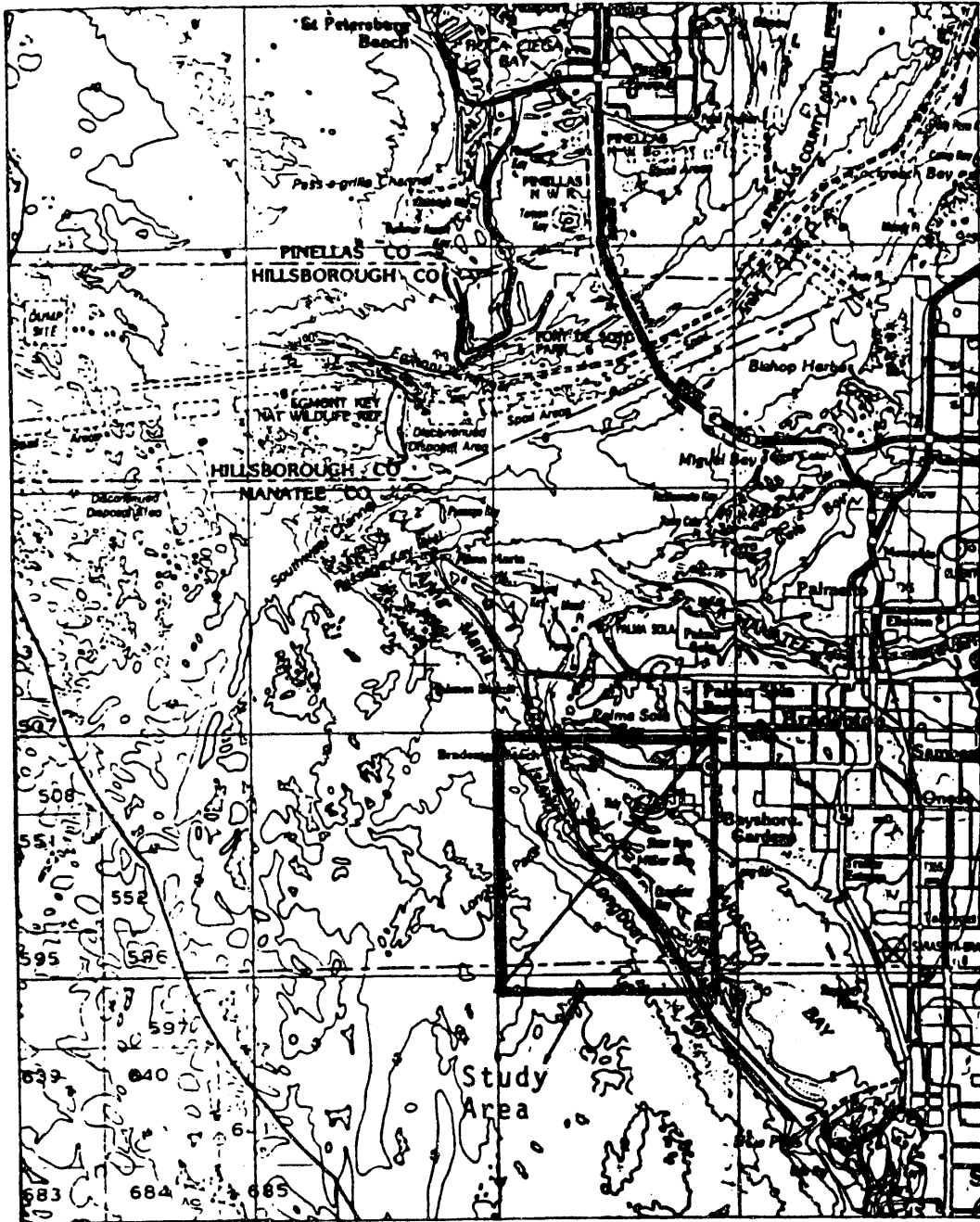


Fig 5.15 Offshore profiles, Bradenton Beach, Florida.

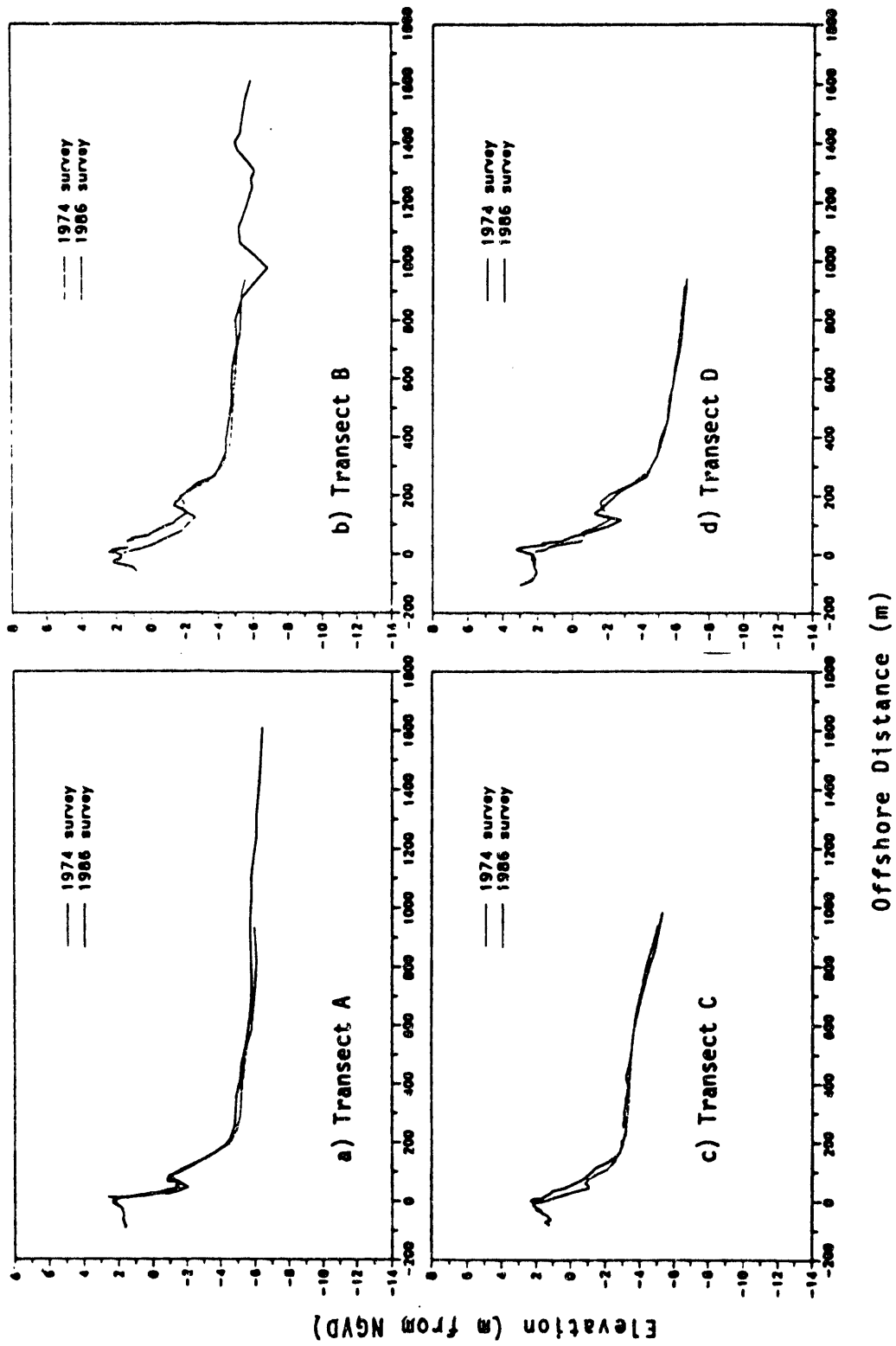


Fig 5.16 Location of cross-shore transects, Bradenton Beach, Florida.

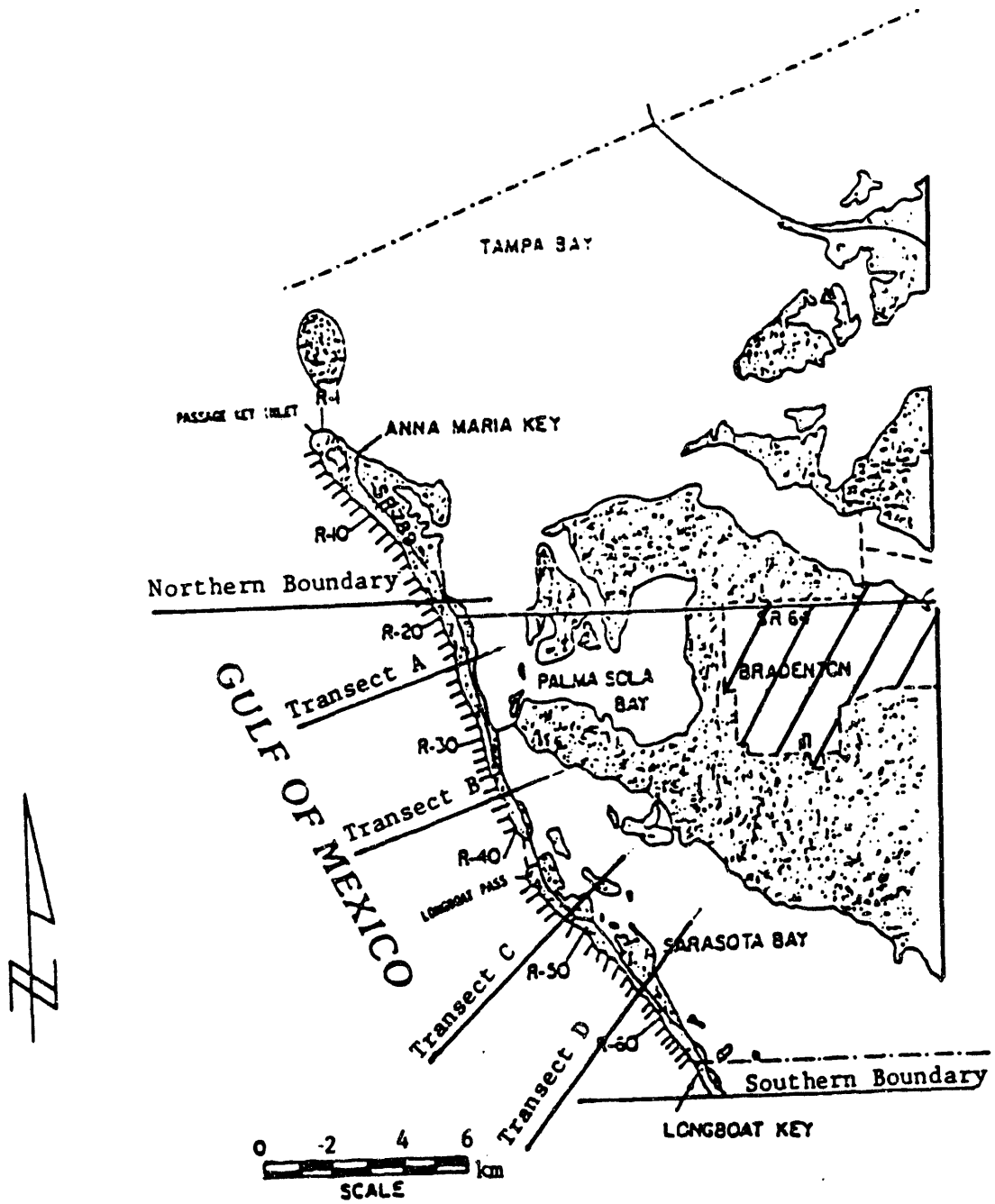
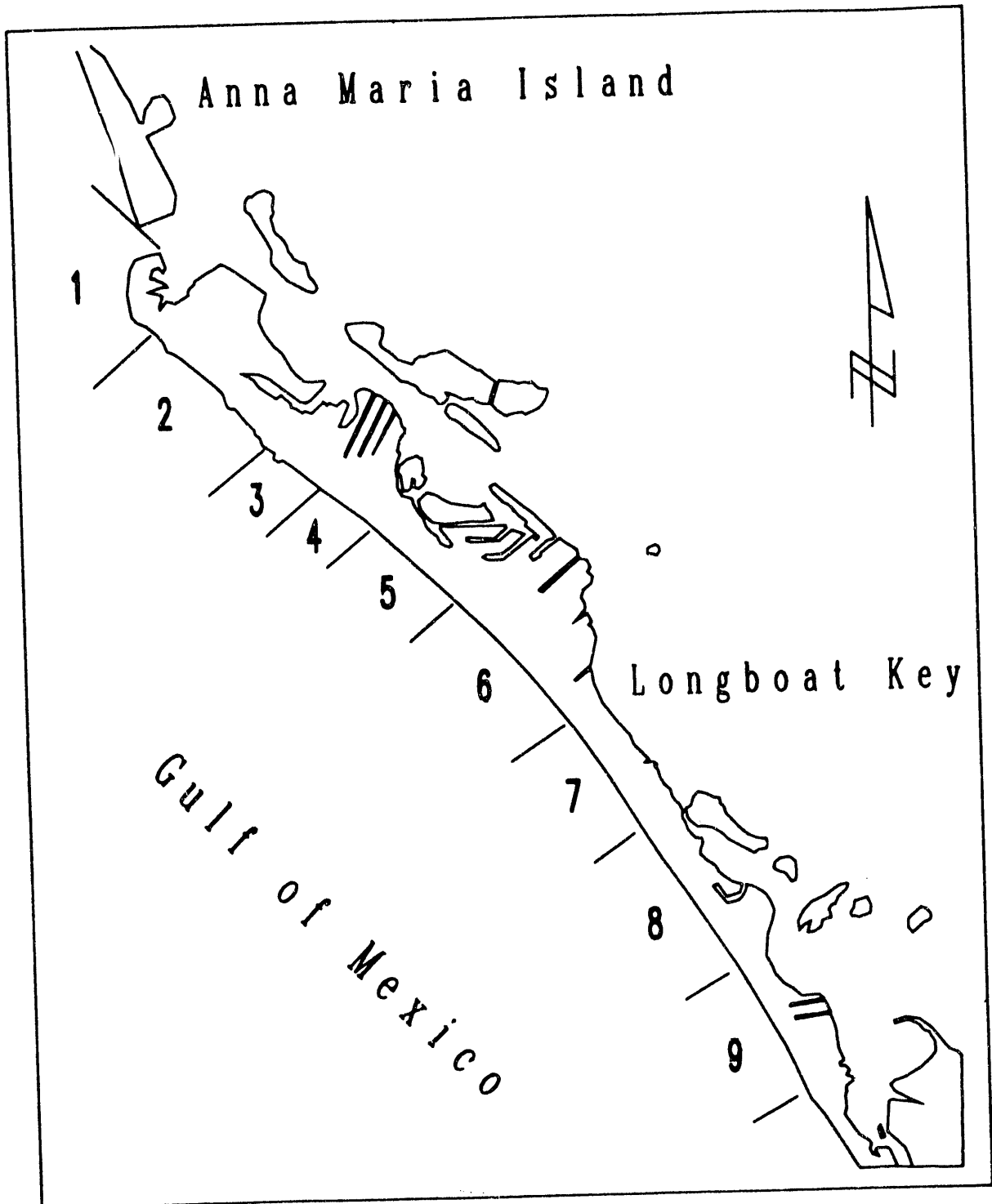


Fig 5.17 Beach segments referenced in Table 5.12.





**Fig 5.18** Historical shoreline positions, Bradenton Beach, Florida.

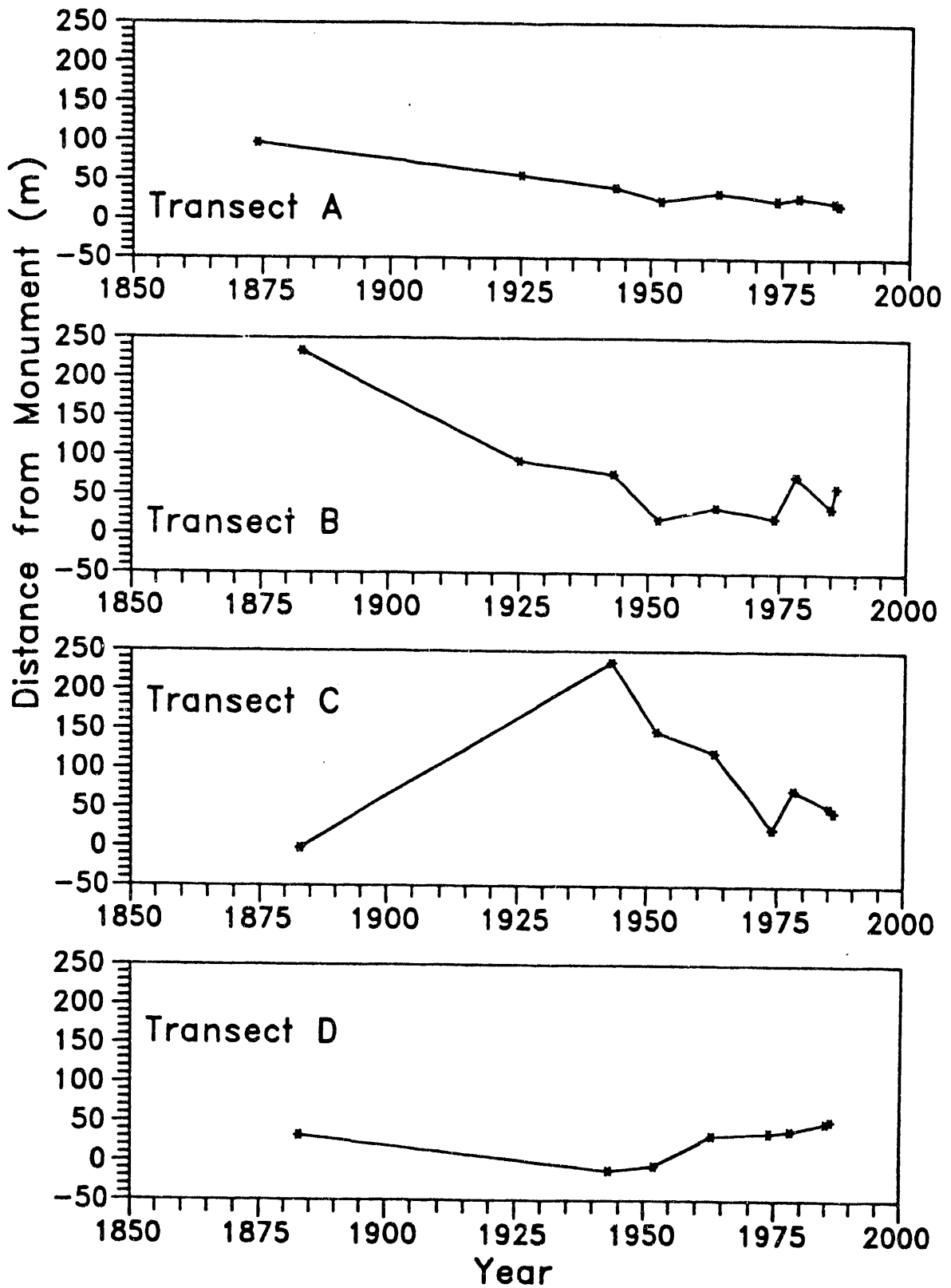


Fig 5.19

Longboat Pass bathymetry, Bradenton Beach, Florida (adapted from Harvey 1982).

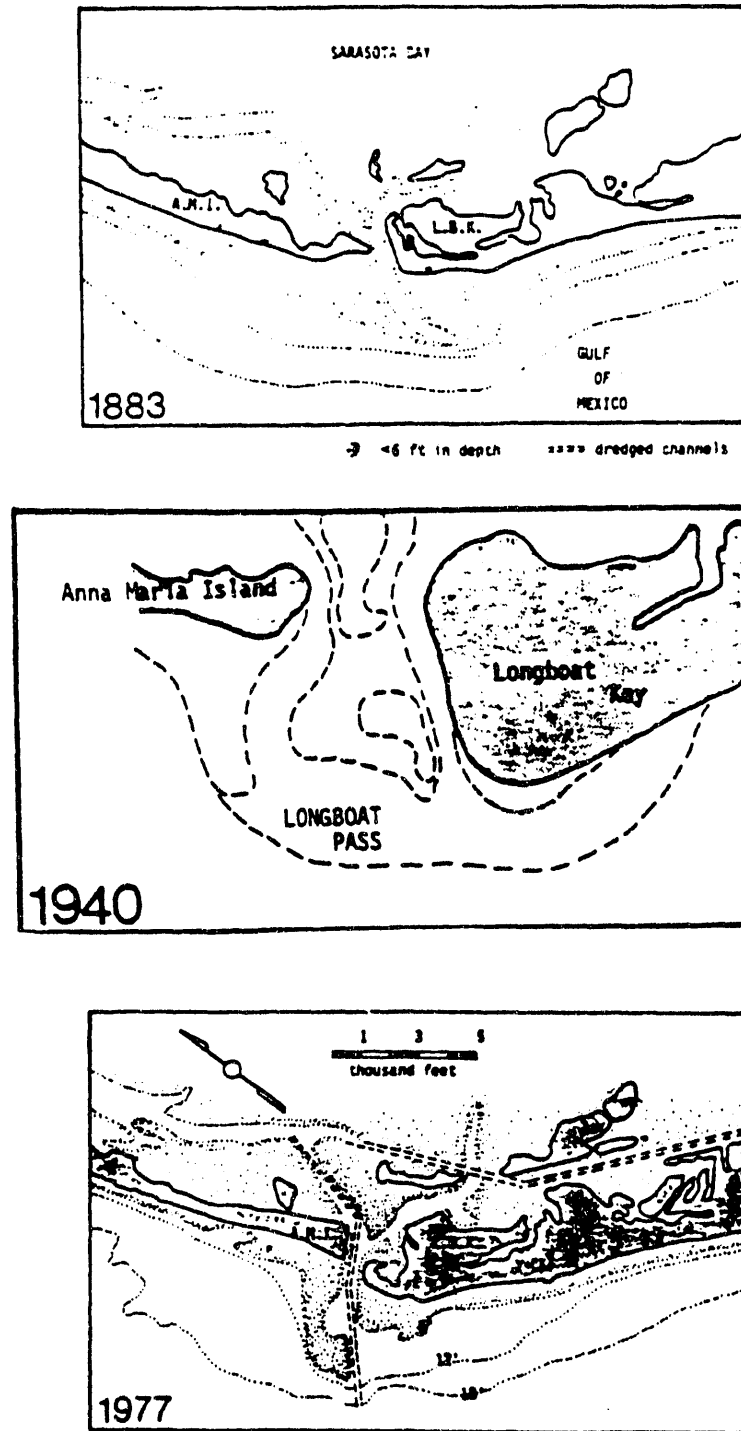
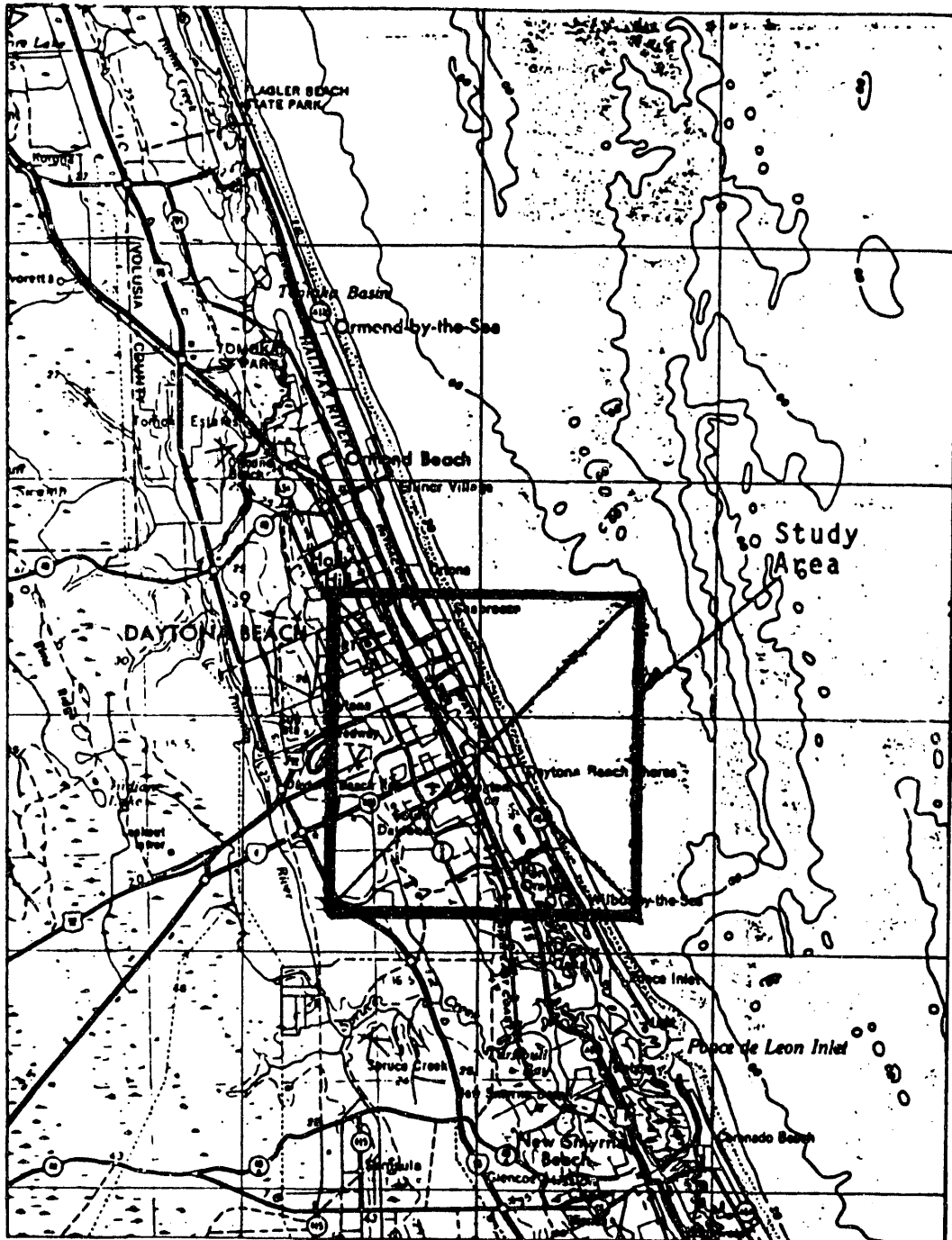


FIGURE REPRINTED WITH PERMISSION

Fig 5.20 Study area, Daytona Beach, Florida.



**Fig 5.21** Offshore profiles, Daytona Beach, Florida.

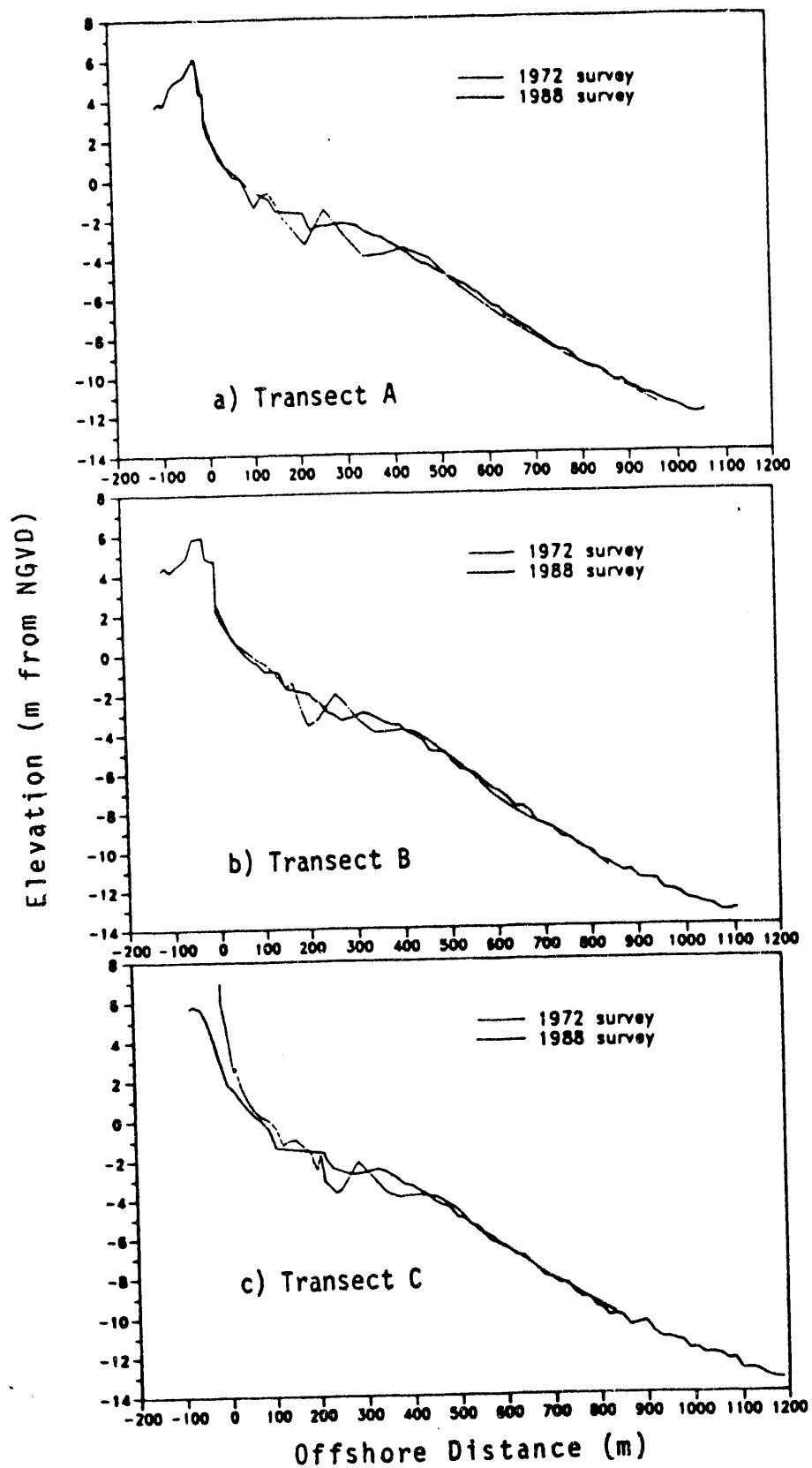
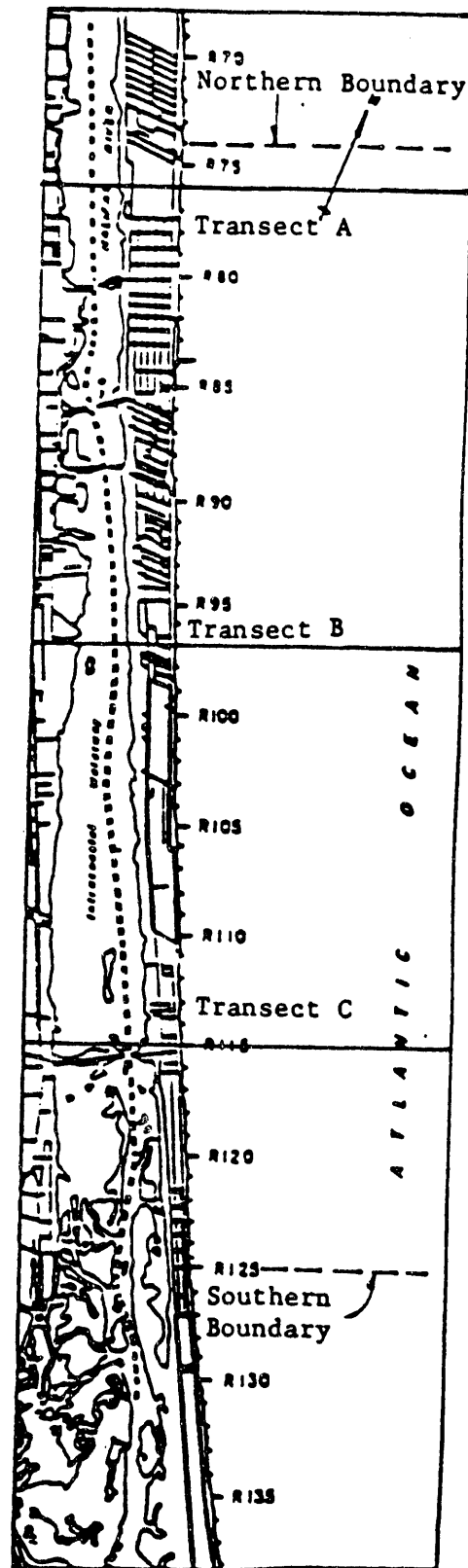
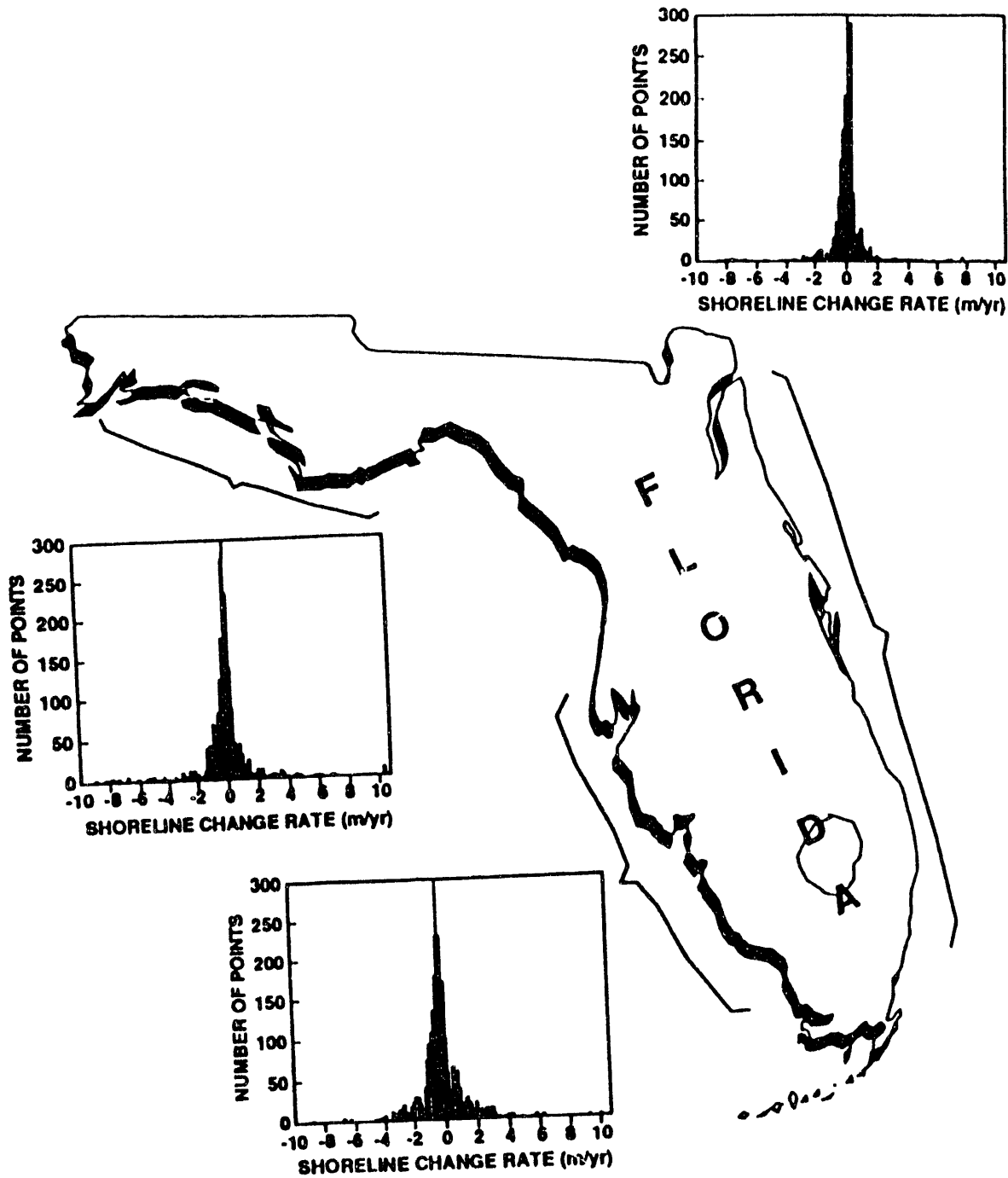


Fig 5.22 Location of cross-shore transects, Daytona Beach, Florida.



**Fig 5.23** Regional histogram of long-term shoreline change rates, Florida (Grant 1992).



*FIGURE REPRINTED WITH PERMISSION*

**Fig 5.24 Historical shoreline positions, Daytona Beach Florida.**

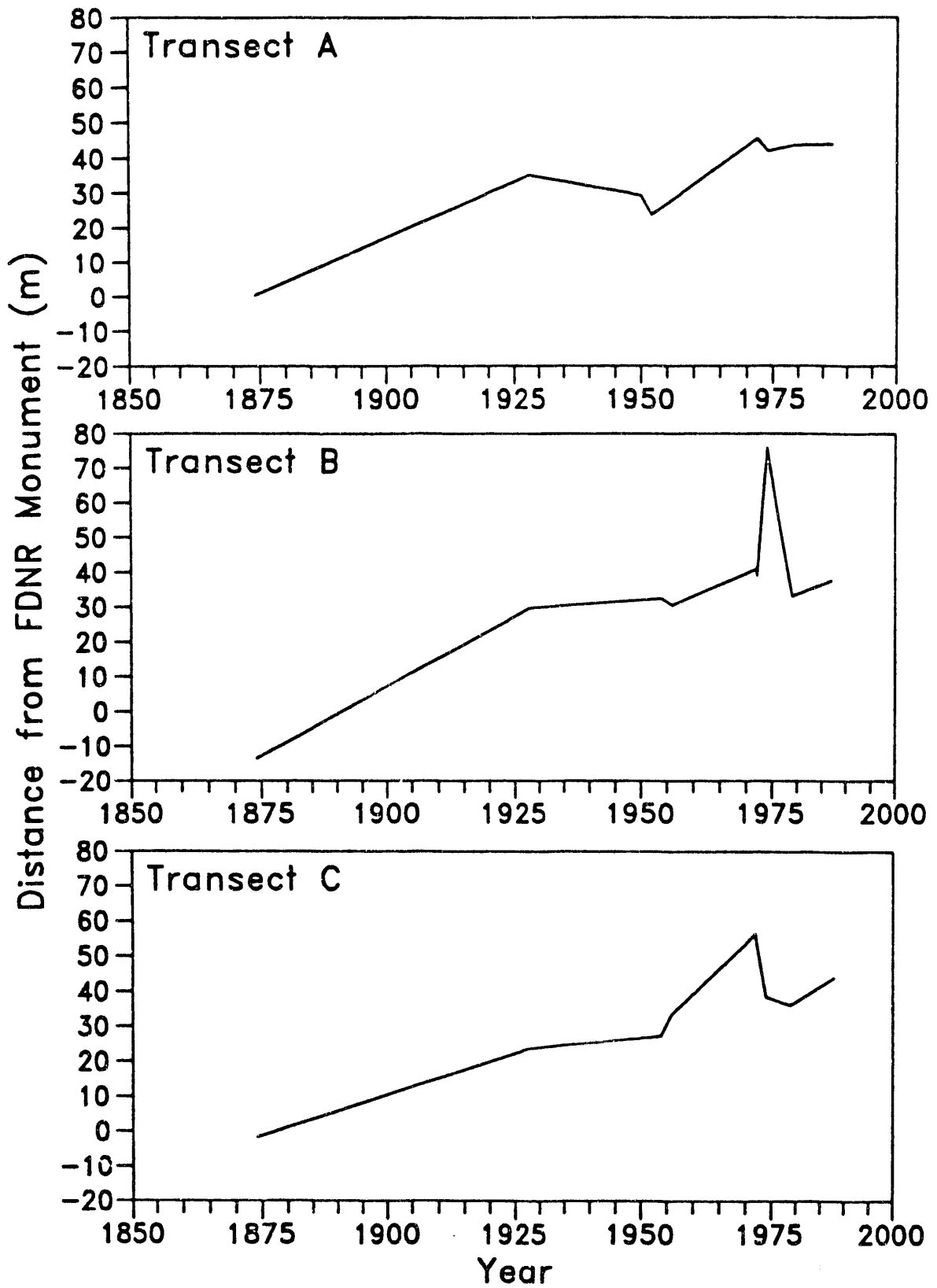
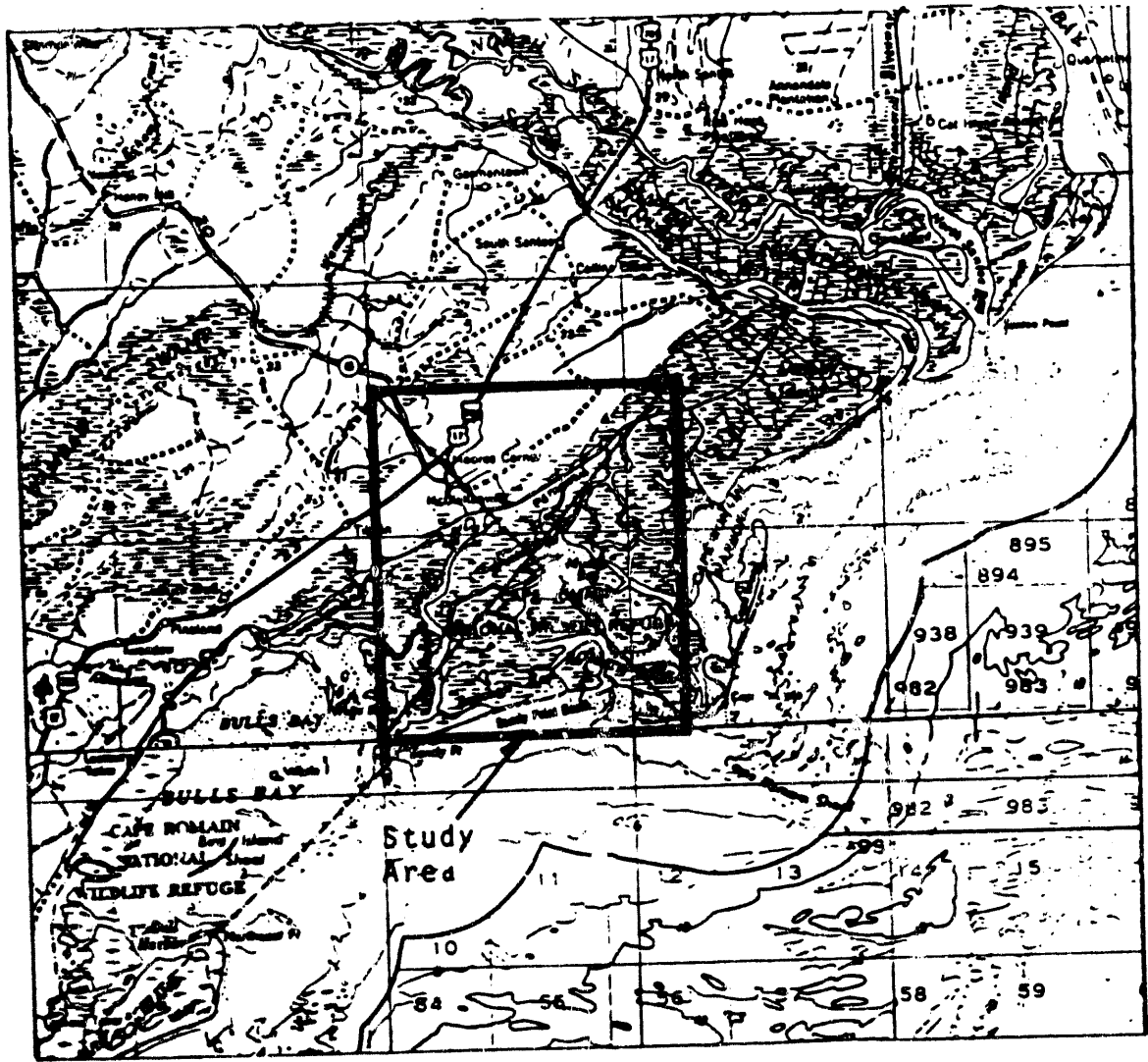


Fig 5.25 Study area, McClellanville, South Carolina.





**Fig 5.26** Offshore profiles, McClellanville, South Carolina (based on U.S. Nautical Charts).

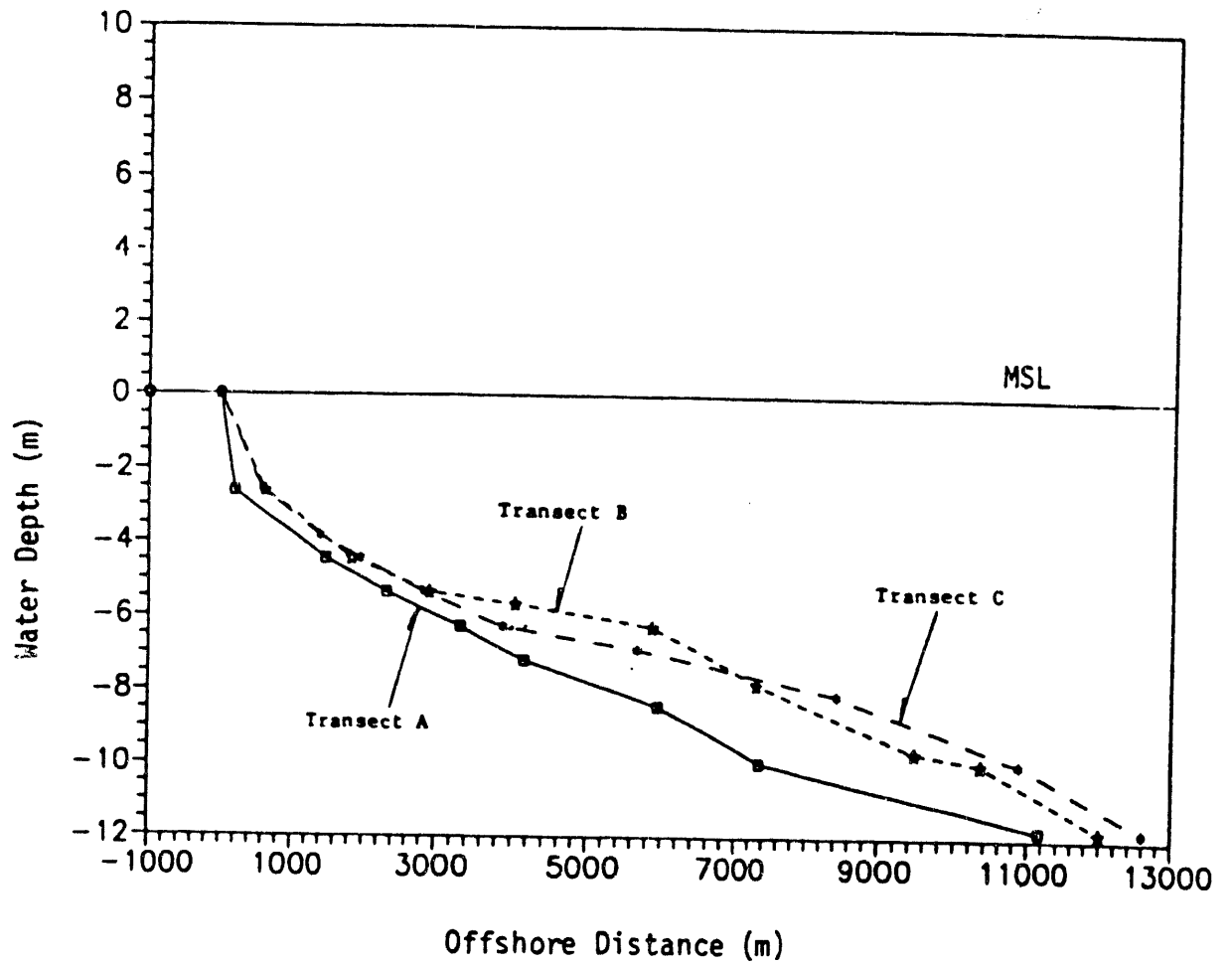
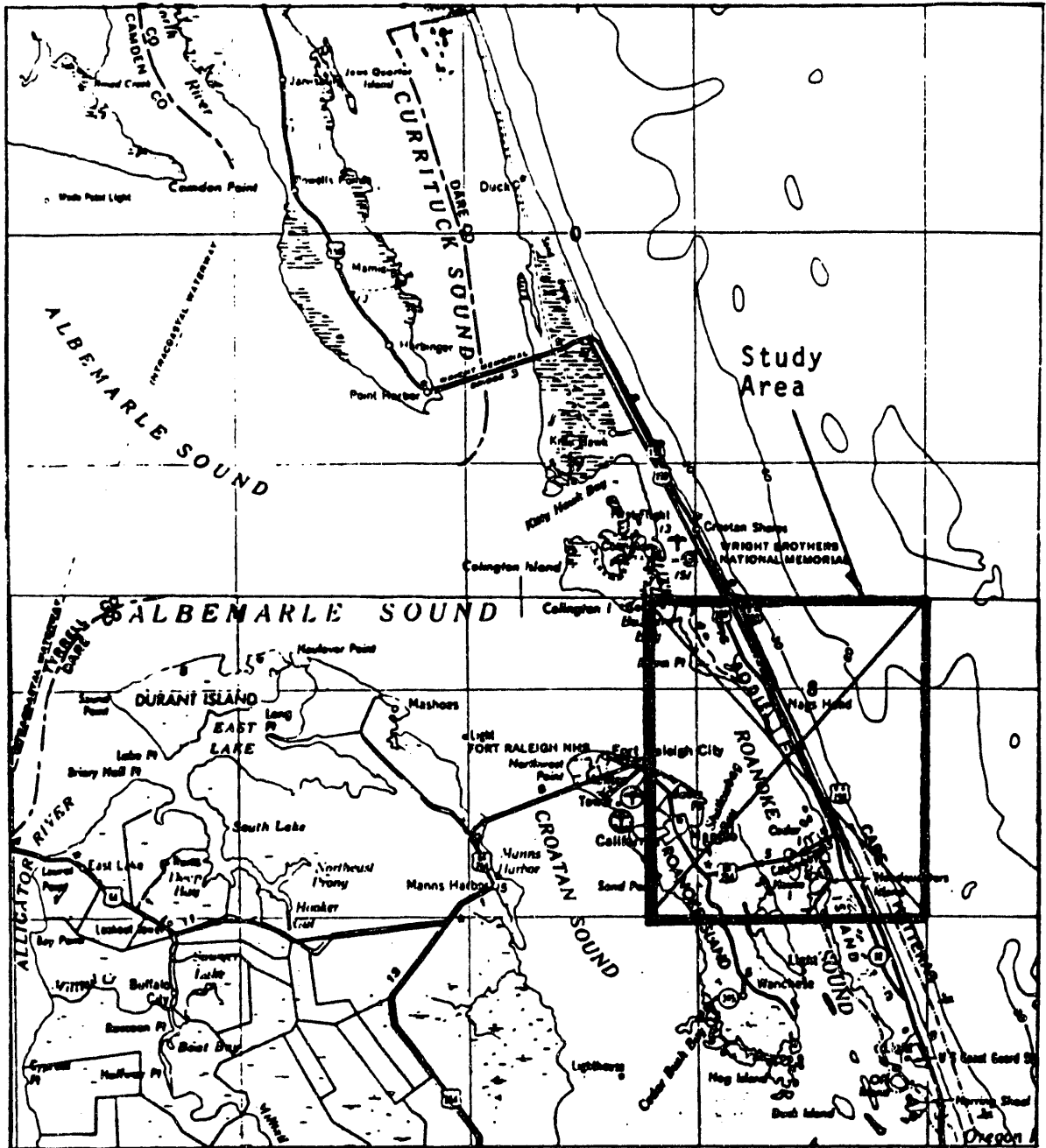


Fig 5.27 Locations of cross-shore transects, McClellanville, South Carolina.



Fig 5.28 Study area, Nags Head, North Carolina.



**Fig 5.29** Offshore profiles, Nags Head, North Carolina (based on U.S. Nautical Charts).

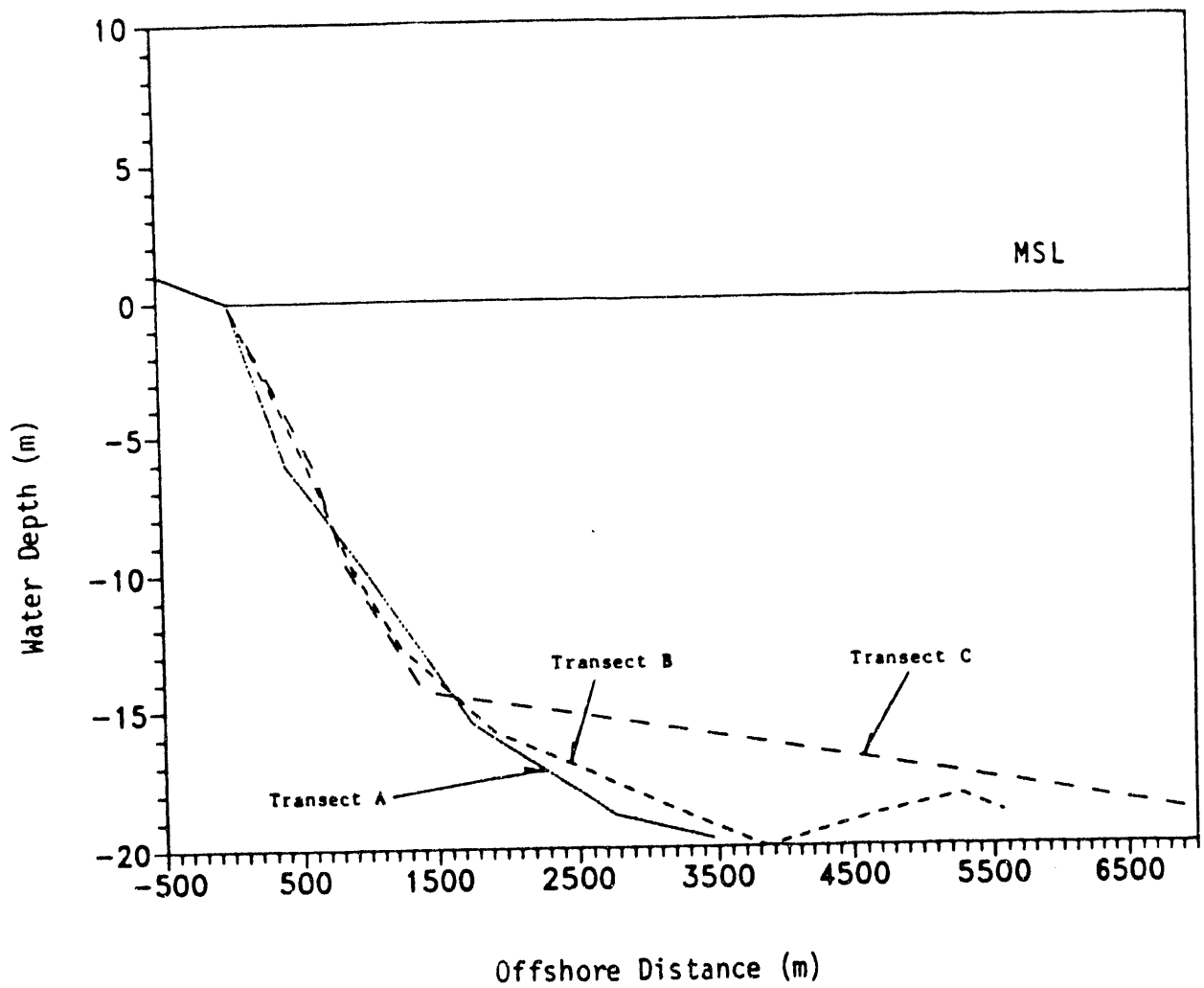
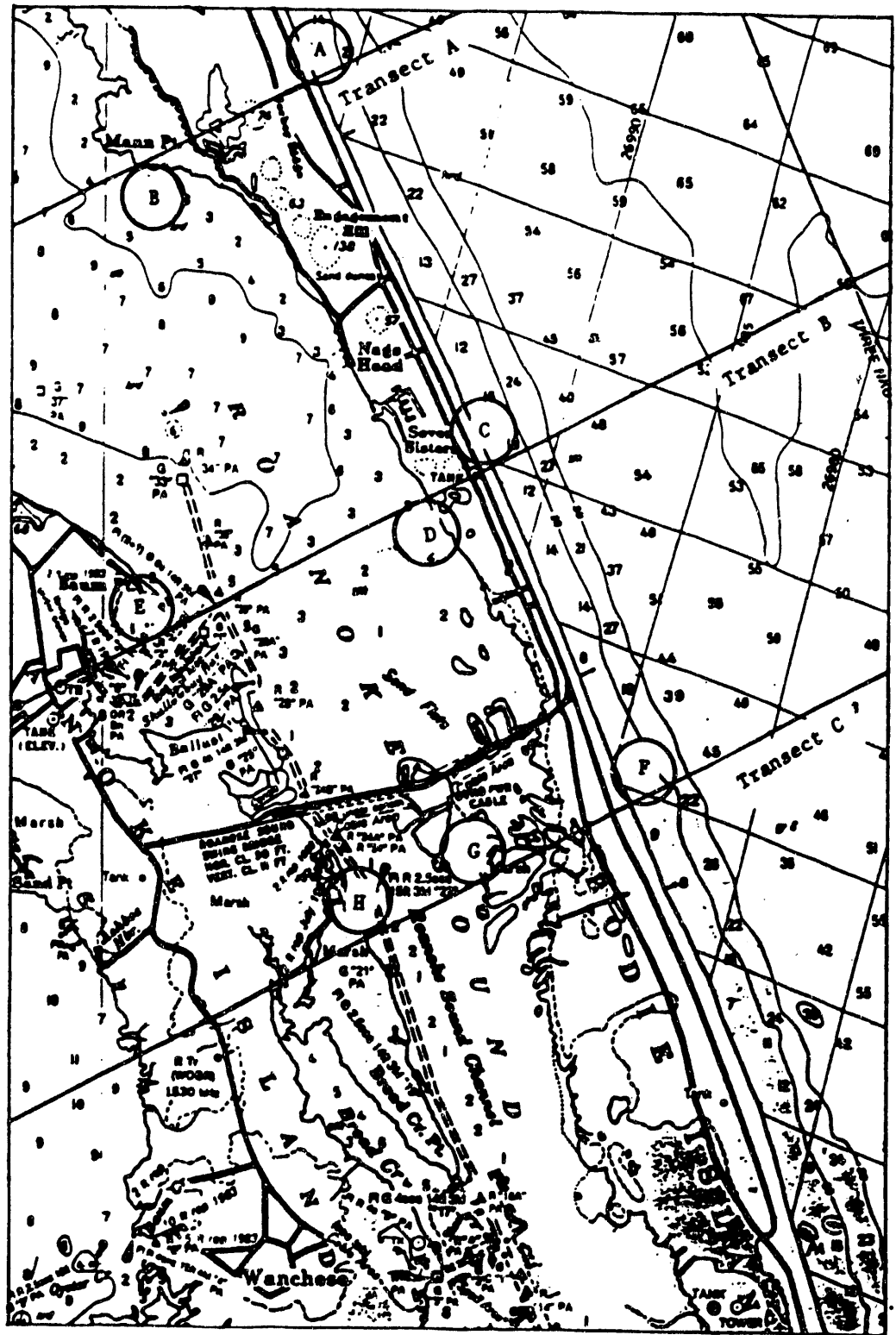
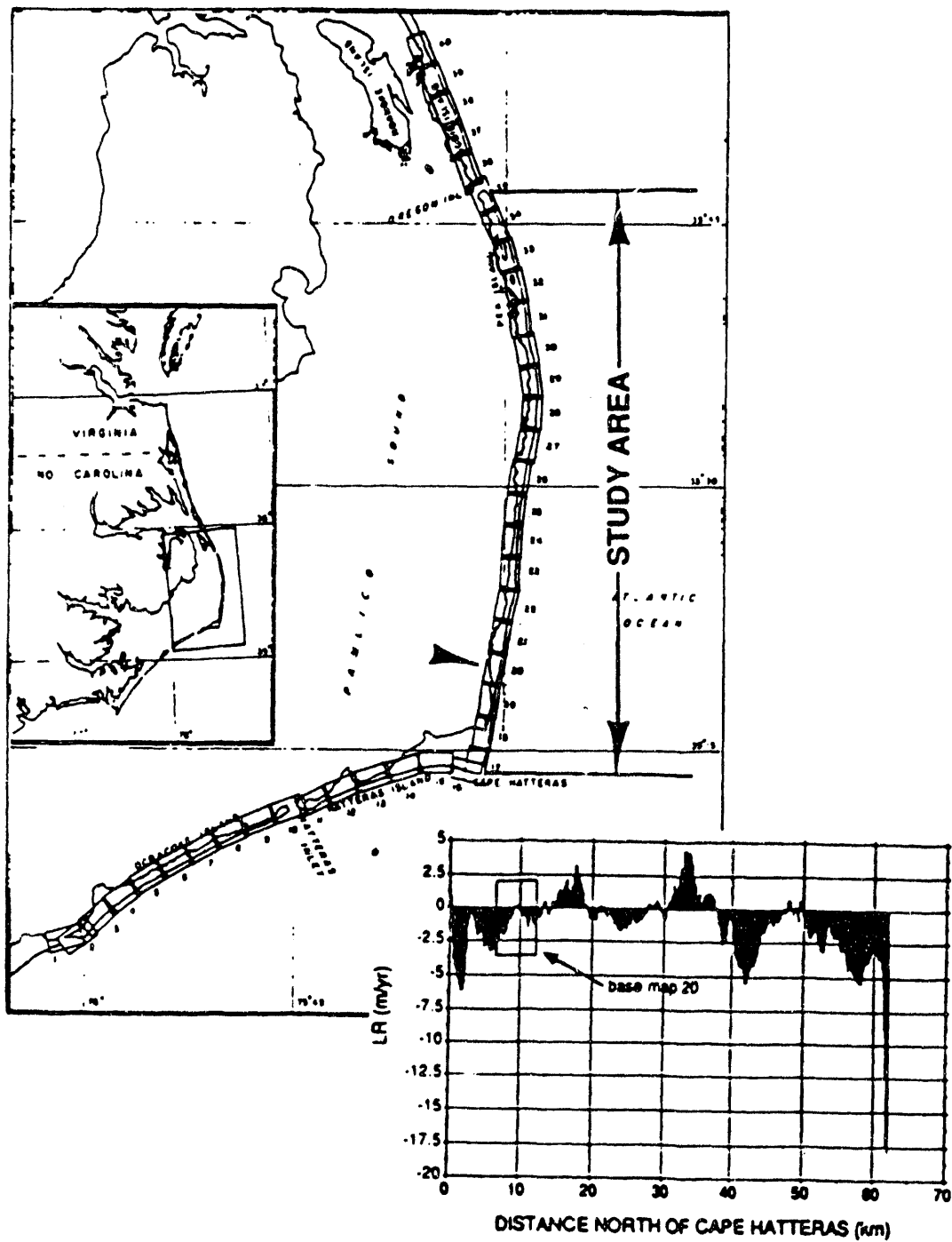


Fig 5.30 Locations of cross-shore transects, Nags Head, North Carolina.

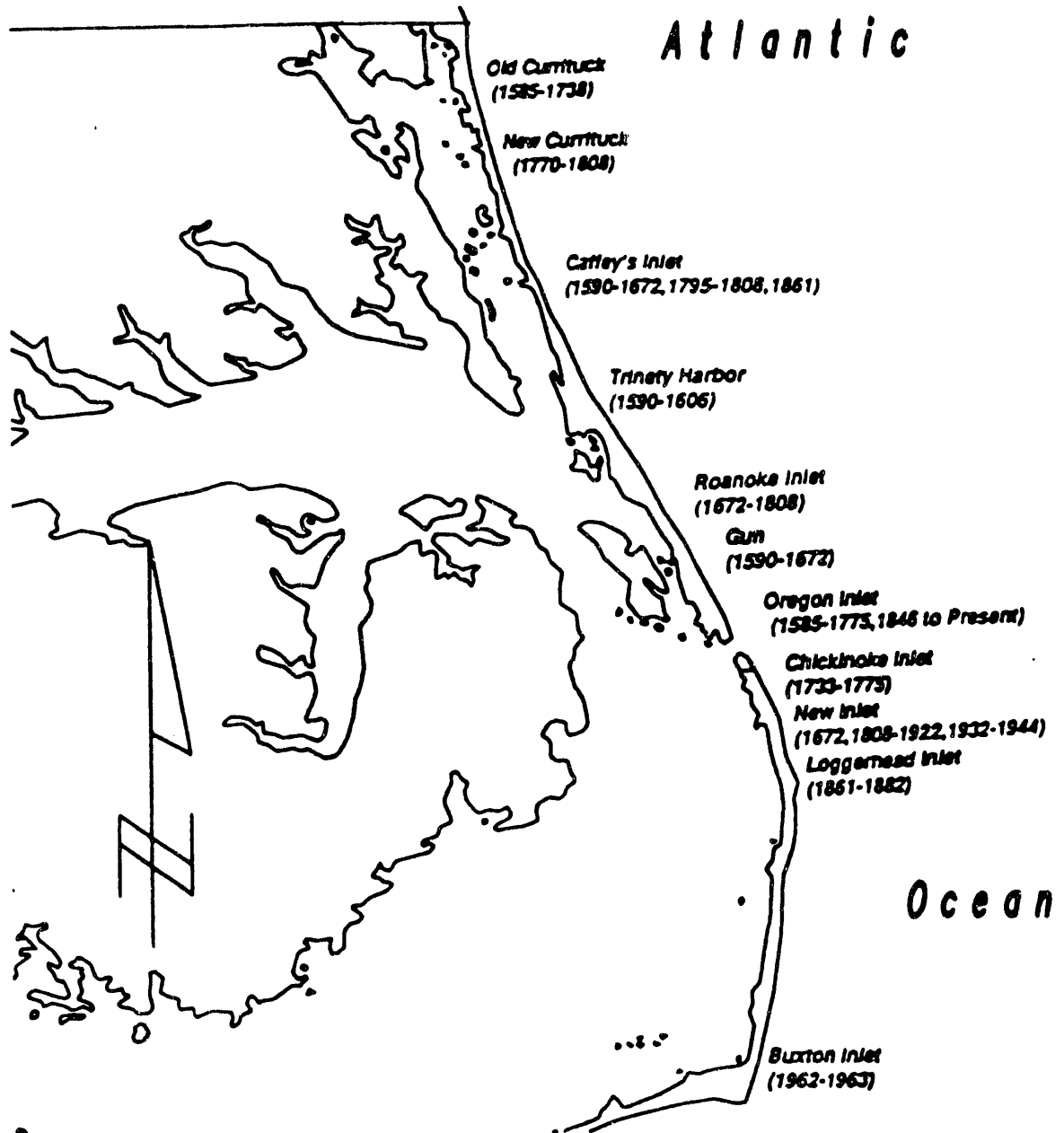


**Fig 5.31 Study area and plot of shoreline rate-of-change values, Cape Hatteras to Oregon Inlet, North Carolina (Dolan et al. 1991).**



*FIGURE REPRINTED WITH PERMISSION*

**Fig 5.32** Historical inlet locations from the Virginia/North Carolina state line to Cape Hatteras (Mehta and Montague 1991).



Note:  
Dates in parenthesis indicate periods in which inlets were open

FIGURE REPRINTED WITH PERMISSION

## **SUMMARY AND FINDINGS**

### **6.1 SUMMARY**

Rising sea levels from global warming, in conjunction with storms, threaten coastal areas in many parts of the world, and especially the southeastern United States, with temporary and/or permanent inundation and erosion. Three options have been proposed as possible responses to this threat: (1) hardening the shoreline for all affected areas; (2) raising the land surface and nourishing beaches, especially for barrier islands, in developed areas only; and (3) abandoning the coast and retreating inland. The third option has been suggested as being especially appropriate when the level of investment within an area does not warrant the massive expenditures that would be necessary if the coast were maintained at its present location.

In this project the impact that sea-level rise would have for the third option (i.e., abandoning the current shoreline) was analyzed. During this project the following steps/tasks were undertaken and completed: (1) identification of coastal areas of the U.S. Southeast most vulnerable to inundation and erosion from rising sea levels and storms; (2) examination, in greater detail, of six high-risk localities with different dominant land uses (i.e., urban, resort, rural); (3) evaluation of the potential inland encroachment of the sea, by land use type, based on elevation alone for each case study area; (4) identification of infrastructure and biophysical factors that could protect the land and interfere with the rising sea as predicted in item 3; and (5) reappraisal of the total amount of land that would be lost to the sea in each study area based on the factors identified in item 4.

### **6.2 FINDINGS**

The significant findings of this project were derived from the statistical analysis of the risk maps constructed for the U.S. Southeast, in Sect. 3, and from the conclusions drawn from the six detailed case studies, in Sects. 4 and 5. These findings are listed below:

1. Thirty percent of the Gulf Coast has been identified as being at very high risk to sea-level rise and erosion, versus only 15% of the East Coast (southern half).
2. The six case studies were conducted in several distinct geologic regions; when these study areas were ordered from high to low on the basis of their subsidence rates, it was found that areas with high subsidence rates will suffer the greatest loss of land to sea-level rise (especially wetlands).



3. In areas that have low topographies and sand lithologies and that are not significantly influenced by inlet processes, the use of elevation for determining the amount of land that will be lost to the sea in response to sea-level rise produces estimates that may be used for preliminary planning. These estimates are within  $\pm 30\%$  of those obtained from more complicated, physically based models.
4. Inlets produce local variations in the direction and speed of nearshore and longshore currents. These variations affect the sediment transport mechanisms (i.e., erosion/accretion rates) in a finite zone on either side of an inlet. Thus, the location of inlets must be considered when determining if static inundation models are suitable for use in a given study area.
5. The undeveloped case study areas (i.e., Caminada Pass, Louisiana; and McClellanville, South Carolina) will lose from 60 to 99.9% of their land to the sea by 2100 if the rates of sea-level rise and subsidence surpass the mean wetland vertical accretion rate in the given study area ( $\approx 5$  mm/year). This rate is surpassed in the moderate and high sea-level-rise scenarios in McClellanville, South Carolina, and for all scenarios in Caminada Pass, Louisiana.
6. The developed case study areas (i.e., Galveston, Texas; Bradenton Beach, Florida; Daytona Beach, Florida; and Nags Head, North Carolina) would lose a minimum of 31% to a maximum of 88% of their land area to sea-level rise by 2100 if no steps are taken to protect the coast.
7. On the basis of the perceived economic and social value of the areas that would be inundated in Galveston, Texas; Bradenton Beach, Florida; and Daytona Beach, Florida, it can be stated that retreat to sea-level rise in developed areas is not an option (under current law and political conditions) and that funds will be spent to protect the current coastline.
8. As sea levels continue to rise the viability of small communities located on coastal islands, such as Nags Head, North Carolina, may be in question, as federal, state, and local governments may not have the resources to both protect the coast from sea-level rise and to restore the coastline in the face of recurrent episodic events (e.g., hurricanes).

### **6.3 IMPLICATIONS FOR FUTURE STUDIES**

This study considered biophysical factors only (e.g., elevation, terrain, vertical movements of the land, ocean, and climate). As such, it indicates only what is potentially at risk: land that could be subject to increased erosion or inundation and today's land uses and infrastructures that could stand in the way of the sea's inland advance. The answers to many logical questions that are raised by this study and the specter of sea-level rise are not addressable on the biophysical level. Some questions, for example, are these:

At what point does the level of investment in an area make it cost-effective to protect the present coastline?

What is a rational societal response to these potential impacts?

Which resources are worth protecting, which ones are not, and how does society make such decisions (currently and in the future)?

Will decisions made to protect one resource affect another resource (e.g., increase erosion down or up the coast) and if so, how will these trade-offs be evaluated?

How does the uncertainty concerning the magnitude and timing of impacts affect decisions relative to other uncertainties (e.g., socioeconomic trends) or relative to the decision-making process (e.g., the NIMTOO ["not in my term of office"] effect?)

One logical extension of this project would be an elaboration on the biophysical level (e.g., more sites, larger sites, greater spatial resolution or diversity, development of site-specific sediment-transport models). Another interesting and useful extension would be an integrated analysis of the physical, socioeconomic, and political factors needed to address the above questions. The analysis could include such things as identifying the location of key resources (i.e., using an expanded Coastal Hazards Data Base), assessing the value of these resources, determining the useful lifetime of the resources, estimating the costs of protecting the resources from sea-level rise, and identifying socioeconomic trends that would affect the ability of the public or private sector to finance the three options to sea-level rise (for key locations).

## LITERATURE CITED

- Anders, F.J., and D.W. Reed. 1989. Shoreline change along the South Carolina coast. pp. 296-310. In D.K. Stauble (ed.), *Barrier Islands: Process and Management*. ASCE, New York, N.Y.
- Anderson, J.R., Hardy, E.E., and J.T. Roach. 1976. A Land use and Land Cover Classification System for Use with Remote Sensing Data. Geological Survey Professional Paper 964. Revised circular 671. U.S. Geological Survey, Washington, D.C.
- Aubrey, D.G., and P.E. Speer. 1985. Updrift migration of tidal inlets. *Journal of Geology*, 92:531-545.
- Ball, T.F. 1986. Historical evidence and climatic implications of a shift in the boreal forest tundra transition. *Climate Change*, 8:121-134.
- Barnett, T.P. 1988. Global sea level. In NCPO, *Climate Variations over the Past Century and the Greenhouse Effect: A report based on the First Climate Trends Workshop*. September 7-9, 1988, Washington, D.C., NOAA, National Climate Program Office, Rockville, Md.
- Barnett, T.P. 1984. The estimate of "global" sea level change: a problem of uniqueness. *Journal of Geophysical Research*, 89:7980-7988.
- Barnett, T.P. 1983. Recent changes in sea level and their possible causes. *Climate Change*, 5:15-38.
- Beltrami, H., and J.C. Mareschal. 1991. Recent warming in eastern Canada inferred from geothermal measurements. *Geophysical Research Letters*, 18:605-608.
- Birdwell, K.R., and R.C. Daniels. 1991. A global geographic information system data base of storm occurrences and other climatic phenomena affecting coastal zones. NDP-035, ORNL/CDIAC-40. Oak Ridge National Laboratory, Oak Ridge, Tenn.
- Blatt, F.J. 1983. *Principles of Physics*. Allyn and Bacon Publishing, Boston, Mass.
- Bruun, P. 1983. Review of conditions for uses of the Bruun Rule of erosion. *Coastal Engineering*, 7:77-89.
- Bruun, P. 1966. *Tidal Inlets and Littoral Drift*. H. Skipnes Offsettrykkeri, Trondheim, Norway.

- Bruun, P. 1962. Sea level rise as a cause of shore erosion. *Journal of the Waterways and Harbor Division*, 88:117-130.
- Callendar, G.S. 1938. The Artificial Production of Carbon Dioxide and its Influence on Temperature. *Quarterly Journal of the Royal Meteorological Society*, 64:223-240.
- Chiu, T.Y. 1989. Coastal Construction Control Line Review and Reestablishment Study for Volusia County. Beaches and Shore Resource Center, Institute of Science and Public Affairs, Florida State University, Tallahassee, Fla.
- Church, J.A., Godfrey, J.S., Jackett, D.R., and T.J. McDougall. 1991. A model of sea level rise caused by ocean thermal expansion. *Journal of Climate*, 4:438-456.
- Clark, R.R. 1990. Beach Condition in Florida: A Statewide Inventory and Identification of Beach Erosion Problem Areas in Florida (Update). Beach and Shores Technical and Design Memorandum 89-1. Florida Department of Natural Resources, Tallahassee, Fla.
- Coastal Engineering Research Center. 1984. Shore Protection Manual, Vol. 1. U.S. Army Corp of Engineers, Vicksburg, Miss.
- Curtis, J. 1984. Longboat Key: Yesterday, Today, and Tomorrow. Lindsay-Curtis Publishing, Sarasota, Fla.
- Dahl, T.E., and C.E. Johnson. 1991. Status and trends of wetlands in the conterminous United States, mid-1970's to mid-1980's. U.S. Department of the Interior, Fish and Wildlife Service, Washington D.C.
- Daniels, R.C. 1992. Sea-level rise on the South Carolina coast: Two case studies for 2100. *Journal of Coastal Research*, 8:56-70.
- Davis, Jr., R.A., and J.L. Gibeaut. 1990. Historical Morphodynamics of Inlets in Florida. Technical Paper 66, Florida Sea Grant College, Gainesville, Fla.
- Dean, R.G. 1991. Impacts of global change: Engineering solutions. In *Our Changing Planet: Joining Forces for a Better Environment. Proceedings of the Symposium in Commemoration of the 20th Anniversary of the Graduate Collage of Marine Studies*, University of Delaware, Newark, Del.
- Dean, R.G. 1990. Equilibrium Beach Profiles: Characteristics and Applications. UFL/COEL-90/001. University of Florida, Gainesville, Fla.
- Dean, R.G. 1983. Shoreline Erosion due to Extreme Storms and Sea Level Rise. UFL/COEL-83/007. University of Florida, Gainesville, Fla.

- Dean, R.G. 1977. Equilibrium Beach Profiles: U.S. Atlantic and Gulf Coasts. Ocean Engineering Technical Report No. 12. University of Delaware, Newark, Del.
- Dean, R.G., and E.M. Maurmeyer. 1983. Models for beach profile response. In Handbook of Coastal Processes and Erosion. CRC Press, New York, N.Y.
- Dean, R.G., and M.P. O'Brian. 1987. Florida's West Coast Inlets Shoreline Effects and Recommended Action. UFL/COEL-87/018. University of Florida, Gainesville, Fla.
- Delaune, R.D., Bauman, R.H., and J.G. Gosselink. 1983. Relationships among vertical accretion, coastal submergence, and erosion in a Louisiana Gulf Coast marsh. *Journal of Sediment Petrology*, 53:147-157.
- Denison, P.S. 1981. The North Carolina experience. *Shore and Beach*, 49:15-17.
- Dolan, R., Ferm, J.C., and J. McCoy. 1967. Analysis of variations in nearshore beach profiles along the Outer Banks of North Carolina. *Shore and Beach*, 35:26-28.
- Dolan, R. Ferm, J.C., and D.S. McArthur. 1969. Measurement of Beach Variables, Outer Banks, North Carolina. Louisiana State University, Baton Rouge, La.
- Dolan, R., Hayden, B.P., and J. Heywood. 1978. A new photogrammetric method for determining shoreline erosion. *Coastal Engineering*, 2:21-39.
- Dolan, R., Hayden, B.P., May, P., and S. May. 1980. The reliability of shoreline change measurements from aerial photographs. *Shore and Beach*, 48:22-29.
- Dolan, R., Trossbach, S.J., and M.K. Buckley. 1989. Patterns of erosion along the Atlantic Coast. pp. 17-22. In *Coastal Zone '89, Proceedings of the 5th Symposium on Coastal and Ocean Management*. ASCE, New York, N.Y.
- Dolan, R., Trossbach, S.J., and M.K. Buckley. 1990. New shoreline erosion data for the mid-Atlantic Coast. *Journal of Coastal Research*, 6:471-477.
- Dolan, R., Fenster, M.S., and S.J. Holme. 1991. Temporal analysis of shoreline recession and accretion. *Journal of Coastal Research*, 7:723-744.
- Douglas, B. 1991. Global sea level rise. *Journal of Geophysical Research*, 96:6981-6992.
- Emanuel, K.A. 1987. The Dependency of Hurricane Intensity on Climate. *Nature*, 326:483-485.
- Emery, K.O. 1980. Relative sea levels from tide-gauge records. *Proceedings of the National Academy of Science*, 77:6968-6972.

- Everts, C.H. 1985. Sea level rise effects on shoreline erosion. *Journal of the Waterway, Port, Coastal and Engineering Divison*, 111:985-999.
- Fairbridge, R.W., and O.A. Krebs. 1962. Sea level and the southern oscillation. *Geophysical Journal*, 6:532-545.
- Finkelstein, K., and C.S. Hardaway. 1988. Late holocene sedimentation and erosion of estuarine fringing marshes, York River, Virginia. *Journal of Coastal Research*, 4:447-456.
- Fisher, W.L., McGowen, J.H., Brown, Jr., L.F., and C.G. Groat. 1972. *Environmental Geologic Atlas of the Texas Coastal Zone: Galveston-Houston Area*. University of Texas, Auston, Tex.
- Foster, E.R., and R.J. Savage. 1989. Methods for analysis of historic shoreline data. In *Proceedings of the 8th Symposium on Coastal Sedimentology*, Department of Geology, Florida State University, Tallahassee, Fla.
- Godfrey, P.J. 1976. Comparative ecology of East Coast barrier islands: Hydrology, soil, vegetation. *Technical Proceedings of the 1976 Barrier Islands Workshop*, U.S. Department of Commerce, Annapolis, Md.
- Gornitz, V., White, T.W., and R.M. Cushman. 1991. Vulnerability of the U.S. to Future Sea Level Rise. pp. 2354-2368. In *Coastal Zone'91, Proceedings of the 7th Symposium on Coastal and Ocean Management*, ASCE, New York, N.Y.
- Gornitz, V. 1990. Vulnerability of the East Coast, U.S.A. to future sea level rise. *Journal of Coastal Research*, Special Issue, 9:201-237.
- Gornitz, V., and P. Kanciruk. 1989. Assessment of global coastal hazards from sea level rise. pp. 1345-1359. In *Coastal Zone '89, Proceedings of the 5th Symposium on Coastal and Ocean Management*, ASCE, New York, N.Y.
- Gornitz, V., Lebedeff, S., and J. Hansen. 1982. Global sea level trend in the past century. *Science*, 215:1611-1614.
- Gornitz, V., and S. Lebedeff. 1987. Global sea level changes during the past century. pp. 3-16. In Nummedal, D., Pilkey, O.H., and J.D. Howard (eds.), *Sea Level Fluctuation and Coastal Evolution*. SEPM Special Publication 41.
- Grant, J.R.H. 1992. *Historical Shoreline Response to Inlet Modifications and Sea Level Rise*. M.S. thesis. University of Florida, Gainesville, Fla.

- Grove, J.M. 1988. *The Little Ice Age*. Methuen, London.
- Hallermeier, R.J. 1981. A profile zonation for seasonal sand beaches from wave climate. *Coastal Engineering*, 4:253-277.
- Hands, E.B. 1976. Observations of Barred Coastal Profiles under the Influence of Rising Water Levels, Eastern Lake Michigan, 1967-1971. TR-76-1. U.S. Army Corp of Engineers, Coastal Engineering Research Center, Vicksburg, Miss.
- Hands, E.B. 1981. Predicting Adjustments in Shore and Offshore Sand Profiles on the Great Lakes. CETA 81-4. U.S. Army Corp of Engineers, Coastal Engineering Research Center, Vicksburg, Miss.
- Hands, E.B. 1983. The Great Lakes as a test model for profile response to sea level changes. In *Handbook of Coastal Processes and Erosion*. CRC Press, New York, N.Y.
- Hansen, J., and S. Lebedeff. 1987. Global trends of measured surface air temperature. *Journal of Geophysical Research*, 92D:345-372.
- Harvey, J. 1982. An assessment of beach erosion and outline of management alternatives, Longboat Key, Florida. Longboat Key Town Commission, Longboat Key, Fla.
- Hicks, S.D., Debaugh, Jr., H.A., and L.E. Hickman. 1983. *Sea Level Variations for the United States 1855-1980*. NOAA, National Ocean Service, Rockville, Md.
- Hicks, S.D., and J.E. Crosby. 1974. Trends and variability of yearly mean sea level (1893-1972). NOS-13. NOAA, National Ocean Service, Washington, D.C.
- Hine, A.C. 1989. *Evaluation of the Volusia County Coastline: Dominant Processes, Shoreline Change, Stabilization Efforts, and Recommendations for Beach Management*. University of South Florida, St. Petersburg, Fla.
- Hoffman, J.S., Keyes, D., and J.G. Titus. 1983. *Projecting Future Sea Level Rise, Methodology, Estimates to the year 2100, and research needs*. EPA 230-09-007. U.S. Environmental Protection Agency, Washington, D.C.
- Hoffman, J.S., Wells, J.B., and J.G. Titus. 1986. Future global warming and sea level rise. In *Iceland Coastal and River Symposium '85*. National Energy Authority, Reykjavik, Iceland.
- Houghton, R.A., and G.M. Woodwell. 1989. Global Climate Change. *Scientific America*, 260:36-44.

- Houghton, J.T., Jenkins, G.J., and J.J. Ephraums (eds.). 1990. *Climate Change, the IPCC Scientific Assessment*. Cambridge University Press, Cambridge, U.K.
- Howd, P.A., and W.A. Birkemeier. 1987. *Beach and Nearshore survey data: 1981-1984*. CERC-87-9. U.S. Army Corp of Engineers, Coastal Engineering Research Center, Vicksburg, Miss.
- Hubertz, J.M., and R.M. Brooks. 1989. *Gulf of Mexico Hindcast Wave Information*. WIS-18. U.S. Army Corp of Engineers, Coastal Engineering Research Center, Vicksburg, Miss.
- International Panel on Climate Change. 1990. *Strategies for Adaption to Sea Level Rise*. Response Strategies Working Group, Cambridge University Press, New York, N.Y.
- Jacoby, Jr., G.C., and R. D'Arrigo. 1989. *Reconstructed northern hemisphere annual temperature since 1671 based on high-latitude tree-ring data from North America*. *Climate Change*, 15:39-59.
- Jensen, R.E. 1983. *Atlantic Coast Hindcast, shallow water, significant wave information*. WIS-9. U.S. Army Corp of Engineers, Hydraulics Laboratory, Waterways Experiment Station, Vicksburg, Miss.
- Jones, C.P., and A.J. Mehta. 1978. *Ponce de Leon Inlet: Glossary of Inlets Report No. 6*. Report 23, Florida Sea Grant Program, Gainesville, Fla.
- Jones, P.D., Kelly, P.M., Goodess, G.B., and T.R. Karl. 1989. *The effect of urban warming on the Northern Hemisphere temperature average*. *Journal of Climate*, 2:285-290.
- Jones, P.D., Wigley, M.L., and P.B. Wright. 1990. *Global and hemispheric annual temperature variations between 1861 and 1988*. NDP-022/R1, ORNL/CDIAC-31. Oak Ridge National Laboratory, Oak Ridge, Tenn.
- Kana, T.W. 1988. *U.S.A.-South Carolina. Artificial Structures and Shorelines*, Klumwer Academic Publishers.
- Kana, T.W., Baca, B.J., and M.L. Williams. 1988a. *Charleston case study*, In: *Greenhouse Effects, Sea Level Rise, and Coastal Wetlands*. EPA-230-05-86-03. U.S. Environmental Protection Agency, Washington, D.C.
- Kana, T.W., Eiser, W.C., Baca, B.J., and M.L. Williams. 1988b. *New Jersey case study*. In *Greenhouse Effects, Sea Level Rise, and Coastal Wetlands*. EPA-230-05-86-03. U.S. Environmental Protection Agency, Washington, D.C.



- Kana, T.W. 1989. The South Carolina Coast I: Natural Processes and Erosion. pp. 265-273. In *Barrier Islands, Sea level rise, and Coastal Wetlands*. ASCE, New York, N.Y.
- Keeling, C.D., and T.P. Whorf. 1991. Atmospheric CO<sub>2</sub> - Modern Record, Mauna Loa. pp 12-15. In Boden, T.A., Sepanski, R.J., and F.W. Stoss (eds.), *Trends'91: A Compendium of Data on Global Change*. ORNL/CDIAC-46. Carbon Dioxide Information Analysis Center, Oak Ridge National Laboratory, Oak Ridge, Tenn.
- Komar, P. 1976. *Beach Processes and Sedimentation*. Prentice Hall Publishing, New York, N.Y.
- Kriebel, D.L., and R.G. Dean. 1985. Numerical simulation of time-dependent beach and dune erosion. *Coastal Engineering*, 9:221-245.
- Krone, R.B. 1985. Simulation of marsh growth under rising sea levels. pp. 106-115. In *Proceedings of the Conference on Hydraulics and Hydrology in the Small Computer Age*, ASCE, New York, N.Y.
- Lachenbruch, A., and B.V. Marshall. 1986. Changing climate: geothermal evidence from permafrost in the Alaskan Arctic. *Science*, 234:689-696.
- Langfelder, L.J. 1971. Coastal erosion in North Carolina. In *Proceedings of the Coastal Processes and Shore Protection Seminar*. Coastal Plains Center for Marine Development Services, Wilmington, N.C.
- Leatherman, S.P. 1979a. *Barrier Island Handbook*. U.S. Department of the Interior, National Park Service, Washington, D.C.
- Leatherman, S.P. (ed.). 1979b. *Barrier Islands: From the Gulf of St. Lawrence to the Gulf of Mexico*. Academic Press, New York, N.Y.
- Leatherman, S.P. 1981. *Barrier Island migration: An annotated bibliography*. University of Maryland, College Park, Md.
- Leatherman, S.P. 1983. Coastal effects of projected sea level rise: a case study of Galveston Bay, Texas. pp. 2890-2901. In *Coastal Zone'83, Proceedings of the 3rd Symposium on Coastal and Ocean Management*, ASCE, New York, N.Y.
- Leatherman, S.P. 1984. Coastal geomorphic response to sea level rise: Galveston Bay, Texas. In *Greenhouse Effect and Sea Level Rise: A Challenge for This Generation*. Van Nostrand Reinhold Company, New York, N.Y.
- Leontyev, O.K. 1965. On the causes of the present-day erosion of barrier bars. *Coastal Research Notes*, 12:5-7.

- List, J.H., Jaffe, B.E., and A.H. Sallenger. 1991. Large-scale coastal evolution of Louisiana's barrier islands. pp.1532-1546. In Coastal Sediments'91. ASCE, New York, N.Y.
- Louisiana Wetland Protection Panel. 1987. Saving Louisiana's Coastal Wetlands. EPA-230-02-87-026. U.S. Environmental Protection Agency, Washington, D.C.
- Lyles, S.D., Hickman, Jr., L.E., and H.A. Debaugh Jr. 1987. Sea-Level Variations for the United States, 1855-1986. National Ocean Service, Rockville, Md.
- Macchio, W.J. (ed.). 1990. Hurricane Hugo, Storm of the Century. J.R. Rowell Printing, Charleston, S.C.
- McAnally, W.H., Thomas, W.A., Letter, Jr., J.V., and J.P. Stewart. 1984. The Atchafalaya River Delta: Interim Summary Report of Growth Predictions. HL-82-15. U.S. Army Corp Of Engineers, Waterways Experiment Station, Vicksburg, Miss.
- McBride, R.A., Hiland, M.W., Penland, S., Williams, S.J., Byrnes, M.R., Westphal, K.A., Jaffe, B.E., and A.H. Sallenger Jr. 1991. Mapping barrier island changes in Louisiana: techniques, accuracy, and results. pp. 1011-1026. In Coastal Sediments'91. ASCE, New York, N.Y.
- McElyea, W.D., Brower, D.J., Godschalk, D.R., and B. Seymour. 1984. Before the storm: Managing development to reduce hurricane damages. University of North Carolina, Chapel Hill, N.C.
- Mehta, A.J., and H.K. Brooks. 1973. Mosquito Lagoon Barrier Beach Study. Shore and Beach, 41:27-34.
- Mehta, A.J., Dean, R.G., Kunz, H., Law, V.J., Tarapore, Z.S., and R.I. Wiegall. 1991. Global Warming and Coastal Hazards. Unpublished report, National Institute for Global Environmental Change, Southern Region, Tulane University, New Orleans, La.
- Mehta, A.J., and C.L. Montague. 1991. A brief review of flow circulation in the vicinity of natural and jetted inlets: Tentative observations on implications for larval transport at Oregon Inlet, North Carolina. UFL/COEL/MP-91/3. University of Florida, Gainesville, Fla.
- Mehta, A.J., and R.M. Cushman (eds.). 1989. Workshop on Sea Level Rise and Coastal Processes. DOE/NBB-0086. U.S. Department of Energy, Washington D.C.

- Mehta, A.J., Dean, R.G., Dally, W.R., and C.L. Montague. 1987. Some Considerations on Coastal Processes Relevant to Sea Level Rise. UFL/COEL-87/012. University of Florida, Gainesville, Fla.
- Meier, M.F. 1990. Reduced rise in sea level. *Nature*, 343:115-116.
- Meier, M.F. 1984. The contribution of small glaciers to global sea level. *Science*, 226:1418-1421.
- Mitsch, W.J., and J.G. Gosselink. 1986. *Wetlands*. Van Nostrand Reinhold, New York, N.Y.
- National Research Council. 1990. *Managing Coastal Erosion*. National Academy Press, Washington, D.C.
- National Research Council. 1987. *Responding to Changes in Sea Level, Engineering Implications*. National Academy Press, Washington, D.C.
- Neumann, C.J., Jarvinen, B.R., and A.C. Pike. 1987. *Tropical Cyclones of the North Atlantic Ocean: 1871-1986*. Historical Climatology Series 6-2. NOAA, National Weather Service, Hurricane Center, Coral Gables, Fla.
- North Carolina Department of Natural Resources and Community Development. 1984. *Coastal Resources Commission's Outer Banks Erosion Task Force Report*. Raleigh, N.C.
- Odum, H.T., Copeland, B.J., and E.A. McMahan. 1974. *Coastal Ecological Systems of the United States, Vol. II*. World Wildlife Fund, Washington, D.C.
- Oerlemans, J. 1989. A projection of future sea level. *Climate Change*, 15:151-174.
- Orme, A.R. 1990. Wetland morphology, Hydrodynamics and sedimentation. In Williams, M. (ed.), *Wetlands: A Threatened Landscape*. Basil Blackwell Publishers, Cambridge, Mass.
- Orson, R., Panageotou, W., and S.P. Leatherman. 1985. Response of tidal salt marshes to rising sea levels along the U.S. Atlantic and Gulf coasts. *Journal of Coastal Research*, 1:29-37.
- Park, R.A., Trehan, M.S., Mausel, P.W., and R.C. Howe. 1989. The effects of sea level rise on U.S. coastal wetlands. In Smith, J.D., and D.A. Tirpak (eds.), *The Potential Effects of Global Climate Change on the United States*. EPA-230-05-89-052. U.S. Environmental Protection Agency, Washington, D.C.

- Peltier, W.R., and A.M. Tushingham. 1989. Global sea level rise and the greenhouse effect: might they be connected? *Science*, 244:806-810.
- Penland, S., and R. Boyd. 1981. Shoreline changes on the Louisiana barrier coast. *OCEANS*, 209-218.
- Penland, S., Boyd, R., Nummedal, D., and H. Roberts. 1981. Deltaic barrier development along the Louisiana coast. *Transactions of the Gulf Coast Association, Geological Society*. 31:471-477.
- Phillips, J.D. 1986. Coastal submergence and marsh fringe erosion. *Journal of Coastal Research*, 2:427-436.
- Pierce, J.W., and Colquhoun, D.J. 1970. Holocene evolution of a portion of the North Carolina coast. *Geological Society of America Bulletin*, 81:3697-3714.
- Pilkey, O.H. 1980. *New York Times*. December 1, 1980.
- Pilkey, Jr., O.H., Neal, W.J., and O.H. Pilkey. 1978. From Currituck to Calabash. North Carolina Science and Technology Research Center, Raleigh, N.C.
- Pugh, D.T., Spencer, N.E., and P.L. Woodworth. 1987. Data Holdings of the Permanent Service for Mean Sea Level. Bidston Observatory, Birkenhead, U.K.
- Ramanathan, V. 1987. The Role of Earth Radiation Budget Studies in Climate and General Circulation Research. *Journal of Geophysical Research*, 92:4075-4095.
- Sallenger, Jr., A.H., Penland, S., Williams, S.J., and J.R. Suter. 1987. Louisiana barrier island erosion study. pp. 1503-1516. In *Coastal Sediment'87*, ASCE, New York, N.Y.
- Schneider, S.H. 1989. The Changing Climate. *Scientific America*, 260:70-79.
- Shepard, F.P. (ed.) 1960. Gulf coast barriers: Recent sediments, Northwest Gulf of Mexico. American Association of Petroleum Geologists, Tulsa, Okla.
- Smith, J.B., and D. Tirpak (eds.). 1989. The Potential effects of Global Climate Change on the United States: Report to Congress. EPA-230-05-89-050. U.S. Environmental Protection Agency, Washington, D.C.
- Smith, J.B., and J.G. Titus. 1990. The Potential Impacts of Climate Change on the Southeast. In *Global Change: A Southern Perspective*. Southeast Regional Climate Symposium, Southeast Regional Climate Center, Charleston, S.C.

- Smith, T.D. 1991. Manatee County, Florida Shore Protection Project, GENESIS shoreline change simulation, Anna Maria Key. pp. 339-354. In Proceedings of the 4th Annual Beach Preservation Technology Conference. Florida Shore and Beach Protection Preservation Association, Tallahassee, Fla.
- South Carolina Water Resources Commission. 1970. South Carolina Tidelands Report. Columbia, S.C.
- Stauble, D.K., Seabergh, W.C., and L.Z. Hales. 1990. The initial impact of Hurricane Hugo on the reaches, dunes, and inlets of South Carolina. pp. 363-377. In Proceedings of the 3rd Annual National Beach Preservation Technology Conference. Florida Shore and Beach Preservation Association, Tallahassee, Fla.
- Stephen, M.F., Brown, P.J., FitzGerald, D.M., Hubbard, D.K., and M.O. Hayes. 1975. Beach Erosion Inventory of Charleston County, South Carolina: A Preliminary Report. South Carolina Sea Grant Technical Report No. 7, Columbia, S.C.
- Stevenson, J.C., Ward, L.G., and M.S. Kearney. 1986. Vertical accretion in marshes with varying rates of sea level rise. In Wolf, D.A. (ed.), Estuarine Variability. Academic Press, New York, N.Y.
- Thomas, R. 1986. Future sea level rise and its early detection by satellite remote sensing. pp. 19-36. In Titus, J.G. (ed.), Effects of Changes in Stratospheric Ozone and Global Climate, Vol. 4. UNEP and EPA, Washington, D.C.
- Thompson, R.E. 1982. Harris-Galveston Coastal Subsidence District, Houston, Texas. Esley Houston and Associates, Houston, Tex.
- Tiner, R.W. 1991. Recent changes in estuarine wetlands of the Coterminous United States. pp. 100-109. In Coastal Wetlands. ASCE, New York, N.Y.
- Titus, J.G. 1991. Greenhouse Effect and Coastal Wetland Policy: How Americans Could Abandon an Area the Size of Massachusetts at Minimum Cost. Environmental Management, 15:39-58.
- Titus, J.G. 1990. Greenhouse Effect, Sea Level Rise, and Barrier Islands: Case Study of Long Beach Island, New Jersey. Coastal Management, 18:65-90.
- Titus, J.G., Leatherman, S.P., Everts, C.H., Kriebel, D.L., and R.G. Dean. 1985. The Potential Impacts of Sea Level Rise on the Beach at Ocean City, Maryland. EPA-230-10-85-013. U.S. Environmental Protection Agency, Washington, D.C.
- Trupin, A., and J. Wahr. 1990. Spectroscopic analysis of global tide gauge sea level data. Geophysical Journal Internal, 100:441-453.

- U.S. Army Corp of Engineers. 1990. Hurricane Hugo, After-action Report. Charleston District, S.C.
- U.S. Army Corp of Engineers. 1972. Beach Erosion Control Study on Manatee County, Florida. Jacksonville District, Fla.
- U.S. Army Corp of Engineers. 1971. National Shoreline Study, Inventory Report - Lower Mississippi Delta. New Orleans District, La.
- U.S. Department of Commerce. 1979. Meteorological Criteria for Standard Project Hurricane and Probable Maximum Hurricane Windfields, Gulf and East Coasts of the United States. Technical Report NWS-23. NOAA, National Weather Service, Washington, D.C.
- U.S. Department of the Interior. 1983. Final Environmental Statement: Undeveloped Coastal Barriers. Coastal Barriers Task Force, Washington, D.C.
- U.S. Geological Survey. 1990. Storm-tide Elevations Produced by Hurricane Hugo Along the South Carolina Coast, September 21-22, 1989. Open-file report 90-386. Reston, Va.
- Wahr, J., and J. Trupin. 1990. New computation of global sea level rise from 1990 tide gauge data. abstract, EOS, 71:1267.
- Walker, H.J., and J.M. Coleman. 1987. Atlantic and Gulf Coastal Provinces. pp. 51-107 In Graf, W.L. (ed.), Geomorphic Systems of North America, Vol. 2. Geological Society of America, Boulder, Colo.
- Walton, T.L. 1977. Coastal History Notes: Anna Maria Key. Florida Sea Grant Publication, Gainesville, Fla.
- Walton, T.L. 1976. Littoral Drift Estimates along the Coastline of Florida. Florida Sea Grant Program Report 13, Gainesville, Fla.
- Wang, H. 1990. Water and erosion damage to coastal structures -South Carolina coast, Hurricane Hugo, 1989. pp. 1-25. In Proceedings of the Third Annual National Beach Preservation Technology Conference. Florida Shore and Beach Preservation Association, Tallahassee, Fla.
- Ward, L.G., and D.D. Domeracki. 1978. The stratigraphic significance of back-barrier tidal channel migration. Geological Society of America, Abstract with program, Vol. 10., p. 201.

- Warrick, R.A., and J. Oerlemans. 1990. Sea level rise. pp. 257-281. In Houghton, J.T., Jenkins, G.J., and J.J. Ephraums (eds.), *Climate Change —The IPCC Scientific Assessment*. Cambridge University Press, Cambridge, U.K.
- Weggel, J.R. 1979. A Method for Estimating Long-term Erosion Rates from a Long-term Rise in Water Level. CETA-79-2. U.S. Army Corp of Engineers, Coastal Engineering Research Center, Vicksburg, Miss.
- Wigley, T.M.L., and S.C.B. Raper. 1992. Implications for climate and sea level of revised IPCC emissions scenarios. *Nature*, 357:293-300.
- Wigley, T.M.L. 1989. *Scientific Assessment of Climate Change and its Impact*. p 131. cited In *Climate Change: Meeting the Challenge*. Commonwealth Secretariat, London.
- Wigley, T.M.L., and S.C.B. Raper. 1987. Thermal expansion of sea water associated with global warming. *Nature*, 330:127-131.
- Wolaver, T.G., Dame, R.F., Spurrier, J.D., and A.B. Miller. 1988. Sediment exchange between a euhaline salt marsh in South Carolina and the adjacent tidal creek. *Journal of Coastal Research*, 4:17-26.
- Zimmerman, R.J., Minello, T.J., Klima. E.F., and J.M. Nance. 1991. Effects of accelerated sea level rise on coastal secondary production. *Coastal Wetlands*, ASCE, New York, N.Y.

## MAPS CITED

- National Ocean Service. 1991. Approaches to Galveston Bay. Scale 1:80,000. U.S. Nautical Chart 11323, Washington, D.C.
- National Ocean Survey. 1991. Barataria Bay and Approaches. Scale 1:80,000. U.S. Nautical Chart 11358, Washington D.C.
- National Ocean Survey. 1990. Currituck Beach Light to Wimble Shoals. Scale 1:80,000. U.S. Nautical Chart 12204, Washington D.C.
- National Ocean Survey. 1991. Galveston Bay Entrance. Scale 1:25,000. U.S. Nautical Chart 11324, Washington D.C.
- National Ocean Survey. 1990. Winyah Bay Entrance - Isle of Palms. Scale 1:80,000. U.S. Nautical Chart 11531, Washington D.C.
- U.S. Geological Survey. 1964 (Revised 1987). Bradenton Beach, Florida. Scale 1:24,000. 7.5-Minute Series (Topographic), Washington, D.C.
- U.S. Geological Survey. 1957 (Revised 1979). Caminada Pass, Louisiana. Scale 1:24,000. 7.5-Minute Series (Topographic), Washington, D.C.
- U.S. Geological Survey. 1952 (Revised 1988). Daytona Beach, Florida. Scale 1:24,000. 7.5-Minute Series (Topographic), Washington, D.C.
- U.S. Geological Survey. 1954 (Revised 1974). Galveston, Texas. Scale 1:24,000. 7.5-Minute Series (Topographic), Washington, D.C.
- U.S. Geological Survey. 1953 (Revised 1983). Manteo, North Carolina. Scale 1:24,000. 7.5-Minute Series (Topographic), Washington, D.C.
- U.S. Geological Survey. 1942 (Revised 1973). McClellanville, South Carolina. Scale 1:24,000. 7.5-Minute Series (Topographic), Washington, D.C.
- U.S. Geological Survey. 1956 (Revised 1977). Port Orange, Florida. Scale 1:24,000. 7.5-Minute Series (Topographic), Washington, D.C.
- U.S. Geological Survey. 1957 (Revised 1973 and 1981). Breton Sound, Louisiana. Scale 1:250,000. Topographical/Bathymetric Map NH 16-7, Reston, Va.
- U.S. Geological Survey. 1954 (Revised 1972). Daytona Beach, Florida. Scale 1:250,000. Map series V501 NH 17-8, Reston, Va.



- U.S. Geological Survey. 1972. Daytona Beach, Florida: Land use and land cover. Scale 1:250,000. Land use series, Washington, D.C.
- U.S. Geological Survey. 1946 (Revised 1969). Eastville, Reston, Va; North Carolina; Maryland. Scale 1:250,000. Map series V501 NI 18-8,11, Reston, Va.
- U.S. Geological Survey. 1974 (Revised 1978). Georgetown, South Carolina; North Carolina. Scale 1:250,000. Topographical/Bathymetric Map NI 17-9, Reston, Va.
- U.S. Geological Survey. 1973. Georgetown, South Carolina: Land use and land cover. Scale 1:250,000. Land use series, Washington, D.C.
- U.S. Geological Survey. 1975. Houston, Texas. Scale 1:250,000. Topographic/Bathymetric Map, Washington, D.C.
- U.S. Geological Survey. 1973. Houston, Texas: Land use and land cover. Scale 1:250,000. Land use series, Washington, D.C.
- U.S. Geological Survey. 1969. James Island, South Carolina. Scale 1:250,000. Topographical/Bathymetric Map NI 17-12, Reston, Va.
- U.S. Geological Survey. 1957 (Revised 1973). Manteo, North Carolina. Scale 1:250,000. Map series V501 NI 18-2, Reston, Va.
- U.S. Geological Survey. 1975. Manteo, North Carolina: Land use and land cover. Scale 1:250,000. Land use series, Washington, D.C.
- U.S. Geological Survey. 1963 (Revised 1972 and 1979). New Orleans, Louisiana. Scale 1:250,000. Topographical/Bathymetric Map NH 15-9, Reston, Va.
- U.S. Geological Survey. 1978. New Orleans, Louisiana: Land use and land cover. Scale 1:250,000. Land use series, Washington, D.C.
- U.S. Geological Survey. 1988. St. Petersburg, Florida. Scale 1:250,000. Topographical/Bathymetric Map 27082-A1-TB-250, Reston, Va.
- U.S. Geological Survey. 1972. Tampa, Florida: Land use and land cover. Scale 1:250,000. Land use series, Washington, D.C.

**INTERNAL DISTRIBUTION**

- |                                     |   |
|-------------------------------------|---|
| 1. L. W. Barnthouse, 1505, MS-6036  | 20. F. E. Sharples, 1505, MS-6036                 |
| 2. L. D. Bates, K-1001, MS-7169     | 21. D. S. Shriner, 1505, MS-6036                  |
| 3. T. A. Boden, 1000, MS-6335       | 22. F. W. Stoss, 1000, MS-6335                    |
| 4. J. B. Cannon, 4500N, MS-6189     | 23. S. H. Stow, 1505, MS-6038                     |
| 5. J. H. Cushman, 1503, MS-6352     | 24. R. W. Van Dyke, 4500N, MS-6205                |
| 6. R. M. Cushman, 1000, MS-6335     | 25. R. I. Van Hook, 1505, MS-6037                 |
| 7. R. C. Daniels, 1000, MS-6335     | 26. T. W. White, 1000, MS-6335                    |
| 8. J. E. Dobson, 4500N, MS-6237     | 27-126. CDIAC, 1000, MS-6335                      |
| 9. M. P. Farrell, 1505, MS-6038     | 127. Central Research Library, 4500N, MS-6175     |
| 10. D. E. Fowler, 1505, MS-6035     | 128. ESD Library, 1505, MS-6035                   |
| 11. C. W. Gehrs, 1505, MS-6036      | 129-130. Laboratory Records Dept., 4500N, MS-6285 |
| 12. D. L. Greene, 4500N, MS-6207    | 131. Laboratory Records Dept., RC                 |
| 13. S. G. Hildebrand, 1505, MS-6035 | 132. ORNL Patent Section, 4500N, MS-6258          |
| 14. E. L. Hillsman, 4500N, MS-6206  | 133. ORNL Public Relations, 4500N, MS-6213        |
| 15. J. Kahn, 4500N, MS-6206         |   |
| 16. P. Kanciruk, 0907, MS-6490      |   |
| 17. G. Marland, 1000, MS-6335       |   |
| 18. R. D. Perlack, 4500N, MS-6205   |   |
| 19. D. E. Reichle, 4500N, MS-6253   |   |

**EXTERNAL DISTRIBUTION**

134. D. Alvic, EERC, University of Tennessee, Pellissippi Office, Ste. 100, 10521 Research Drive, Knoxville, TN 37932
135. A. Andersen, U.S. Department of Energy, Code EI-62, Independence Avenue, SW, Washington, DC 20585
136. T. V. Armentano, Holcomb Research Institute, Butler University, 4600 Sunset Avenue, Indianapolis, IN 46208
137. D. G. Aubrey, Department of Geology and Geophysics, Woods Hole Oceanographic Institution, Woods Hole, MA 02543
138. R. H. Ball, U.S. Department of Energy, Office of Environmental Analysis, EP-63, 1000 Independence Avenue, SW, Washington, DC 20585
139. C. Berish, Environmental Protection Agency, Region 4, 345 Courtline, NE, Atlanta, GA 30365
140. R. Beirbaum, Office of Technology Assessment, U.S. Congress, Washington, DC 20510
141. M. Bowman, Tidewater Administration, Tawes State Office Building, 580 Taylor Avenue, Annapolis, MD 21401

142. R. J. Braithwaite, Geological Survey, Oster Voldgade 10, DK-1350, Kobenhavn K, Greenland, DENMARK
- 143-152. B. Breed, U. S. Department of Energy, Office of Environmental Analysis, EP-63, Forrestal Building, Room 4G-036, Washington, DC 20585
153. P. Brunn, 34 Baynard Cove Road, Hilton Head Island, SC 29928
154. J. R. Busby, Environmental Resources Information Network, G.P.O. Box 636, Canberra, A.C.T. 2601, AUSTRALIA
155. R. Calender, Oceanographer of the Navy, U.S. Naval Observatory, 34th St. and Massachusetts Ave., NW, Washington, DC 20392-5101
156. J. Callaway, Wetland Biogeochemistry Institute, Louisiana State University, Baton Rouge, LA 70803-7511
157. D. Canning, Shorelands and Coastal Zone Management Program, Washington Department of Ecology, PV-11, Olympia, WA 98054
158. K. K. Chapman, 928 View Harbor Road, Knoxville, TN 37922
159. C. Christensen, Department of Interior, Office of Information Resources Management, 1849 C. St., NW, MS-5321, Washington, DC 20240
160. W. Conner, Belle W. Baruch Forest Science Institute, P.O. Box 596, Georgetown, SC 29442
161. W. R. Dally, Oceanography and Ocean Engineering, Florida Institute of Technology, 150 West University Boulevard, Melbourne, FL 32901
162. R. A. Dalrymple, Department of Civil Engineering, University of Delaware, Newark, DE 19716
163. L. Davis/Refuge Manager, Cape Romain National Wildlife Refuge, 390 Bulls Island Road, Awendaw, SC 29429
164. R. G. Dean, Coastal and Oceanographic Engineering Dept., 336 Weil Hall, University of Florida, Gainesville, FL 32611
165. L. DeMouy, U.S. Department of Energy, Code EI-623, 1000 Independence Avenue, SW, Washington, DC 20585
166. J. G. de Ronde, Rijkswaterstaat, P.O. Box 20904, 2500 EX The Hague, NETHERLANDS
167. D. P. de Sylva, School of Marine and Atmospheric Science, 4600 Rickenbacker Causeway, University of Miami, Miami, FL 33149
168. R. Dolan, Department of Environmental Sciences, University of Virginia, Clark Hall, Room 101, Charlottesville, VA 22903

169. J. J. Easton, Jr., Assistant Secretary for International Affairs and Energy Emergencies, IE-1, Department of Energy, Washington, DC 20585
170. G. Evans, U.S. Department of Agriculture, Global Change Program Office, 1621 N. Kent Street, Room 60LL, Arlington, VA 22209
171. W. Ferrell, U.S. Department of Energy, 1000 Independence Ave., SW, Washington, DC 20585
172. C. W. Finkl, Editorial Office, Journal of Coastal Research, 4310 25th Avenue, NE, Fort Lauderdale, FL 33308
173. J. F. Franklin, Bloedel Professor of Ecosystem Analysis, College of Forest Resources, University of Washington, Anderson Hall (AR-10), Seattle, WA 98195
174. B. Friedman, Office of Technology Assessment, U.S. Congress, Washington, DC 20510
175. D. G. Friedman, Travelers Corporation, Corporate Strategy and Research, 6 Plaza Building, 1 Tower Square, Hartford, CT 06183-7200
176. J. B. Grace, Botany Department, Louisiana State University, Baton Rouge, LA 70803
- 177-178. V. M. Gornitz, Goddard Institute for Space Studies, 2880 Broadway, New York, NY 10025
179. T. J. Gross, Environmental Sciences Division, Office of Health and Environmental Research, ER-74, U. S. Department of Energy, Washington, DC 20585
180. R. C. Harris, Institute for the Study of Earth, Oceans, and Space, Science and Engineering Research Bldg., University of New Hampshire, Durham, NH 03824
181. W. Haeberli, VAW, AHG, ETH-Zentrum, CH-8092, Zurich, SWITZERLAND
182. J. R. Hanchey/Director, U.S. Army Corps of Engineers, Institute for Water Resources, Casey Building, Fort Belvoir, VA 22060-5586
183. W. Harrison, Energy and Environmental System Division, Argonne National Laboratory, Argon, IL 60439
184. R. Hayes, Oceanographer of the Navy, U.S. Naval Observatory, 345th St. and Massachusetts Ave., NW, Washington, DC 20392-5101
185. D. Hayward, Mote Marine Laboratory, 1600 Thompson Parkway, Sarasota, FL 34236-1096
186. S. D. Hicks, National Oceanic and Atmospheric Administration, N/OMA 12, Room 315, 6001 Executive Boulevard, Rockville, MD 20852
187. G. Hunolt, NASA, Code SED, 600 Independence Ave., SW, Washington, DC 20546

188. G. Y. Jordy, Director, Office of Program Analysis, Office of Energy Research, ER-30, G-226, U.S. Department of Energy, Washington, DC 20545
189. J. Joyce, National Science Foundation, Atmospheric Science Division, 1800 G. St., NW, Washington, DC 20550
190. H. E. Jurcso, Finance Department, Town Hall, 501 Bay Isles Road, Longboat Key, FL 34228
191. T. R. Karl, National Climatic Data Center, Federal Building, Asheville, NC 28801
192. J. Klink, Department of Geography, Miami University, Oxford, OH 45056
193. A. Krapfenbauer, O. Universitätsprofessor, Universität Für Bodenkultur, Peter Jordan-Strasse 81, AUSTRIA
194. S. P. Leatherman/Director, Laboratory for Coastal Research, University of Maryland, 1113 Lefrak Hall, College Park, MD 20742
195. J. K. Lee, School of Public and Environmental Affairs, Indiana University, Bloomington, IN 47405
- 196-197. Say-Chong Lee, Coastal and Oceanographic Engineering Department, 336 Weil Hall, University of Florida, Gainesville, FL 32611
198. R. J. Livingston/Director, Center for Aquatic Research and Resource Mgmt., 136-B Conradi Building, Florida State University, Tallahassee, FL 32306
199. T. H. Mace, U.S. Environmental Protection Agency, Room 1123 West Tower, 401 M St. SW, Washington, DC 20460
200. P. W. Mausel, Department of Geography and Geology, Indiana State University, Terre Haute, IN 47809
201. W. H. McAnnally, Estuaries Division, USAW Waterways Experiment Station, P.O. Box 631, Vicksburg, MS 39180-0631
- 202-203. A. J. Mehta, Coastal and Oceanographic Engineering Dept., 336 Weil Hall, University of Florida, Gainesville, FL 32611
204. C. L. Montague, Environmental Engineering Department, 217 Black Hall, University of Florida, Gainesville, FL 32611
205. L. H. Motz, Civil Engineering Department, 346 Weil Hall, University of Florida, Gainesville, FL 32611
206. S. Z. Meschkow, The Editing Works, 126 Colfax Road, Havertown, PA 19083
207. J. Oerlemans, Institute Meteorologic Ocean, Princetonplein 5, Utrecht 2506, NETHERLANDS

208. G. Oertel, Old Dominion University, Department of Oceanography, Norfolk, VA 23508-8512
209. R. H. Olsen, Vice President for Research, University of Michigan, Medical Science Building II, #5605, 1301 East Catherine Street, Ann Arbor, MI 48109-0610
210. R. A. Park/Coordinator, Holcomb Research Institute, Butler University, 4600 Sunset Avenue, Indianapolis, IN 46208
211. A. Patrinos, Director, Environmental Sciences Division, Office of Health and Environmental Research, ER-74, U. S. Department of Energy, Washington, DC 20585
212. L. Pettinger, National Mapping Division, USGS/DOI, 590 National Center, Reston, VA 22092
213. A. B. Pittovk, CSIRO, Division of Atmospheric Research, Private Bag No. 1, Mordialloc, Vic. 3195, AUSTRALIA
214. S. Ichtiague Rasool, IGBP Data and Information System Office, Université Paris, Tour 26, 4 Etage, Aile 26-16, 4 Place Jussieu, 73230 PARIS Cedex 06, FRANCE
215. M. R. Riches, Environmental Sciences Division, Office of Health and Environmental Research, ER-74, U.S. Department of Energy, Washington, DC 20585
216. T. J. Smith III, Department of Wildlife and Range Science, 117 Newins-Ziegler, University of Florida, Gainesville, FL 32611
217. P. M. Steurer, National Climatic Data Center, Database Management Branch, Federal Building, Asheville, NC 28801
218. P. Stokoe, School for Resources and Environmental Studies, Dalhousie University, 1312 Robie Street, Halifax, Nova Scotia B3H 3E2, CANADA
219. D. J. P. Swift, Old Dominion University, Department of Oceanography, Norfolk, VA 23508-8512
220. J. G. Titus, Office of Policy Analysis, PM-220, U.S. Environmental Protection Agency, 401 M Street, SW, Washington, DC 20460
221. J. Van de Kreeke, School of marine and Atmospheric Sciences, 4500 Rickenbacker Causeway, University of Miami, Miami, FL 33149
222. H. Wang, Coastal and Oceanographic Engineering Dept., 336 Weil Hall, University of Florida, Gainesville, FL 32611
223. R. A. Warrick, Climatic Research Unit, University of East Anglia, Norwich, Norfolk NR4 7TJ, UNITED KINGDOM
224. C. Watts, NOAA/Library, 6009 Executive Blvd., Rockville, MD 20852

225. J. R. Weggel, Department of Civil and Architectural Engr., Drexel University, Philadelphia, PA 19104
226. A. Q. White, Marine Sciences Department, Jacksonville University, Jacksonville, FL 32211
227. T. M. L. Wigley, School of Environmental Sciences, University of East Anglia, Norwich, Norfolk NR4 7TJ, UNITED KINGDOM
228. R. S. Williams, Jr., U.S. Geological Survey, Geologic Division, 927 National Center, Reston, VA 22092
229. L. Wolf, National Academy of Sciences, 2001 Wisconsin Ave., NW, Harris Building 372, Washington, DC 20007
230. G. W. Yohe, Department of Economics, Wesleyan University, Middletown, CT 06457
231. Office of Assistant Manager for Energy, Research and Development, Oak Ridge Field Office, P.O. Box 2001, U.S. Department of Energy, Oak Ridge, TN 37831-8600
- 232-241. Office of Scientific and Technical Information, P.O. Box 62, Oak Ridge, TN 37831
242. Clark University, Central Library, Attn: J. X. Kasperson, Worcester, MA 01610
243. Coastal Engineering Research Center, Waterways Experiment Station, Central Research Library, P.O. Box 631, Vicksburg, MS 39180
244. Louisiana State University, A & M C Government Documents Dept., Librarian, Baton Rouge, LA 70803
245. North Carolina State University, Government Documents Dept., Librarian, Raleigh, NC 27607
246. Rutgers State University, Government Documents Dept., Librarian, New Brunswick, NJ 08903
247. The Florida State University, Government Documents Dept., Librarian, Tallahassee, FL 32306
248. University of Alabama, Government Documents Dept., Librarian, Tuscaloosa, AL 35486
249. University of California, Government Documents Dept., Librarian, Davis, CA 95616-5292
250. University of East Anglia, Climatic Research Unit, Library, Norwich, Norfolk NR4 7TJ, UNITED KINGDOM
251. University of Florida, Government Documents Dept., Librarian, Gainesville, FL 32601
252. University of Georgia, Government Documents Dept., Librarian, Athens, GA 30601

253. University of Houston, Government Documents Dept., Librarian, Houston, TX 77004
254. University of Maryland, College Park, Government Documents Dept., Librarian, College Park, MD 20742
255. University of South Carolina, Government Documents Dept., Librarian, Columbia, SC 29208
256. University of Washington, Government Documents Dept., Librarian, Seattle, WA 98195
257. University of Wisconsin-Eau Claire, Government Documents Dept., Librarian, Eau Claire, WI 54701



**END**

**DATE  
FILMED**

6 / 22 / 93

quadrangle). However, the term *vegetated wetlands* as used in the above context include both freshwater and salt marshes. The prognosis for salt marshes is very bleak; it shows a very rapid decline in acreage with a SLR of 0.1 m (> 60%) and close to a complete wipe-out at a SLR of 0.7 m.

#### 5.4.4 Results and Discussion

Numerous factors have been identified as contributing to the long-term erosion and subsidence being experienced in Louisiana. Chief among these are human impacts (e.g., jetty and canal construction, reef removal, sand mining), indirect human impacts (e.g., reduction in available sediment, accelerated subsidence, flood controls), SLR, and increased frequency of hurricane landfall (Louisiana Wetland Protection Panel 1987). Not all of these elements result in a change in the relative sea level. Therefore, not all the erosional losses can be attributed to SLR. Also, at present, eustatic SLR accounts for only 10 to 15% of the relative SLR being experienced along the Louisiana coast. However, relative SLR principally induced by subsidence, has always been tacitly acknowledged as the primary agent of change of the land-sea interface along the coast of Louisiana. Some of the supports for this claim may have been eroded by the preliminary study results based on bathymetric change information by List et al. (1991). They suggested that the longshore removal of sand appears to be the primary factor in causing coastal erosion along the Bayou Lafourche (Moreau-Caminada) headland, despite the extremely high relative SLR rate in the area. However, the same authors also pointed out that their result must be tempered by the possibility that SLR may exert some control over the rate of longshore erosion. Hence, the use of the trend line method, while subject to the uncertainty just mentioned, produces acceptable results with the proviso that SLR is the primary agent of change. In the present study, the historical rate of erosion,  $R_h$ , is taken from McBride, et al. (1991).

Various data on the historical rate of relative SLR are available for the intensively studied Louisiana coast. Based on a National Ocean Survey Tide Station at Eugene Island, Louisiana, the rate of relative SLR during the period 1940-1972 is reported to be 9.2 mm/year (Hicks and Crosby 1974). The reported rates of relative SLR listed in Table 5.1 (Sect. 5.2.2) range from 8.5 to 9.5 mm/year for the Louisiana coast. For the seven sampled sites within Louisiana referred to in Sect. 5.4.3, the corresponding range is from 8.5 to 9.3 mm/year, with the exception of Pelican Pass, which registered a subsidence rate of 13.8 mm/year (Park et al. 1989). For the present study, the historical rate of relative SLR,  $S_h$ , is assumed to be 8.2 mm/year.

However, the assessment approach adopted is not uniform for the three selected transects. For transects C, which is dominated by salt marshes, another relevant controlling parameter is the cut-off rate of natural vertical accretion of marshes (this aspect is further discussed in Sect. 5.7 for McClellanville, South Carolina). As seen in Table 5.1, the mean accretion rates in Louisiana range from 6.6 to 7.8 mm/year. In the study by Park et al. (1989) the accretion rate has been taken as 5 mm/year (except for Pelican Pass, which was 10 mm/year). Since the present rate of subsidence adopted for the study is already 8.2 mm/year, it can be concluded at the outset that the salt marshes will be progressively